

INFORMATION TO USERS

This reproduction was made from a copy of a document sent to us for microfilming. While the most advanced technology has been used to photograph and reproduce this document, the quality of the reproduction is heavily dependent upon the quality of the material submitted.

The following explanation of techniques is provided to help clarify markings or notations which may appear on this reproduction.

1. The sign or "target" for pages apparently lacking from the document photographed is "Missing Page(s)". If it was possible to obtain the missing page(s) or section, they are spliced into the film along with adjacent pages. This may have necessitated cutting through an image and duplicating adjacent pages to assure complete continuity.
2. When an image on the film is obliterated with a round black mark, it is an indication of either blurred copy because of movement during exposure, duplicate copy, or copyrighted materials that should not have been filmed. For blurred pages, a good image of the page can be found in the adjacent frame. If copyrighted materials were deleted, a target note will appear listing the pages in the adjacent frame.
3. When a map, drawing or chart, etc., is part of the material being photographed, a definite method of "sectioning" the material has been followed. It is customary to begin filming at the upper left hand corner of a large sheet and to continue from left to right in equal sections with small overlaps. If necessary, sectioning is continued again—beginning below the first row and continuing on until complete.
4. For illustrations that cannot be satisfactorily reproduced by xerographic means, photographic prints can be purchased at additional cost and inserted into your xerographic copy. These prints are available upon request from the Dissertations Customer Services Department.
5. Some pages in any document may have indistinct print. In all cases the best available copy has been filmed.

University
Microfilms
International
300 N. Zeeb Road
Ann Arbor, MI 48106

8323955

Barneyback, Robert Seay, Jr.

ALKALI-SILICA REACTIONS IN PORTLAND CEMENT CONCRETE

Purdue University

Ph.D. 1983

**University
Microfilms
International** 300 N. Zeeb Road, Ann Arbor, MI 48106

32705
5-2-83

ALKALI-SILICA REACTIONS IN PORTLAND CEMENT CONCRETE

A Thesis

Submitted to the Faculty

of

Purdue University

by

Robert S. Barneyback, Jr.

In Partial Fulfillment of the
Requirements for the degree

of

Doctor of Philosophy

May 1983

PURDUE UNIVERSITY

Graduate School

This is to certify that the thesis prepared

By Robert S. Barneyback, Jr.

Entitled Alkali-Silica Reactions in Portland Cement Concrete

Complies with the University regulations and that it meets the accepted standards of the Graduate School with respect to originality and quality

For the degree of:

Doctor of Philosophy

Signed by the final examining committee:

Sidney Diamond, chairman
JR West
W. D. Miller
Charles B. Roth

Approved by the head of school or department:

May 5, 1983 Harold J. Michael

To the librarian:

is-

This thesis is not to be regarded as confidential

Sidney Diamond
Professor in charge of the thesis

ACKNOWLEDGEMENTS

I wish to express my sincere appreciation for the guidance and patient support of my Major Professor, Dr. Sidney Diamond, and to the other members of my committee; Dr. William L. Dolch, Dr. Charles B. Roth, and Dr. Terry R. West, for their invaluable counsel in various technical aspects of this work.

I am particularly indebted to Bryant and Katharine Mather for their support and assistance in obtaining special materials for the study, providing analyses of materials, and many valuable suggestions and references.

I am thankful for the considerable assistance of the staff of the Material Laboratory of the Indiana State Highway Commission for allowing the use of their facilities and providing assistance in the processing of mortar samples to obtain pore solutions for analysis.

I extend my gratitude to the three principal typists who worked on the many revisions of the manuscript; Mrs. Marian Sipes, Ms. Mellann Farmer and Miss Susan Coffman.

I wish to thank my wife, Charleen Anne Barneyback, for her patience, good humor, support and assistance during the long, and frequently trying course of this work, and our son, Carl J. Barneyback, for his considerable help in mining and milling the several tons of Beltane Opal, used in this and similar studies worldwide.

The program of research in which the development of the apparatus and procedures described here was accomplished was supported by the U.S. National Science Foundation (Grants No. ENG74-21495 and ENG77-09166) and by the U.S. Department of Energy (Grant No. EM-78-S-02-5207). The support of these agencies is gratefully acknowledged.

This work is dedicated
to the memory of
Alexander Klein
who aroused my interest
in this area of concrete technology.

TABLE OF CONTENTS

	Page
LIST OF TABLES.....	viii
LIST OF FIGURES.....	xvii
ABSTRACT.....	xxii
CHAPTER 1 - INTRODUCTION.....	1
CHAPTER 2 - LITERATURE REVIEW.....	6
2.1 Historical.....	6
2.2 The Problem Returns.....	10
CHAPTER 3 - MATERIALS USED IN THE STUDY.....	23
3.1 Standard Reactive Aggregate.....	23
3.2 Portland Cements Used.....	36
3.3 Pozzolanic Materials Used.....	38
CHAPTER 4 - APPARATUS AND EXPERIMENTAL METHODS.....	40
4.1 Pore Fluid Expression Die.....	40
4.2 Atomic Absorption Spectrophotometer.....	49
4.3 Preparation of Standards and Reagents.....	49
4.4 Determination of Cations.....	50
4.5 Scheme of Analysis and Analytical Conditions.....	51
4.6 Determination of Anions.....	55
4.7 Determination of pH.....	58
4.8 Acquisition and Reduction of Data From the Spectrophotometer	59
4.9 Pozzolan Grinding.....	60
4.10 Determination of Cement and Pozzolan Specific Surface..	61

	Page
4.11 Determination of Chemically Bound Water.....	61
4.12 Adjustment of Pore Solution Concentrations to Compensate for Chemically Bound Water.....	74
4.13 Thermogravimetry and Derivative Thermogravimetry.....	79
4.14 Specimen Molds.....	89
4.15 Storage Containers for Prisms.....	92
4.16 Length Change Measurements.....	98
4.17 Constant Temperature Storage Facilities.....	98
4.18 Mixing Mortars and Molding Specimens.....	99
CHAPTER 5 - EXPERIMENTAL RESULTS.....	100
5.0 Introduction.....	100
5.1 Mix Series 4 - 14.....	102
5.2 Mix Series 15 - 21.....	112
5.3 Mix Series 22 - 24.....	116
5.4 Mix Series 25 - 27.....	116
5.5 Mix Series 28 - 31.....	116
5.6 Mix Series 32 - 33.....	134
5.7 Mix Series 34 - 35.....	137
5.8 This section not used.....	151
5.9 This section not used.....	151
5.10 Mix Series 44 - 45.....	152
5.11 Mix Series 46 - 48.....	162
5.12 Mix Series 49 - 51.....	183
5.13 This section not used.....	199
5.14 Mix Series 58.....	200
5.15 Mix Series 59 - 64.....	203
5.16 This section not used.....	247

	Page
5.17 This section not used.....	247
5.18 This section not used.....	247
5.19 Mix Series 78 ~ 81.....	247
5.20 Mix Series 82 ~ 91.....	271
CHAPTER 6 - THE ROLE OF DIFFUSION IN ALKALI-SILICA REACTIONS.....	304
6.1 Alkali Diffusion in Mortars and Cement Paste.....	304
6.2 Alkali Diffusion in Reactive Aggregate.....	305
6.3 Computation of Diffusion Coefficients.....	312
6.4 Interpretation of Anomalous Diffusion of Potassium in Opal	322
CHAPTER 7 - CONCLUSIONS.....	332
BIBLIOGRAPHY.....	341
VITA.....	352

LIST OF TABLES

Table	Page
2.1 Chemical Analyses of Cements Used by Longuet, et al. (246).....	19
2.2 Concentrations of Ions in Expressed Pore Solutions Reported by Longuet, et al. (246).....	20
2.3 Observed OH ⁻ , pH, and Calculated pH (From Data Reported by Longuet et al. (246).....	22
3.1 Typical Chemical Composition of Some Alkali-Silica Reactive Aggregates and Research Standards.....	27
3.2 Summary of the Observations of Tufts (315) on X-Ray Diffraction Patterns From Opaline Materials Before and After Heat Treatment at 1000° C.....	30
3.3 Reported Refractive Indices of Beltane Opal Grains in Powder Immersion Mounts (319).....	34
3.4 Lot Chemical Analyses of Portland Cements Used in This Study.....	37
3.5 Lot Chemical Analyses of Pozzolans Used in This Study.....	39
4.1 Analytical Conditions Used for Selected Elements.....	53
4.2 Calibration Standards for Sulfate Determination.....	57
4.3 Batch Weights and Factors for Calculation of Oven-Dry and Ignited Batch Weights of Mix 81.....	64
4.4 Calculation of Wo', Wod, and Wig for a Typical Mixture From Which Some of the Pore Solution Has Been Expressed.....	65
4.5 Relationship of Observed Wn/c and Estimated Wn/c to Time for Control Mixes at 20° C.....	72
4.6 Key and Part List for Figure 4.10.....	94
4.7 Key and Part List for Figure 4.11.....	97
5.1.1 Batch Weights, grams, for Mixes 4 - 14.....	103

LIST OF TABLES, cont.

Table	Page
5.1.2 Expansion and SiO ₂ /Na ₂ O eq for mix series 4-14.....	107
5.2.1 Batch Weights, grams, for Mixes 15 - 21.....	114
5.2.2 Expansion and SiO ₂ /Na ₂ O eq. for Mix Series 15 - 21.....	115
5.5.1 Batch Weights, grams, for Mixes 28 - 31.....	117
5.5.2 Weight Ratios of Component Materials Oven-Dry/ Batch, Ignited/Batch.....	118
5.5.3 Observed Expansions of Mortar Prisms, Mixes 28 - 31.....	120
5.5.4 Observed Concentrations of Ions in Expressed Pore Solution (Not Corrected for Bound Water) Mix 28, Control for Mix Series 28 - 31.....	122
5.5.5 Observed Concentrations of Ions in Expressed Pore Solution (Not Corrected for Bound Water) Mix 29, 1% Li ₂ CO ₃	123
5.5.6 Observed Concentrations of Ions in Expressed Pore Solution (Not Corrected for Bound Water) Mix 30, 8% Opal Sand.....	124
5.5.7 Observed Concentrations of Ions in Expressed Pore Solution (Not Corrected for Bound Water) Mix 31, 8% Opal Sand and 1% Li ₂ CO ₃	125
5.5.8 Concentrations of Alkali Metal Cations in Expressed Pore Solution (Corrected for Bound Water) Mix 28, Control for Mix Series 28 - 31.....	126
5.5.9 Concentrations of Alkali Metal Cations in Expressed Pore Solutions (Corrected for Bound Water) Mix 29, 1% Li ₂ CO ₃ ..	127
5.5.10 Concentrations of Alkali Metal Cations in Expressed Pore Solution (Corrected for Bound Water) Mix 30, 8% Opal Sand.....	128
5.5.11 Concentrations of Alkali Metal Cations in Expressed Pore Solutions (Corrected for Bound Water) Mix 31, 8% Opal Sand and 1% Li ₂ CO ₃	129
5.5.12 Concentrations of Alkali Metal Cations in Expressed Pore Solutions (Corrected for Bound Water) Mix 31, 8% Opal Sand and 1% Li ₂ CO ₃	130
5.6.1 Batch Weights, grams, for Mixes 32 - 33.....	135

LIST OF TABLES, cont.

Table	Page
5.5.2 Observed Expansions of Mortar Prisms ($\mu\text{in/in}$), Mixes 32 - 33.....	135
5.7.1 Batch Weights, grams, for Mixes 34 - 35.....	138
5.7.2 Observed Concentrations of Ions in Expressed Pore Solution (Not Corrected for Bound Water) Mix 34, Control for Mix Series 34 - 35	139
5.7.2 Observed Concentrations of Ions in Expressed Pore Solution (Not Corrected for Bound Water) Mix 34, Control for Mix Series 34 - 35.....	140
5.7.3 Observed Concentrations of Ions in Expressed Pore Solution (Not Corrected for Bound Water) Mix 35, 10. Percent Opal Pozzolan, BP-2.....	141
5.7.3 Observed Concentrations of Ions in Expressed Pore Solution (Not Corrected for Bound Water) Mix 35, 10. Percent Opal Pozzolan, BP-2.....	142
5.7.4 Concentrations of Alkali Metal Cations in Expressed Pore Solution (Corrected for Bound Water) Mix 34, Control for Mix Series 34 - 35.....	143
5.7.4 Concentrations of Alkali Metal Cations in Expressed Pore Solution (Corrected for Bound Water) Mix 34, Control for Mix Series 34 - 35 (cont.).....	144
5.7.5 Concentrations of Alkali Metal Cations in Expressed Pore Solution (Corrected for Bound Water) Mix 35, 10. percent Opal Pozzolan, BP-2.....	145
5.7.5 Concentrations of Alkali Metal Cations in Expressed Pore Solution (Corrected for Bound Water) Mix 35, 10. Percent Opal Pozzolan, BP-2 (cont.).....	146
5.7.6 Observed Expansions of Mortar Prisms ($\mu\text{in/in}$), Mixes 34 - 35.....	150
5.10.1 Batch Weights, grams, for Mixes 44 - 45.....	153
5.10.3 Observed Concentrations of Ions in Expressed Pore Solution (Not Corrected for Bound Water) Mix 44, Control for Mix Series 44 - 45.....	154
5.10.4 Observed Concentrations of Ions in Expressed Pore Solution (Not Corrected for Bound Water) Mix 45, 8% Opal Sand.....	155

LIST OF TABLES, cont.

Table	Page
5.10.5 Nonevaporable Water, $W_{n/c}$, as a Function of Beltane Opal Addition and Time.....	156
5.10.6 Concentrations of Alkali Metal Cations in Expressed Pore Solution (Corrected for Bound Water) Mix 44, Control for Mix Series 44 - 45.....	157
5.10.7 Concentrations of Alkali Metal Cations in Expressed Pore Solution (Corrected for Bound Water) Mix 45, 8% Opal Sand. 158	
5.10.8 Observed Expansions of Mortar Prisms ($\mu\text{in/in}$), Mixes 44 - 45.....	161
5.11.1 Batch Weights, Grams, for Mixes 46 - 48.....	164
5.11.2 Weight Ratios of Component Materials Oven-Dry/Batch, Ignited/Batch.....	164
5.11.3 Observed Concentrations of Ions in Expressed Pore Solution (Not Corrected for Bound Water) Mix 46, Control for Mix Series 46 - 48.....	165
5.11.4 Observed Concentrations of Ions in Expressed Pore Solution (Not Corrected for Bound Water) Mix 47, 8% Opal Sand.....	166
5.11.5 Observed Concentrations of Ions in Expressed Pore Solution (Not Corrected for Bound Water) Mix 48, 8% Opal Sand, 19.6% Pozzolan BP-2.....	167
5.11.6 Nonevaporable Water, W_n /c, as a Function of Beltane Opal Addition* and Time.....	168
5.11.7 Concentrations of Alkali Metal Cations in Expressed Pore Solution (Corrected for Bound Water) Mix 46, Control for Mix Series 46 - 48.....	169
5.11.8 Concentrations of Alkali Metal Cations in Expressed Pore Solution (Corrected for Bound Water) Mix 47, 8% Opal Sand. 170	
5.11.9 Concentrations of Alkali Metal Cations in Expressed Pore Solution (Corrected for Bound Water) Mix 48, 8% Opal Sand, 19.6% Pozzolan BP-2.....	171
5.11.10 Observed Expansions ($\mu\text{in/in}$) of Mortar Prisms, Mixes 46 - 48.....	180
5.12.1 Batch Weights, Grams, for Mixes 49 - 51.....	184

LIST OF TABLES, cont.

Table	Page
5.12.2 Weight Ratios of Component Materials Oven-Dry/Batch, Ignited/Batch.....	184
5.12.3 Observed Concentrations of Ions in Expressed Pore Solution (Not Corrected for Bound Water) Mix 49, Control for Mix Series 49 - 51.....	185
5.12.4 Observed Concentrations of Ions in Expressed Pore Solution (Not Corrected for Bound Water) Mix 50, 8% Opal Sand.....	186
5.12.5 Observed Concentrations of Ions in Expressed Pore Solution (Not Corrected for Bound Water) Mix 51, 8% Opal Sand, 1% Li ₂ CO ₃	187
5.12.6 Nonevaporable Water, W /c, as a Function of Beltane Opal Sand Addition* and Time ⁿ	188
5.12.7 Concentrations of Alkali Metal Cations in Expressed Pore Solution (Corrected for Bound Water) Mix 49, Control for Mix Series 49 - 51.....	190
5.12.8 Concentrations of Alkali Metal Cations in Expressed Pore Solution (Corrected for Bound Water) Mix 50, 8% Opal Sand..	191
5.12.9 Concentrations of Alkali Metal Cations in Expressed Pore Solution (Corrected for Bound Water) Mix 51, 8% Opal Sand, 1% Li ₂ CO ₃	192
5.12.9 Concentrations of Alkali Metal Cations in Expressed Pore Solution (Corrected for Bound Water) Mix 51, 8% Opal Sand, 1% Li ₂ CO ₃	193
5.14.1 Batch Weights, grams, for Mix 58.....	201
5.14.2 Expansion Measurements (μ in/in) of Specimens Representing Mix Series 58.....	202
5.15.1 Batch Weights, grams, for Mixes 59 - 64.....	205
5.15.2 Weight Ratios of Component Materials Oven-Dry/Batch, Ignited/Batch.....	205
5.15.3 Observed Concentrations of Ions in Expressed Pore Solution (Not Corrected for Bound Water) Mix 59, Control for Mix Series 59 - 64.....	206
5.15.4 Observed Concentrations of Ions in Expressed Pore Solution (Not Corrected for Bound Water) Mix 60, 8 Percent Opal Sand	207

LIST OF TABLES, cont.

Table	Page
5.15.5 Observed Concentrations of Ions in Expressed Pore Solution (Not Corrected for Bound Water) Mix 61, 8 Percent Opal Sand, 10 Percent Pozzolan L.....	208
5.15.6 Observed Concentrations of Ions in Expressed Pore Solution (Not Corrected for Bound Water) Mix 62, 8 Percent Opal Sand, 25 Percent Pozzolan L.....	209
5.15.7 Observed Concentrations of Ions in Expressed Pore Solution (Not Corrected for Bound Water) Mix 63, 10 Percent Pozzolan L.....	210
5.15.8 Observed Concentrations of Ions in Expressed Pore Solution (Not Corrected for Bound Water) Mix 64, 25 Percent Pozzolan L.....	211
5.15.9 Nonevaporable Water, W_n /c, as a Function of % POZZeq.....	213
5.15.10 Concentrations of Alkali Metal Cations in Expressed Pore Solution (Corrected for Bound Water) Mix 59, Control for Mix Series 59 - 64.....	216
5.15.11 Concentrations of Alkali Metal Cations in Expressed Pore Solution (Corrected for Bound Water) Mix 60, 8 Percent Opal Sand.....	217
5.15.12 Concentrations of Alkali Metal Cations in Expressed Pore Solution (Corrected for Bound Water) Mix 61, 8 Percent Opal Sand, 10 Percent Pozzolan L.....	218
5.15.13 Concentrations of Alkali Metal Cations in Expressed Pore Solution (Corrected for Bound Water) Mix 62, 8 Percent Opal Sand, 25 Percent Pozzolan L.....	219
5.15.14 Concentrations of Alkali Metal Cations in Expressed Pore Solution (Corrected for Bound Water) Mix 63, 10 Percent Pozzolan L.....	220
5.15.15 Concentrations of Alkali Metal Cations in Expressed Pore Solution (Corrected for Bound Water) Mix 64, 25 Percent Pozzolan L.....	221
5.15.16 Equations of Trend Lines Relating $*M^+$ to Percent Added Pozzolan L.....	232
5.15.17 Percent Addition of Pozzolan L Required to Effect the Same Alkali Metal Ion Concentration Reduction as Effected by Addition of One Percent Beltane Opal Sand.....	234

LIST OF TABLES, cont.

Table	Page
5.15.18 Free Ca(OH) ₂ Found by Thermogravimetry in Mix Series 59 - 64.....	236
5.15.19 Expansion (Microstrain) of Mortar Specimens, Mix Series 59 - 64.....	244
5.15.20 Expansion (Microstrain) of Mortar Cylinders, Mix Series 59 - 64 After Removal of Butyl Rubber Jackets and Storage Over Water.....	246
5.19.1 Batch Weights, grams, for Mixes 78 - 81.....	248
5.19.3 Observed Concentrations of Ions in Expressed Pore Solution (Not Corrected for Bound Water) Mix 78, Control for Mix Series 78 - 81.....	249
5.19.4 Observed Concentrations of Ions in Expressed Pore Solution (Not Corrected for Bound Water) Mix 79, 10 Percent Pozzolan Addition, Mix Series 78 - 81.....	250
5.19.5 Observed Concentrations of Ions in Expressed Pore Solution (Not Corrected for Bound Water) Mix 80, 15 Percent Pozzolan Addition, Mix Series 78 - 81.....	251
5.19.6 Observed Concentrations of Ions in Expressed Pore Solution (Not Corrected for Bound Water) Mix 81, 30 Percent Pozzolan Addition, Mix Series 78 - 81.....	252
5.19.7 Nonevaporable Water, W _n /c, as a Function of Percent Pozzolan L Added.....	254
5.19.8 Concentrations of Alkali Metal Cations in Expressed Pore Solution (Corrected for Bound Water) Mix 78, Control for Mix Series 78 - 81.....	256
5.19.9 Concentrations of Alkali Metal Cations in Expressed Pore Solution (Corrected for Bound Water) Mix 79, 10 Percent Pozzolan L.....	257
5.19.10 Concentrations of Alkali Metal Cations in Expressed Pore Solution (Corrected for Bound Water) Mix 80, 15 Percent Pozzolan L.....	258
5.19.11 Concentrations of Alkali Metal Cations in Expressed Pore Solution (Corrected for Bound Water) Mix 81, 30 Percent Pozzolan L.....	259
5.19.12 Total Alkali Metal Ion Concentration, *M ⁺ , as a Function of Percent Pozzolan L Added.....	260

LIST OF TABLES, Cont.

Table	Page
5.20.1 Batch Weights, grams, for Mixes 82 - 91.....	273
5.20.2 Weight Ratios of Component Materials Oven-Dry/Batch, Ignited/Batch.....	274
5.20.3 Nonevaporable water, W_c , as a Function of Time at 15 Percent Pozzolan Replacement.....	275
5.20.4 Observed Concentrations of Ions in Expressed Pore Solution (Not Corrected for Bound Water) Mix 82, Control for Mixes 82, 84, 86, 88 and 90.....	276
5.20.5 Observed Concentrations of Ions in Expressed Pore Solution (Not Corrected for Bound Water) Mix 84, 15 Percent Pozzolan L.....	277
5.20.6 Observed Concentrations of Ions in Expressed Pore Solution (Not Corrected for Bound Water) Mix 86, 15 Percent Pozzolan S.....	278
5.20.7 Observed Concentrations of Ions in Expressed Pore Solution (Not Corrected for Bound Water) Mix 88, 15 Percent Pozzolan A.....	279
5.20.8 Observed Concentrations of Ions in Expressed Pore Solution (Not Corrected for Bound Water) Mix 90, 15 Percent Pozzolan R.....	280
5.20.9 Observed Concentration of Ions in Expressed Pore Solution (Not Corrected for Bound Water) Mix 83, Control for Mixes 83, 85, 87, 89, and 91.....	281
5.20.10 Observed Concentrations of Ions in Expressed Pore Solution (Not Corrected for Bound Water) Mix 85, 30 Percent Pozzolan L.....	282
5.20.11 Observed Concentrations of Ions in Expressed Pore Solution (Not Corrected for Bound Water) Mix 87, 30 Percent Pozzolan S.....	283
5.20.12 Observed Concentrations of Ions in Expressed Pore Solution (Not Corrected for Bound Water) Mix 89, 30 Percent Pozzolan A.....	284
5.20.13 Observed Concentrations of Ions in Expressed Pore Solution (Not Corrected for Bound Water) Mix 91, 30 Percent Pozzolan R.....	285
5.20.14 Concentrations of Alkali Metal Cations in Expressed Pore Solution (Corrected for Bound Water) Mix 82, Control for Mixes 82, 84, 86, 88 and 90.....	286

LIST OF TABLES, cont.

Table	Page
5.20.15 Concentrations of Alkali Metal Cations in Expressed Pore Solution (Corrected for Bound Water) Mix 84, 15 Percent Pozzolan L.....	287
5.20.16 Concentrations of Alkali Metal Cations in Expressed Pore Solution (Corrected for Bound Water) Mix 86, 15 Percent Pozzolan S.....	288
5.20.17 Concentrations of Alkali Metal Cations in Expressed Pore Solution (Corrected for Bound Water) Mix 88, 15 Percent Pozzolan A.....	289
5.20.18 Concentrations of Alkali Metal Cations in Expressed Pore Solution (Corrected for Bound Water) Mix 90, 15 Percent Pozzolan R.....	290
5.20.19 Concentrations of Alkali Metal Cations in Expressed Pore Solution (Corrected for Bound Water) Mix 83, Control for Mixes 83, 85, 87, 89, and 91.....	291
5.20.20 Concentrations of Alkali Metal Cations in Expressed Pore Solution (Corrected for Bound Water) Mix 85, 30 Percent Pozzolan L.....	292
5.20.21 Concentrations of Alkali Metal Cations in Expressed Pore Solution (Corrected for Bound Water) Mix 87, 30 Percent Pozzolan S.....	293
5.20.22 Concentrations of Alkali Metal Cations in Expressed Pore Solution (Corrected for Bound Water) Mix 89, 30 Percent Pozzolan A.....	294
5.20.23 Concentrations of Alkali Metal Cations in Expressed Pore Solution (Corrected for Bound Water) Mix 91, 30 Percent Pozzolan R.....	295

LIST OF FIGURES

Figure	Page
3.1 X-Ray Diffraction Pattern for Beltane Opal.....	32
4.1 Isometric Half Section of Pore Fluid Expression Die.....	44
4.2 Flow Chart for Analysis of Expressed Pore Fluid.....	52
4.3 Plot of $t/(W_n/c)$ vs. t , Illustrating Rectified Relationship Between Nonevaporable Water and Time.....	73
4.5 Schematic Representation of Alkali Metal Ion Distribution in Portland Cement Mortar.....	76
4.6 Schematic Representation of Alkali Metal Ion Distribution in Portland-Pozzolan Cement Mortar.....	78
4.7 Sketch of the Cahn Thermobalance.....	82
4.8 Illustration of the Use of Thermogravimetric and Derivative Thermogravimetric Curves for a Typical Mortar Mix to Determine Weight Loss Due to Thermal Decomposition of Calcium Hydroxide.....	87
4.9 Isometric Sketch of 0.5 in (12.7 mm) Gang Prism Mold and Isometric Half-Section of Finsihed Prism.....	91
4.10 Sketch of Diametral Cross Section of 50 mm Diameter Sealed Expansion Specimen.....	93
4.11 Diametral Cross Section of Storage Container for Miniature Mortar Prisms.....	96
5.1.2 Expansion vs. Time for Mixes 4 - 7, and Mix 14.....	105
5.1.1 Expansion vs. Time for Mixes 9 - 13.....	106
5.1.3 Expansion vs. Mole Ratio $\text{SiO}_2/\text{Na}_2\text{O}$ eq Data from Vivian (501). 109	
5.1.4 Expansion vs. Mole Ratio $\text{SiO}_2/\text{Na}_2\text{O}$ eq from Mix Series 4 - 14, and 15 - 21.....	110
5.5.1 Mortar Prism Expansion vs. Time.....	121
5.5.2 Alkali Metal Ion Concentration vs. Time.....	131

LIST OF FIGURES, Cont.

Figure	Page
5.5.3 Alkali Metal Ion Concentration vs. Time.....	132
5.7.1 Change in Combined Alkali Metal Ion Concentration vs. Time as a Result of Alkali-Silica Reaction.....	149
5.10.1 Alkali Metal Ion Concentration vs. Time.....	159
5.10.2 Alkali Metal Ion Concentration vs. Time.....	160
5.11.1 Alkali Metal Ion Concentrations (Compensated for W _n /c) as a Function of Time for Mix 46, Control for Mix Series ⁿ 46 - 48.	172
5.11.2 Alkali Metal Ion Concentrations (Compensated for W _n /c) as a Function of Time for Mix 47, 8% Beltane Opal Sand.....	173
5.11.3 Alkali Metal Ion Concentrations (Compensated for W _n /c) as a Function of Time for Mix 48, 8% Beltane Opal Sand and 19.6% BP-2.....	174
5.11.4 Total Alkali Metal Ion Concentration (Compensated for W _n /c) as a Function of Added Beltane Opal.....	177
5.11.5 Total Alkali Metal Ion Concentration (Compensated for W _n /c) as a Function of Added Beltane Opal.....	178
5.11.6 Total Alkali Metal Ion Concentration (Compensated for W _n /c) as a Function of Added Beltane Opal.....	179
5.11.7 Comparison of Total Alkali Metal Ion Concentration (Compensated for W _n /c) and Expansion of Hardened Mortar Prisms With Time.....	181
5.11.8 Comparison of Total Alkali Metal Ion Concentration (Compensated for W _n /c) and expansion of Hardened Mortar Prisms With Time.....	182
5.12.1 Alkali Metal Ion Concentrations (Compensated for W _n /c) as a Function of Time for Mix 49, Control for Mix Series ⁿ 49 - 51.	194
5.12.2 Alkali Metal Ion Concentrations (Compensated for W _n /c) as a Function of Time for Mix 50, *% Beltane Opal Sand.....	195
5.12.3 Alkali Metal Ion Concentrations (Compensated for W _n /c) as a Function of Time for Mix 51, 8% Beltane Opal Sand, 1.0% Li ₂ CO ₃ for Specimens Stored at 20° C.....	196
5.12.4 Alkali Metal Ion Concentrations (Compensated for W _n /c) as a Function of Time for Mix 51, 8% Beltane Opal Sand, 1.0% Li ₂ CO ₃ for Specimens Stored at 40° C.....	197

LIST OF FIGURES, Cont.

Figure

5.15.1	Effect of Reactive Mix Component, % POZZeq' on W_n/c	215
5.15.2	Alkali Metal Ion Concentration (Compensated for W_n/c) as a Function of Time for Mix 59, Control for Mix Series 59 - 64.....	222
5.15.3	Alkali Metal Ion Concentration (Compensated for W_n/c) as a Function of Time for Mix 60, 8% Beltane Opal Sand.....	223
5.15.4	Alkali Metal Ion Concentration (Compensated for W_n/c) as a Function of Time for Mix 61, 8% Beltane Opal Sand, 10% Pozzolan L.....	224
5.15.5	Alkali Metal Ion Concentration (Compensated W_n/c) as a Function of Time for Mix 62, 8% Beltane Opal Sand, 25% Pozzolan L.....	225
5.15.6	Alkali Metal Ion Concentration (Compensated for W_n/c) as a Function of Time for Mix 63, 10% Pozzolan L.....	226
5.15.7	Alkali Metal Ion Concentration (Compensated for W_n/c) as a Function of Time for Mix 64, 25% Pozzolan L.....	227
5.15.8	Total Alkali Metal Ion Concentration (Compensated for W_n/c) as a Function of % Pozzolan L Addition.....	229
5.15.9	Total Alkali Metal Ion Concentration (Compensated for W_n/c) as a Function of % Pozzolan L Addition.....	230
5.15.10	Total Alkali Metal Ion Concentration (Compensated for W_n/c) as a Function of % Pozzolan L Addition.....	231
5.15.11	Grams of Calcium Hydroxide, $Ca(OH)_2$, Found per Gram of Cement Batched vs. Percent Pozzolan Equivalent.....	237
5.15.12	Grams of Calcium Hydroxide, $Ca(OH)_2$, Found per Gram of Cement Batched vs. Percent Pozzolan Equivalent.....	238
5.15.13	Derivative Thermogravimetric Curves for Mixes 59 (Control), 63 (10% Pozzolan L), and 64 (25% Pozzolan L), 432 Days at $20^{\circ} C$	239
5.15.14	Derivative Thermogravimetric Curves for Mixes 60 (8% Beltane Opal Sand), 61 (8% Beltane Opal Sand + 10% Pozzolan L), and 62 (8% Beltane Opal Sand + 25% Pozzolan L), 432 Days at $20^{\circ} C$	240
5.15.15	Derivative Thermogravimetric Curves for Mixes 59 (Control), 63 (10% Pozzolan L), and 64 (25% Pozzolan L), 423 Days at $40^{\circ} C$	241

LIST OF FIGURES, Cont.

Figure	Page
5.15.16 Derivative Thermogravimetric Curves for Mixes 60 (8% Beltane Opal Sand), 61 (8% Beltane Opal Sand + 10% Pozzolan L), and 62 (8% Beltane Opal Sand + 25% Pozzolan L), 423 Days at 40° C.....	242
5.15.16 Effect of Addition of Pozzolan L on Estimated Ultimate Expansion of Sealed 50-mm Cylinders.....	245
5.19.1 Effect of Pozzolan L Addition on Nonevaporable Water, W_n/c , at 10 and 128 Days.....	253
5.19.2 Alkali Metal Ion Concentration (mMol/L) in Expressed Pore Solution, Compensated for W_n/c , Mix 78 Stored at 20° C.....	261
5.19.3 Alkali Metal Ion Concentration (mMol/L) in Expressed Pore Solution, Compensated for W_n/c , Mix 78 Stored at 40° C.....	262
5.19.4 Alkali Metal Ion Concentration (mMol/L) in Expressed Pore Solution, Compensated for W_n/c , Mix 81 Stored at 20° C.....	263
5.19.5 Alkali Metal Ion Concentration (mMol/L) in Expressed Pore Solution, Compensated for W_n/c , Mix 81 Stored at 40° C.....	264
5.19.6 Effect of Pozzolan L Addition on Alkali Metal Ion Concentration, Compensated for W_n/c , at 2.75 Days.....	266
5.19.7 Effect of Pozzolan L Addition on Alkali Metal Ion Concentration, Compensated for W_n/c , at 5.75 Days.....	267
5.19.8 Effect of Pozzolan L Addition on Alkali Metal Ion Concentration, Compensated for W_n/c , at 10. Days.....	268
5.19.9 Effect of Pozzolan L Addition on Alkali Metal Ion Concentration, Compensated for W_n/c , at 27. Days.....	269
5.19.10 Effect of Pozzolan L Addition on Alkali Metal Ion Concentration, Compensated for W_n/c , at 124. Days.....	270
5.20.1 Alkali Metal Ion Concentration (Compensated for W_n/c) vs. Time.....	296
5.20.2 Alkali Metal Ion Concentration (Compensated for W_n/c) vs. Time.....	297
5.20.3 Alkali Metal Ion Concentration (Compensated for W_n/c) vs. Time.....	298
5.20.4 Alkali Metal Ion Concentration (Compensated for W_n/c) vs. Time.....	299

LIST OF FIGURES, Cont.

Figure	Page
5.20.5 Alkali Metal Ion Concentration (Compensated for W_n/c) vs. Time.....	300

ABSTRACT

Barneyback, Robert S., Jr., Purdue University, May 1983.
ALKALI-SILICA REACTIONS IN PORTLAND CEMENT CONCRETE. Major Professor:
Dr. Sidney Diamond.

The traditional method of studying alkali-silica expansion reactions has been to cast rectangular prisms or cylinders of mortar or concrete, expose them to various regimen's of temperature and moisture, and observe length changes of the specimens.

While this approach yields information on expansion potential, it reveals nothing about the chemcial reactions taking place in the mortar or concrete.

In order to obtain samples or the pore solution in reacting mortars a pore fluid expression die was designed and built to operate at pressures up to 80,000 psi (522 MPa). These expressed solutions were then analyzed by atomic absorption spectroanalysis and microchemical methods. It was found that major chemical changes could take place in the pore solutions prior to the initiation of expansion and these changes frequently went to completion days or even months before expansion approached completion.

Studies with pozzolans revealed that pore solution chemical changes associated with their reactions were similar to those associated with expansive reactions, but were generally much more rapid.

Studies of the amount of water chemically bound by a unit weight of portland cement revealed that water chemically bound by

portland cement is apparently reduced as a linear function of the ratio of pozzolan to cement.

Data from a study of the effect of the presence of available calcium on the diffusion of potassium in opal suggests that, in the presence of calcium, the amount of potassium found in the outer layers of the opal may be nearly ten times as great as that in the absence of calcium.

CHAPTER 1

INTRODUCTION

Durable concrete results from a thorough understanding of the service requirements of the structure (resistance to service loads, chemical attack, weathering, and abrasion) and appropriate concrete mixture design (selection of component materials and mix proportions with due regard for their chemical and physical properties, cost, the anticipated service life of the structure, and the consequences of its premature failure).

One class of durability problems involves chemical reactions between certain aggregate constituents and alkali hydroxides, usually derived from the portland cement, and generally classed as "alkali-aggregate" reactions. Alkali aggregate reactions fall into three categories:

- Alkali-Silica Reactions - Alkali attack on amorphous or metastable silica minerals or mineraloids. This attack may lead to the formation of alkali-silica gels which may, in turn, imbibe water and expand with considerable force.
- Alkali-Silicate Reactions - Exfoliation and expansion, generally as a result of water uptake, by some silicate rocks, primarily argillites, phyllites, and graywackes containing large amounts of argillaceous material.

- Alkali Carbonate Reactions - Generally restricted to argillaceous dolomitic limestones in which dedolomitization of the rock is followed by imbibition of water by the dehydrated clay minerals, formerly sealed within the rock structure, and followed by expansion (101).

This investigation is concerned with alkali silica reactions, and constitutes an attempt to study some of the details of their chemical and physiochemical aspects, with the aim of providing further insight into their mechanisms and kinetics. It was undertaken in the hope that the results obtained would be helpful in indicating how the durability problems that arise as a result of these responses can be prevented or ameliorated.

For the purpose of this investigation the alkali-silica reaction is characterized as a chemical reaction between alkaline solutions (primarily potassium and sodium-bearing solutions) within the pores of hardened concrete or mortar, and unstable or metastable siliceous components of the aggregate phase of the mortar or concrete.

Under certain conditions this initial chemical reaction may be followed by a physical-chemical response in which some portion of the alkali-silica reaction products imbibe water and swell with sufficient force to result in deleterious expansion of the mass. It should be noted that expansion is not a necessary consequence of the alkali-silica reaction. Indeed, the inclusion of sufficient amounts of finely divided siliceous materials, i.e. pozzolans, appears to result in the formation of alkali-silica reaction products with significantly reduced expansive capacity. It is also possible that some siliceous aggregates

with high specific surface due to interior pores and voids (e.g. welded tuff, pumice, and bloated lightweight aggregates made from pyroprocessed clays, shales and slates) may also produce reaction products with low expansion potential and therefore be self protected.

In this study the primary reactive aggregate used was a naturally occurring largely amorphous siliceous material referred to as Beltane Opal (see Chapter 3). In essentially all of the mixtures all of the alkalies were derived from the portland cement used. A few of the mixtures contained additional alkali introduced in the form of Li_2CO_3 . The aggregates and pozzolanic materials were, with few exceptions, selected for their relative freedom from alkali components.

In practical field concretes alkalies can be derived not only from the hydrating portland cement but can be inadvertently supplied by aggregate components such as zeolitic or other alkali-bearing minerals or as aggregate contaminants. Attack by alkalies released from the hydrating cement may decompose such components to release their constituent alkalies. Furthermore, pozzolanic materials or chemical admixtures may contribute significant amounts of alkalies. Finally, alkalies may enter the concrete from the environment in which the structure is located or from materials or processes within the structure.

It has been established that the actual reactions involved are dependent on the dissolved alkalies being in the form of alkali hydroxides. Under most circumstances in concrete the existence of a reservoir of solid calcium hydroxide results in added alkali compounds liberating an equivalent molar quantity of hydroxide ions into solution.

In most of the investigations cited in Chapter 2, expansion potential arising as a result of alkali-silica reactions has been evaluated in terms of measured length changes of specimens prepared from materials of known properties, e.g. cements containing known quantities of alkali metal compounds, admixtures of known chemical composition, and aggregates of known chemical and petrographic character. Correlations between the material properties and the proportions added, and the consequent observed expansion potential have then been attempted. These largely empirical, and frequently poorly understood, relationships have, in the past, been used to set specification limits for permissible amounts of component materials considered to be deleterious from the standpoint of alkali-silica expansion reactions.

A number of attempts have been made to study the alkali-silica reaction. Many of these have taken the form of studies of the physiochemical properties of synthetic alkali-silica gels and sols, with or without the addition of calcium. While these are of interest, the methods used to prepare the gels are not directly related to the formation of gels *in situ* in the concrete. Chemical analyses of reaction products separated manually from concretes evidencing alkali-silica expansion have been conducted, but these materials are the end products of the reaction, and the probability that they contain contaminants is great. Applications of electron microprobe analysis and energy dispersive X-ray analysis have come closer to providing information on some of the chemical properties of *in situ* reaction products, but leave many questions. Diamond, Young, and Lawrence (102) discussed

the applications of energy dispersive X-ray analysis to cement hydration products and indicate some of the problems associated with the method. In addition to problems outlined in this reference, neither method is adaptable to the determination of water contents of the reaction products, and quantitative determination of sodium and elements with atomic numbers below it is difficult, if not impossible, with presently available equipment.

The approach taken in this work involves primarily the study of the effect of alkali silica reactions on pore solution chemistry. This mode of study also contains a number of uncertainties in that it usually involves an attempt to deduce the course and extent of reaction from changes taking place in the complex solution from which one of the reactants is drawn.

Further uncertainties must be recorded. It seems likely that the role of calcium in the alkali-silica reaction, particularly when pozzolans are involved, may be significantly greater than is reflected by its low concentration in the expressed pore solutions. Further, while the bulk concentration of the pore solutions is likely to be reasonably represented by the chemical properties of the expressed pore solution, films immediately adjacent to reacting aggregate and pozzolan particles may vary in composition from the bulk solution.

Finally, it should be borne in mind that the reactive aggregate component used in these experiments was an opaline material which is highly reactive. Attempts to extrapolate these results to other perhaps less highly reactive aggregates, e.g. volcanic glasses, strained quartzites, etc., may not be valid.

CHAPTER 2

LITERATURE REVIEW

2.1 - Historical

For well over a century it has been common knowledge that portland cements contain water soluble alkali metal compounds and that these compounds tend to accelerate the rate of set of the cement. The remarks of Gilmore, writing in 1879, are typical:

"Recent analyses of American cements show that they all contain more or less of the alkalies, sometimes caustic and sometimes in the form of chlorides of sodium and potassium. ... The alkalies promote hydraulic induration in their own peculiar way. We know that Mortars of American cements part with soda and potash when immersed in water, and render the latter alkaline; ...". (201, pp. 305, f.)

More recent writers recognized the importance of alkali metal compounds as fluxes (202, pp. 30, & 132) during clinker production as well as accelerators (203, p. 41) during hydration of the cement.

While it is virtually certain that deleterious alkali-silica reactions took place, none of these early authors described distress which in the light of present knowledge, would be positively interpreted as indicating alkali-silica reaction. There are occasional cryptic remarks, for example Blount (204, p. 217, f.) remarked, under the heading of "Effects of Aggregates":

"It is obvious that questions of freight come in, as it is easier to bring cement to the site than to carry aggregate, however good, from a distance: but sometimes it happens that

the local aggregates may have a bad influence on the cement with which it is to be mixed, and difficulties often arise from this cause."

In 1940 the observations and experiments of Stanton (205), of the California Division of Highways, led him to conclude that alkalies could react with some aggregate constituents, thus causing expansion and disruption of the concrete. The initial publication of Stanton's findings and observation of similar problems by the Bureau of Reclamation at Parker Dam (206) led to a meeting of interested parties at Denver, Colorado in February of 1941.

The phenomenon was aptly described by Blanks early in the Denver conference:

"When the concrete cores are extracted and stored in the presence of water, a gel-like substance exudes from their surfaces. This gel is also found throughout the concrete in the small cavities and voids. On drying, the gel hardens to a whitish-gray deposit with enormous shrinkage. The gel has been positively identified as sodium silicate."

"The cores taken from Parker Dam further reveal that certain aggregate particles in the concrete are not content with the role of an inert filler material and evidence such dissatisfaction by undergoing chemical alteration. Apparently the sodium silicate gel is a product of reaction between alkalies in the cement and siliceous minerals contained in andesite and rhyolite particles. These rocks constitute less than 2 percent of the aggregate used in the Parker concrete." (207, p. 9)

Subsequent work, much of it inspired by this conference, resulted in confirmation of the hypotheses advanced as to the apparent causes of the cracking and development of methods of test to identify potentially reactive materials. This work suggested, empirically, solutions which would lead to elimination of the problem, or at least to its mitigation. Much of this work was published as a result of an ASTM

Symposium held in San Francisco, California in October 1949 (208). Interest in the alkali-silica problem was not confined to the Western United States. In 1942 the Cement and Concrete Association of Australia entered into an agreement with the Commonwealth of Australia Council for Scientific and Industrial Research to support research on cement and concrete. A series of 26 papers were published during the period 1947 through 1958 (209-210) that dealt with various aspects of the alkali-silica reaction problem. The Danish Institute of Building Research and the Academy of Technical Sciences sponsored work by the Committee on Alkali Reactions in Concrete. During the period 1957 through 1964 this organization issued 23 reports. Much of this material was incorporated in the Ph.D. thesis of Idorn (211). The work involved extensive surveys of concrete structures in Denmark, many of which exhibited classic symptoms of alkali-silica attack. Numerous samples were obtained from selected structures for detailed laboratory examination. Lerch (212, pp. 334-345) reviewed progress on the problem in the United States in 1955, citing 48 references.

By the time of Lerch's review, intensive research in many different laboratories had confirmed Stanton's original findings. In addition, a wide range of test methods had been developed to measure the potential expansion of reactive cement-aggregate combinations (214), assist in evaluation of potential aggregate resources (215-219), and evaluate admixtures intended for use as inhibitors of expansion (220).

At the time the problem and its avoidance seemed quite simple. Simply stated, the problem resulted from combination of a high alkali cement with aggregates containing metastable or unstable siliceous

constituents. These constituents were attacked by the alkali metal hydroxides released during hydration of the cement. The resulting reaction products, alkali silica gels, imbibed water and expanded producing tensile stresses within the concrete which resulted in local disruption and gross expansion.

Aggregate constituents found to be particularly susceptible to attack include opal, frequently found as a secondary mineral filling cavities and fissures in igneous rocks and which may occur as coatings on sand and gravel particles; tridymite, and cristobalite. When microcrystalline or when they contain natural glass the extrusive volcanic rocks rhyolite, andesite, and some basalts may be reactive. The glassy volcanic rocks such as obsidian, pitchstone, and perlite are generally reactive. Some argillites, phyllites, and slates may be reactive as well. These reactive materials may constitute a relatively small fraction of an aggregate and still cause deleterious effects. It should be remembered that the Parker Dam aggregate contained less than 2 percent andesite and rhyolite.

Accepted methods of avoidance of the problem fell into three classifications:

1. In the absence of accepted service records to the contrary, a fine or coarse aggregate should be considered potentially deleteriously reactive if petrographic examination reveals any of the following:
 - a. The presence of any opal
 - b. More than 5 percent chert in which chalcedony is detected.

- c. More than 3 percent glassy igneous rocks in which acid (more than 65 percent silica) or intermediate (55 to 65 percent silica) glass is detected. Glasses with more than 55 percent silica generally have an index of refraction lower than 1.57 (221, pp. B-1 through B-3).
2. Limit the equivalent Na_2O content ($\text{Na}_2\text{O} + 0.658 \text{K}_2\text{O}$) of the cement to a maximum of 0.60 percent.
3. Utilize pozzolans as admixtures or replacement for part of the portland cement.

2.2 - The Problem Returns

With few exceptions research interest in the alkali-silica reaction declined in the mid 1960's. There were occasional theoretical debates over various aspects of the physical chemistry of the expansion associated with the alkali-silica reaction, the role of pozzolans as inhibitors of the expansion reaction, and some reports of alleged distress of concretes containing granites, quartzites, and similar rock types then thought to be innocuous. With the above noted exceptions, the alkali-silica expansion problem was considered solved until the early 1970's when three significant factors intervened:

2.2.1 - Alkali Silica Reactions With Quartz

Variations in optical properties of mineral grains due to stress and deformation, i.e. undular, undulatory, or strain extinction, are well known (222-225). Gogte (226) conducted extensive studies on a suite of seemingly innocuous aggregates, e.g. granites, charnockites, quartzites, etc. He found that their susceptibility to alkali-silica

attack was related to the magnitude of the strain effects present in the quartz grains in these rocks, and that the strain effects could be quantified by measuring the angle of undular extinction (223). Normal quartz grains, when oriented in the position of highest birefringence and viewed between crossed polarizers, exhibit a relatively sharp extinction. In contrast, a deformed or strained quartz grain may exhibit partial extinction for 20 to 60 degrees or more with waves of extinction moving across the crystal like a thunderstorm across the sky. The increased potential for alkali-silica reactivity of the quartz seems likely to be due to the presence of dislocations in the crystal lattice of the quartz. Microfractures produced in the quartz may also serve to increase the effective specific surface of the mineral grains.

2.2.2 - Increasing Alkali Content of Cements

Low alkali cement, containing less than 0.60 percent Na₂O equivalent, is becoming a rarity. Virtually all raw materials used in the manufacture of portland cement may contribute alkalies, but clay and shale are the major sources. If coal is used to fire the kiln its ash may contribute significant amounts of CaO, SiO₂, alkalies and sulfur. Prior to the advent of serious environmental concern in the 1960's, excess alkalies could be removed from the kiln charge by allowing them to volatilize and venting them to the atmosphere as an aerosol along with the kiln gases and part of the dust. Alternative procedures involved bypassing part of the dust and kiln gases at points where kiln effluent gases are rich in alkalies. This effluent could then be

precipitated and wasted. Efficiency of volatilization could be improved by the addition of calcium chloride, first done in the United States by Brownmiller in 1937 (227). Woods (228) undertook extensive studies involving the use of calcium chloride and heat treatments to remove excess alkalies from clinker.

With the advent of environmental concern and rapidly increasing energy costs these methods have become impractical. The requirement that virtually all particulate material be removed from kiln gases before they are discharged into the atmosphere results in the accumulation of large quantities of dust that represents a considerable investment. Since these dusts are largely the fine fraction of the raw kiln feed it is logical that they should be returned to the raw feed circuit. However they also contain high concentrations of alkalies relative to the virgin raw feed, and their return significantly increases the alkali content of the kiln charge. If some method of eliminating the circulating load of alkalies is not used, coatings of alkali bearing materials are deposited in the kiln and dust collecting system, eventually causing blockage. One solution to this problem is to increase the sulfur content of the raw feed either by the introduction of sulfur bearing materials, or by use of high sulfur fuels. This results in the formation of alkali sulfates which, due to their relatively high vaporization temperatures, are more readily retained in the clinker and pass out of the kiln with it. This results in clinkers with higher alkali contents, but this increase in alkali content is an unavoidable consequence of the current technology required to improve energy efficiency.

While the major portion of current U.S. portland cement production comes from plants utilizing large rotary kilns, the trend is toward more energy efficient equipment for replacement or new construction.

Three general kiln arrangements are currently favored:

Lepol-kiln - A short rotary kiln completing ignition of a raw mix which has been precalcined on a chain grate. The grate calciner draws hot exhaust gases from the rotary kiln through a compact bed of raw mix effecting greater efficiency in heat exchange, reduced dust in the waste gas stream, and results in conditioning of the waste gas stream for more efficient operation of electrostatic precipitation equipment. An energy saving of greater than 50 percent is claimed for this system which was first introduced in 1928. (229, pp. 375-378).

Suspension Preheaters - Systems of various combinations of cyclones in which raw feed flows counter-current to exhaust gases from a rotary kiln in which calcination and ignition of the clinker is completed. This system was first introduced in 1934. Reduction in thermal energy requirements depends on raw mix gradation and composition as well as the number of stages in the system. (229, pp. 379-407)

Suspension Preheaters with Precalciners - Similar to the suspension preheater, but with the addition of a chamber in which heat energy is supplied by combustion of fossil fuel. Materials entering the rotary kiln are approximately 90 percent calcined as opposed to approximately 15 percent for the simple suspension preheater

systems. The fuel energy requirements for systems of this design are claimed to be approximately 40 percent of that required for a standard rotary kiln design of similar capacity. (229, pp. 407-436).

While all of these systems significantly increase fuel efficiency, all of them increase retention of alkalies in the finished clinker nodules and on their exterior surfaces. Some reduction in alkali content may be effected in these systems through dust bypasses that allow the removal of alkali rich dusts at various points in the system, but a general increase in alkali content of finished clinker appears to be a concomitant cost of increased fuel efficiency.

The most complete review of the effects of alkalies and their effects on both the clinkering process and on the hydration and performance of portland cements has been prepared by Jawed and Skalny (230,231).

Diamond (232, 233) has summarized knowledge of the mechanism of alkali-silica reactions through 1974, and an extensive annotated bibliography on alkali-aggregate reactions, also covering material up to 1974, has been prepared by Figg (234). Five international symposia have been held on the general subject of alkalies in cement and their effects on performance of concrete, the last in April 1981. Proceedings volumes were generated by three conferences (235-237), and a fourth is in press.

The specific subject of the chemistry of pore solutions in hydrating portland cement pastes, mortars and concretes has been addressed by only a few researchers. The earliest appears to be that of Roller (238, 239). He used six portland cement clinkers obtained from production plants over a wide geographic distribution. The clinkers were ground

in the laboratory to approximate particle sizes encountered in normal cement production. Finely ground gypsum (approximately $2.5 \mu\text{m}$) was blended with the ground clinker prior to preparation of "normal consistency" cement pastes for test. The liquid phase was separated from the paste approximately 15 minutes after introduction of the mixing water by application of mechanical force. The system used consisted of a small cylindrical mold fitted with a piston. A pressure of 280 kgf/cm² (27.5 MPa) was applied by the piston and the liquid phase flowed upward "through the clearance of a few thousandths of a centimeter between the piston and the walls of the die." (238, p. 670). The liquid was collected, filtered, and subjected to chemical analysis. Kalousek, Jumper, and Tregoning (240) worked with a similar series of portland cement clinkers which were blended with gypsum as well as a number of admixtures. They worked with cement pastes with a water-cement ratio of 0.35 and separated the liquid phase by air pressure filtration 7 and 115 minutes after addition of mixing water to their pastes. Strelkov (241) employed a pressure-filtration device in studies of the liquid phase of hydrating portland cements with water-cement ratios in the range 0.4 to 0.5. Eitel (242, pp. 353-355) illustrates the device used, but provides no data or discussion of the findings resulting from these studies. Kurbatova (243) expressed the liquid phase from hydrating portland cement pastes with 0.50 water-cement ratio. Although the paper contains no description of the device used, data are presented in graphical form for analyses of fluids expressed in the time range 3 minutes to 24 hours after the introduction of mixing water.

The results of all of these studies, with respect to those portions dealing with portland cement clinkers with added gypsum, can be summarized as follows:

- Within a few minutes after the initial mixing of water and cement, the liquid phase is at or above saturation with respect to $\text{Ca}(\text{OH})_2$.
- Within the same time frame the liquid phase is essentially a solution of sulfates and hydroxides of calcium, sodium, and potassium. The $\text{SO}_4^{=}$ concentration remains relatively constant throughout the first two hours of hydration and then begins to disappear from solution, being replaced on an equivalent basis by OH^- . Kalousek et al. (240) reported on color observed in the freshly separated pore solutions. It appears that concentrations of $\text{SO}_4^{=}$ in excess of 10 mMol/L are yellow in color, the color being more intense with increasing $\text{SO}_4^{=}$ concentration. Roller (238, p. 671) observed, "The liquors are, in general, yellowish but are colorless in the absence of dissolved sulfate".

Pore solutions expressed in this study and concurrent work with other cements confirms these observations. In addition it should be noted that in these same studies $\text{SO}_4^{=}$ may return to solution after periods of several months to three years. These expressed pore solutions also exhibit a pale slightly greenish yellow color similar to that observed in pore solutions expressed from fresh pastes. The reason for the yellow appearance of the fluid is puzzling since the sulfate ion is colorless.

- Kurbatova observed that alite clinkers released their alkalies much more rapidly than belite clinkers, and that not all of the alkalies present in the original clinkers had been transferred to solution within 24 hours.

The studies referred to thus far have involved relatively short hydration times. Up to the time of final set separation of the liquid phase from hydrating pastes, mortars, and concretes is relatively easily accomplished. Application of gas or mechanical pressures to samples aged one to three days, which are supported on some form of filter arrangement has met with some success, but beyond this time period extreme measures are required. The use of organic fluids to displace the aqueous phase, or leaching of powdered samples of the material have been attempted. Some investigators have elected to work with dilute slurries, e.g. Lawrence (244), but these approaches have little relevance to practical concrete mixtures.

It appears the first successful device for expressing pore solutions from hardened portland cement paste specimens was developed by Peginin, Rubaud, Longuet, and Zelwer (245) in the early 1970's. This device, or others like it, were used to obtain samples of pore solutions from cement pastes a year or more old (246-248). The primary interest of these investigators was the study of chemical factors relating to corrosion resistance afforded by pore solutions to embedded reinforcing materials.

The paper by Longuet, Burglen, and Zelwer (246) is of particular interest and some of the tables from this reference have been recast in units used in this investigation and included here. These

investigators worked with 0.50 water cement ratio pastes of portland cement (CPA) and pastes consisting of mixtures of slag cement with portland cement (CLK). Their specimens, weighing about 300 g. each, were cast in molds and subsequently demolded and stored in plastic bags to maintain a constant moisture content. These specimens were expressed at a pressure of 3500 Bar (350. MPa). The reported chemical analyses of the cements used are listed in Table 2.1 and the partial analyses of the expressed pore solutions are listed in Table 2.2. These concentrations have not been adjusted for chemically bound water since no data for estimation of bound water were available in the original reference. It should be noted that these data are for cement pastes, i.e. mixtures without any aggregate or filler material.

In Table 2.3 the OH^- concentration (millimoles/liter) and pH, as determined by Longuet et al. (246), have been listed. Calculated values of pH, assuming unit activity of OH^- , have been included in Table 2.3.

As observed by previous investigators, the initial pore solutions consisted mainly of sulfates and hydroxides of calcium and alkali metals. In the cases of cements CPA 1 and CPA 2, the initially high sulfate content falls to near zero within 28 days and then returns after several months. It is also of interest to note that the concentrations of alkali metal ions in expressed pore solutions go through a maximum at about six months and then decline slightly. These results are in agreement with the findings of the work reported herein.

Table 2.1

Chemical Analyses of CementsUsed by Longuet, et al. (246)

<u>Component</u>	<u>CPA 69</u>	<u>CPA 1</u>	<u>CPA 2</u>	<u>CLK</u>
SiO ₂	21.85	20.51	19.74	29.82
Al ₂ O ₃	4.79	5.14	4.94	9.69
Fe ₂ O ₃	2.09	3.12	3.00	1.50
CaO	63.46	61.69	60.89	47.77
MgO	2.39	4.82	4.64	4.11
Na ₂ O	0.19	0.24	0.23	0.20
K ₂ O	1.00	1.21	1.16	0.39
SO ₃	3.64	2.76	4.97	4.71
S	--	--	--	0.56
Cl	--	0.01	0.01	0.02
TiO ₂	0.25	0.31	0.29	0.36
P ₂ O ₅	0.12	0.11	0.11	0.13
MnO	<u>0.05</u>	<u>0.06</u>	<u>0.05</u>	<u>0.61</u>
Total	99.83	99.98	100.03	99.87

Table 2.2

Concentrations of Ions in Expressed Pore SolutionsReported by Longuet, et al. (246)(Not Corrected for Bound Water)
(Concentrations in millimoles/liter)Cement CPA 69

Age, Days at 20°C	Si^{4+}	Ca^{++}	Na^+	K^+	$\Sigma +*$	OH^-	$\text{SO}_4^=$	$\Sigma -*$	$\Sigma +-*$
0.125	0.2	24	24	201	272	n.r.	65	--	--
0.208	0.2	21	29	246	361	132	89	310	+6
4.	0.2	4	73	372	453	453	2	457	-4
28.	n.r.	1	120	515	638	698	7	698	-73
91.	1.5	1	92	454	549	541	11	562	-13
182.	0.9	0	110	442	552	546	4	554	-2
364.	n.r.	1	100	404	506	502	5	512	-6

Cement CPA 1

Age, Days at 20°C	Si^{4+}	Ca^{++}	Na^+	K^+	$\Sigma +*$	OH^-	$\text{SO}_4^=$	$\Sigma -*$	$\Sigma +-*$
0.208	0.3	14	29	255	312	176	66	308	+3
2.	n.r.	2	72	353	429	435	1	437	-7
7.	n.r.	2	115	502	622	623	7	636	-15
28.	n.r.	2	160	556	721	717	0	717	-4
91.	0.005	3	133	531	670	625	0	625	+45
182.	n.r.	0	156	546	702	689	3	695	+7
364.	0.4	0	143	554	697	670	11	691	+6

Cement CPA 2

Age Days at 20°C	Si^{4+}	Ca^{++}	Na^+	K^+	$\Sigma +*$	OH^-	$\text{SO}_4^=$	$\Sigma -*$	$\Sigma +-*$
0.208	0.2	21	28	223	292	129	82	293	-1
2	0.9	3	111	467	584	452	4	459	+124
7	0.6	2	168	531	703	687	0	687	+16
28	n.r.	2	160	532	696	685	10	705	-9
56	1.2	0	159	626	785	740	13	766	+19
182	0.9	0	173	517	690	651	19	688	-2
364	1.6	0	137	565	702	670	15	700	+2

Table 2.2 (Continued)

Concentrations of Ions in Expressed Pore SolutionsReported by Longuet, et al. (246)

(Not Corrected for Bound Water)

(Concentrations in millimoles/liter)

Age, Days at 20° C	Cement CLK								
	Si ⁴⁺	Ca ⁺⁺	Na ⁺	K ⁺	$\Sigma +*$	OH ⁻	SO ₄ ⁼	$\Sigma -*$	$\Sigma +e*$
0.17	0.2	34	10	45	124	83	19	120	+3
2.	0.0	26	26	73	151	77	35	147	+4
7.	0.0	3	41	89	136	137	0	137	-1
36.	n.r.	3	49	85	140	160	1	162	-22
112.	0.05	0	51	86	137	143	3	150	-13
182.	0.4	0	55	87	141	129	3	135	+7
224.	n.r.	0	44	73	118	128	n.r.	128	-10

* milliequivalents/liter, Si⁴⁺ not included.
n.r. = not reported

Table 2.3

Observed OH⁻, pH, and Calculated pH
(From Data Reported by Longuet et al. (246))

(Concentrations in millimoles/liter)

Age, Days	Cement CPA 69			Cement CPA 1			Cement CPA 2			Cement CLK		
	Observed OH	pH	Calc. pH									
0.125	n.d.	n.d.	n.d.	---	---	---	---	---	---	---	---	---
0.17	83	n.d.	13.11	---	---	---	---	---	---	83	n.d.	12.92
0.208	132	13.1	13.12	176	13.1	13.25	129	13.2	13.11	---	---	---
2.	---	---	---	435	13.5	13.64	452	13.35	13.66	77	12.7	12.89
4.	453	13.7	13.66	---	---	---	---	---	---	---	---	---
7.	---	---	---	623	13.7	13.79	687	13.6	13.84	137	12.95	13.14
28.	698	13.7	13.84	717	13.45	13.86	685	13.55	13.84	---	---	---
36.	---	---	---	---	---	---	---	---	---	160	12.95	13.20
56.	---	---	---	---	---	---	740	n.d.	13.87	---	---	---
91.	541	13.25	13.73	625	13.2	13.80	---	---	---	---	---	---
112.	---	---	---	---	---	---	---	---	---	143	13.1	13.16
182.	546	n.d.	13.74	689	13.9	13.84	651	13.9	13.81	129	13.1	13.11
224.	---	---	---	---	---	---	---	---	---	128	n.d.	13.11
364.	502	13.75	13.70	670	13.65	13.83	670	n.d.	13.83	---	---	---

n.d. = not determined

CHAPTER 3

MATERIALS USED IN THE STUDY

3.1 - Standard Reactive Aggregate

Study of the alkali-silica expansion reaction requires a homogeneous source of reactive aggregate. The aggregate should be sufficiently reactive so that when it is incorporated in the mixture, expansion will commence within a reasonable length of time and ideally should be rapid enough to approach a limit within 90 to 180 days.

Any standard reactive aggregate used should be selected with due regard to its chemical composition as well as its potential reactivity. Some natural materials contain alkalies and their presence complicates interpretation of test results because attack of the aggregate by alkaline solutions, derived from the hydrating portland cement, may release alkalies bound in crystalline or glassy components of the aggregate. Such alkalies released from the aggregate may then act in concert with alkalies derived from the cement phase of the mixture and result in more extensive attack on the aggregate or other reactions not directly related to the cement properties.

Fused quartz would probably have been satisfactory as a standard reactive aggregate, however facilities for melting large batches of silica sand at 1600°C were not available.

Crushed and graded Pyrex* lump cullet No. 7740 is currently used as a standard reactive aggregate for evaluating pozzolanic materials in ASTM Designation C 441-75. The initial use of Pyrex glass in this role appears to have been in U.S. Bureau of Reclamation Specifications for "Calcined Reactive Siliceous Material for Use in Concrete", for the Davis Dam Project, Arizona-Nevada, in 1947 (301). The specification including the requirement for the initial use of this test method for qualification of project materials was cited by Moran and Gilland (302, p. 109, f.), and the original test method is quoted at length (302, pp. 123-125).

The original intent of specifying Pyrex lump cullet No. 7740 was to obtain a potentially reactive standard aggregate of controlled chemical composition. While the chemical properties of this product may lie within a reasonably narrow range, it should be noted that what is frequently encountered as "lump cullet" may range from large blocks through tear-drop pendants to fragments of culled laboratory glassware. The cooling rates of these solids are hardly comparable and their differing strain properties may have significant effects on the rate of alkali-silica attack on aggregates made by crushing and grading them. Perhaps it would be well to consider modifying the test method to allow the use of some commonly available size of Pyrex glass rod as the source of raw material for the standard aggregate.

While Pyrex glass may be a satisfactory reactive standard aggregate for pozzolan evaluation in the ASTM method cited above, it contains a significant amount of alkali metal compounds that, as pointed out

*Registered Trade Mark of Corning Glass Works, Corning, New York.

above, complicate interpretation of the test results for other applications. Further, the high concentration of boron is atypic of natural reactive aggregates. The boron ion, B^{3+} , is not stable in aqueous solutions and, if alkali attack on Pyrex glass results in decomposition of the boron compounds, it is probable that hydrolysis will produce boric acid, $B(OH)_3$. At the high pH found in these pore solutions, $B(OH)_3$ will react further according to the reaction $B(OH)_3 + H_2O \rightarrow B(OH)_4^- + H^+$ (303, p. 104). This would lower the alkalinity of the pore solutions. For these reasons it was decided not to adopt Pyrex glass as a standard reactive aggregate for this work.

3.1.1 - Beltane Opal

The standard reactive aggregate selected for this work was Beltane Opal. The name Beltane is derived from a station formerly located on a long defunct branch-line railroad which once passed along the eastern side of the Sonoma Valley, Sonoma County, California. The name was selected because it is not known to have been previously applied to any geologic formation in the area. Details of the geologic origin of the material are included in Section 3.1.2.

The deposit was located in an abandoned open-pit mine from which a number of products, primarily kaolin clay and decorative stone, were harvested during various periods of activity back to about 1900. The mine has been permanently closed and reclamation procedures initiated to make it compatible with the surrounding land use.

The bulk of the Beltane opal was obtained from a massive bed of opaline material approximately 20 ft. (6. m) thick, which strikes approximately N. 50°W., and dips approximately 55° W.S.W. The bed

was originally exposed along the entire length of its strike across the floor of the pit and the full height of the working face. To the west lie additional badly sheared and distorted beds of opaline materials which were probably on top of this material prior to formation of the valley. These beds grade into a light colored gritty material and finally into a deposit of white, moderately plastic kaolin clay. During the period when the mine was worked for clay, a number of fire opals were alleged to have been recovered from the deposit.

Mining the Beltane opal used in this study involved removal of a thin topsoil cover from the floor of the mine pit along the axis of the trace of the opal bed. Blocks of the opal were then loosened by repeated passes with a tractor mounted ripper, gradually working inward from one side of the bed. Once the bed had been opened up many large blocks would be removed by the use of pry bars. Blocks were hand-picked from the deposit and placed in 55 gal (0.21 m^3) steel drums. Blocks weighing more than about 100 lbs (45. kg) were broken with a sledge to obtain manageable sized pieces. The mine-run opal was trucked to a custom milling plant and crushed to about 95 percent passing one inch (2.5 cm), mixed to insure homogeneity, and sealed in open-head steel drums for shipment and storage.

3.1.1.1 - Chemical and Physical Properties of Beltane Opal

A complete chemical analysis was performed on samples taken from a 25 lb (10. kg) representative sample of crushed product. The analysis was performed by the Research Department of the California Portland Cement Company, Colton, California (304), and appears in the first column of Table 3.1. For comparative purposes, average chemical

Table 3.1
Typical Chemical Compositions of Some Alkali-Silica
Reactive Aggregates and Research Standards

Material	Beltane Opal	Rhyolite	Basalt Glass	Pyrex #7740
Reference	(304)	(305, p. 1012)*	(305, p. 1021)*	(306, p.102)
Oxide				
SiO ₂	87.96%	73.66%	50.83%	81. %
TiO ₂	-	0.22	2.03	-
Al ₂ O ₃	3.91 **	13.54	14.07	2.
Fe ₂ O ₃	0.29	1.25	2.88	-
FeO	-	0.75	9.05	-
MnO	-	0.03	0.18	-
MgO	0.28	0.32	6.34	-
CaO	0.56	1.13	10.42	-
Na ₂ O	0.14	2.99	2.23	4.
K ₂ O	0.26	5.35	0.82	-
P ₂ O ₅	-	0.07	0.23	-
SO ₃	Nil	-	-	-
B ₂ O ₃	-	-	-	13.
H ₂ O	-	0.78	0.91	-
LOI	6.54	-	-	-
Totals	99.94%	100.00%	100.00%	100.00%
No. of anal's		22	137	

* Also cited by Carmichael et al. (307, p. 9)

** Al₂O₃ + P₂O₅ + TiO₂

analyses of typical reactive components of natural aggregates, rhyolite and basalt glass, have been included in the table as well as an analysis of Pyrex lump cullet No. 7740.

Opal is classed as amorphous, i.e. without long-range atomic structure. X-ray diffraction patterns of amorphous siliceous materials are characterized by broad diffuse bands which are few in number, generally less than three, the most intense generally being centered in the range 4.1 to 4.4 Å.

Levin and Ott (308) and Taliferro (309), and other investigators published papers in the period 1931 - 1935 in which they noted that apparently amorphous hyalites, fire opal, wood opal, and Eocene and Miocene opaline cherts gave X-ray diffraction patterns characteristic of beta-cristobalite (high-temperature). This form of silica is normally considered stable between 1470 and 1732°C, and metastable from 1420 down to 272°C at atmospheric pressure (310, p. 38). In many ways pressure is equivalent to temperature as a controlling variable in phase equilibrium and beta-cristobalite could be preserved down to ambient atmospheric temperature locked within a matrix of glass or mineral material. While preservation of high-temperature cristobalite below its inversion temperature by this mechanism is possible it should be noted that Taliferro (309, p. 459) was not able to find any traces of crystals or crystallites of cristobalite in his samples. He noted that freshly prepared silica gels as well as Recent and Tertiary opals and cherts and wood opals, show faint beta-cristobalite (high-temperature) X-ray diffraction patterns. He concluded that the tendency toward formation of a crystalline structure in these materials is not the

result of slow aging, but is produced during the formation of the gel. Krejci and Ott (311) noted that freshly prepared silica gels, which at no time had been heated above 100°C, also yielded X-ray diffraction patterns of the cristobalite type. Florke (312), and others cited by Sosman (310, pp. 117, f.), believed the evidence insufficient to prove that the structure of opal is that of beta-cristobalite. They concluded that the characteristic pattern of most opals tended to be that of the low-temperature form, alpha-cristobalite, metastable at all temperatures below 272°C.

More recently investigators, e.g. Jones and Segnit (313), Jones, Sanders, and Segnit (314), have reported that opals tend to fall into one of two general classifications:

1. Specimens which give X-ray diffraction patterns of well crystallized alpha-cristobalite (low-temperature)
2. Specimens which give only a few diffuse bands.

Tufts examined about 100 specimens of opaline materials. Her findings (315, p. 64) are summarized as follows: "Opaline materials consist of hydrated silica in an amorphous or crystalline state before heat treatment (1000°C for 24 hours), but are always crystalline after heating". Her results for a number of materials are summarized in Table 3.2. She also found that, in general, the presence of small amounts of certain cations had a significant effect on the type of X-ray diffraction pattern observed before or after heating. Less than 0.7 percent Al_2O_3 tends to favor tridymite, while more than this amount tends to favor cristobalite. The presence of other cations, e.g. more

Table 3.2

Summary of the Observations of Tufts (315) on X-Ray DiffractionPatterns From Opaline Materials Before and AfterHeat Treatment at 1000° C

<u>Opal Type</u>	<u>Before Heat Treatment</u>	<u>After Heat Treatment</u>
Tripolite	amorphous with quartz	cristobalite & quartz
Geyserite	amorphous	cristobalite
Precious opal	cristobalite	cristobalite
Wood Opal	tridymite	tridymite
Hyalite	amorphous	cristobalite & quartz
Common opal	amorphous	cristobalite
	cristobalite	cristobalite
	tridymite	tridymite

than about 1. percent of Na_2O or K_2O , tends to favor alpha-cristobalite patterns.

Perhaps some of the confusion concerning whether patterns for opals resemble alpha- or beta-cristobalite stems from the limitations of pre-1935 X-ray diffraction technology, and relate to the work of Barth (316) in which he proposed a cubic unit cell for alpha-cristobalite with a_0 of approximately 7.01 Å. Alpha-cristobalite is currently considered to be tetragonal with $a_0 = 4.971$, $b_0 = 6.918$, but the structure is quite similar to that of beta-cristobalite. A unit cell edge as short as 7.09 Å (317, p. c174) has been reported and the three most prominent peaks for this pattern would approximate those presently accepted for alpha-cristobalite.

A typical X-ray diffraction pattern for Beltane opal has been reproduced in Figure 3.1. Numerous X-ray diffraction patterns were prepared from both powder mounts and sawed slab specimens of Beltane opal. This work was repeated in several laboratories and all of the patterns indicate that the material is largely amorphous but does exhibit recognizable X-ray diffraction peaks attributable to the following minerals:

alpha-cristobalite (SiO_2)	JCPDS*	11-0695
alpha-tridymite (SiO_2)	JCPDS	18-1170
alpha-quartz (SiO_2)	JCPDS	05-0490
alunite ($\text{K},\text{Na}\text{Al}_3(\text{SO}_4)_2(\text{OH})_6$ **)	JCPDS	14-0136

* Joint Committee on Powder Diffraction Standards

** See also Parker (318, pp. 127-136)

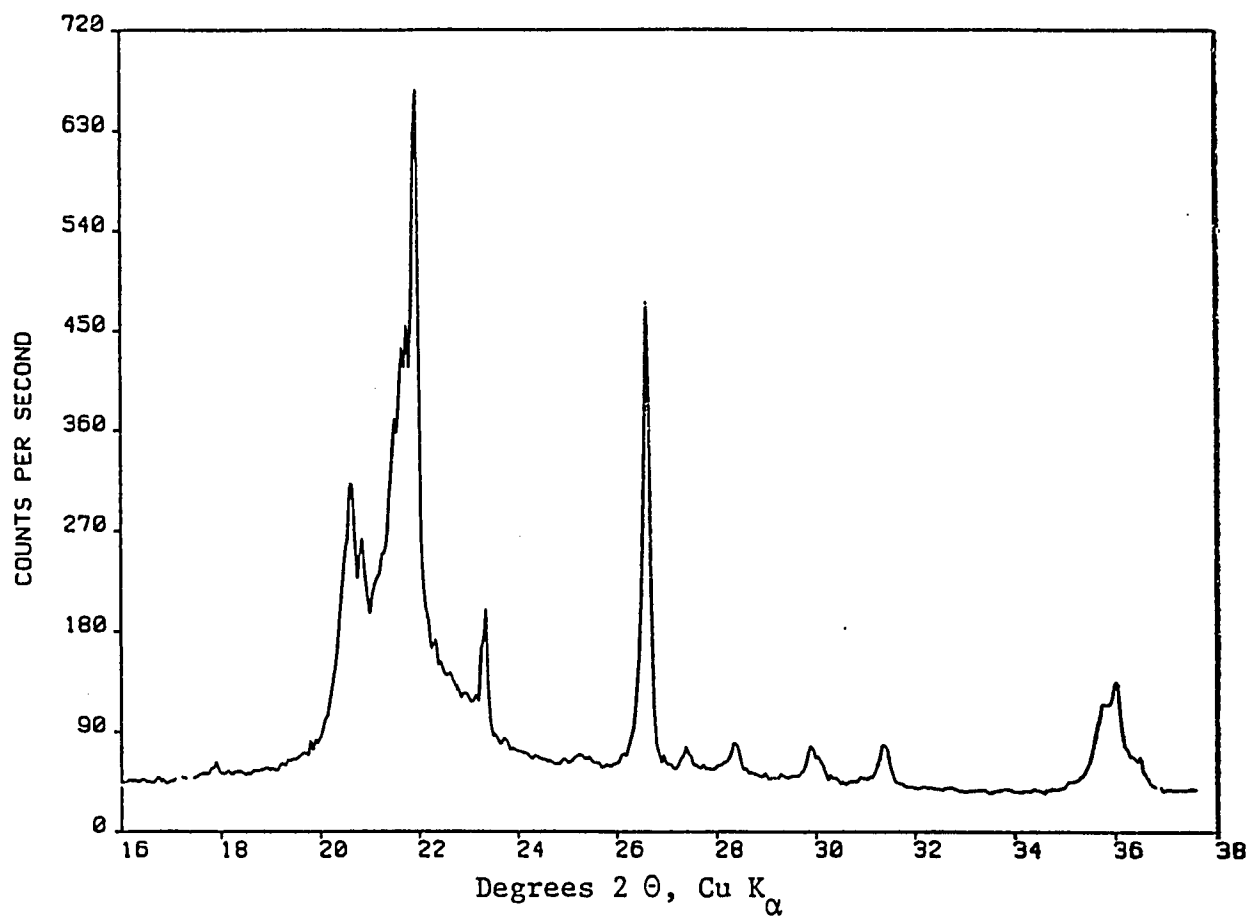


Figure 3.1 - X-Ray Diffraction Pattern for Beltane Opal

Note that the peak intensities in Figure 3.1 which correspond to these crystalline compounds are relatively small due to the presence of amorphous material in the opal.

The alunite peaks were found in only a few of the samples and are significant only in that they tend to confirm the probable mode of formation of the deposit (see Section 3.1.2).

Samples of the Beltane opal were forwarded to the Concrete Research Laboratory of the U.S. Army Corps of Engineers Waterways Experiment Station at Vicksburg, Mississippi for optical, chemical and X-ray examination and test. The following material has been abstracted from this report (319).

Three small pieces of opal were sawn from hand specimens identified as "D", "E", and "G". Powder immersion mounts were prepared by crushing representative portions of these fragments and examining them under a polarizing microscope at 320X. Cargille Refractive Index liquids were used in a room in the temperature range of 24-25°C.

It was anticipated that the following materials might be found:

<u>Mineral or Mineraloid</u>	<u>Range of Indices (320)</u>
opal	1.44 - 1.46
cristobalite	1.484 - 1.487
tridymite	1.469 - 1.473

Results of the examination of powder immersion mounts of the three samples of Beltane opal have been listed in Table 3.3. It is of interest to note that none of the samples contained a significant amount of particles outside the range 1.444 to 1.464. This suggests that opal is the primary constituent of Beltane opal. Several

Table 3.3

Reported Refractive Indices of Beltane Opal Grains
in Powder Immersion Mounts (319)

<u>Index of Refraction</u>	<u>D</u>	<u>E</u>	<u>G</u>
1.500	None	None	None
1.480	n.d.	None	n.d.
1.470	n.d.	None	n.d.
1.464	n.d.	None	n.d.
1.462	n.d.	Minor	n.d.
1.460	None	Abundant	n.d.
1.458	Minor	Abundant	Abundant
1.456	Minor	Minor	Minor
1.454	n.d.	Minor	Minor
1.450	Minor	Minor	n.d.
1.448	Abundant	Minor	Minor
1.446	Abundant	Minor	n.d.
1.444	Minor	n.d.	n.d.
1.440	None	n.d.	n.d.
	None	None	None

Note: Index values are cell limits and values between limits are relative abundance of grains with indices in that cell.

n.d. = Not determined

particles exhibited refractive indices nearly as high as the lower limit for tridymite (1.469) but none even approaching the lower limit of cristobalite (1.484). Apparently the observed X-ray diffraction peaks for cristobalite are due to the presence of opal and there is no alpha-cristobalite present as such.

Thin sections were also prepared by the Corps of Engineers Petrographic Section. These were found to contain tridymite twins, quartz, feldspar microlites, dirty glass, and some minor amounts of unidentifiable material. From this work it was concluded that what has been designated as Beltane opal is the end product of intense alteration and silicification of acid igneous rock to produce common opal.

3.1.2 Geologic Setting

The Beltane opal deposit is located within the Sonoma Volcanics, named for Mr. Sonoma, located approximately 70 miles (113 km) N.N.E. of San Francisco, California. The Sonoma Volcanics are made up of a complex series of lava flows and tuff beds that are, in some areas, interbedded with sand stone, gravel, and conglomerate. The lava flows, which constitute more than 60 percent of the entire sequence, are primarily andesitic with local accumulations of materials which approximate basalt in chemical and mineralogic composition (321, p. 63).

The St. Helena Member of the Sonoma Volcanics usually forms the upper part of the sequence and is found in parts of the Santa Rosa and Sonoma Quadrangles. Three types of rhyolite are recognized in this member:

- A bluish-gray, coarse textured, porphyritic rock with well defined banding and flow structure
- A creamy-white, dense vitreous rock, in which phenocrysts are invisible to the unaided eye, and with a well developed flow structure
- Obsidian and pitchstone

Weaver (321, p. 65) considered the Sonoma Volcanics to be of Middle Pliocene and the St. Helena Rhyolite Member to be of Late Pliocene Age. Previous work in this area by Burnett and Barneyback (322) indicated that the St. Helena Rhyolite Member of the Sonoma Volcanics contained several deposits of aggregates which were potentially alkali-silica reactive.

A quite similar geologic setting, in which kaolin, opal, and alunite were found, is reported by Shurtz (323). This deposit, located in West Texas, is considered to be of hydrothermal origin.

3.2 Portland Cements Used

The bulk of the work reported herein involved a single lot of high-alkali Type I portland cement, here designated as AT-1. For comparison purposes two other high-alkali cements, designated PI and RZ-354, were used in several of the mix series. The available chemical and physical properties of these cements have been listed in Table 3.4. Aside from their relatively high alkali contents, these are considered normal production cements.

Table 3.4

Lot Chemical Analyses of PortlandCements Used in This Study

<u>Component</u>	<u>AT-1</u>	<u>PI</u>	<u>RZ-354</u>
SiO ₂	21.14	20.1	19.9
Al ₂ O ₃	5.81	4.5	6.2
Fe ₂ O ₃	2.25	3.2	2.1
CaO	63.24	62.3	62.9
MgO	3.45	2.8	2.7
SO ₃	2.70	3.5	2.9
Na ₂ O	0.30	1.39	0.28
K ₂ O	0.91	0.38	1.57
LOI	0.73	---	1.0
Insoluble	<u>0.22</u>	<u>---</u>	<u>0.17</u>
Total	100.75	98.17	99.72
Water Sol. Na ₂ O	0.29	---	---
Water Sol. K ₂ O	0.50	---	---
Potential Bogue Compounds			
C ₃ S	46.8	56.1	52.
C ₂ S	25.3	15.3	12.7
C ₃ A	11.6	6.5	18.
C ₄ AF	6.8	9.7	6.
Specific Surf. cm ² /g (Blaine)	3680	---	3770

3.3 - Pozzolanic Materials Used

Five pozzolans and one pozzolan substitute, ground quartz sand, were used in various parts of this work. Two of these materials were commercially available pozzolans, "A" and "L", and two were experimental pozzolans, "R" and "S". The experimental pozzolans were not in commercial use at the time of this study, but were being considered for commercial use. The remaining materials; "Q", ground quartz sand; and BP-2, ground Beltane opal, were produced in the laboratory. Pozzolan substitute "Q" was intended as an inert filler material for use in control mixtures to maintain a reasonably consistent gradation of particles. As will be noted in the tabulations of the results in Chapter 5, this material was not entirely inert as may be inferred from its effect on alkali ion concentration in expressed pore solutions.

Chemical analyses and selected physical properties of these pozzolans have been listed in Table 3.5.

Table 3.5

Lot Chemical Analyses of Pozzolans

<u>Component</u>	<u>Used in This Study</u>					
	L	A	R	C*	S	BP-2**
SiO ₂	67.98	71.18	71.78		95.98	87.96
Al ₂ O ₃	17.4	18.94	18.78		1.26	3.91
Fe ₂ O ₃	5.49		0.51		0.12	0.29
MgO	0.8	2.04	0.92		0.03	0.28
CaO	2.28	3.34	1.18		0.26	0.56
SO ₃	0.88	0.95	---		0.12	Nil
Na ₂ O	0.16	0.18	3.05		0.03	0.14
K ₂ O	0.19	0.31	4.47		0.00	0.26
Free Water	1.37	0.17	---		0.27	---
LOI	1.58	0.8	---		1.13	6.54
Total	98.13	97.91	100.69		99.2	99.94
Specific Surf. cm ² /g (Blaine)	11840		8465	4080	26680	10860
cm ² /cm ³	28180		20850	10810	58700	22480
Specific Gravity	2.38	2.48	2.46	2.65	2.20	2.07
B.E.T. Specific Surface, m ² /g	17.08	11.53	1.62	<0.5	20.00	17.43

* Ground C 109 Ottawa Silica Sand, essentially quartz

** Analysis from Beltane opal sample

CHAPTER 4
APPARATUS AND EXPERIMENTAL METHODS

4.1 - Pore Fluid Expression Die

Pore fluids were expressed from fresh and hardened mortars in a steel die based on a similar device used by Longuet, et al. (401). Their die was designed for expressing pore fluids from hardened cement pastes at 3500 bar (350. MPa). It was considered desirable to be able to operate at a higher pressure for expressing pore fluids from hardened mortars and the die used in these studies was designed for a maximum operating pressure of 80,000 psi (551.6 MPa). SAE 4340 alloy steel, recommended for use in high stress service where fatigue resistance is important, was selected for fabrication of the die. It was specified that all components of the die made from this alloy be heat treated to attain a potential yield strength of 190 ksi (1.310 GPa) and a potential ultimate tensile strength of 210 ksi (1.448 GPa), (402, p. 2034).

4.1.1 - Design of the Die

The die was designed as a jacketed cylinder, a problem treated in detail by Seely and Smith (403, Ch. 10), and in other standard texts on advanced mechanics of materials. The design equations which appear in this section have been adapted from this reference.

The design of the die was begun with the selection of an internal radius for the die liner. The internal radius of the finished die liner depends on the internal radius of the specimen mold. A heavy plastic salve jar, which could be sealed vapor-tight and which had an internal radius of 25.5 mm, was selected as an appropriate and economical specimen mold. To assure remolding of the specimen under load and to accommodate variations in mold radii, the die liner radius (r_1 below) was increased by four percent over that of the mold. The following equations were used to select optimum proportions for die components:

$$S_w = S_y / F_s \quad \quad \text{Eq. 4.1.1}$$

$$C^2 = \frac{1 + (p/S_w) + 2(1 + (p/S_w))^{0.5}}{3 - (p/S_w)} \quad \quad \text{Eq. 4.1.2}$$

$$r_2 = r_1^2 \times C^2 \quad \quad \text{Eq. 4.1.3}$$

$$r_3 = C^2 \times r_1 \quad \quad \text{Eq. 4.1.4}$$

$$p_s = \frac{r_2^2 - r_1^2}{2 \times r_2^2} \times p \times \frac{r_3^2 + r_1^2}{r_3^2 - r_1^2} - S_w \quad \quad \text{Eq. 4.1.5}$$

$$d = \frac{p_s \times r_2}{E} \times \frac{r_3^2 + r_2^2}{r_3^2 - r_2^2} + \frac{r_2^2 + r_1^2}{r_2^2 - r_1^2} \quad \quad \text{Eq. 4.1.6}$$

where

r_1 = Inner radius of die liner

r_2 = Nominal outer radius of die liner and inner radius of die jacket

r_3 = Outer radius of die jacket

d = Difference in radius which must be added to nominal outer
radius of die liner for obtaining prestress

S_w = Working strength of material chosen

S_y = Ultimate tensile yield strength of material chosen

Fs = Safety factor

p = Internal pressure to be resisted

p_s = Potential surface contact pressure between die jacket and
liner due to prestress

C = Constant

E = Young's modulus of elasticity for material chosen.

4.1.1 - Design of the Die

The reader is cautioned that, as with all high pressure apparatus, a potential hazard exists should the die burst under load. Even with careful design and the use of adequate safety factors, defects in materials, faulty heat treatment of alloys, errors in machining, and other deficiencies or errors, may contribute to unexpected failure of the device. A careful reading of Bridgeman's remarks (404, Ch. IV) on the "special sorts of rupture peculiar to high pressures", is recommended. The following paragraph summarizes the more salient points of Bridgeman's remarks.

Simple elastic theory suggests rupture will initiate at the inner surface when maximum shearing stress capacity (Coulomb-Tresca failure criteria) is exceeded. This was not confirmed by Bridgeman's many tests. He found that cylinders designed by these criteria could stand significantly higher pressures than was anticipated, assuming no

material defects, and that ruptures of cylinders made from ordinary steel invariably initiate at the outside surface and travel inward. The rupture may progress along an approximately equiangular spiral for the entire wall thickness or it may, on approaching the inner surface, branch along two planes of shear at nearly 90° to each other so that a triangular prism is detached at the inside, which may be projected through the opening crack by the internal pressure with great violence (404, pp. 81-82).

An isometric half-section of the pore fluid expression die used in these experiments is shown in Figure 4.1. The support cylinder was fabricated from SAE 4340 alloy steel, heat treated to attain a potential yield strength of 190. ksi (1.310 GPa). The Teflon* seal was turned from bar stock and generally lasted 40 to 50 expression cycles before requiring replacement. The top of the platen was scribed with a drain ring that is intersected by the fluid drain, drilled upward from the bottom surface of the platen. This hole was tapered with a standard taper pin reamer of sufficient size to allow insertion of a short length of heavy plastic tubing approximately one-third of the way up the fluid drain, thus forming an air-tight seal.

After heat treatment and final assembly of the die body, the bore of the liner was honed to size and the top and bottom surfaces of the die body and the top surface of the platen were surface ground plane ± 0.0005 in. (0.0127 mm) on any six inch (15.25 cm) diameter. These surfaces, and the piston shaft and face, were then hard chrome plated to improve chemical and abrasion resistance.

*DuPont Trademark.

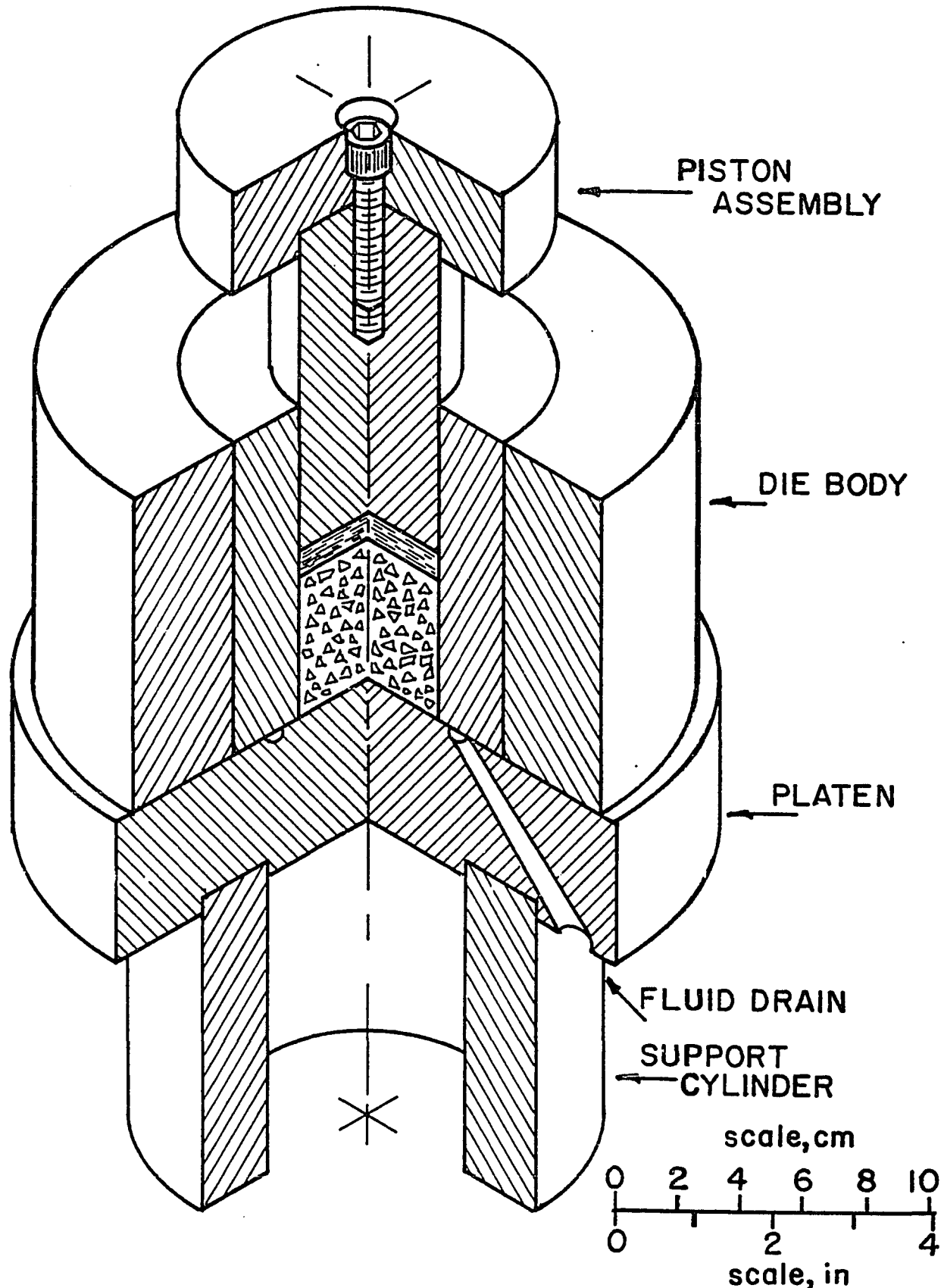


Figure 4.1 - Isometric Half Section of Pore Fluid Expression Die

4.1.2 - Operation and Maintenance of the Die

Prior to the use of the unit a thin coating of film-bonding grade fluorocarbon was sprayed in the bore of the die body, on the mating surfaces of the die body and platen, and on the shaft of the piston. The die body was mounted on the center of the platen, the specimen was dropped into the bore, and the Teflon seal and piston were inserted. Specimens were loaded with their as-cast bottoms in contact with the platen. The Teflon seal must be tipped into a vertical orientation, forced into the bore, and then rotated into the approximate plane of the top of the specimen. On loading, the piston forced the Teflon seal to complete its rotation into position.

Immediately prior to applying the pressurizing load to the die, the plastic hypodermic syringe (to receive the expressed pore fluid) was attached to the die by a short (5 cm) length of heavy plastic tubing. The required capacity of the syringe is a function of the volume and age of the specimen. In this investigation the volume of specimens for pore fluid expression ranged from 80 to 100 cm^3 . During the first 24 hours after mixing, 30 cm^3 syringes were used. Beyond one day to three days, 20 cm^3 syringes were used. At all later ages, 10 cm^3 syringes were used. Although the expressed pore fluid may fill no more than 20 percent of the 10 cm^3 syringe, gases from collapsed voids within the specimen, and trapped in the die before complete crushing of the specimen, are expelled with the pore fluids, thus making the additional capacity desirable.

Specimens 24 hours or more old were loaded at approximately 400 psi/s (2.76 MPa/s) to a total load equivalent of 80,000 psi (551.7 MPa).

The loading rate is not critical, however it was found that a relatively slow loading rate resulted in greater yield of pore fluid, and this rate seemed to be optimum. As expressed pore fluid and gas collected in the syringe, its plunger was withdrawn a short distance to put a slight negative pressure on the pore fluid drain system. This cycle can be repeated several times to draw most of the expressed fluid down from the drain ring. The syringe was then removed from the delivery tube, the gas was expelled from it, and the syringe was reconnected without loss of fluid. Loading of the die was continued to the maximum associated with the desired specimen stress and then was held constant for three to five minutes. It was deemed desirable to obtain a minimum pore fluid sample of 3 cm^3 . If this amount could not be collected on the first loading cycle, a static negative pressure was again applied to the pore fluid drain system, and the load on the specimen was reduced to approximately 50,000 psi (345 MPa).

Elastic rebound of the mortar specimen caused a slight separation of the die body from the platen, and nearly all of the remaining expressed pore fluid was withdrawn from the drain system in response to the negative pressure applied by the syringe. Gas and air collected in the syringe were expelled, and the specimen was reloaded as before. It was seldom possible to significantly increase pore fluid recovery by applying more than three or four reloading cycles.

After final unloading of the specimen, the syringe was removed from the delivery tube, gas was expelled, and the cap was replaced over the Luer fitting on the syringe. After application of an identifying code on the syringe, it was placed in a protective storage box.

Cleaning of the pore fluid expression die was begun with removal of the die body and piston assembly with the contained remains of the mortar specimen from the platen. The plastic fluid drain tube was removed from the platen, flushed with absolute ethanol, and placed in a container to drain and dry. The platen surface and drain system were flushed with absolute ethanol and wiped clean with soft facial tissue, this process being repeated twice before the platen was set aside to dry.

A plastic receiving cup, fabricated from a 250 ml plastic beaker, was inserted in the support cylinder, and the die body and piston, with its cap removed, were mounted on the support cylinder. A mild steel plunger, 1.25 in. dia. x 4 in. long (3.18 cm dia. x 10.2 cm long), was placed on top of the piston. To protect the loading surface of the upper head of the testing machine it was desirable to interpose a piece of cold finished plate, 1 in. thick and 3 in. square (25 mm thick and 75 mm square) between the plunger and the loading surface. This assembly was loaded in the testing machine to eject the remains of the mortar specimen. The force that must be applied depends on the force required to express the pore fluids and its duration of application. While a force in excess of 20,000 lbf (89.0 KN) has been required for some specimens, the range of 5,000 to 7,000 lbf (22.2 to 31.1 KN) is more typical. The remains of the mortar specimen ejected from the die was generally a coherent solid, and was recovered from the plastic receiving cup and sealed in a code numbered plastic bag for return to the laboratory for determination of bound water or other tests. After the remains of the mortar sample is ejected it may be possible to force the piston from the die by hand, but if prolonged or cyclic loading

has been required to express pore fluids from the specimen, a film of Teflon from the seal will have been extruded into the annulus between the piston and the die body, and the piston must be forced out by the testing machine.

With the die now completely disassembled, the die body and piston were flushed with absolute ethanol and dried with facial tissues. The bore of the die body was inspected carefully for residual cement paste smeared on the inside. Any residual materials must be removed by careful scraping of the bore of the die body with a straight-edged stainless steel spatula.

After cleaning and inspection of the die, a thin film of film-bonding grade fluorocarbon was sprayed on all surfaces that come in contact with pore fluids. If the die was to be used again within 30 minutes, the coating on the platen and mating surface of the die body were sufficiently thick to form an air-tight seal.

Because of the unavailability of a high capacity testing machine close to the specimen preparation laboratory, it was necessary to use what amounted to a calibrated hydraulic jack for expression of pore fluid from specimens aged 30 minutes to one day. This device was limited to application of a force that resulted in an expression pressure of 57,500 psi (396.4 MPa). Fresh mortars were removed from the mold with a spatula and remolded in the die by spading with the spatula. Hardened specimens were demolded by removing the cap and plastic sheet seal from the plastic jars, striking the inverted jar on a solid surface to cause the specimen to move away from the bottom of the mold. When the specimen was clear of the bottom of the mold, the

mold was shattered by striking it on the bottom adjacent to the mold wall with a small hammer.

4.2 - Atomic Absorption Spectrophotometer

The volume of pore fluid that can be expressed from an 80 to 100 cm³ mortar specimen ranged from 15 to 20 ml at 30 minutes after mixing, 5 to 7 ml at 7 days after mixing, and 2 to 3 ml, or less, one year after mixing of the mortar. Traditional wet methods of chemical analysis are obviously inadequate because of this small sample size. A Perkin-Elmer Model 503 Atomic Absorption Spectrophotometer was used. The instrument is capable of operation in both atomic absorption and flame emission modes. The flame emission mode was used for the alkali metals and for barium (for indirect determination of SO₄⁼). The remaining cations of interest, i.e. Si⁴⁺, Al³⁺, Mg⁺⁺ and Ca⁺⁺, were determined in the absorption mode. Hydroxide ion concentration was determined by titration with standard hydrochloric acid solution.

4.2.1 - Operation of the Spectrophotometer

Compressed air, medical grade nitrous oxide (N₂O), and industrial grade acetylene (C₂H₂) were used as oxidants and fuel. Instrument operating procedures outlined in the Perkin-Elmer instruction manual were generally observed.

4.3 - Preparation of Standards and Reagents

Specific details of the preparation of standard solutions appear in the reference manual accompanying the spectrophotometer. Where deviations from the recommended practice have been deemed necessary or where special solutions have been required they will be described.

The standard solutions were single element standards (See Figure 4.2 for exceptions) prepared from reagent grade chemicals and deionized water.

Standard solutions for Si^{4+} were prepared by diluting a proprietary concentrated solution of SiCl_4 in aqueous NaOH solution with deionized water to make 1.0 L of stock standard solution. A check against a multi-element standard solution, prepared from an NBS standard cement sample did not produce significantly different results.

4.4 - Determination of Cations

Direct determination of elements by flame emission and atomic absorption is limited to those for which strong resonance lines lie within the visible and ultraviolet portions of the spectrum, i.e. 1000 to 190 nm (405, p. 211). This condition restricts the methods generally to metals and semimetals. Indirect methods can be employed for some anions, e.g. precipitation of barium from solutions of known concentration of BaCl_2 by $\text{SO}_4^=$.

4.4.1 - Effect of Glassware on Determination for Silicon

When glass volumetric apparatus is used in the determination for Si^{4+} in alkaline solutions, the apparent concentration of Si^{4+} found usually increases significantly with time of storage. The apparent concentration of Si^{4+} found in typical solutions used in this study ranged from 1 to 5 mMol/L for samples tested within six hours of preparation to as much as 50 mMol/L for the same samples retested 48 hours later. The use of plastic volumetric ware or storage containers was considered, but plastic containers tend to adsorb Si^{4+} from solution and increase the possibility of contamination of contained solutions.

4.5 - Scheme of Analysis and Analytical Conditions

As previously noted the methods used generally followed those recommended in the Perkin-Elmer manual, "Analytical Methods for Atomic Absorption Spectrophotometry" (406). Some modifications were introduced, based on experience in this and other laboratories.

The nebulizing system (sprayer) was adjusted for optimum delivery by aspirating a 5 $\mu\text{g}/\text{ml}$ solution of Cu^{++} and making appropriate adjustments to produce maximum instrument response in atomic absorption mode. Copper was chosen because of its relative insensitivity to flame chemistry.

Fuel-oxidant mixtures, and burner elevations were selected on the basis of maximum response of the system and it was found that minor changes were necessary during the course of the investigation. A 50 mm single slot nitrous oxide burner was used for all determinations involving nitrous oxide. The same burner, turned 30° away from the axis of the optical system, was used for determination of all of the alkali metals. This was done to reduce the sensitivity of the instrument, enabling determinations to be made on relatively concentrated solutions of the alkali metals, thus reducing the potential dilution error. A 100 mm single slot burner was used for the determination of Fe^{3+} .

In Figure 4.2, the general scheme of analysis is outlined in the form of a flow chart. In some cases, generally resulting from low pore solution yield, significant modifications of this scheme were required.

In Table 4.1, the analytical conditions used in the analyses have been listed. Minor modifications were found to be desirable as lamps and other portions of the equipment aged.

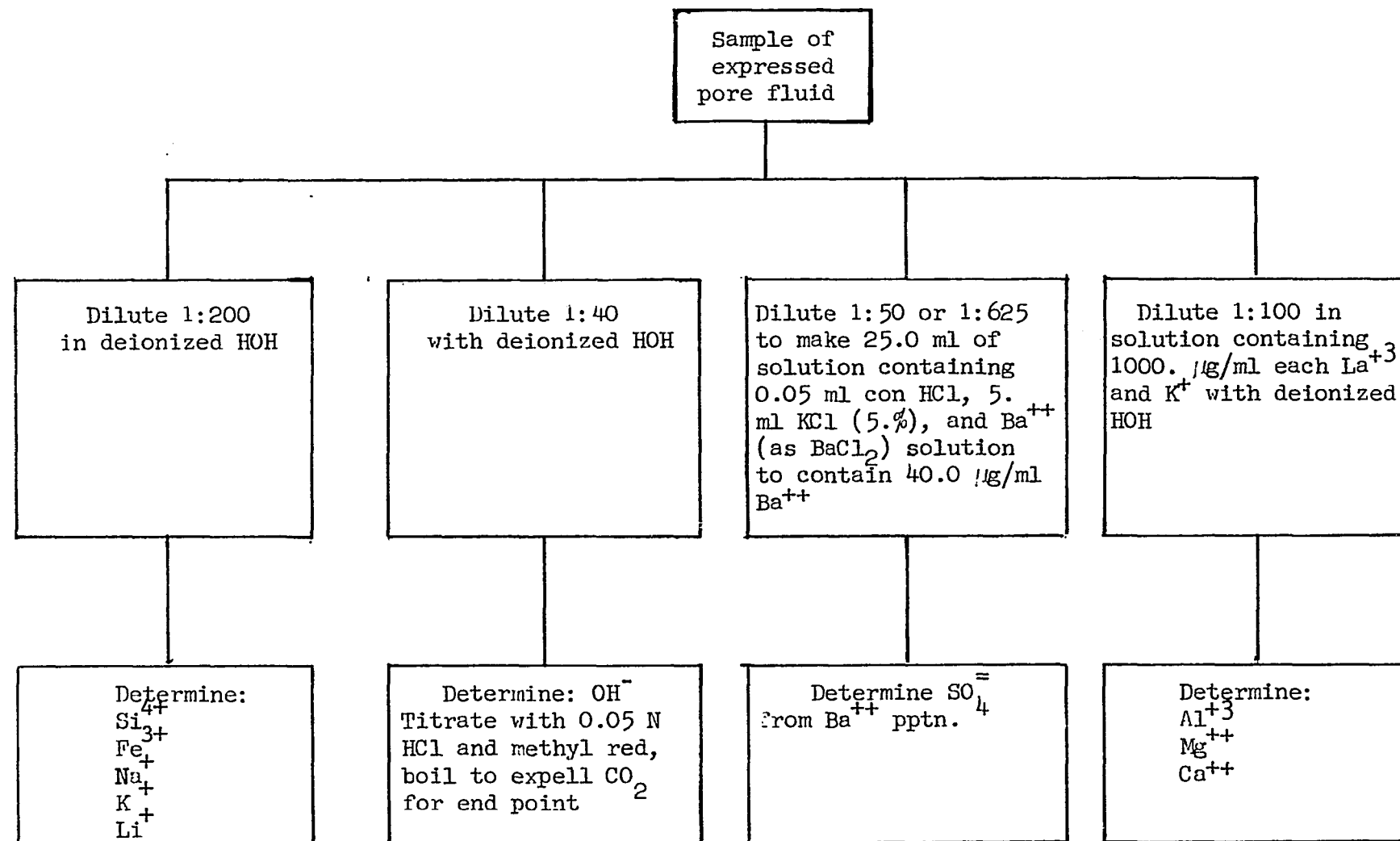


Figure 4.2 Flow Chart for Analysis of Expressed Pore Fluid

Table 4.1
Analytican Conditions Used for Selected Elements

	Si	Al	Fe	Mg	Ca	Na	K	Li	Ba
Monochrometer, nm	251.6	309.3	248.4	285.2	422.7	589.0	766.5	670.8	553.6
Slit, nm	0.2	0.7	0.2	0.7	1.4	0.4	1.4	0.2	0.4
Hollow Cathode Lamp	Si	Al	Fe	Mg	Ca	--	--	--	--
Lamp Current, ma	40	28	30	12	20	--	--	--	--
Emission Mode	No	No	No	No	No	Yes	Yes	Yes	Yes
Primary Oxidant Flow, L/min	N ₂ O 13.2	N ₂ O 13.3	Air 21.6	N ₂ O 15.6	N ₂ O 14.2	Air 21.7	Air 21.7	Air 21.7	N ₂ O 14.6
Fuel Flow, l/min	C ₂ H ₂ 6.4	C ₂ H ₂ 6.8	C ₂ H ₂ 2.7	C ₂ H ₂ 6.8	C ₂ H ₂ 6.8	C ₂ H ₂ 2.7	C ₂ H ₂ 2.7	C ₂ H ₂ 2.7	C ₂ H ₂ 6.8
Burner Length, mm	50	50	100	50	50	50	50	50	50
Elevation, mm*	9	9	7	9	8	14	14	14	7
Calibration Standards	0	0	0	0	0	0	0	0	0
/g/ml	5	5	5	5	5	10	20	5	10
	50				10	25	50	50	20
						50	100	100	30
						100	200	40	56
Notes (see following page)	1	1, 2	3	2, 4	2, 5	3, 6, 7	3, 6, 7	3, 6	5

* Distance below optic axis, mm

Notes for Table 4.1

1. Optic axis should pass through the "red feather" of rich N₂O - C₂H₂ flame.
2. Add sufficient concentrated stock solutions of lanthanum and potassium to both standards and unknowns to result in a concentration of 1000 $\mu\text{g}/\text{L}$ of each.
3. Use lean blue flams.
4. Use slightly fuel-rich N₂O - C₂H₂ flame.
5. Use bright red fuel-rich N₂O - C₂H₂ flame.
6. Use 50 mm burner turned 30° from optic axis.
7. Use duplex stock solution 500 $\mu\text{g}/\text{L}$ sodium and 1000 $\mu\text{g}/\text{L}$ potassium.
8. Insert filter in optical system.

4.6 - Determination of Anions

Some anions can be determined indirectly by flame emission or atomic absorption spectrophotometry, but indirect determinations are complicated and should be avoided. The only indirect determination used extensively in this study was that of $\text{SO}_4^{=}$. The major anion determined was OH^- , and this was done by titration with 0.05 normal HCl standard acid (407, pp. 777 ff.).

4.6.1 - Determination of Sulfate ($\text{SO}_4^{=}$)

The method for determination of sulfate is based on the reaction of the sulfate ion in the unknown with a known concentration of barium and precipitation of barium sulfate. The amount of $\text{SO}_4^{=}$ in the test solution must be within the range of zero to 40 $\mu\text{g}/\text{ml}$. An excess of BaCl_2 is necessary to assure that equilibrium of the precipitation is favorably shifted and the precipitation is complete. Thus, although the calibration curve is carried to 56 $\mu\text{g}/\text{ml}$, the portion beyond 40 $\mu\text{g}/\text{ml}$ is used only to provide a calibration end point. If it is not possible to estimate the $\text{SO}_4^{=}$ concentration, test solutions should be prepared at two or more dilution factors for analysis. At the same time the unknown solutions are prepared, calibration standards are prepared. Unknown and calibration standard solutions were stored at 40°C for 18 to 24 hours before analysis to insure complete reaction and precipitation.

Stock Standard Solutions:

Barium chloride solution containing 400 $\mu\text{g}/\text{ml}$ Ba^{++}

Sodium Sulfate solution containing 1000 $\mu\text{g}/\text{ml}$ $\text{SO}_4^=$

Potassium chloride ionization suppressant solution,

5 percent KCl

Preparation of Unknowns:

Unknowns were prepared in 25 ml class A borosilicate volumetric flasks. Ten ml of deionized water was dispensed by syringe into the flasks, followed by the analyte. At early ages, i.e. 30 minutes to about 12 hours after mixing the mortar from which the pore fluid was expressed, 40 μL of analyte was found to be adequate (dilution factor 1:625). At most later ages, 500 μL aliquots (dilution factor 1:50) were appropriate. The analyte was followed by 0.05 ml (1 drop) of conc HCl and 5.00 ml of 400 $\mu\text{g}/\text{ml}$ Ba^{++} solution (for a final concentration of 80 $\mu\text{g}/\text{ml}$ Ba^{++}). The flasks were then filled to the mark.

Preparation of Calibration Standards:

Calibration standards were prepared in 50 ml class A borosilicate volumetric flasks in accordance with the schedule outlined in Table 4.2. All calibration standards contained 2 drops of concentrated HCl and 2.0 ml of 5 percent KCl ionization suppressant solution.

The analytical conditions for determination of residual Ba^{++} are listed in Table 4.1.

Table 4.2
Calibration Standards for Sulfate Determination

$\text{SO}_4^{=}$ Concentration $\mu\text{g/ml}$	ml Stock Standard Solutions				Approximate Instrument Response
	Ba^{++}		$\text{SO}_4^{=}$		
0	10	(80)*	0	(0)*	56
10	10	(80)	0.5	(10)	51
20	10	(80)	1.0	(20)	42
30	10	(80)	1.5	(30)	31
40	10	(80)	2.0	(40)	20
56	10	(80)	2.8	(56)	1

* Equivalent concentration when diluted to 50 ml.

4.7 - Determination of pH

At high concentrations the activity coefficient of OH^- departs significantly from unity and it was desired to attempt to evaluate the activity coefficient of OH^- in the expressed pore solutions by potentiometric methods. Two miniature combination glass electrodes, designed for use in highly alkaline solutions, were tried. Neither yielded satisfactory results. Three major problems were encountered:

1. No adequate standards above pH 12.63 (saturated $\text{Ca}(\text{OH})_2$ solution at 20°C (408, p. 5-71) exist and the apparent pH values of most of the pore solutions in this study exceeded 13.6.
2. The volume of expressed pore solution was barely sufficient for the other determinations and little could be spared for conditioning the pH electrode and the determination of pH. One of the electrodes tried was claimed by the manufacturer to yield accurate results from a sample as small as $5\mu\text{L}$ and had a potassium leak rate sufficiently low to permit the determination to be made directly in the expressed pore solution sample without measurable contamination. The other electrode required a sample approximately 100 times as great and the potassium leak rate was sufficient to contaminate the bulk sample, making it unsuitable for other determinations.
3. The concentration of OH^- in the expressed pore solutions was sufficiently high that the glass membrane of the electrode was attacked and both electrodes failed after about five to ten determinations.

4.8 - Acquisition and Reduction of Data

From the Spectrophotometer

In atomic absorption and flame emission analysis it is desirable to work at concentrations within the linear range of the instrument if possible. With the limited amounts of expressed pure solution available and the extreme range of concentrations present in the solutions, e.g. alkali metals in hundreds of millimoles per liter and other elements of interest present in tens to tenths millimoles per liter, this was not practical. While inverse interpolation from calibration curves can introduce some potential for error, this is offset by the use of smaller dilution factors when more concentrated solutions are used.

The concentrations of some elements were sufficiently low as to lie within the linear range of the instrument, e.g. silicon, aluminum, iron, and magnesium. In these cases calibration involved establishing only zero and maximum concentration points and employing simple inverse linear interpolation to convert the instrument responses from the unknowns to equivalent concentrations of the element of interest. For the remaining elements it was necessary to establish the end points of the curve and then present a series of standards for analysis that contained intermediate concentrations suitable to define the remainder of the curve. Each point on the calibration curve was represented by the mean value of five representative responses from the instrument using a three second integrating period for each of the responses. Points for the unknowns were obtained from a similar series of five responses. Observations were verbally recorded on magnetic tape and transcribed to punch cards for data reduction by a digital computer.

Several interpolating functions were tried, but the cubic spline method (409), (410), (411) was deemed the most appropriate. The mathematical development of cubic spline functions began about 1946 (410, p.70), but the mechanical analog is a very old device used by draftsmen to draw smooth curves through a series of points.

4.9 - Pozzolan Grinding

Pozzolans BP-2 and R were ground in the laboratory in a Norton No. 1 porcelain jar mill with an outside diameter of approximately 9 in. (23 cm). Grinding time was controlled by a time clock and the mill was driven at approximately 62 rpm.

The raw feed consisted of 300 cm³ loose volume of the material to be ground, all of which passed 4.75 mm. The ball charge consisted of approximately 6 kg of nominal 22 mm diameter forged manganese-steel grinding balls. The mill product was passed through a 850 µm sieve prior to storage to remove surviving chips of the raw materials. In no case was more than a trace of material retained on the 850 µm sieve.

The required grinding time was determined from the results of two grinding time trials. Fineness, as determined by the air permeability method, ASTM Designation C 204-79, can be related to grinding time by the relationship $S_S = a + b \log t$, where S_S = specific surface, cm²/g; a and b are empirical constants; and t = time, minutes. The required grinding times for the materials used in this study ranged from 3.5 to 4.5 hours. Fineness was determined for each batch as it was ground and a lot fineness was determined after all batches had been ground and mixed.

4.10 - Determination of Cement and Pozzolan

Specific Surface

In common with industry practice, the specific surface areas of cements and pozzolans used in this study were determined by the Blaine air permeability method. The apparatus, and its use, is discussed in ASTM Designation C 204-79. This device provides a relative value of specific surface and is particularly useful in grinding mill applications.

Absolute specific surface areas for some selected materials used in this study were also determined by Dr. Arnon Bentur (510) using a Micromeritics Instrument Corporation Model 2100 Orr Surface-Area Pore Volume Analyzer. This device uses the principle of nitrogen adsorption, developed by Brunauer, Emmett, and Teller (412), to determine surface area. Both the exterior surface of the particle and all of its pores accessible to nitrogen are included in the surface area measurement. The surface areas for pozzolans reported by Dr. Bentur are listed in Table 3.5, and the surface areas for beltane opal sand are reported in Section 3.1.

4.11 - Determination of Chemically Bound Water

For the purpose of this study, water contained in hydraulic cement pastes and mortars has been divided into two classifications; evaporable water (W_e), which can be driven off by oven drying at 105°C at atmospheric pressure, and chemically bound or nonevaporable water (W_n), which can be driven off from a specimen previously dried at 105°C by ignition at 1050°C . In general, the weight ratios of each of these classes of water to the weight of unhydrated cement in the sample is

of interest, and these ratios are represented by the symbols W_e/c and W_n/c respectively. For specimens from which part of the water has been removed by partial drying or expression just prior to the determinations, the amount of evaporable water will be reduced by some amount and the ratio is then expressed by W_e'/c .

4.11.1 - Specimen Preparation, Drying and Ignition

After that portion of the pore solution that could be expressed from the specimen loaded to 80,000 psi (551.6 MPa) had been expressed, the specimen was ejected from the die and immediately stored in a sealed plastic bag.

The cylindrical specimen representing each mix was then split into three layers with a cold chisel and hammer. The outer 0.5 to 1 cm of the central disc was cut away, and the remainder of the central disc was broken into lumps 0.5 to 1 cm in diameter. The test sample, consisting of 10 to 15 g of these fragments, was loaded into a previously ignited and tared porcelain crucible. After determination of the gross weight of the crucible and sample to 0.0001 g, approximately 7 ml of acetone was poured over the sample to prevent further hydration and reduce the potential for carbonation. The samples were dried for 24 hours at $105 \pm 5^\circ C$. The samples were then cooled in a desiccator, weighed and transferred to an electric muffle furnace for two hours at $1050 \pm 50^\circ C$. After ignition the samples were again cooled in a desiccator, and the ignited weights were determined. Tests of the ignition procedure indicated that the weight loss after 30 minutes averaged about 99.6 percent of that at three hours, and that the average loss in porcelain was about 100.4 percent of that in platinum crucibles, for a three hour ignition period.

4.11.2 - Development of Equations for Data Reduction

Determination of the nonevaporable water (W_n/c) was complicated by two factors:

1. With only a few exceptions, some portion of the pore solution had been expressed from the available specimen. Thus, the weight of the sample, including both evaporable water and nonevaporable water could not be determined directly.
2. The specimens were of mortar mixtures which contained one or more aggregates and/or pozzolans.

These complications made it necessary to base all computations on ignited ($1050^{\circ} C$) weights and to make adjustments for drying and ignition loss contributions of the original mix components. This also required determination of the evaporable water (W_e/c) by difference, i.e. the difference between the original water-cement ratio (W/c) and W_n/c , the nonevaporable water.

Adjustment factors for the mix components were determined by the same methods used to determine the oven-dry and ignited weights of the mortar samples, but without the addition of acetone. In Table 4.3, batch weights for a typical mix (Mix 81) have been listed with factors for calculating oven-dry and ignited weights. In Table 4.4, the calculation of oven-dry and ignited weights of a sample cut from a specimen of Mix 81 is illustrated.

Development of the equations used to calculate the original weight of unhydrated cement (c) in a representative sample of mortar, and the weights of evaporable (W_e) and chemically bound or nonevaporable water (W_n), at some time after mixing but before loss or expression of any

Table 4.3

Batch Weights and Factors for Calculation of
Oven-Dry and Ignited Batch Weights of Mix 81

Material	Batch Wts., g	Parts by Weight	Wod/Wo	Wig/Wo
Cement, AT-1	1590.2	1.00	0.99809	0.99483
Water	795.1	0.50	--	--
Pozzolan, L	477.0	0.30	0.99807	0.98924
Opal Sand	0.0	0.0	0.99442	0.95298
Sand, C-109	<u>2649.1</u>	<u>1.666</u>	0.99993	0.99868
Totals	5511.4	2.966	--	--

Where: Wo = Initial weight (material in as-batched or as-received condition)

Wod = Weight, oven-dry ($105 \pm 5^\circ C$)

Wig = Weight, ignited ($1050 \pm 50^\circ C$)

Table 4.4.

Calculation of Wo', Wod, and Wig for a Typical Mixture
From Which Some of the Pore Solution Has Been Expressed
(Mix 81, 124 days at 40° C)

Gross weight (sample as received)	25.8648
Tare (ignited crucible)	-11.1557
Net weight, Wo'	14.7091
Gross oven dry weight	24.7060
Tare	-15.1557
Net weight, Wod	13.5503
Gross ignited weight	23.9833
Tare	-11.1557
Net weight, Wig	12.8276

pore solution, is illustrated below.

$$W_o = c + P + B + A + W_e + W_n \dots \dots \dots \quad \text{Eq. 4.11.1}$$

Where: W_o = Weight of the representative sample

c = Original weight of unhydrated cement

P = Weight of pozzolan

B = Weight of Beltane Upai aggregate

A = Weight of quartz aggregate

$W_e + W_n$ = Original weight of mixing water

In a representative sample taken from an expressed or partially dried mortar specimen, the quantities W_o and W_e are reduced by the weight of the pore solution expressed or weight of the water evaporated and are then represented by W_o' and W_e' . Quantitative recovery of the expressed pore solution is not possible and W_e for expressed specimens must be found by difference:

$$W_e = W - W_n$$

or:

$$W_e/c = W/c - W_n/c \dots \dots \dots \dots \dots \quad \text{Eq. 4.11.2}$$

Where: W = Original weight of mixing water

W/c = Original water-cement-ratio

W_e/c = Ratio of evaporable water to cement

W_n/c = Ratio of nonevaporable water to cement

For an expressed specimen, Eq. 4.11.1 becomes:

$$W_o' = c + P + B + A + W_e' + W_n \dots \dots \dots \quad \text{Eq. 4.11.3}$$

Here only W_o' , the weight of the sample taken from the expressed specimen, is known; the remaining six terms are unknowns. It is possible to reduce these unknowns, and any others added by the addition of other aggregates and/or pozzolans, to three by replacing the actual weights of the solid materials by their weight ratios to the weight of cement. For the example that concludes this development, numerical values of these ratios are listed under "Parts by Weight" in Table 4.3.

Making the above substitution:

$$W_o' = cRc + cRp + cRb + cRa + W_e' + W_n$$

$$\text{Where: } R_c = c/c = 1.00$$

$$R_p = P/c = 0.30$$

$$R_b = B/c = 0.00$$

$$R_a = A/c = 1.666$$

$W_e' + W_n$ = Residual mixing water

Factoring and solving for W_e' :

$$W_e' = W_o' - c(1 + R_p + R_b + R_a) - W_n \quad . \quad . \quad . \quad . \quad . \quad \text{Eq. 4.11.4}$$

If it is assumed that W_e' is zero in an oven-dried sample of weight W_{od} :

$$W_{od} = cD_c + cR_p D_p + cR_b D_b + cR_a D_a + W_n$$

Where: D_c = Oven-dry weight of cement/c

D_p = Oven-dry weight of pozzolan/P

D_b = Oven-dry weight of Beltane Opal/B

D_a = Oven-dry weight of aggregate/A

Factoring and solving for W_n :

$$W_n = W_{od} - c(Dc + RpDp + RbDb + RaDa) \quad . \quad . \quad . \quad . \quad . \quad \text{Eq. 4.11.5}$$

If it is assumed that both W_e' and W_n are zero in an ignited sample of weight W_{ig} :

$$W_{ig} = cI_c + cRpIp + cRbIb + cRaIa$$

Where: I_c = Ignited weight of cement/c

I_p = Ignited weight of pozzolan/c

I_b = Ignited weight of Beltane Opal/B

I_a = Ignited weight of aggregate A/A

Factoring and solving for c:

$$c = W_{ig}/(I_c + RpIp + RbIb + RaIa) \quad . \quad . \quad . \quad . \quad . \quad . \quad \text{Eq. 4.11.6}$$

Introducing appropriate constants from Table 4.3 and sample weights from Table 4.4, the equations are solved in inverse order:

$$c = 12.8276/(0.99483 + 0.98924 \times 0.30 + 0.95298 \times 0.00 + 0.99868 \times 1.666) \quad . \quad \text{Eq. 4.11.6}$$

$$c = 4.3404 \text{ g}$$

$$W_n = 13.5503 - 4.3404(0.99809 + 0.99807 \times 0.30 + 0.99442 \times 0.00 + 0.99993 \times 1.666) \quad . \quad . \quad . \quad . \quad . \quad \text{Eq. 4.11.5}$$

$$W_n = 0.6880 \text{ g}$$

$$W_e' = 14.7091 - 4.3404(1.00 + 0.30 + 0.00 + 1.666) - 0.6880 \quad . \quad \text{Eq. 4.11.4}$$

$$W_e' = 1.1475 \text{ g}$$

The values of W_n/c and W_e'/c are then found to be:

$$W_n/c = 0.1585 \text{ g nonevaporable water/g cement}$$

$$W_e'/c = 0.2644 \text{ g residual evaporable water/g cement}$$

Since some of the pore solution has been expressed from the mortar specimen prior to sampling, W_e/c must be found by difference:

$$W_e/c = 0.50 - 0.1585 = 0.3415 \text{ g evaporable water/g cement.}$$

To facilitate solution of these equations a program was prepared for an HP-67 programmable calculator. The constants were loaded from magnetic card records and the variables were entered from the keyboard.

For purposes of this calculation all chemically bound water in hydration and reaction products has been formally assigned to the portland cement. As will be discussed in later sections, addition of reactive mix components, e.g. pozzolans and/or reactive aggregates results in apparent reduction of chemically bound or nonevaporable water. This was an entirely unexpected result.

4.11.3 - Interpolation and Extrapolation

As will be seen in Chapter 5, apparent values of W_n/c observed in this study tend to decrease with increasing additions of reactive mix components for mixes of a constant age:

$$W_n/c = a + b P Eq. 4.11.7$$

Where: W_n/c = Nonevaporable or chemically bound water

a and b = Empirical constants

P = Percent, by weight of portland cement, of added reactive component

In common with many natural processes that tend asymptotically toward some limiting value with increasing time, nonevaporable water data respond reasonably well to hyperbolic estimating equations of the form proposed by Lipka (413, p. 137 ff):

$$W_n/c_t = \frac{t}{a + b t} \dots \dots \dots \dots \dots \quad \text{Eq. 4.11.8}$$

Where: W_n/c_t = Observed W_n/c at time t

a and b = Empirical constants

A useful property of this equation is its ability to predict ultimate values. As time tends toward infinity the constant "a" becomes insignificant and the ultimate value of W_n/c approaches $1/b$.

It is frequently found that, over some limited range of values, the points are better fit by the obvious extension of Eq. 4.11.8:

$$W_n/c = \frac{t}{a + b t + c t^2 \dots m^n} \dots \dots \quad \text{Eq. 4.11.9}$$

In general, a second order polynomial divisor is found to be adequate. Unfortunately, this form precludes extrapolation.

An additional modification that may improve agreement between observed and estimated values is that of applying a constant offset "k" to the time value:

$$W_n/c = \frac{(t + k)}{a + b (t + k)} \dots \dots \quad \text{Eq. 4.11.10}$$

For each value of "k" a value for the standard error of the estimate, " $S_{y.x}$ " can be calculated by the method of least squares.

A plot of the points $(k, S_{y,x})$ generates a parabola. By setting the derivative of the equation for the parabola equal to zero it is possible to select the optimum value of "k".

Prior to attempts to fit Equations of the forms 4.11.8 through 4.11.10 to experimental data it is recommended that a rough plot of $(t, (W_n/c)/t)$ be prepared to investigate the fit of early data. It will frequently be found that early points deviate significantly from the linearity exhibited by later data, indeed the first point if taken early enough should approach infinity. These points should be deleted from the set employed to derive the estimating equation.

In the following example constants for an estimating equation of the form of Eq. 4.11.9 are computed for the relationship of nonevaporable water to curing time (W_n/c vs. t). The data have been taken from mixes 44, 49, 59, and 78. These are all control mixes (1 : 0.5 : 2, cement ; water ; sand), cured continuously at 20°C in sealed containers for the periods indicated. Table 4.5 contains the observed data, estimates resulting from the use of the estimating equation, and deviations of the estimates from the observed values.

Figure 4.3 illustrates the rectifying effect of plotting $t/(W_n/c)$ vs. t . The result is nearly linear for the range 0.333 through 30.5 days. Note that the point for 0.125 days lies significantly above the plotted line, and has been omitted from the data used to compute the coefficients for Eq. 4.10.9. When this type of plot is applied to other kinds of data, e.g. potential drying shrinkage measurements of mortars and concretes, early points will lie significantly above the linear relationship exhibited by the remainder of the data points.

Table 4.5

Relationship of Observed Wn/c and Estimated Wn/c
to Time for Control Mixes at 20° C

Time, Days	Mix No.	Wn/c Observed	Wn/c Computed	Error of Estimate	t/(Wn/c)
0.125	44	0.0069	--	--	18.116
0.333		.0329	0.0361	+.0032	10.122
1.125		.0781	.0843	+.0062	14.405
0.46	49	.0360	.0465	+.0105	12.778
4.		.1563	.1414	-.0149	25.592
30.5		.1835	.1850	+.0015	166.213
2.	59	.1331	.1118	-.0213	15.026
32.		.1847	.1855	+.0008	173.254
128		.1958	.1968	+.0010	653.728
432		.2167	.2167	+.0000	1993.539
1.	78	.1041	.0788	-.0253	9.606
3.75		.1518	.1390	-.0128	24.704
5.75		.1572	.1539	-.0033	36.578
10.		.1610	.1684	+.0074	62.112
27.		.1792	.1838	+.0064	150.670
124.		.1981	.1965	-.0016	625.946

Estimating equation:

$$W_n/c \approx \frac{t}{7.496 + 5.2022 \times t - 0.0014 \times t^2} \quad \dots \quad \text{Eq. 4.11.11}$$

Standard error of the estimate, $S_{y.x} = \pm 0.0108$, $N = 15$

Estimating equation (points at 0.125 days for Mix 44, 2 days for Mix 59, and 1 day for Mix 78 not used):

$$W_n/c \approx \frac{t}{7.0397 + 5.2093 \times t - 0.0014 \times t^2} \quad \dots \quad \text{Eq. 4.11.12}$$

Standard error of the estimate, $S_{y.x} = \pm 0.0071$, $N = 13$

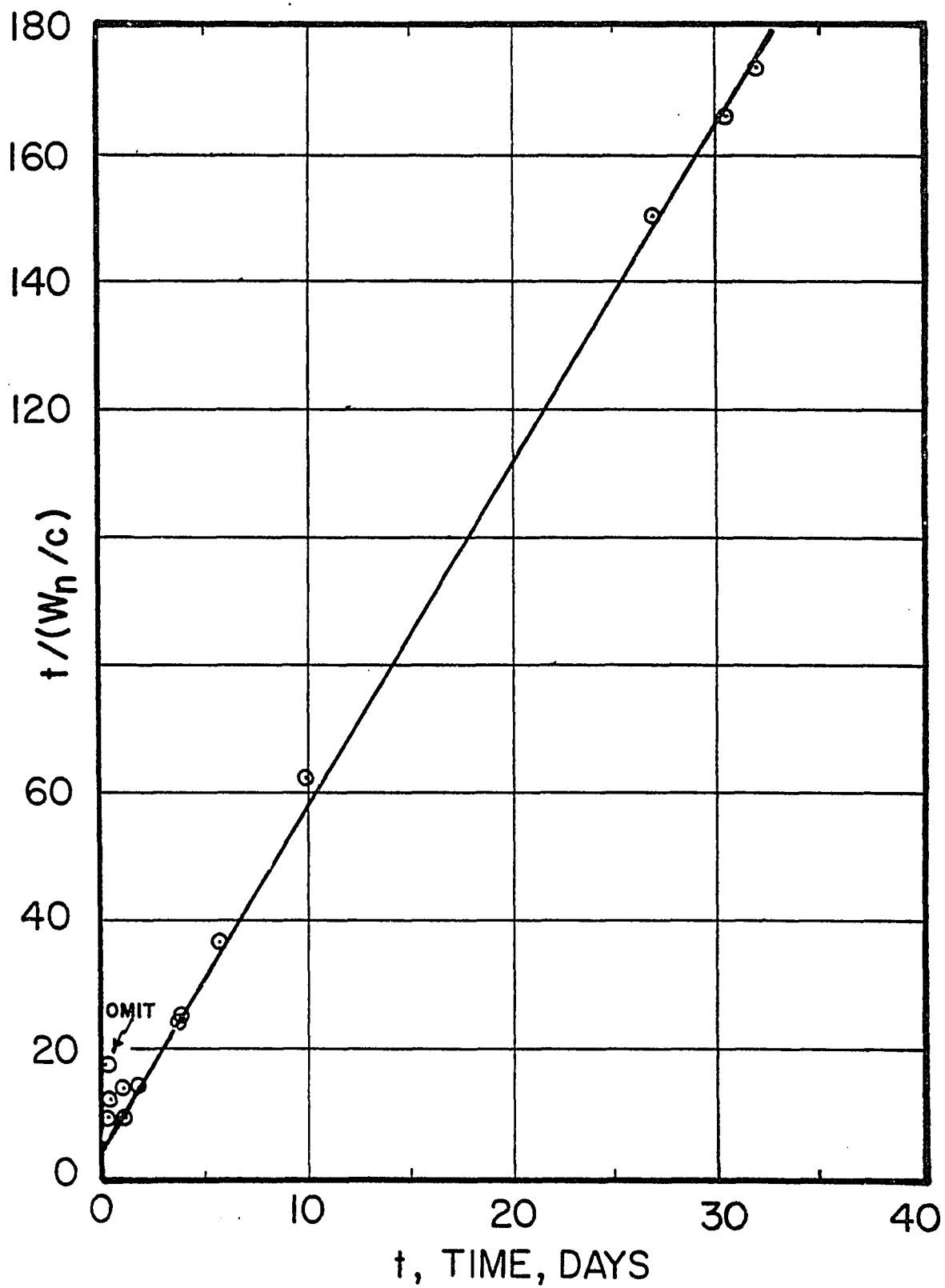


Figure 4.3 - Plot of $t/(W_n/c)$ vs. t , Illustrating Rectified
Relationship Between Nonevaporable Water and Time.

Using the 15 points in Table 4.5, the standard error of the estimate is 0.0108. This can be reduced to 0.0071 by eliminating the point at 2 days in mix 59 and the point at 1 day in mix 78.

4.12 - Adjustment of Pore Solution Concentrations

to Compensate for Chemically Bound Water

As hydration of the portland cement proceeds, part of the free water added at the time of mixing is chemically bound in hydration products, thus reducing the volume of the solvent phase of the pore solution. Even if the absolute quantity of the solutes in solution were to remain constant, i.e. none added from hydration, taken up in hydration products, or precipitated from solution, the apparent concentration of ions in solution would increase.

The concentration observed due to this decrease in solvent volume, n_i , can be calculated from Equation 4.11.1:

$$n_i = \frac{W/c}{W/c - W_n/c} \times n_o \quad . \quad Eq. \quad 4.12.1$$

Where: n_o = Normality of original solution

n_i = Normality of observed solution

W/c = Original water-cement ratio

W_n/c = Nonvaporable (chemically bound) water

For convenience in calculating the normality of the original solution, the bound water constant, bwk , is defined as:

$$\left(\frac{W/c}{W/c - W_n/c} \right)^{-1} = bwk \quad . \quad Eq. \quad 4.12.2$$

Then: $n_o = n_i \times bwk$

For a given series of mixes consisting of a control mix and companion mixes each containing a fixed amount of some test substance, admixture, aggregate or both, or for companion mixes containing known amounts of test substance, adjustment of the observed ionic concentrations by compensation for chemically bound water allows evaluation of the effect of the test substances on pore fluid chemical properties. It also seems safe to assume that if the alkali metal ion concentration, after compensation for chemically bound water, remains constant or falls gradually beyond about 28 days, that at ages beyond about 100 days virtually all of the alkalies originally present in the cement clinker have found their way into solution. Thus, to a first approximation, the alkalies bound in hydration and reaction products should be reflected by the difference between the potential contribution of the cement clinker and the residual alkali content in the pore solution, all expressed in moles per liter of original pore solution. This also requires the assumption that no alkalies are contributed by the aggregate, a fair assumption if an aggregate free of alkali containing minerals, e.g. quartz sand, is used.

Unfortunately the final dispositions of alkalies in a mortar can not be stated without ambiguity from data provided by analyses of expressed pore solutions. In Figure 4.4 the alkali ion flow in the relatively simple system involving a cement paste is diagrammed. On addition of mixing water to the portland cement, the rapidly soluble alkali metal components, primarily alkali metal sulfates, appear in the pore solution. As hydration progresses additional alkalies held within the crystalline and glassy phases of the cement clinker appear in the

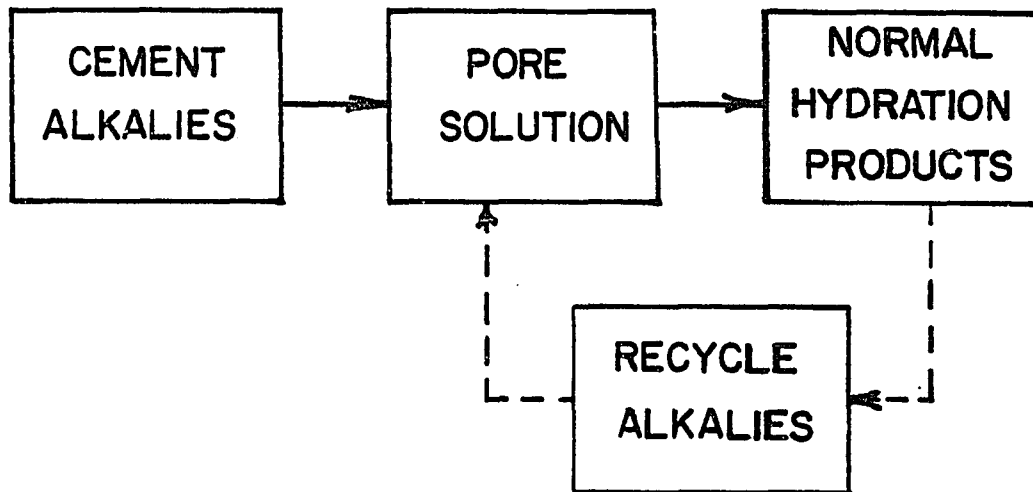


Figure 4.4 - Schematic Representation of Alkali Metal Ion Distribution in Portland Cement Paste

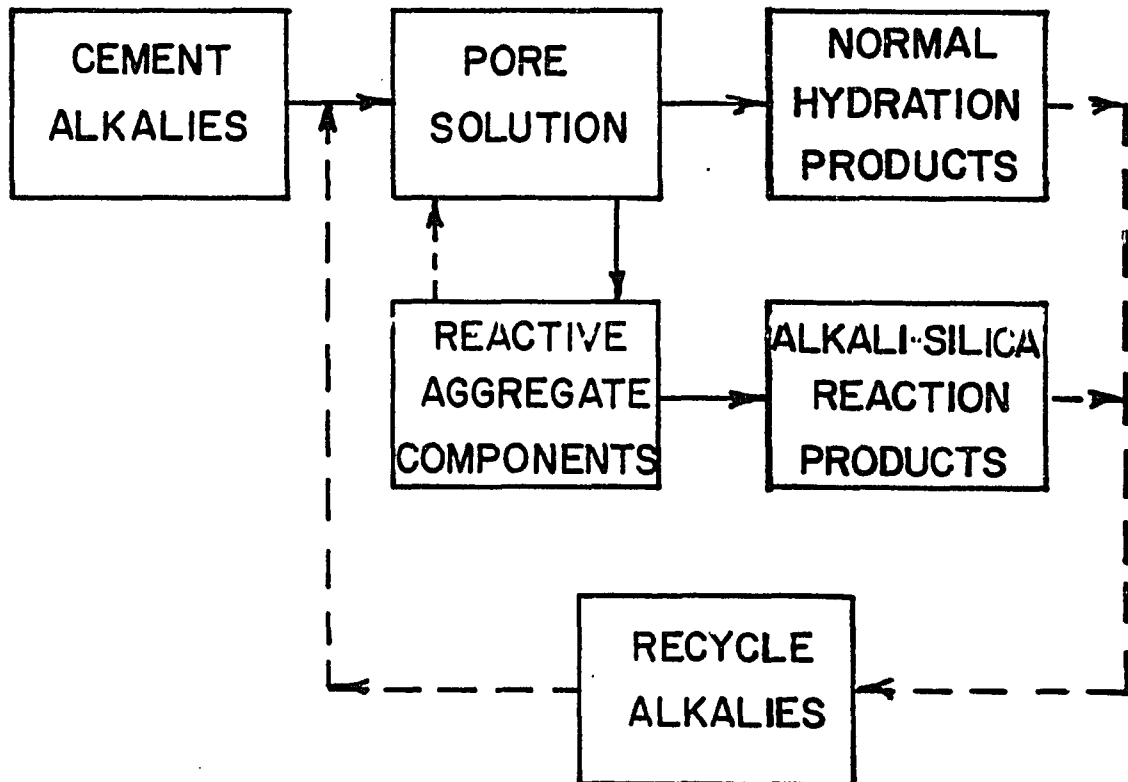


Figure 4.5 - Schematic Representation of Alkali Metal Ion Distribution in Portland Cement Mortar

pore solution. At the same time it seems probable that some of these ions are incorporated into hydration products. To further complicate the situation, it is possible that calcium or other cations may displace some of the alkali metals from hydration products, thus recycling the alkalies. This may be a factor, but, as will be discussed in Chapter 6, the evidence available from this study suggests that if alkali metal ions are recycled the quantity is small. For this reason the alkali recycle paths are represented by dashed lines in the figures.

In Figure 4.5, an aggregate containing reactive components has been added to the system. It should be borne in mind that virtually all commonly used aggregate materials react chemically with components of the hydrating cement paste resulting in improved paste-aggregate bond. The reaction contemplated here is between alkalies derived from hydrating cement paste and siliceous components of the aggregate. The amount of the reaction product and its properties are dependent on the relative aggressiveness of the pore solution and the nature of the reactive components of the aggregate. The reaction products appear to bind alkali metal ions, and the attack may release additional alkalies from aggregate components. If released by this action, these alkalies may go into pore solution or, more likely, be incorporated into other reaction products adjacent to the site of their release. These circuits are also shown as dashed lines.

In Figure 4.6, a pozzolanic material has been added to the mortar. By definition, pozzolanic materials contain reactive components. This system is analogous to the previous system, but more rapid and more extensive reaction would be expected owing to the high specific surface

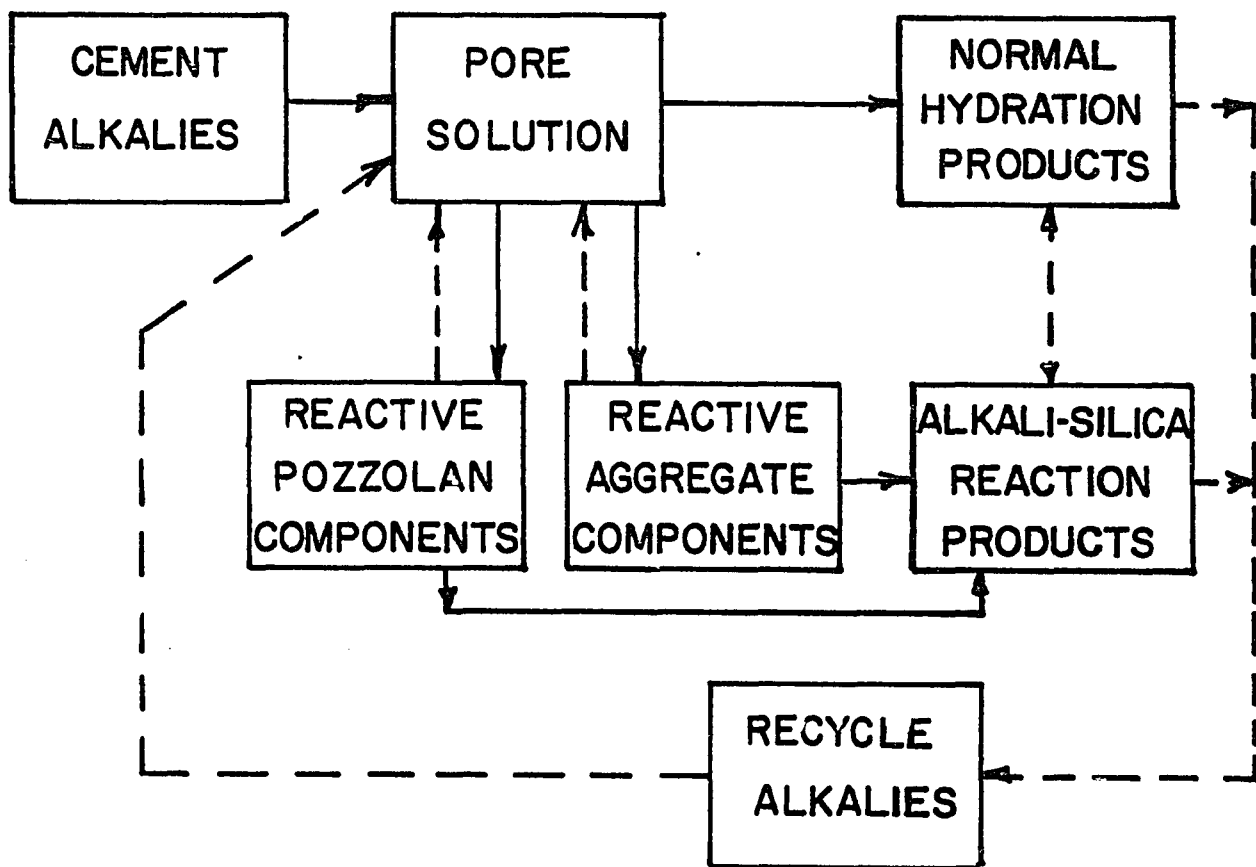


Figure 4.6 - Schematic Representation of Alkali Metal Ion

Distribution in Portland-Pozzolan Cement Mortar

of the pozzolanic material. Further, the presence of the pozzolanic material or its reaction products can significantly alter the hydration products of the portland cement (414, 415, 416). From the preceding it can be appreciated that changes in ionic concentrations observed in expressed pore solutions are difficult to interpret.

4.13 - Thermogravimetry and Derivative Thermogravimetry

In this study thermogravimetry (TG) involved measurement and recording of the change in weight of samples subjected to a constantly increasing temperature. Simultaneously a plot of the first derivative of the TG curve was recorded (DTG). Theory, instrumentation, and application of thermogravimetric methods to analytical and physical chemistry determinations have been discussed by Duval (417), Garn (418), Schwenker and Garn (419), Wendlandt (420), and many others.

4.13.1 - Cahn Thermobalance

The primary equipment used in this study consisted of a Cahn Model RG Automatic Electrobalance and Cahn Mark II Time Derivative Computer. The balance unit was isolated from random vibrations in the laboratory building by supporting it on a series of three 75 mm thick foam rubber pads. Low frequency cyclic vibrations from ventilating equipment necessitated loading the unit with various combinations of weights to damp sympathetic vibration of the unit. A Marshall Model 2011 tube furnace, hinged to open parallel to its long axis was used to supply heat under the control of a Barber-Colman temperature control system. This unit employed a synchronous motor driven programmer and solid state power control to maintain a temperature increase in the furnace of 5° C/min. The furnace temperature was sensed by a chromel-alumel

thermocouple installed in the furnace. The sample temperature was sensed by a platinum vs. platinum - 10% rhodium thermocouple placed approximately 1 mm below the sample boat. A similar thermocouple, immersed in an ice bath in a vacuum bottle, provided the reference temperature signal. The amplified signal from the noble metal thermocouple system drove the X axis of a Houston Instruments Omnigraphic X-Y, Y' flat-bed plotter. A signal from the thermobalance drove the Y pen to provide a cumulative record of sample weight loss. The Y' pen, offset 0.50 in. (one major chart division) behind the Y pen to prevent mechanical interference, was driven by a signal from the time derivative computer.

Immediately prior to each run the thermobalance and recorder span calibration were checked by application of a 50 mg Class M primary standard weight to the sample boat. The thermobalance calibration remained constant throughout the series of runs required for this study, but minor adjustments of the recorder span calibration were generally required after each run. The least division provided on the electrobalance mass dial was 0.10 mg and it was possible to estimate dial readings to 0.01 mg. The recorder chart used had a 0.50 in. rectangular grid with 10 minor subdivisions. The electrobalance output and recorder scale factors available allowed plotting output from the sample temperature sensing thermocouple at 1.0 mV/in. on the X axis, and cumulative weight loss at 1.0 mg/2.5-in on the Y axis. Areas defined by well-formed troughs of the derivative curve were determined by integrating polar planimeter and it was found that
 $1.0 \text{ in.}^2 = 1.086 \text{ mg sample weight change}$ ($1.0 \text{ cm}^2 = 0.168 \text{ mg.}$)

The sample, prepared and preconditioned as outlined below, was placed in the platinum sample boat and this, in turn, was placed in the balance stirrup. If this initial rough weight determination indicated the sample weight did not lie within the range 55 ± 5 mg, the sample boat was removed from the stirrup and the amount of sample was adjusted to fall within these limits. After a satisfactory sample weight was obtained, the sample, its support system and thermocouple were enclosed by the installation of a quartz hangdown tube (see Figure 4.7. The tube furnace was centered about the apparatus, closed, and adjusted to provide a 3-4 mm annular air space about the hangdown tube.

A delay of three to five minutes was required for vibration within the system to be damped prior to determination of the sample weight, W_0 , to the nearest 0.01 mg. Following the determination, the system was pumped down to 80 ± 5 mm Hg and the sample weight at this reduced pressure, W_I , determined. The pressure of 80 ± 5 mm Hg was maintained throughout the run and until the final weight, W_F , had been determined at $1000^\circ C$. Operation of the system at reduced pressure is desirable to minimize apparent weight changes resulting from convection currents within the hangdown tube and to reduce the tendency of CaO , resulting from the decomposition of $Ca(OH)_2$, to combine with CO_2 from the atmosphere to form $CaCO_3$.

4.13.2 - Sample Preparation and Preconditioning

The sample for thermogravimetric analysis was obtained as described in Section 4.11.1. A representative sample of approximately 3 g of the freshly broken cylinder was selected and immediately crushed in a

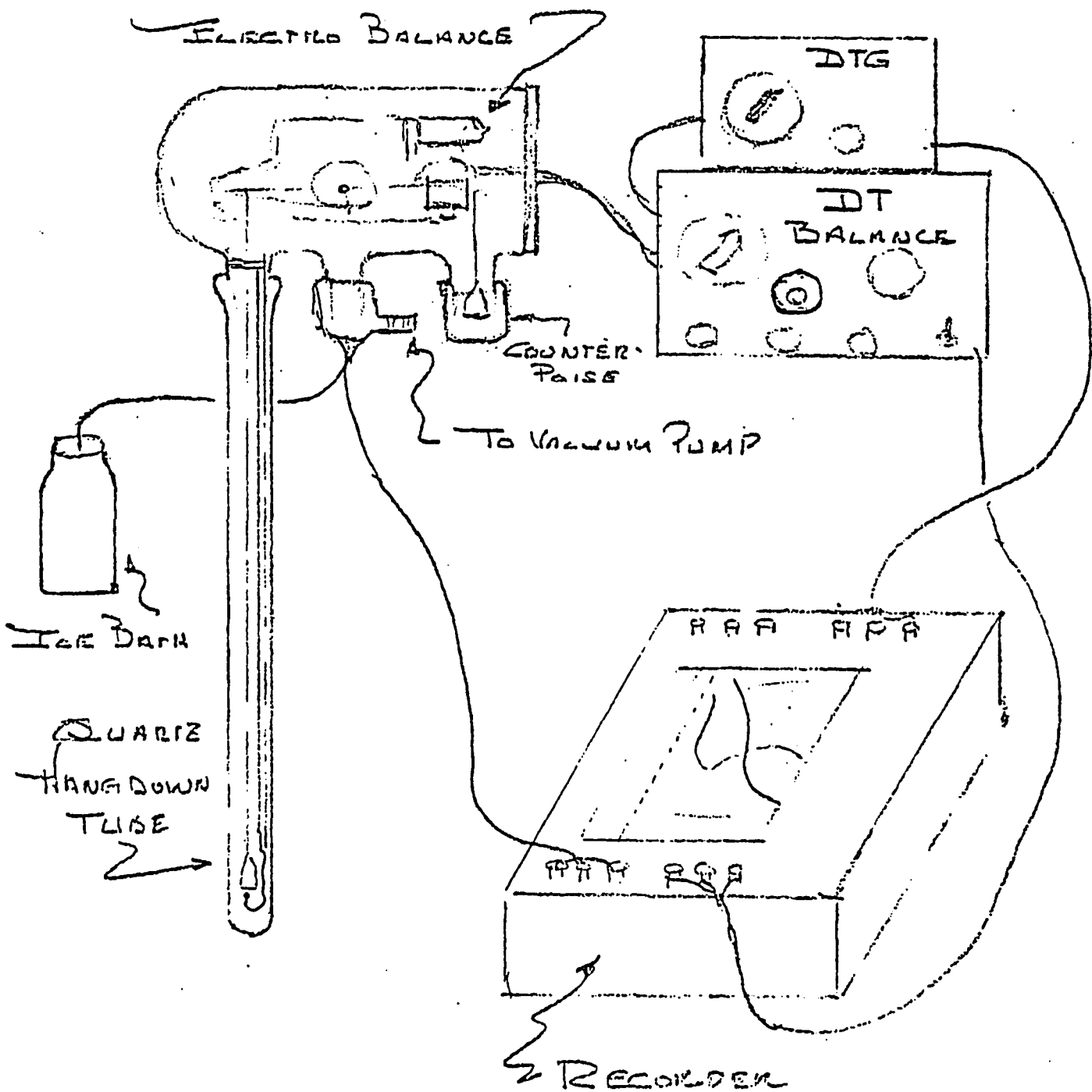


Figure 4.7 - Sketch of the Cahn Thermobalance

Plattner mortar. The crushed sample was transferred to a mullite mortar and ground under acetone until all particles were judged to be less than 75 μm . The ground slurry was transferred to a 75 mm watch glass and placed under a heat lamp at $30 - 40^\circ\text{C}$ to drive off the acetone. Crushing, grinding and drying required about 20 minutes, about half of which was devoted to evaporating the acetone. To reduce the potential for carbonation, the sample was not sieved, but was transferred from the watch glass to an open weighing bottle and was then stored in a desiccator over a saturated solution of $\text{Mg}(\text{NO}_3)_2 \cdot 6\text{H}_2\text{O}$ at $22 \pm 3^\circ\text{C}$. The International Critical Tables list the equilibrium relative humidity above this solution as 56 percent at 18.5°C and 52 percent at 24.5°C (421, pp. 67-68). The samples were allowed a minimum of five days of such preconditioning prior to test. Weighing bottles were covered as soon as they were removed from the desiccator for sample loading on the thermobalance, and the caps were removed again on return to the desiccator.

A complete cycle for each run required approximately ten hours: 0.75 hours for cleaning sample boat, calibration of balance and recorder, loading new sample, and obtaining W_0 ; 3.25 hours for the run from 25 to 1000°C ; and 6 hours furnace cooling time. Thus a minimum of three days were required for a suite of six samples. To determine the possible effect of prolonged storage in the preconditioning desiccator, several samples were retested after approximately 15 days storage at 52-54 percent R.H.. No significant deviations from the previous curves were noted.

4.13.3 - Interpretation of Thermogravimetic Data

Biffen reported on the determination of $\text{Ca}(\text{OH})_2$ and CaCO_3 in calcium silicate hydrates (C-S-H) (422). He used a Chevenard thermo-balance with a heating rate of $8^\circ \text{ C}/\text{min}$. The sample was exposed to an atmosphere free from CO_2 and moisture.

His studies indicated the TG curves for C-S-H could be characterized as a straight line in the temperature interval $375\text{--}650^\circ \text{ C}$ and that the rate of weight loss, presumably due to loss of water of hydration, with increasing temperature was small in comparison to the rate of water loss from $\text{Ca}(\text{OH})_2$ decomposition in this interval. Further, with the start of $\text{Ca}(\text{OH})_2$ decomposition, the vapor pressure of water present increases rapidly, further reducing the rate of water loss from the C-S-H gel. He also found that the loss of CO_2 from CaCO_3 resulted in a separate dip in the TG curve at a temperature above that for decomposition of $\text{Ca}(\text{OH})_2$. His quantitative determination, assuming that weight loss in these intervals represented loss of water from $\text{Ca}(\text{OH})_2$ and CO_2 from CaCO_3 , checked with determinations on mixtures of known composition for $\text{Ca}(\text{OH})_2$ and with wet chemical methods for CaCO_3 .

The procedural decomposition temperature, i.e. the apparent temperature at which decomposition of a compound appears to start depends on several factors. This temperature tends to be lower for smaller samples or those in which the compound of interest is diluted, finer particle sizes, less ordered crystallinity, and reduced pressure. In the experiments conducted here, the mortar samples were ground to pass $75 \mu\text{m}$ and a pressure of 80 mm Hg was maintained in the hangdown tube during the run. Halstead and Moore studied the thermal decomposition of

Ca(OH)_2 . From their data (423, p. 3874) the following relationship can be derived, using the Clausius-Clapeyron equation:

$$\log_e P = 21.869 - 11940.13 \times 1/T \quad . \quad . \quad . \quad . \quad . \quad . \quad \text{Eq. 4.13.1}$$

Where: P = Equilibrium decomposition pressure, mm Hg.

T = Temperature, Kelvin

In their experiments, P ranged from 19.0 to 671.0 mm Hg and T from 635 to 776.5°K ($361.8 - 503.4^\circ \text{C}$). From Eq. 4.13.1, the equilibrium decomposition temperature for Ca(OH)_2 at 80 mm Hg is found to be 409°C .

Southard and Royster studied the thermal decomposition of CaCO_3 . From their data (424, p. 437) the following relationship was derived:

$$\log_e P = 23.644 - 19855.95 \times 1/T \quad . \quad . \quad . \quad . \quad . \quad . \quad \text{Eq. 4.13.2}$$

Their sample was composed of calcite grains "crushed to about 100 mesh", and tested in a static atmosphere in the pressure range 826 to 109.3 mm Hg.

Using Eq. 4.13.2 and extrapolating to 80 mm Hg, the equilibrium decomposition temperature is found to be 758°C . These data confirm those of Webb and Heystek (425, pp. 331-334).

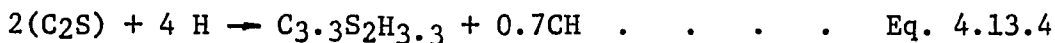
Based on the above information it is reasonable to assume that decomposition of Ca(OH)_2 should be indicated by initiation of an endotherm at approximately 410°C , and that decomposition of CaCO_3 , if present, should be indicated by initiation of an endotherm at approximately 760°C .

Major endotherms were observed for Ca(OH)_2 in the appropriate temperature range (e.g. see Figure 4.8), but no significant endotherms

were observed above 600° C, suggesting the absence of CaCO₃, formed during hydration or sample preparation due to carbonation.

The amount of Ca(OH)₂ produced in a fully hydrated portland cement will depend on the compound composition of the cement, W/c, and to a small extent, the hydration temperature in the range 20 - 40° C.

Kantro, et al. (426) suggest the following reactions reasonably represent the hydration of the two main compounds in portland cement:



Applying the Bogue equations (ASTM C 150) to the reported chemical analysis of cement AT-1, the potential Ca(OH)₂ in the fully hydrated paste of this cement is 3.588 mMol/g cement or 0.266 g Ca(OH)₂/g cement. There is evidence to suggest that the C/S ratio of the hydrates may be greater than these equations indicate, perhaps approaching 2 or even more in some cases (427, 428, 429, 430). Thus, the value of 0.266g of free Ca(OH)₂/g cement should be considered an upper bound in this cement. In mortars the free Ca(OH)₂ will be further reduced as a result of secondary reactions with other mix components, e.g. pozzolans or reactive aggregates.

In Figure 4.8, a complete TG and DTG curve for Mix 59 is reproduced. The offset required for mechanical clearance between the Y and Y' pens has been eliminated so that both curves refer to the scales on the temperature millivolt axis. The procedural decomposition temperature is taken as the point of departure of the DTG curve from a tangent line segment drawn across the opening of a trough and is indicated as T_i, the initiation temperature. Completion of the

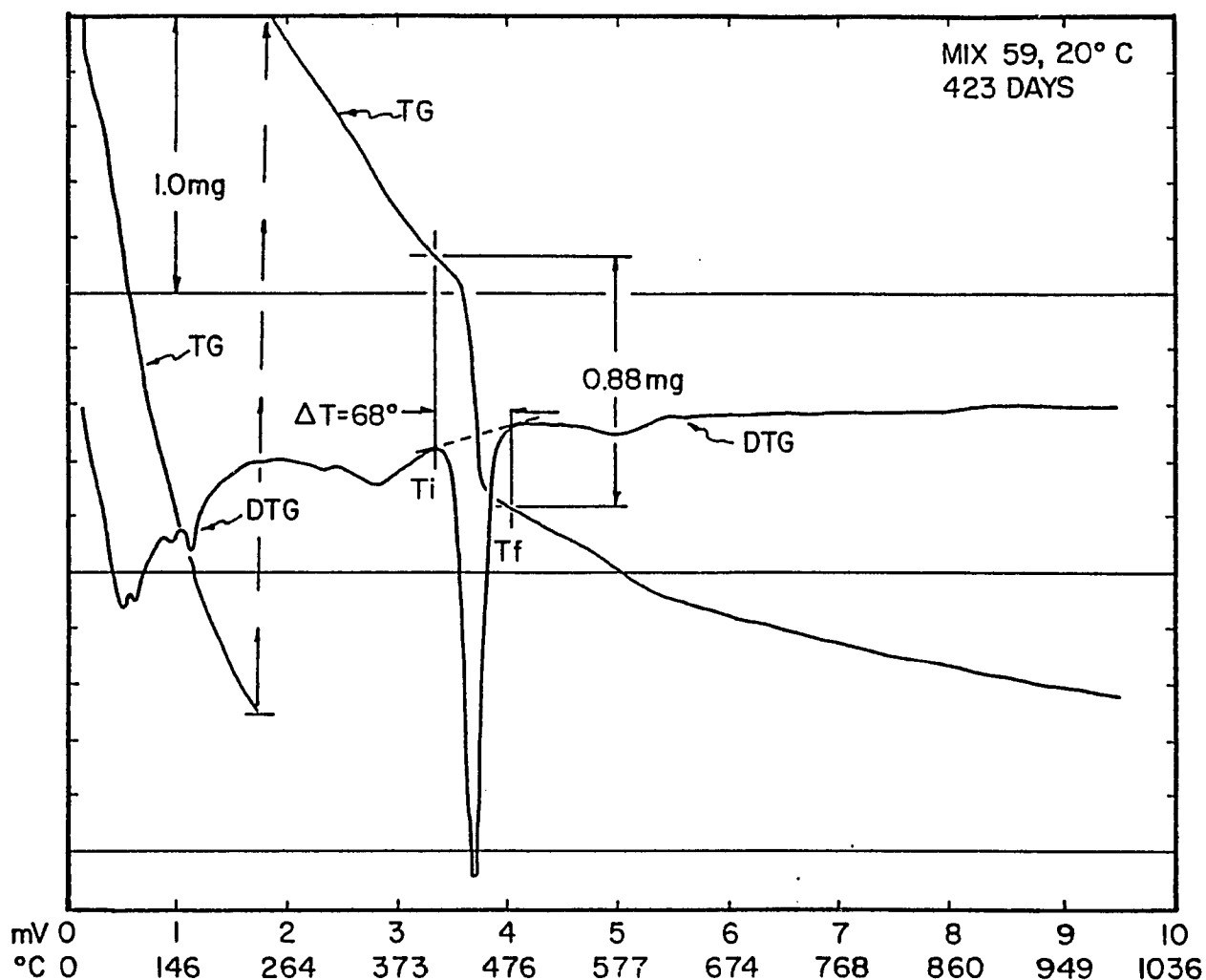


Figure 4.8 - Illustration of the Use of Thermogravimetric and Derivative Thermogravimetric Curves for a Typical Mortar Mix to Determine Weight Loss Due to Thermal Decomposition of Calcium Hydroxide

reaction is taken as the point of return of the DTG curve to the tangent line segment, T_f . Vertical line segments are extended from T_i and T_f to intersect the TG curve. The weight loss in this temperature interval can then be scaled from the TG plot.

For the sample:

$$\Delta W = \text{Weight loss of sample due to thermal decomposition of } Ca(OH)_2 = 0.88 \text{ mg}$$

$$W_I = \text{Initial weight prior to heating} = 50.2 \text{ mg}$$

$$W_F = \text{Final weight after heating to } 1000^\circ C = 45.3 \text{ mg}$$

The mean correction factor for buoyancy of the specimen at reduced pressure was found to be 1.007. The weight of the cement represented by this sample was found by the following modification of Eq. 4.11.6:

$$c = W_F \times 1.007 / (I_c + R_p I_p + R_b I_b + R_a I_a) \text{ Eq. 4.13.5}$$

Where: W_F = Final weight of TG specimen at $1000^\circ C$ and 80mm Hg.

1.007 = Buoyancy factor

and other variables are as defined in Section 4.11.2

Substituting appropriate values in the above equation:

$$c = 45.3 \text{ mg} \times 1.007 / (0.99483 + 2 \times 0.99868)$$

$$c = 15.243 \text{ mg unhydrated portland cement}$$

The weight of residual $Ca(OH)_2$ resulting from hydration of the cement and subsequent additional reactions prior to sampling is:

$$g Ca(OH)_2/g Cement = \frac{\text{Mol. Wt. } Ca(OH)_2}{\text{Mol. Wt. } H_2O} \times \frac{W}{c} . . . \text{ Eq. 4.13.6}$$

$$\text{g Ca(OH)}_2/\text{g Cement} = 4.113 \times (0.88/15.243) = 0.237 \text{ g/g}$$

This is approximately 90 percent of the value obtained from Eqs. 4.13.3 and 4.13.4. Considering the uncertainties involved in the use of the Bogue equations and the probably greater C/S ratio of hydrates than found by Kantro et al. (426), this is a satisfactory result.

4.14 - Specimen Molds

Molds used in this study for casting specimens for pore solution expression and specimens for measurement of potential length change are described below.

4.14.1 - Pore Solution Specimens

Plastic salve jars of nominal 4 oz (118 cm^3) volume were used to mold and store specimens for pore solution expression. The jars selected had an internal diameter of approximately 50 mm at the bottom and 51 mm at the top. They were filled with 80 to 90 cm^3 of fresh mortar. The seal in the caps supplied with the jars was supplemented by a sheet of heavy plastic film (Parafilm) applied over the jar mouth prior to sealing the jars with their caps.

4.14.2 - Molds for 1 in (25.4 mm) square Cross Section Prisms

The molds for casting 1 in (25.4 mm) square cross section mortar prisms with 10 in (254 mm) gage length were constructed and fitted with gage studs as specified and illustrated in ASTM Designation C 490.

4.14.3 - Molds for 0.5 in (12.7 mm) Square Cross Section Prisms

The molds for casting 0.5 in (12.7 mm) square cross section mortar prisms with 2.75 in (69.8 mm) long gage length were fabricated from

cold finished steel plates and bar (key) stock. An isometric sketch of one of the assembled molds and isometric half section of a finished mortar prism are provided in Figure 4.9. The mold bars were clamped in position on the base plates by retaining plates attached with small machine screws. Two servings of plastic electrical tape were applied over each end of the mold bars normal to their long axes. The tape servings prevent lateral or vertical displacement of the bars during molding and curing. Stainless steel gage studs were fabricated from #1 x 64 (M1.8 x 0.35-6g) threaded rod. Each mold was capable of forming 6 prisms.

4.14.4 - Molds for 0.25 in (6.35 mm) Square Cross Section Prisms

The molds for casting 0.25 in (6.35 mm) square cross section mortar prisms with 2.75 in (69.8 mm) gage length were similar in construction to those described in Section 4.13.3.

4.14.5 - Molds for 50 mm Diameter

Sealed Expansion Specimens

These specimens were cast in molds made from split acrylic plastic tubing. Thick brass plates were provided as mold closures and bearing surfaces for the butyl rubber jackets (applied after the specimens had hardened), and to carry stainless steel gage studs for length change measurements.

During casting the plastic tubing was clamped to the mold base plate by a worm-drive hose clamp. All joints were coated with water-pump grease to prevent loss of mixing water from the mortar. In addition, the halves of the acrylic plastic cylinder were taped at the longitudinal joints with transparent plastic surgical tape. The

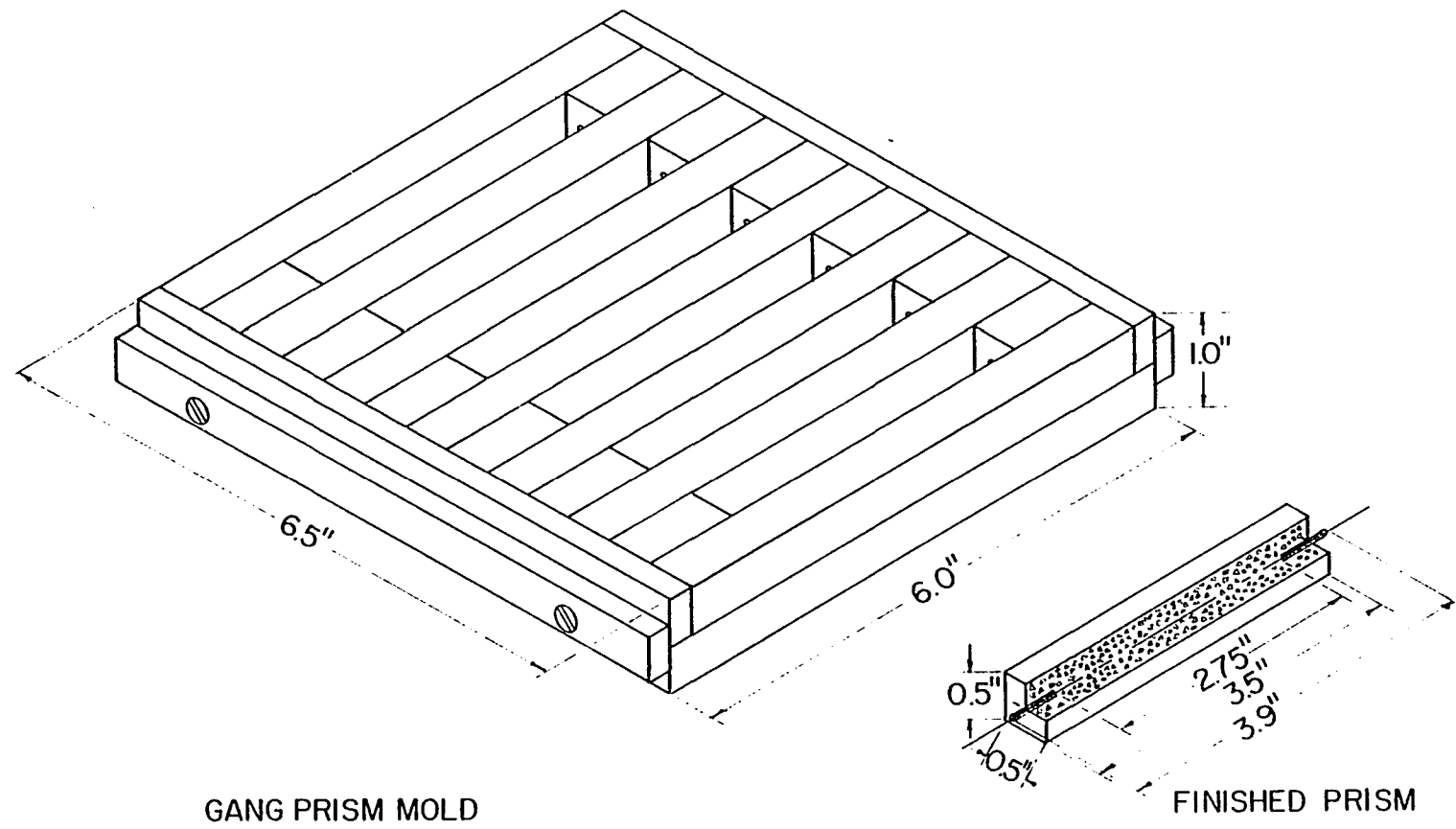


Figure 4.9 - Isometric Sketch of 0.5 in (12.7 mm) Gang Prism Mold
and Isometric Half-Section of Finished Prism

molds were filled and vibrated to contain a column of mortar 70 mm high. The top bearing plate was then pressed into the mold, excess mortar being vented through the vent plug opening. When the top of the top bearing plate was flush with the top of the acrylic plastic mold body, the top clamp was then applied and tightened. The vent plug hole threads were swabbed clean and a machine screw, coated with rubber cement, was inserted and tightened to seal the vent.

Twenty-four hours after casting, the specimens were demolded and butyl rubber jackets, cut from bicycle innertube, were applied. Butyl rubber (butene-diene copolymer) was selected because of its low permeability to air, less than 10 percent of that of natural rubber (408, p. 7-457). The ends of the jacket were turned back to form a cuff of double thickness over the end plates. Before the clamps were replaced a coating of rubber cement was applied to the circumference of the brass end plates to cement the rubber jacket to the end plates. The hose clamps were then applied and tightened to form a vapor tight seal. A sketch of a diametral cross section of a typical specimen is shown in Figure 4.10. Table 4.6 contains a parts list for the specimen and a key to Figure 4.10.

After each length measurement, the weight of the sealed expansion specimens was determined to the nearest 0.1 gram as a check for leaks in the jacket.

4.15 - Storage Containers for Prisms

The optimum storage environment for accelerating most forms of the alkali-silica reaction is thought to be a water vapor saturated atmosphere at approximately 100° F (37.8° C). For this work three storage

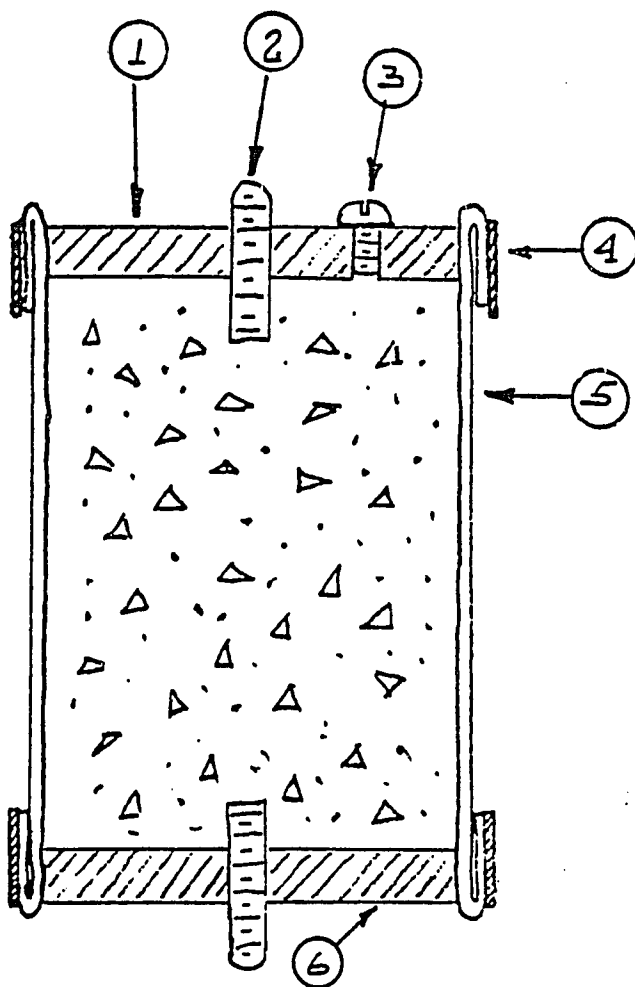


Figure 4.10 - Sketch of Diametral Cross Section
of 50 mm Diameter Sealed Expansion Specimen

NOTE: Nominal gage length is 2.25 in (57 mm).

See Table 4.6 for Key and Parts List.

Table 4.6

Key and Part List for Figure 4.10

1. Top plate, Naval bronze disc, 1.95 in diameter, 0.25 in thick (50 mm x 6.35 mm), turned from bar stock. Drill and tap center for 1/4 x 20 (M6 x 1-6g) stainless steel gage stud (Item 2), and drill and tap 0.55 in (14 mm) off center for #10 x 24 (M5 x .8-6g) vent plug (Item 3). One required per specimen.
2. Stainless steel gage stud, 1/4 x 20 (M6 x 1-6g) threaded stock 0.75 in (19 mm) long. Two required per specimen.
3. Vent plug, #10 x 24 (M5 x 0.8-6g) brass machine screw, 0.25 in (6.35 mm) long. One required per specimen.
4. Stainless steel worm drive hose clamp, 3 in (75 mm) nominal diameter. Two required per specimen. Note: Same clamps are used to hold acrylic plastic mold halves together.
5. Butyl rubber jacket. Fabricate from 4.5 in (115 mm) length of bicycle innertube, nominal 20 x 2.125 in (508 x 54 mm). One required per specimen.
6. Base plate. Identical to top plate, but has no bleed plug. One required per specimen.

temperatures were selected; 20°, 40°, and 60° C. Most of the work was done on specimens stored at either 20° or 40° C. To eliminate the possibility of cross contamination of the specimens, i.e. diffusion of alkali metal ions through water films from one set of specimens to another, specimens representing only a single mixture were placed in each storage container.

4.15.1 - Storage Containers for 1 in (25.4 mm)

Square Cross Section Mortar Prisms

These specimens were stored in transparent styrene plastic sweater storage boxes. The prisms were supported at their quarter points on two pieces of 12 mm diameter glass tubing. A 3 to 5 mm deep layer of water was maintained in the bottom of the boxes. To insure high humidity and retard loss of water from the boxes plastic electrical tape was applied around the perimeter of the lid, sealing it to the box. Although specimens appeared to be equally moist on all sides, they were rotated 90° following each measurement. Great care was required in handling these storage containers to prevent splashing water on to the mortar specimens.

4.15.2 - Storage Containers for 0.5 in (12.7 mm) and

0.25 in (6.35 mm) Square Cross Section Mortar Prisms

These specimens were small enough to be stored in 16 oz (500 ml) wide-mouth specimen jars. A sketch of the diametral cross section of one of these storage containers is shown in Figure 4.11. A parts list and key to the figure appears in Table 4.7.

This curing container is designed for storage of either four 0.5 x 3.5 in (12.7 x 90 mm) or six 0.25 x 3.5 in (6.35 x 90 mm) miniature mortar prisms.

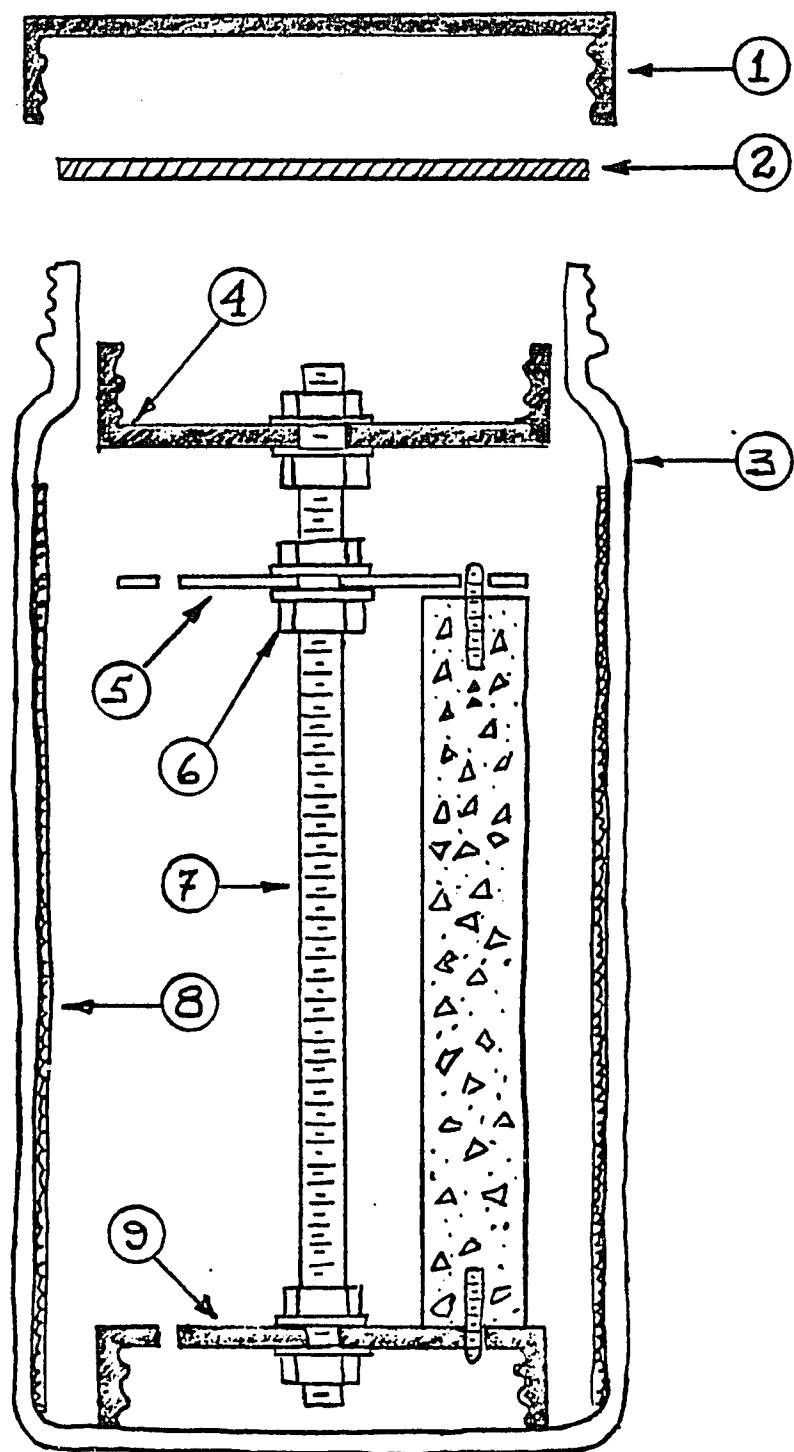


Figure 4.11 - Diametral Cross Section of Storage Container
for Miniature Mortar Prisms

Table 4.7

Key and Part List for Figure 4.11

1. Plastic jar cap, 70 mm, with paper seal disc removed.
One required.
2. Rubber seal disc, 66 mm diameter, die cut from 1/16 in
(1.5 mm) thick rubber packing sheet stock. One required.
3. Standard 16 oz (475 Ml) wide mouth specimen jar. One
required.
4. Plastic jar cap, 53 mm, with paper seal disc removed.
Drill to receive support column (Item 7). One required.
5. Spring brass clips made from 0.016 x 0.5 in (0.4 x 12.7 mm)
stock cut 2 in (50 mm) long. Drill to receive support
column (Item 7) and gage studs in mortar prism specimens.
Number required depends on number and size of specimens to
be stored.
6. Brass nuts and washers, #10 x 24 (M5 x 0.8-6g). Six sets
required.
7. Brass all-thread rod, #10 x 24 (M5 x 0.8-6g) 5 in (125 mm)
long. One required.
8. Blotting paper sheet, 4.5 x 8 in (115 x 200 mm). One
required. Must be replaced periodically.
9. Plastic jar cap, 53 mm, with paper seal disc removed. Drill
to receive support column (Item 7) and gage studs in mortar
prism specimens. One required.

The containers are assembled prior to demolding the mortar prisms and about 20 ml of 5 percent solution of copper sulfate in demineralized water is poured into the storage container over the blotting paper. The container is rolled to insure saturation of the entire sheet of blotting paper and the excess copper sulfate solution is then poured out. Prior to loading new specimens into the storage container, 8 to 10 ml of demineralized water is injected into the bottom of the container with a calibrated syringe. At each measurement the level of the solution in the bottom of the jar is checked to maintain this volume.

4.16 - Length Change Measurements

Mechanical dial gage comparators complying with the requirements of ASTM Designation C 490, were used.

In preliminary studies it was determined that expansion of mixtures containing Beltane opal sand would be rapid. To eliminate possible effects of temperature cycling on expansion and allow measurements to be taken without the necessity of waiting for them to come to equilibrium with the laboratory temperature, measurements were generally taken at the same temperature as that at which the specimens were being stored. Exceptions to this rule are indicated in the tabulations of measurements.

4.17 - Constant Temperature Storage Facilities

Two double-wall insulated cabinets were constructed of plywood for storage of most of the specimens.

A small cabinet was maintained at $20^{\circ} \pm 1^{\circ}\text{C}$ by means of a small heat exchanger constructed from an automobile heater core. House water, at about 15°C , was circulated through the interior of the core

and the air in the cabinet was circulated over its surfaces for cooling. A solid-state thermostat using a thermistor temperature probe controlled electrical heating elements to maintain the desired temperature. Weekly adjustments of the water flow rate were necessary to optimize energy and water consumption.

A similar, but larger cabinet, was constructed for storage of specimens at $40^{\circ} \pm 1^{\circ}\text{C}$. This cabinet was equipped with a viewing window and arm ports so that the specimens could be measured without removing them from the cabinet. Since the laboratory temperature was maintained below 40°C , only termostatically controlled heating was required in this cabinet. Air circulation in this cabinet was maintained by a small fan.

During phases of the work involving 1 in (25.4 mm) square cross section mortar prisms, a room held at $40^{\circ} \pm 2^{\circ}\text{C}$ was used for storage and measurement of these specimens.

4.18 - Mixing Mortars and Molding Specimens

Pilot tests of materials were conducted on batches of mortars that were hand mixed (Sections 5.1 and 5.2). The remainder of the batches were machine mixed in accordance with the provisions of ASTM Designation C 305. Parts of the metal molds for casting mortar prisms for length change measurements were sprayed with two coats of film bonding grade fluorocarbon prior to assembly. Where appropriate, water-pump grease was used as a sealant to prevent leakage of mixing water from the molds. To eliminate the possibility of chemical contamination, no more than one mix was cast in each gang mold.

CHAPTER 5

EXPERIMENTAL RESULTS

5.0 - Introduction

Each mix series is introduced by a brief statement of the nature and purpose of the series, followed by tabulations, figures, and text appropriate to the nature and extent of the experiments conducted.

Test methods and techniques of data reduction used frequently have been discussed and illustrated in Chapter 4. Techniques and methods specific to a single mix series, or a small number of series, are discussed and illustrated where first used and referenced when used subsequently.

The general organization of the material following the introduction of each mix series is outlined below. Not all of the listed items are appropriate for all mix series.

- Batch weights, in grams, of the materials used in each mix of the series. This tabulation also indicates the weight ratios of each material in the batch to the weight of portland cement batched.
- Chemical properties of the pore solution expressed from mortar specimens are reported in millimoles of the ion per liter of expressed solution. Summaries of the cations Ca^{++} , Na^+ , K^+ , and Li^+ , are reported in milliequivalents per liter under the

heading " Σ^+ ". Summaries of the anions OH^- , and $\text{SO}_4^{=}$, have been listed in the same units under the heading " Σ^- ". Differences between these two values have been tabulated under the heading " Σ^{+-} ", positive values denoting an excess of cations, negative values denoting an excess of anions. Ideally this difference should be zero, in the absence of other ions not included in the summation.

- Weight loss of the mix components on drying at 105°C, and on ignition at 1050°C.
- Tabulation of observed values of chemically bound nonevaporable water, W_n/c . In some cases, e.g. Mix Series 34 - 35, values of W_n/c have been estimated from equations fit to data from other mix series.
- Tabulation of ionic concentrations of Na^+ , K^+ , and Li^+ , adjusted to compensate for chemically bound water, W_n/c . In these tabulations the following column heading symbols and abbreviations have been used:

Na^+	Observed sodium ion concentration	Note: Ca^{++} , K^+ , Li^+ may be substituted where Na^+ shown.
ΣM^+	Total alkali metal ion concentration	
$*\text{Na}^+$	Sodium ion concentration corrected for W_n/c	
$\Delta *\text{Na}^+$	Difference in corrected sodium ion concentration in test mix from that in control mix	
$\Sigma * \text{M}^+$	Total alkali metal ion concentration corrected for W_n/c	

Δ^*M^+	Difference in total alkali metal ion concentration in test mix from that in control mix.
$*K^+/*Na^+$	Molecular ratio, potassium ions/sodium ions
bwk	Bound water constant
Na_2O_{eq}	Sodium oxide equivalent ($Na_2O + 0.658 K_2O$)
$POZZ_{eq}$	Pozzolan equivalent (see Section 5.15 and Equation 5.15.1 for development).

5.1 - Mix Series 4 - 14

This series was initiated to determine the expansion potential of a preliminary sample of opal taken from the Beltane Quarry, and to evaluate the use of small (0.25-in (6.35-mm) square cross-section) rectangular prismatic specimens for study of the alkali-silica expansion reaction. The molds and specimen storage containers are described in detail in Sections 4.14.2, 4.14.3, and 4.15.

The mortars were hand-mixed for two minutes in a polypropylene bowl with a rubber spatula. The specimens were compacted in the molds with a Syntron electric vibrating table.

A high alkali portland cement, designated cement PI, known to cause expansion of mortars containing unstable siliceous minerals was used. Its oxide analysis indicated the presence of 1.39 percent Na_2O and 0.38 percent K_2O , or 1.64 percent Na_2O_{eq} . A specific gravity of 2.07 was used for the Beltane opal, and 2.65 was used for the C109 sand.

The specimens were stored in their containers in a cabinet which was maintained at approximately 40°C for the first 60 days of storage, and then allowed to fall to laboratory temperature. All measurements

Table 5.1.1

Batch Weights, grams, for Mixes 4 - 14

Materials	Mix 4, 11.5% Opal Sand		Mix 5, 23.% Opal Sand		Mix 6, 10.% Opal Sand	
	Parts by Weight	Batch Weights	Parts by Weight	Batch Weights	Parts by Weight	Batch Weights
Cement, PI	1.000	15.65	1.000	15.65	1.000	16.00
Water	0.639	10.00	0.575	9.00	0.500	8.00
Beltane Sd.*	0.115	1.80	0.230	3.60	0.100	1.60
Sand, C109*	2.218	34.70	2.102	32.90	1.888	30.20
Totals	3.971	62.15	3.907	61.15	3.488	55.80
Materials	Mix 7, 20.% Opal Sand		Mix 8, Control		Mix 9, 10.4% Opal Sand	
	Parts by Weight	Batch Weights	Parts by Weight	Batch Weights	Parts by Weight	Batch Weights
Cement, PI	1.000	16.00	1.000	16.00	1.000	16.00
Water	0.500	8.00	0.500	8.00	0.500	8.00
Beltane Sd.*	0.200	3.20	0.000	--	0.104	1.66
Sand, C109*	1.776	28.40	1.976	31.60	1.870	31.26
Totals	3.475	55.60	3.475	55.60	3.474	55.58
Materials	Mix 10, 1.9% Opal Sand		Mix 11, 4.1% Opal Sand		Mix 12, 6.% Opal Sand	
	Parts by Weight	Batch Weights	Parts by Weight	Batch Weights	Parts by Weight	Batch Weights
Cement, PI	1.000	16.00	1.000	16.00	1.000	16.00
Water	0.500	8.00	0.500	8.00	0.500	8.00
Beltane Sd.*	0.019	0.31	0.041	0.66	0.060	0.96
Sand, C109*	1.954	31.26	1.934	30.94	1.916	30.64
Totals	3.473	55.6	3.475	55.60	3.475	55.60
Materials	Mix 13, 8.% Opal Sand		Mix 14, 11.9% Opal Sand		* Beltane sand C109 sand graded 50.% 600 x 300 μm, 50. 50 300 x 150 μm.	
	Parts by Weight	Batch Weights	Parts by Weight	Batch Weights		
Cement, PI	1.000	16.00	1.000	16.00		
Water	0.500	8.00	0.500	8.00		
Beltane Sd.*	0.080	1.28	0.119	1.90		
Sand, C109*	1.896	30.32	1.856	29.70		
Totals	3.475	55.60	3.475	55.60		

of the specimens were made at laboratory ambient temperature. An Invar standard bar was used to maintain a constant reference reading for the Menzel-type comparator used to measure the prisms.

Length change measurements for mixes 8 through 13 have been plotted in Figure 5.1.1. The pattern indicates a relatively orderly increase in expansion with increased opal content up to 10.4 percent. In Figure 5.1.2, length change measurements have been plotted for mixes 4 through 7, and 14. The low expansion exhibited by mix 4 is probably owing to its high water-cement ratio, 0.64. Reduced expansion was observed when the added reactive mix component exceeded 11.9 percent by weight of cement batched.

In Table 5.1.2, the maximum expansions observed for Mix Series 4 - 14 have been listed along with the potential molar $\text{SiO}_2/\text{Na}_2\text{O}_{\text{eq}}$ ratios. These ratios were computed as follows:

SiO_2 content of Beltane opal = 87.96 percent

Assume all SiO_2 in the opal is reactive, then:

$$\text{SiO}_2 = (87.96/100)/60.084 = 14.64 \times 10^{-3} \text{ Moles per batch}$$

$$\text{Na}_2\text{O}_{\text{eq}} = (1.64/100)/61.981 = 0.265 \times 10^{-3} \text{ Moles per batch}$$

Therefore:

$$\text{SiO}_2/\text{Na}_2\text{O}_{\text{eq}} = (14.64/0.265) \times (\text{g opal/g cement}). \quad \text{Eq. 5.1.1}$$

In this computation it is assumed that all the SiO_2 reported in the oxide analysis of the opal is reactive, and that all of the $\text{Na}_2\text{O}_{\text{eq}}$ reported in the oxide analysis of the portland cement will become available. This computation, repeated for each mix, provides the apparent value of the x-coordinate to be paired with the y-coordinate, measured expansion of the hardened mortar mix, necessary to locate a

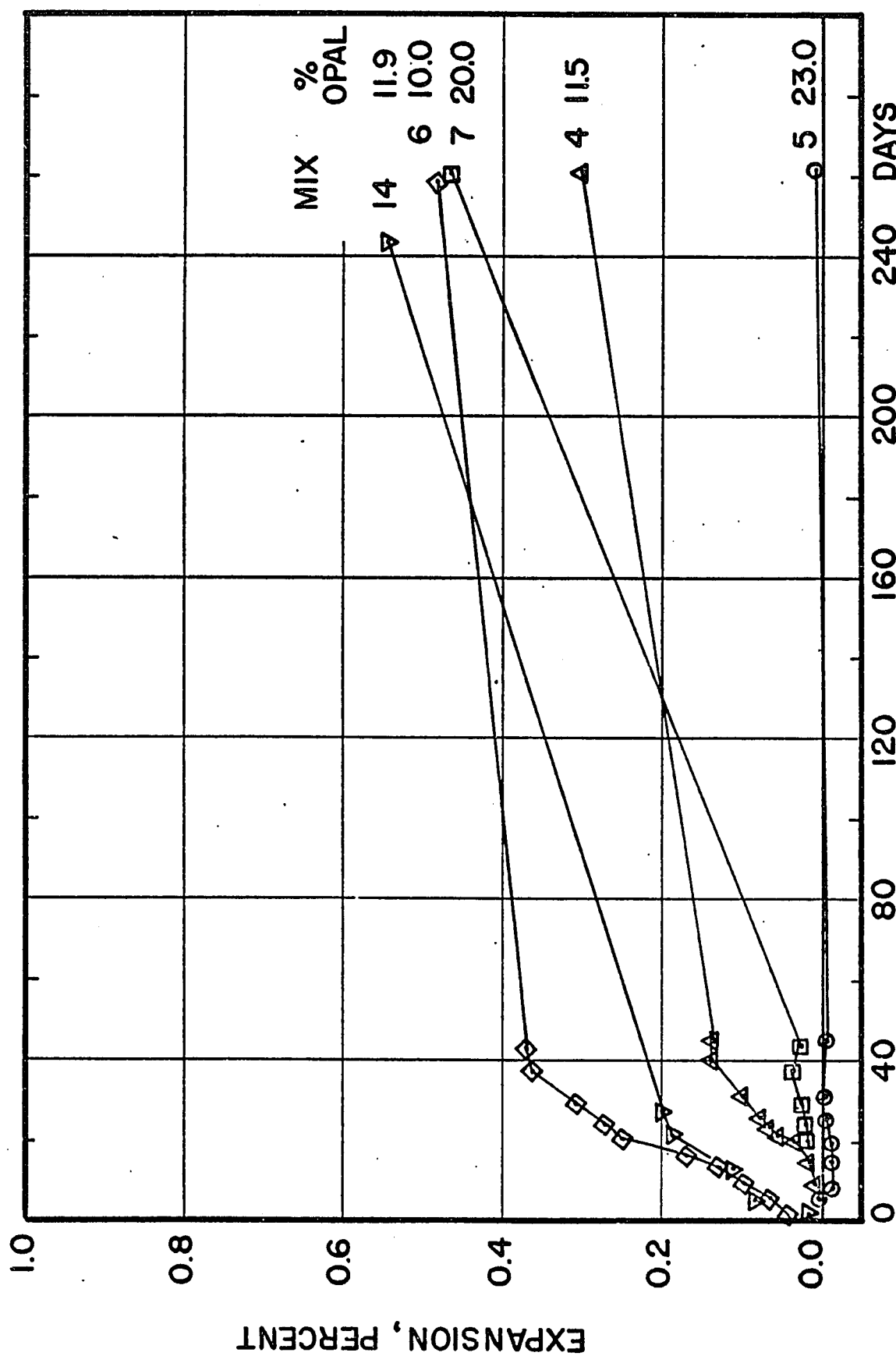


Figure 5.1.2 - Expansion vs. Time for Mixes 4 - 7, and Mix 14

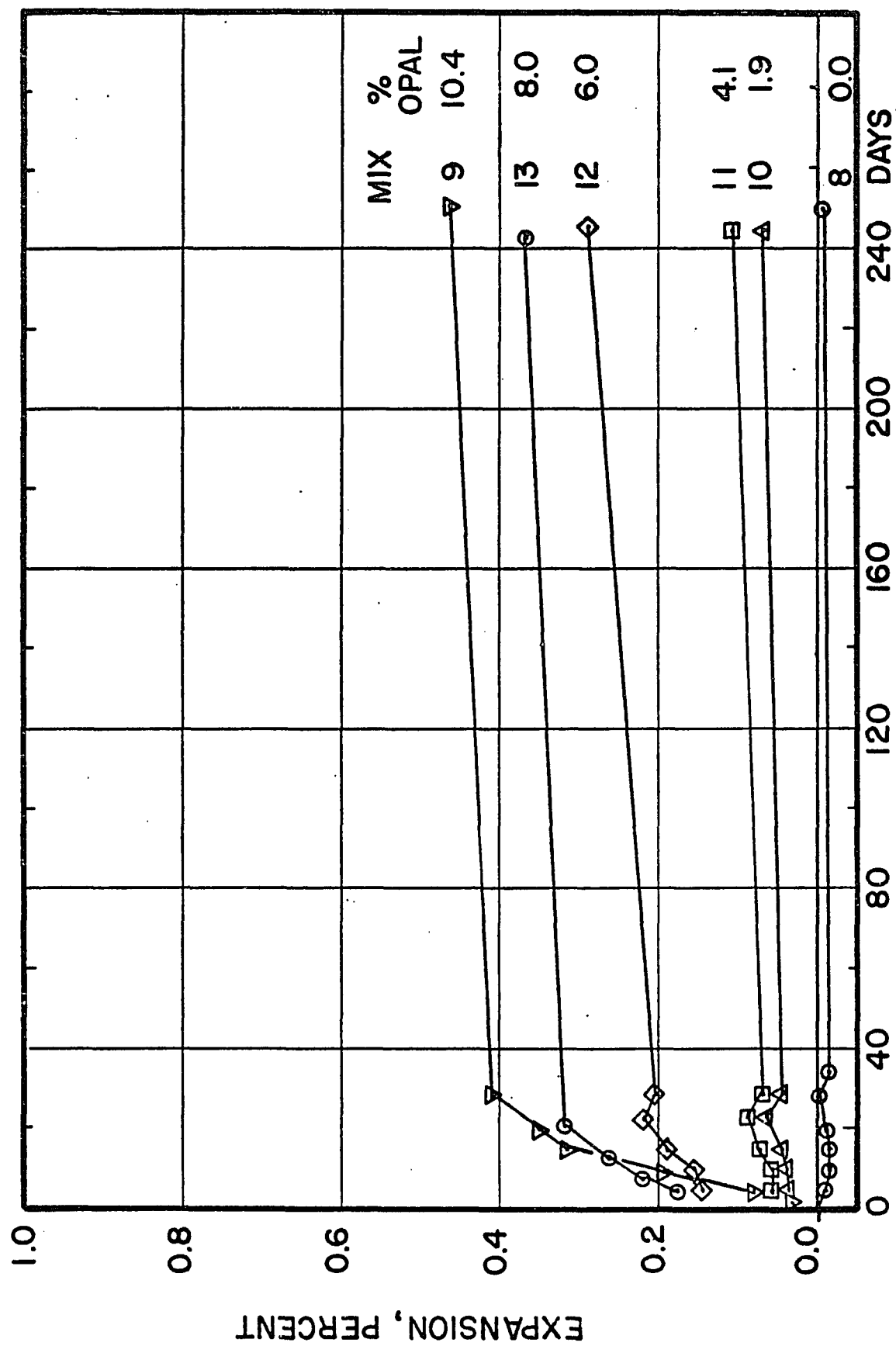


Figure 5.1.1 - Expansion vs. Time for Mixes 9 - 13

Table 5.1.2

Expansion and SiO₂/Na₂O eq for mix Series 4 - 14

Mix	g Opal Sand g Cement	SiO ₂ /Na ₂ O eq	Expansion μ in/in	Age, Days
4	0.115	6.36	3000	261
5	0.230	12.73	80	261
6	0.100	5.53	4787	259
7	0.200	11.07	4653	259
8	-	Control Mix	-80	250
9	0.104	5.75	4613	251
10	0.019	1.05	680	245
11	0.041	2.27	1080	245
12	0.060	3.32	2893	246
13	0.080	4.43	3680	243
14	0.119	6.58	5467	243

point on the plot of expansion versus apparent $\text{SiO}_2/\text{Na}_2\text{O}_{\text{eq}}$ molar ratio (see Figures 5.1.3 and 5.1.4). For Vivian's data (501), and for data presented in this Section, peak expansion is associated with an apparent $\text{SiO}_2/\text{Na}_2\text{O}_{\text{eq}}$ ratio of about 10. It should be noted that this is an apparent, not an effective, ratio of the reactants and that the extent to which the effective ratio approaches the apparent depends on a number of factors:

- The proportion of SiO_2 in the reactive component that is amorphous or unstable. In the case of Beltane opal, X-ray diffraction indicates only a trace of quartz is present.
- The extent to which alkalies in the reactant are released in the process of reaction.
- The compounds in which alkalies are present in the cement. Alkali sulfates and chlorides would be expected to go into solution within minutes after introduction of the mixing water to the batch. Alkalies contained in cement "minerals", e.g. alite, belite, ferrite phases, and the compounds Na_8A_3 , and $\text{KC}_{23}\text{S}_{12}$, will be released more slowly. Some of the alkalies in the cement will be permanently trapped in unhydrated grains of cement.
- The amount of leaching of alkalies that takes place during storage of the mortar specimens over water in sealed containers.
- The cross-sectional area, surface to volume ratio, and the permeability of the specimens. Leaching would be expected to be less for large specimens, with round cross-section, and with low permeability.

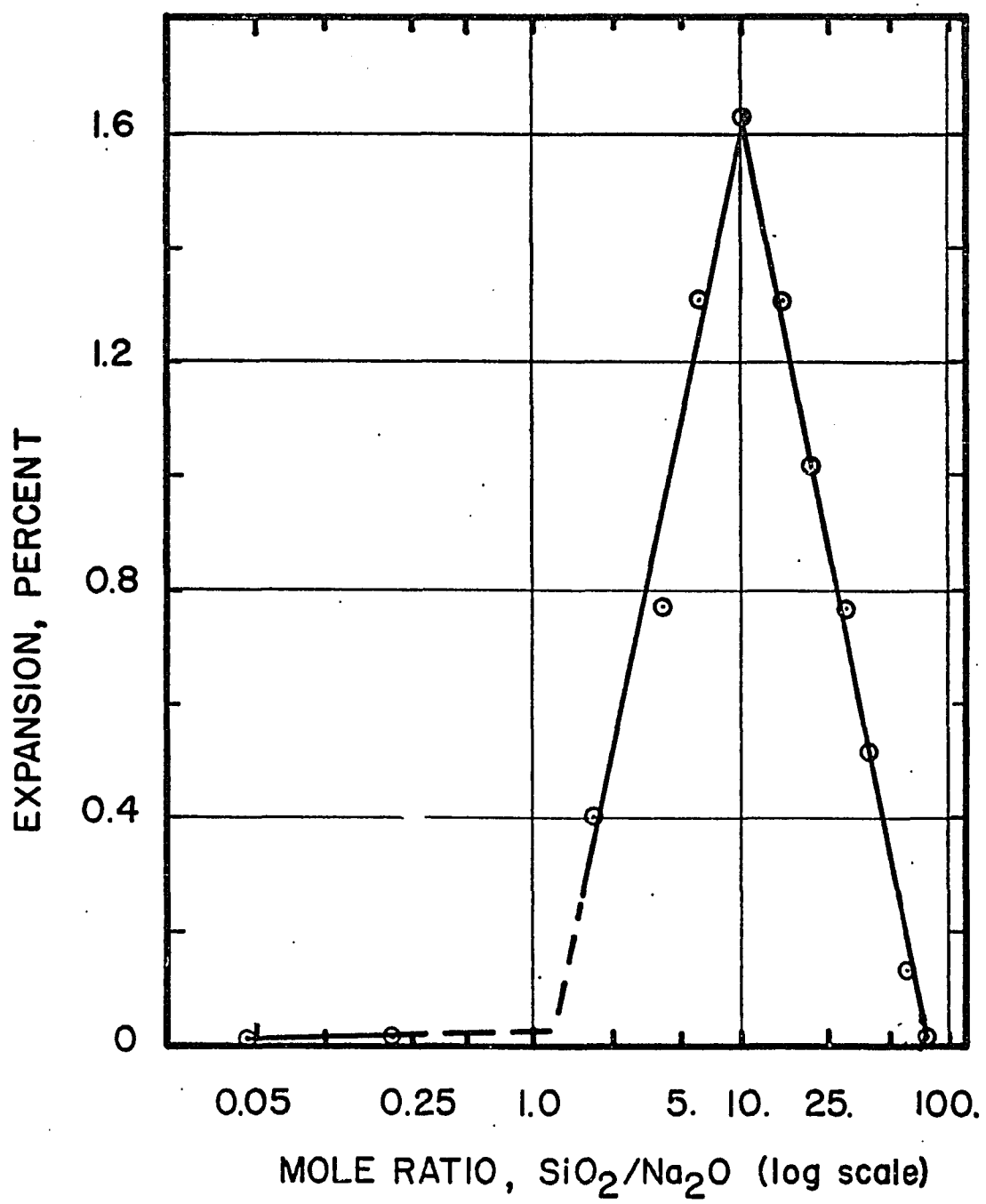


Figure 5.1.3 - Expansion vs. Mole Ratio $\text{SiO}_2/\text{Na}_2\text{O}$ eq

Data from Vivian (501)

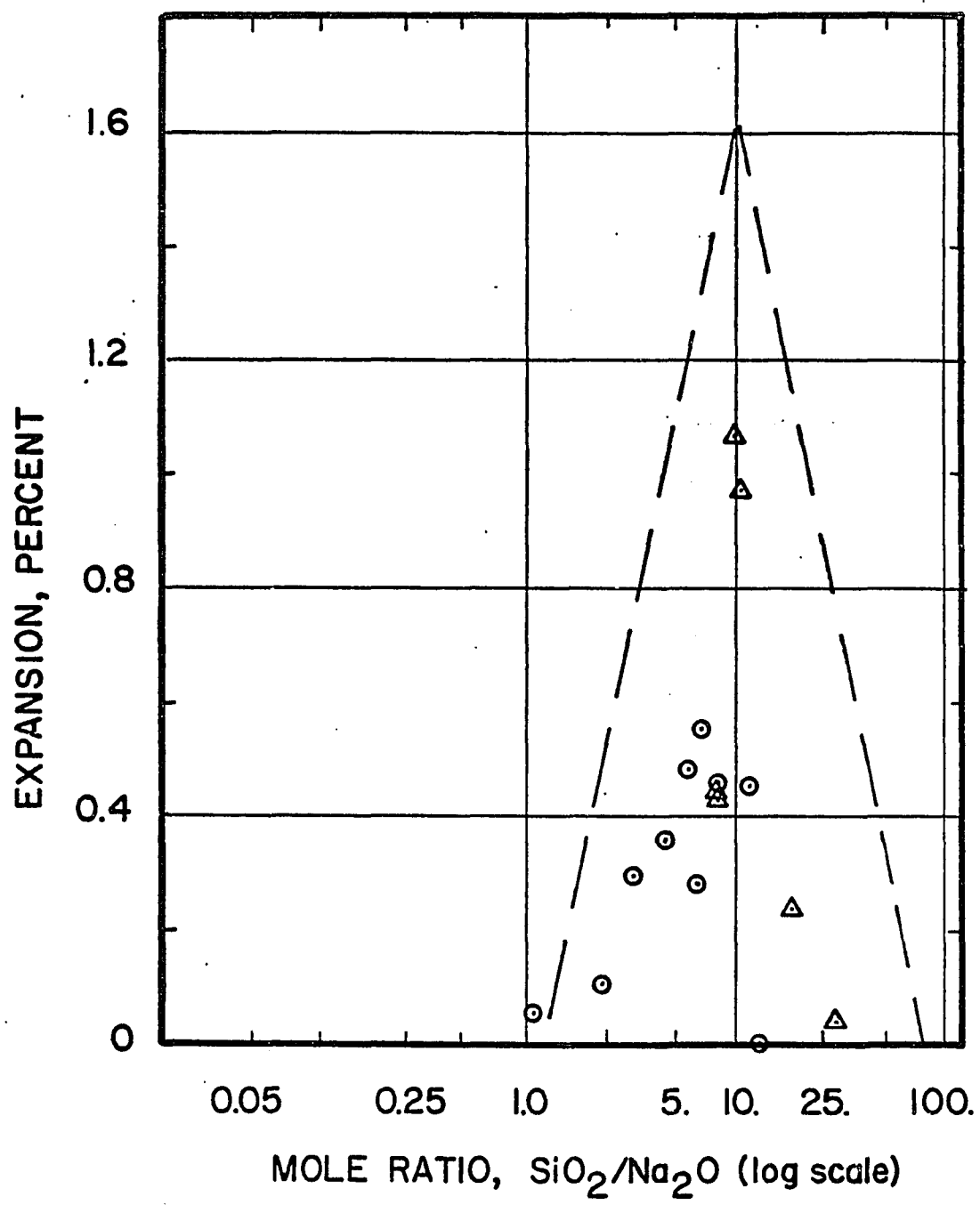


Figure 5.1.4 - Expansion vs. Mole Ratio $\text{SiO}_2/\text{Na}_2\text{O}$ eq
from Mix Series 4 - 14, and 15 - 21.

The combined effects of leaching and trapping of alkalis within unhydrated cement grains will result in a shifting of the $\text{SiO}_2/\text{Na}_2\text{O}_{\text{eq}}$ scale to the right in Figure 5.1.3. Thus, the effective ratio at which peak expansion occurs will be greater than the apparent ratio. In effect, the x-axis is shifted to the right so that apparently lower ratios of $\text{SiO}_2/\text{Na}_2\text{O}_{\text{eq}}$ produce peak expansion. In contrast, the peak expansion occurs at higher apparent ratios for specimens that are sealed or that have low leach rates. Cements with rapid and complete alkali release would be expected to exhibit higher expansions at higher apparent ratios than those with slow and incomplete release of alkalis. This seems a logical explanation of failure of some reactive concretes to expand when submerged, e.g. Parker Dam concrete located below the water line (502), and for apparently different pessimum $\text{SiO}_2/\text{Na}_2\text{O}_{\text{eq}}$ ratios observed by different investigators working with the same materials.

In Figure 5.1.3, data from the work of Vivian (501, p. 15) have been plotted, relating expansion of 1-in square cross-section mortar prisms, stored in moist air for 224 days at room temperature, to the ratio $\text{SiO}_2/\text{Na}_2\text{O}_{\text{eq}}$ on a logarithmic scale. Vivian described the reactive aggregate component used in this series as:

"V.17 Opal, Butcher's Ridge, East Gippsland. Milky-white to brown common opal occurring as veins in basalt. Chiefly opal but chalcedony is plentiful in cracks and vughs. A little quartz and limonite are also present." (503, p. 44)

In Vivian's work this material was crushed and sized to pass the No. 18 sieve and be retained on the No. 52 sieve ($1000 \times 300 \mu\text{m}$). This material was mixed with quartz sand from Leighton Buzzard,

England to provide the various aggregate combinations required. In the absence of specific chemical data it was assumed that the opal was entirely composed of reactive SiO_2 . The cement used contained 0.45 percent Na_2O and 0.81 percent K_2O , or 0.98 percent $\text{Na}_2\text{O}_{\text{eq}}$. The ratio $\text{SiO}_2/\text{Na}_2\text{O}_{\text{eq}}$ for the mixes whose expansions are depicted in Figure 5.1.3 was calculated from:

$$\text{SiO}_2/\text{Na}_2\text{O}_{\text{eq}} = (16.643/0.1586) \times (\text{g opal/g cement}) \quad \text{Eq. 5.1.2}$$

From Figure 5.1.3 the apparent pessimum molar ratio, $\text{SiO}_2/\text{Na}_2\text{O}_{\text{eq}}$ is approximately 10.

In Figure 5.1.4, the outline of the envelope of Vivian's data in the interval $\text{SiO}_2/\text{Na}_2\text{O}_{\text{eq}}$ 1 to 75 has been plotted in broken lines. The points in circles represent data taken from Table 5.1.2. Those points enclosed in triangles are for Mix Series 15 - 21 (see Section 5.2). The ages of the specimens range from 231 to 261 days. Three-quarters or more of that time the specimens were stored at ambient laboratory temperature.

Inspection of the plot suggests that the apparent pessimum molar ratio $\text{SiO}_2/\text{Na}_2\text{O}_{\text{eq}}$ lies in the range 6 to 10 for opaline aggregate contaminants. Similar data can be derived from the results of Stanton (504), Breedsdorff et.al. (505), Wolf (506), and Sprung (507), working with opaline or other highly reactive aggregates.

5.2 - Mix Series 15 - 21

In this group a portion of the experiments conducted in the previous series was repeated with a different cement, AT-1, in which the

proportions of Na_2O and K_2O were nearly reversed: 0.30 percent Na_2O , 0.93 percent K_2O , or 0.91 percent $\text{Na}_2\text{O}_{\text{eq}}$.

Beltane opal sand, prepared from the preliminary sample of opal obtained from the Beltane Quarry, was again used as the reactive component, and all aggregates were sieved and recombined to result in 50 percent being between $600 \times 300 \mu\text{m}$, and 50 percent being between $300 \times 150 \mu\text{m}$. In addition, by grinding some of the crushed Beltane opal in a small laboratory mill, a pozzolanic material, BP-1, was produced with a Blaine specific surface of $7880 \text{ cm}^2/\text{g}$. The specific gravity of this material was 2.07, making the surface area on a volumetric basis $16,320 \text{ cm}^2/\text{cm}^3$. Subsequent microscopic examination of BP-1 indicated that perhaps 20 to 30 percent of the particles were larger than $75 \mu\text{m}$. Perhaps the presence of this coarse material explains the large observed expansion for mix 17, in which the opaline addition was entirely as ground opal. This problem was eliminated in subsequent work by using a large jar mill and substituting steel grinding balls for porcelain slugs and sieving the ground material to remove coarse particles. The same mixing and storage procedures, and conditions employed in the previous series were used in this series.

Batch weights for mixes 15 - 21 are listed in Table 5.2.1.

The course of expansions observed for this series of mixes is similar to that observed for Mix Series 4 - 14, and has not been plotted. The expansions observed at the time the specimens were terminated, together with the apparent $\text{SiO}_2/\text{Na}_2\text{O}_{\text{eq}}$ ratios, are listed in Table 5.2.2, and have been plotted in small triangles in Figure 5.1.4.

Table 5.2.1

Batch Weights, grams, for Mixes 15 - 21

Materials	Mix 15, 10.4% Opal Sand		Mix 16, Control		Mix 17, 10.1% Opal Pozzolan	
	Parts by Weight	Batch Weights	Parts by Weight	Batch Weights	Parts by Weight	Batch Weights
Cement, AT-1	1.000	16.00	1.000	16.00	1.000	16.00
Water	0.500	8.00	0.500	8.00	0.500	8.00
Beltane Sd.*	0.104	1.66	0.000	--	0.000	--
Beltane Pozz.	0.000	--	0.000	--	0.101	1.62
Sand, C109*	1.370	29.92	1.976	31.60	1.874	29.98
Totals	<u>3.474</u>	<u>55.58</u>	<u>3.475</u>	<u>55.60</u>	<u>3.475</u>	<u>55.60</u>

Materials	Mix 18, 8.0% Opal Sand		Mix 19, 8.0% Opal Sd., 10.1% Opal Poz.		Mix 20, 8.0% Opal Sd., 20.% Opal Poz.	
	Parts by Weight	Batch Weights	Parts by Weight	Batch Weights	Parts by Weight	Batch Weights
Cement, AT-1	1.000	16.00	1.000	16.00	1.000	16.00
Water	0.500	8.00	0.500	8.00	0.500	8.00
Beltane Sd.*	0.080	1.28	0.080	1.28	0.080	1.28
Beltane Pozz.	0.000	--	0.101	1.62	0.200	3.20
Sand, C109*	1.896	30.32	1.794	28.70	1.696	29.52
Totals	<u>3.475</u>	<u>55.60</u>	<u>3.475</u>	<u>55.60</u>	<u>3.475</u>	<u>55.60</u>

Materials	Mix 21, 8.0% Opal Sd., 5.0%Opal Pozz	
	Parts by Weight	Batch Weights
Cement, AT-1	1.000	16.00
Water	0.500	8.00
Beltane Sd.*	0.080	1.28
Beltane Pozz.	0.050	0.80
Sand, C109*	1.845	29.52
Totals	<u>3.475</u>	<u>55.60</u>

* Beltane and C109 sand
graded 50% 600 x 300 μm ,
50% 300 x 150 μm .

Table 5.2.2

Expansion and SiO₂/Na₂O eq. for Mix Series 15 - 21

Mix	g Opal Sand g Cement	g Pozzolan BP-1 g Cement	SiO ₂ /Na ₂ O eq.	Expansion μ in/in	Age, Days
15	0.104	-	10.37	9680	244
16	-	-	Control Mix	227	233
17	-	0.101	10.07	10680	233
18	0.080	-	7.98	4307	233
19	0.080	0.101	18.05	2400	233
20	0.080	0.200	27.92	413	231
21	0.080	0.050	12.96	4540	231

The $\text{SiO}_2/\text{Na}_2\text{O}_{\text{eq}}$ ratio for this series of mixes has been computed from the formula:

$$\text{SiO}_2/\text{Na}_2\text{O}_{\text{eq}} + [(0.8796/60.084) / (0.0091/61.981)] \times \\ [(\text{g opal sand} + \text{g opal pozzolan}) / \text{g cement}] \quad \text{Eq. 5.2.1}$$

5.3 - Mix Series 22 - 24

This series consisted of three portland cement paste mixes with water-cement ratios of 0.40, 0.45, and 0.50, by weight. These specimens were used to determine the ability of the pore fluid expression die to express fluids from specimens with a modest range of water-cement ratios. With successful demonstration of ability to perform this task, no further use was made of the specimens from this series.

5.4 - Mix Series 25 - 27

This series consisted of three mortar mixes prepared with the same range of water-cement ratios used in the paste series above, and used for a similar purpose. With successful demonstration of the ability to perform this task no further use was made of the specimens from this series.

5.5 - Mix Series 28 - 31

In this series the effects of the addition of one percent (by weight of cement) lithium carbonate (Li_2CO_3) to mixes with and without 8 percent (by weight of cement) replacement of quartz sand with Beltane opal sand were studied. Batch weights for the mixes are listed in Table 5.5.1. Weight ratios of the component materials, oven-dry/batch and ignited/batch, are listed in Table 5.5.2.

Table 5.5.1

Batch Weights, grams, for Mixes 28 - 31

Materials	Mix 28, Control		Mix 29, 1 % Li ₂ CO ₃		Mix 30, 8% Opal Sand	
	Parts by Weight	Batch Weights	Parts by Weight	Batch Weights	Parts by Weight	Batch Weights
Cement, AT-1	1.00	192.1	1.00	192.0	1.00	191.1
Water	0.50	96.1	0.50	96.0	0.50	95.5
Li ₂ CO ₃	0.00	--	0.01	2.0	0.00	--
Beltane Sd.*	0.00	--	0.00	--	0.08	15.0
Sand, C109	1.97	378.9	1.96	376.6	1.89	361.8
Totals	<u>3.47</u>	<u>667.1</u>	<u>3.47</u>	<u>666.6</u>	<u>3.47</u>	<u>663.4</u>

Mix 31, 8% Opal Sd,
1% Li₂CO₃

Materials	Parts by Weight	Batch Weights
Cement, AT-1	1.00	191.0
Water	0.05	95.5
Li ₂ CO ₃	0.01	2.0
Beltane Sd.*	0.08	15.0
Sand, C109	1.88	359.6
Totals	<u>3.47</u>	<u>663.1</u>

* Beltane opal sand, 50% 600 x 300 μm , 50% 300 x 150 μm .

Table 5.5.2

Weight Ratios of Component MaterialsOven-Dry/Batch, Ignited/Batch

Material	W_{od}/W_o	W_{ig}/W_o
Cement, AT-1	0.99809	0.99483
Beltane Sand	0.99445	0.95298
Sand, C109	0.99993	0.99868

Expansion measurements were made on hardened specimens prepared from all mixes, and the results are listed in Table 5.5.3.

Concentrations of ions found in expressed pore solutions are listed in Tables 5.5.4 through 5.5.7. Data for W_n/c were not obtained for this mix series. In order to make the correction to compensate for W_n/c the estimating equation (Eq. 4.11.11), fitted to data for selected control mixes, was used. The assumptions, only approximately true, were made that additions of reactive silica and Li_2CO_3 , and curing at 40°C, had no significant effect on W_n/c . Nonevaporable water contents, estimated by the use of Eq. 4.15.11, were used to calculate the compensated alkali metal ion concentrations listed in Tables 5.5.8 through 5.5.12. The method of computation is outlined in Section 4.16. Data from these tables have been plotted in Figures 5.5.2 and 5.5.3.

Examination of Figures 5.5.2 and 5.5.3 suggests the following conclusions:

- Concentrations of Na^+ and K^+ in pore solutions expressed from the control mix, mix 28, tended to increase with time, after an initial decrease at about 15 days.
- Addition of Li_2CO_3 , mix 29, had little effect on the above trend. The Li^+ concentration fell to a minimum at 30 days and then rose gradually.
- Addition of opal to the control mix, mix 30, resulted in the usual dramatic reduction in both Na^+ and K^+ , with little change after 10 days.

Table 5.5.3

Observed Expansions of Mortar Prisms, Mixes 28 - 31

(Expansion in Microstrain Units)

Age, Days at 40° C.	Mix 28 Control	Mix 29, 1% Li ₂ CO ₃		Mix 30, 8% Opal Sand		Mix 31, 8% Opal Sand and 1% Li ₂ CO ₃	
	0.25-in ² (6.35-mm ²)	0.25-in ² (6.35-mm ²)	0.50-in ² (12.7-mm ²)	0.25-in ² (6.35-mm ²)	0.50-in ² (12.7-mm ²)	0.25-in ² (6.35-mm ²)	0.50-in ² (12.7-mm ²)
0.84	100		57	187	80	107	0
1.84	40	67	100	380	360	200	80
2.88	100	27	60	540	540	173	80
4.63	100	40	80	700	780	240	180
6.91	80	80	80	960	1060	280	160
8.91	-20	133	100	1160	1200	280	80
14.92	80	53	120	1440	1480	293	80
22.97	80	93	60	1627	1760	307	160
31.28	100	160	100	1867	2080	360	160
49.	100	147	200	1973	2100	400	240
74.	100	267	220	2080	2120	427	240
151.	160	253	280	2160	2160	733	400
243.	280	307	400	2213	2280	827	500

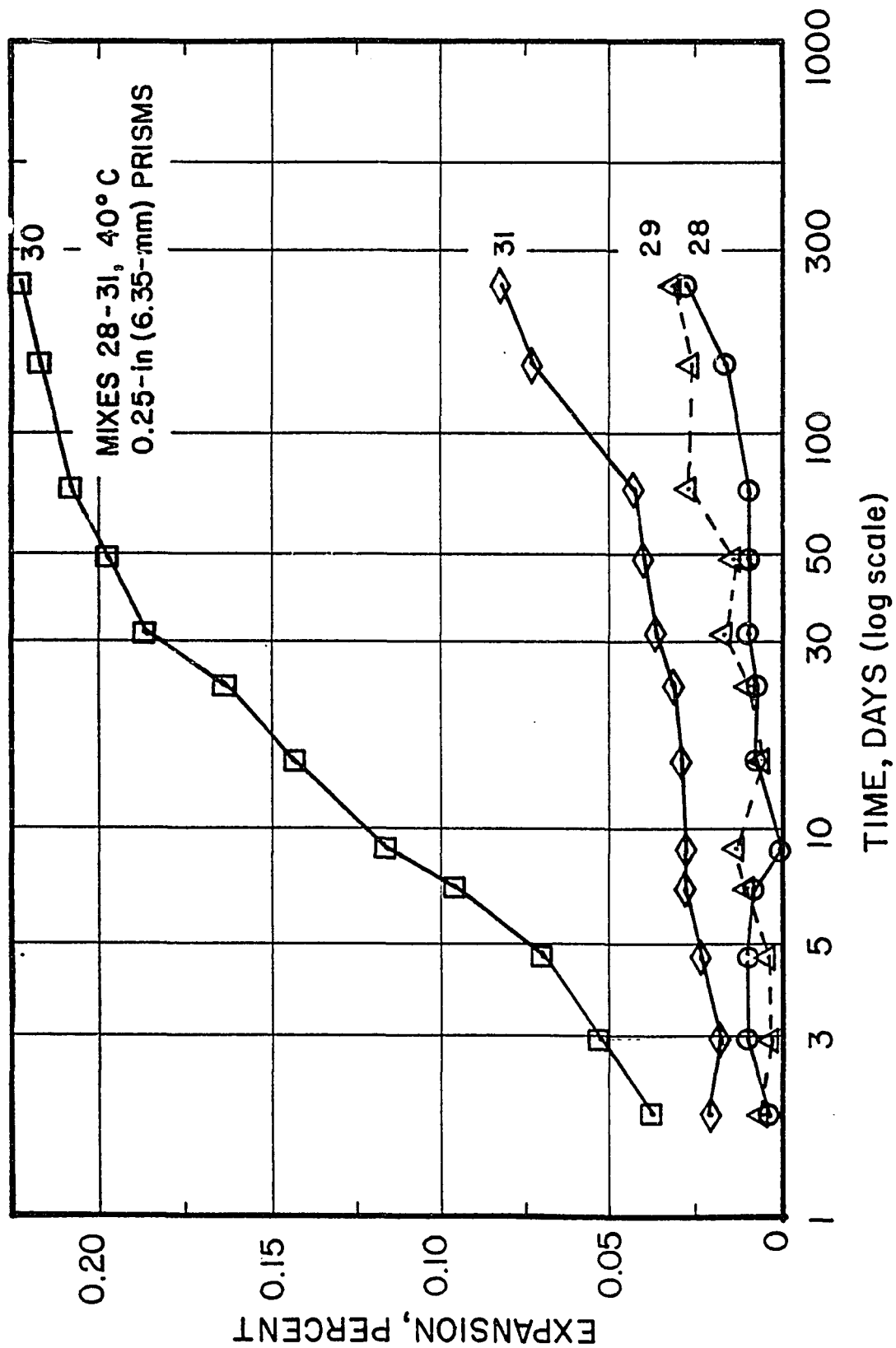


Figure 5.5.1 - Mortar Prism Expansion vs. Time

Table 5.5.4

Observed Concentrations of Ions in Expressed Pore Solution (Not Corrected for Bound Water)Mix 28, Control for Mix Series 28 - 31

(Concentrations in millimoles/liter)

Age, Days at 40° C.	Si ⁴⁺ *	Al ³⁺	Fe ³⁺	Mg ⁺⁺	Ca ⁺⁺	Na ⁺	K ⁺	Li ⁺	$\Sigma +^{**}$	OH ⁻	SO ₄ ⁼	$\Sigma -^{**}$	$\Sigma + -^{**}$
9	2.7	0.0	0.0	0.0	1.	202.	476.	2.	682.	662.	n.d.		
16	5.5	0.0	0.0	0.0	--	218.	440.	--	658.	678.	n.d.		
30	1.8	0.0	0.0	0.0	2.	228.	524.	4.	760.	724.	n.d.		
73	0.2	0.0	0.0	0.0	1.	277.	644.	2.	925.	756.	60	876.	+49.

* See remarks under Section 4.4.1

** milliequivalents/liter

n.d. = not determined

Table 5.5.5

Observed Concentrations of Ions in Expressed Pore Solution (Not Corrected for Bound Water)

Age, Days at 40° C.	(Concentrations in millimoles/liter)												
	Si^{4+} *	Al^{3+}	Fe^{3+}	Mg^{++}	Ca^{++}	Na^+	K^+	Li^+	$\Sigma +^{**}$	OH^-	$\text{SO}_4^{=}$	$\Sigma -^{**}$	$\Sigma +-\^{**}$
9	2.9	0.0	0.0	0.0	1.	198.	491.	432.	1123.	994.	n.d.		
16	2.7	0.0	0.0	0.0	n.d.	212.	471.	416.	1311.	992.	n.d.		
30	1.3	0.0	0.0	0.0	1.	216.	524.	369.	1111.	1030.	n.d.		
73	0.2	0.1	0.0	0.0	1.	249.	610.	401.	1262.	994.	96.	1186.	+76.

* See remarks under Section 4.4.1

** milliequivalents/liter

n.d. = not determined

Table 5.5.6

Observed Concentrations of Ions in Expressed Pore Solution (Not Corrected for Bound Water)

Mix 30, 8% Opal Sand

(Concentrations in millimoles/liter)

Age, Days at 40° C.	Si^{4+*}	Al^{3+}	Fe^{3+}	Mg^{++}	Ca^{++}	Na^+	K^+	Li^+	Σ^{+**}	OH^-	$\text{SO}_4^{=}$	Σ^{-*}	Σ^{+-**}
9	3.6	0.0	0.0	0.0	1.	87.	169.	3.	261.	270.	n.d.		
16	1.6	0.0	0.0	0.0	n.d.	89.	95.	n.d.	184.	275.	n.d.		
30	3.3	0.0	0.0	0.0	3.	76.	141.	9.	232.	246.	n.d.		
73	1.0	0.0	0.0	0.0	1.	150.	196.	12.	360.	305.	7.	319.	+41.

* See remarks under Section 4.4.1

** milliequivalents/liter

n.d. = not determined

Table 5.5.7

Observed Concentrations of Ions in Expressed Pore Solution (Not Corrected for Bound Water)Mix 31, 8% Opal Sand and 1% Li₂CO₃

(Concentration in millimoles/liter)

Age, Days at 40° C.	Si ⁴⁺ *	Al ³⁺	Fe ³⁺	Mg ⁺⁺	Ca ⁺⁺	Na ⁺	K ⁺	Li ⁺	Σ^{+} **	OH ⁻	SO ₄ ⁼	Σ^{-} **	Σ^{+-} **
9	2.9	0.0	0.0	0.0	3.	144.	303.	226.	679.	611.	n.d.		
16	2.2	0.0	0.0	0.0	n.d.	162.	210.	200.	572.	622.	n.d.		
30	1.7	0.0	0.0	0.0	3.	152.	294.	217.	669.	614.	n.d.		
73	0.4	0.0	0.0	0.0	1.	190.	298.	135.	625.	536.	13.	562.	+63.

* See remarks under Section 4.4.1

** milliequivalents/liter

n.d. = not determined

Table 5.5.8

Concentrations of Alkali Metal Cations in Expressed Pore Solution (Corrected for Bound Water)

Mix 28, Control for Mix Series 28 - 31

(Concentrations in millimoles/liter)

Age, Days at 40° C	W _n /c	bwk	Cations Found			Cation Concentration Corrected for W _n /c						*K ⁺ / *Na ⁺
			*Na ⁺	Δ*Na ⁺	*K ⁺	Δ*K ⁺	ΣM ⁺	Δ*M ⁺				
9	0.166	0.668	202	476	678	135	--	318	--	453	--	2.365
16	0.177	0.646	218	440	658	141	--	284	--	425	--	2.018
30	0.185	0.630	228	524	752	144	--	330	--	474	--	2.298
73	0.192	0.616	277	644	921	171	--	397	--	567	--	2.325

Table 5.5.9

Concentrations of Alkali Metal Cations in Expressed Pore Solutions (Corrected for Bound Water)

Mix 29, 1% Li₂CO₃

(Concentrations in millimoles/liter)

Age, Days at 40° C	W _n /c	b/wk	Cations Found			Cation Concentrations Corrected for W _n /c		
			Na ⁺	K ⁺	Li ⁺	*Na ⁺	*K ⁺	Li ⁺
9	0.166	0.668	198	491	432	1121	132	-3
16	0.177	0.646	212	471	420	1103	137	-4
30	0.185	0.630	216	524	369	1109	136	-8
73	0.192	0.616	294	610	401	1305	181	+10
							376	-21
							328	+10
							304	20
							330	0
							376	-21
							289	+289
							271	271
							232	232
							247	247

Age, Days at 40° C	Σ^*M^+	$\frac{\Delta^*M^+}{\Sigma^*M^+}$	$*K^+ / *Na^+$	
			$*K^+$	$*Na^+$
9	749	+296	2.480	
16	713	287	2.222	
30	699	225	2.426	
73	804	237	2.075	

Table 5.5.10
 Concentrations of Alkali Metal Cations in Expresssed Pore Solution (Corrected for Bound Water)
Mix 30, 8% Opal Sand
 (Concentrations in millimoles/liter)

Age, Days at 40° C	M_n/c	bulk	Cations Found			$*\text{Na}^+$	$\Delta *\text{Na}^+$	$*\text{K}^+$	$\Delta *\text{K}^+$	$\Sigma *\text{M}^+$	$\Sigma *\text{M}^+$	V_n/c	$*\text{K}^+/\text{*Na}^+$
			Na^+	K^+	ΣM^+								
9	0.166	0.668	87	169	256	58	-77	113	-205	171	-282	1.943	
16	0.177	0.646	89	95	184	57	-83	61	-223	119	-306	1.067	
30	0.185	0.630	76	149	225	48	-96	94	-236	142	-332	1.961	
73	0.192	0.616	150	196	346	92	-78	121	-276	213	-354	1.307	

Table 5.5.11
Concentrations of Alkali Metal Cations in Expressed Pore Solutions (Corrected for Bound Water)
Mix 31, 8% Opal Sand and 1% Li₂CO₃
(Concentration in millimoles/liter)

Age, Days at 40° C	W _n /c	b _{wk}	Cations Found			Cation Concentrations Corrected for W _n /c		
			Na ⁺	K ⁺	Li ⁺	Na ⁺	K ⁺	Li ⁺
9	0.166	0.668	142	297	187	626	95	-40
16	0.177	0.646	162	210	200	572	105	-36
30	0.185	0.630	152	294	217	663	96	-48
73	0.192	0.616	190	298	135	623	117	-54
							198	-120
							136	-149
							185	-145
							184	-213
							83	83
Age, Days at 40° C	Σ*M ⁺	$\frac{*K^+}{*Na^+}$	$\frac{*K^+}{*Na^+}$	$\frac{*K^+}{*Na^+}$	$\frac{*K^+}{*Na^+}$	$\frac{*K^+}{*Na^+}$	$\frac{*K^+}{*Na^+}$	$\frac{*K^+}{*Na^+}$
9	418	-35	2.092					
16	370	-56	1.296					
30	418	-56	1.934					
73	384	-184	1.568					

Table 5.5.12
Concentrations of Alkali Metal Cations in Expresssed Pore Solutions (Corrected for Bound Water)
Mix 31, 8% Opal Sand and 1% Li₂CO₃
(Concentrations in millimoles/liter)

Age, Days at 40° C	W _{n/c}	bwk	Cations Found			Cation Concentrations Corrected for W _{n/c} **		
			Na ⁺	K ⁺	Σ M ⁺	*Na ⁺	*K ⁺	*Li ⁺
9	0.156	0.668	142	297	187	625	95	-37
16	0.177	0.646	162	210	200	589	105	-32
30	0.185	0.630	152	294	217	663	96	-40
73	0.192	0.616	190	298	135	623	117	-64

Age, Days at 40° C	Σ *M ⁺	$\frac{\Delta *M^+}{\Sigma *M^+}$	*K ⁺ / *Na ⁺	
			** Mix 29, 1% Li ₂ CO ₃ , used as control mix.	** Mix 31, 8% Opal Sand and 1% Li ₂ CO ₃
9	418	-331	2.092	
16	380	-331	1.296	
30	418	-281	1.934	
73	384	-420	1.568	

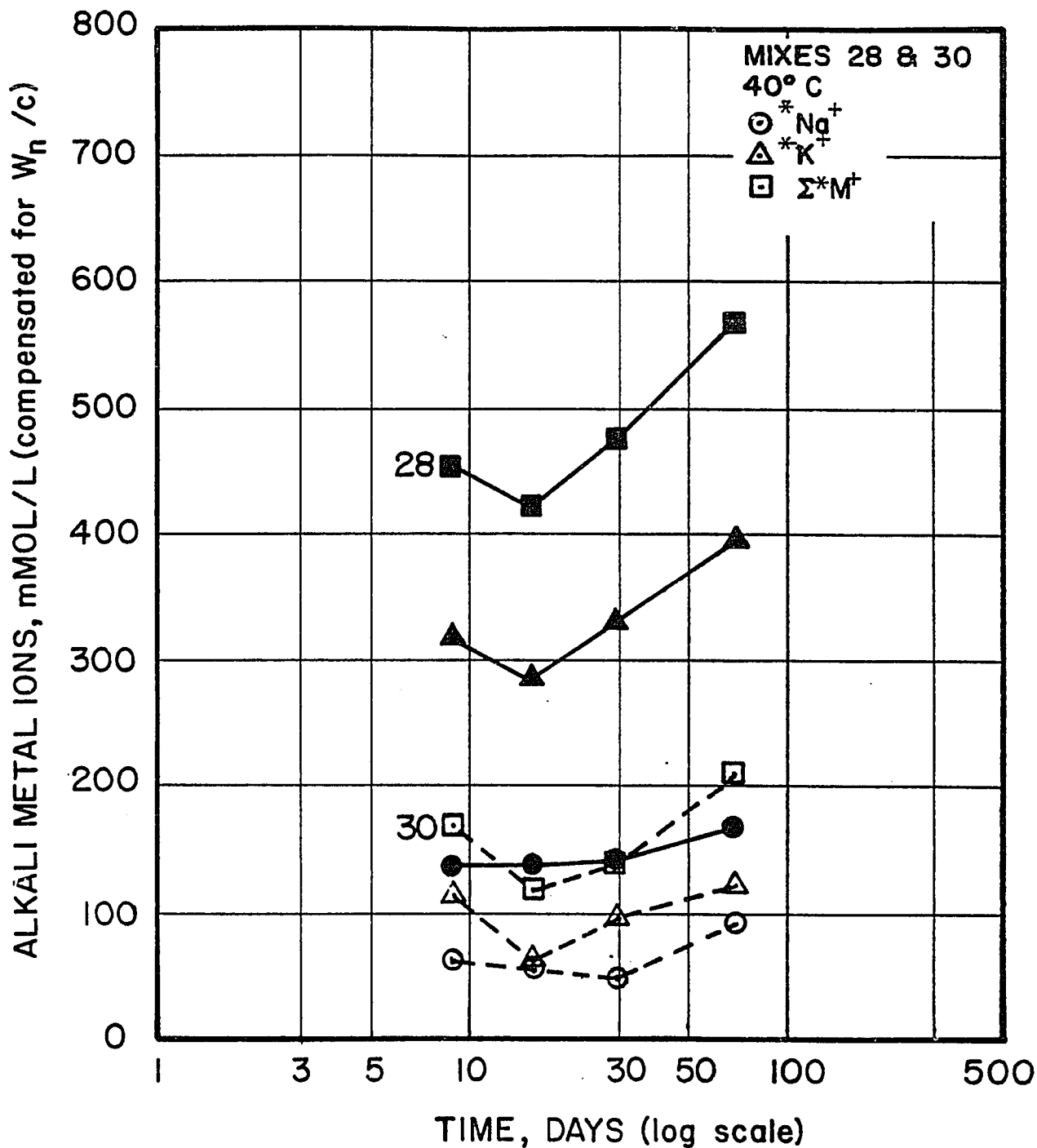


Figure 5.5.2 - Alkali Metal Ion Concentration vs. Time

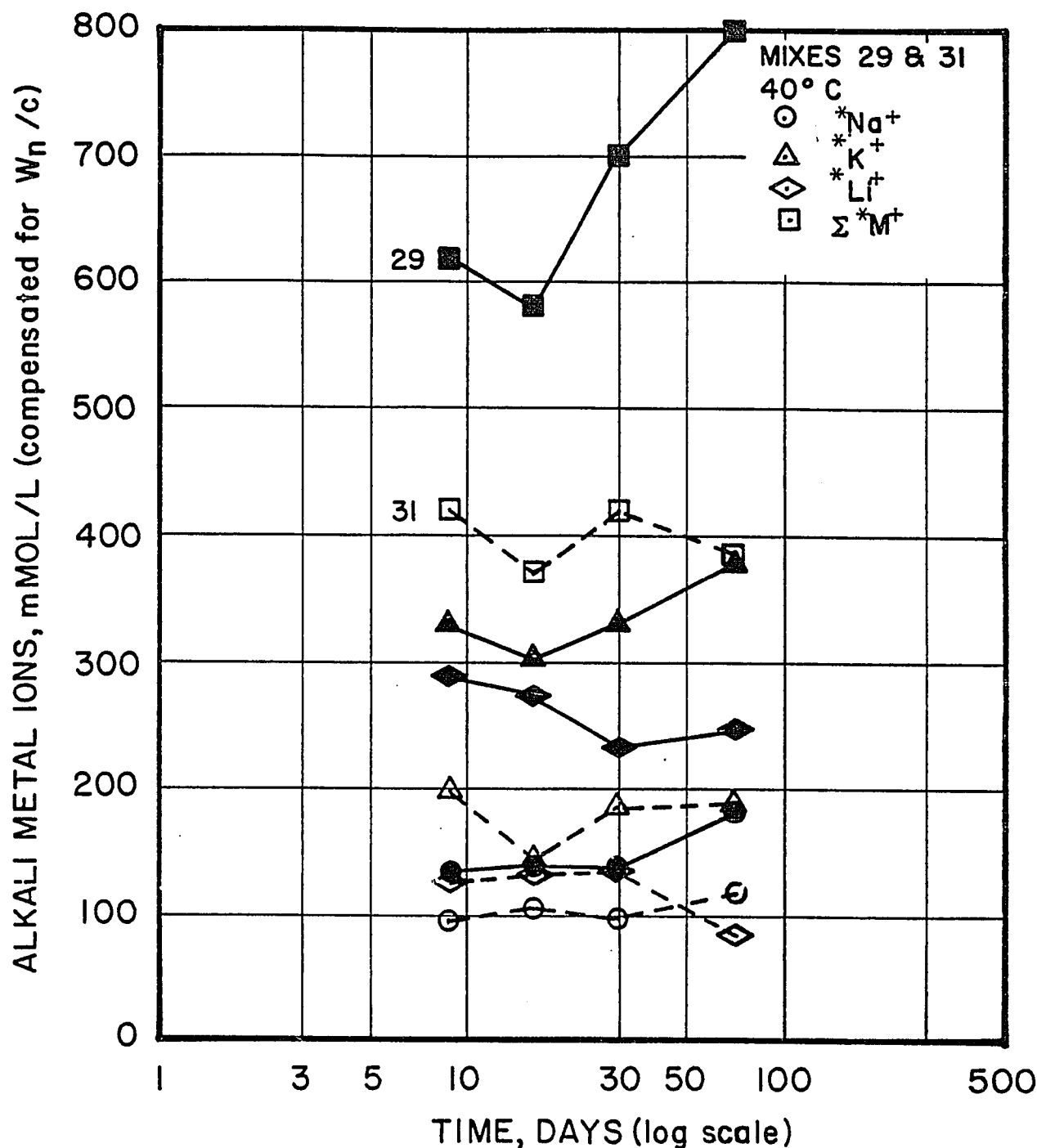


Figure 5.5.3 - Alkali Metal Ion Concentration vs. Time

- Addition of both opal sand and Li_2CO_3 , mix 31, resulted in a reduced rate of removal of Na^+ and K^+ from the pore solution. It appears that the Li^+ is preferentially consumed by the reaction with opal.

These phenomena may, in part, be the result of the relative insolubility of Li_2CO_3 , which is about 0.180 moles/L (360 M Mol Li^+ /of solution in pure water at 20°C (508, Vol. II, p. 384,f.), as compared to the nearly unlimited solubility of the Na^+ and K^+ compounds present. Had all of the added Li_2CO_3 gone into solution the Li^+ concentration of the solution would have been 0.541 moles Li^+/L .

For additional studies containing information on early-age pore solution concentrations of Li^+ , see Section 5.12.

As noted by McCoy and Caldwell (509), the potential expansion of the opal-containing mixes is significantly reduced by the addition of Li_2CO_3 . Observed expansions for mixes 28 through 31 have been listed in Table 5.5.3 and plotted in Figure 5.5.1.

The $\text{SiO}_2/\text{Na}_2\text{O}_{\text{eq}}$ ratios for mixes 30 (8 percent opal sand) and 31 (8 percent opal sand + 1 percent Li_2CO_3) were 8.0 and 4.15 respectively, taking 0.839-g Li_2CO_3 equivalent to one-g of Na_2O . The 243 day expansion measurements for 0.5-in (12.7-mm) prisms were 2280 and 500 $\mu\text{in}/\text{in}$ respectively. It seems possible that the reduction in expansion found to result from the addition of lithium ions may stem from the reduction in the $\text{SiO}_2/\text{Na}_2\text{O}_{\text{eq}}$ balance. Expansion results for the two mixes containing opal sand may be referenced to a plot of the kind Vivian used to relate expansion to $\text{SiO}_2/\text{Na}_2\text{O}_{\text{eq}}$ (See Figure 5.1.3). On this plot decreasing the $\text{SiO}_2/\text{Na}_2\text{O}_{\text{eq}}$ ratio below 10 reduces expansion;

similarly the present demonstrated effectiveness of the added lithium in reducing expansion may result merely from the difference in $\text{SiO}_2/\text{Na}_2\text{O}_{\text{eq}}$ ratio. It is also possible that reduction in expansion observed by McCoy and Caldwell (509) may also have resulted from this same phenomenon.

5.6 - Mix Series 32 - 33

In this series an attempt was made to study the effects of three levels of storage temperature, 20°, 40°, and 60°C, on potential expansion of hardened mortar prisms. A control mix and a mix with 7.8 percent, Beltane opal sand by weight of cement, were used in this series. Batch weights for these mixes are listed in Table 5.6.1.

At the reading following 66 days storage, it was noted that the combination paper-plastic jar seals in several of the storage containers had deteriorated, allowing the specimens to become dry. These mixes were terminated at that point. Expansion data obtained through 66 days are considered valid and are listed in Table 5.6.2.

From the limited data available the following tentative conclusions are drawn with respect to the behavior of mortar specimens containing Beltane opal:

- Based on data at 66 days, expansion is inversely related to storage temperature, being reduced about 54 $\mu\text{in/in}$ for each degree increase in the range 20°-60°C for 0.5-in (12.7-mm) cross-section prisms.
- In general, 0.5-in (12.7-mm) cross-section prisms tend to expand slightly more than 0.25-in (6.35-mm) cross-section prisms. The

Table 5.6.1

Batch Weights, grams, for Mixes 32 - 33

Materials	Mix 32, Control		Mix 33, 8% Opal Sand	
	Parts by Weight	Batch Weights	Parts by Weight	Batch Weights
Cement, AT-1	1.000	192.1	1.000	191.1
Water	0.500	96.1	0.500	95.5
Beltane Sd.*	0.000	--	0.078	15.0
Sand, C109	1.972	378.9	1.893	361.8
Totals	3.472	667.1	3.471	663.4

* Beltane opal sand graded 50% 600 x 300 μm , 50% 300 x 150 μm .

Table 5.5.2

Observed Expansions of Mortar Prisms ($\mu\text{in/in}$), Mixes 32 - 33

Time, Days	Mix 32 Series a	Mix 32 Series b	Mix 33 Series a	Mix 33 Series b	Mix 33 Series c	Mix 33 Series d	Mix 33 Series e	Mix 33 Series f
1	0	160	93	20	27	360	280	760
3	0	187	587	600	80	1280	533	1300
7	53	280	2013	2360	253	2140	907	1640
15	27	307	3173	3680	720	2660	1480	2060
22	27	387	3560	4140	947	3200	2000	2060
40	160	427	4226	4900	1107	3380	2267	2640
66	280	347	4200	4860	1360	3420	2360	2720
235	--	--	4800	5540	--	--	--	--
502	--	--	4720	5780	--	--	--	--
<hr/>								
Temperature of:								
Storage	40° C	60	20	20	40	40	60	60
Measurement	40° C	20	20	20	40	20	20	20
Cross- Section	0.25 in 6.35mm	0.25 6.35	0.25 6.35	0.50 12.7	0.25 6.35	0.50 12.7	0.25 6.35	0.50 12.7

results of series c of mix 33 are considered anomalous, as may be noted in these data and in tabulated data for other series in which this mix has been used.

5.7 - Mix Series 34 - 35

In this series the effects of the addition of a single level of Beltane opal, ground to pozzolan-fineness, on pore solution chemistry and mortar prism expansion were studied. Batch weights for these mixes are listed in Table 5.7.1, and concentrations of ions found in expressed pore solutions are listed in Tables 5.7.2 and 5.7.3.

As a part of the custom milling of the mine-run opal, a portion of the crusher-run material was sized in a laboratory screening plant. A portion of the material passing 4.75-mm and retained on 2.36-mm (no. 4 x no. 8) mesh sieves was ground in a laboratory jar mill to a Blaine specific surface of $10,860 \text{ cm}^2/\text{g}$. The specific gravity of the ground opal, designated BP-2, was 2.07, making the surface area calculated on a volumetric basis $22,480 \text{ cm}^2/\text{cm}^3$. The surface area determined by nitrogen adsorption was $17.4 \text{ m}^2/\text{g}$ (510).

At the time this series was started the significant effect of reactive mix components on chemically bound nonevaporable water, W_n/c , was not appreciated. In the absence of data on W_n/c values specific to this series of experiments, it was necessary to estimate W_n/c from a system of equations fitted to data drawn from several other series. Adjustment of observed alkali metal ion concentrations in the expressed pore solutions to compensate for W_n/c was accomplished by the use of these equations. The results of these computations are listed in Tables 5.7.4 and 5.7.5.

Table 5.7.1

Batch Weights, grams, for Mixes 34 - 35

Materials	Mix 34, Control		Mix 35, 10.% Opal Pozzolan, BP-2	
	Parts by Weight	Batch Weights	Parts by Weight	Batch Weights
Cement, AT-1	1.000	763.3	1.000	763.3
Water	0.500	381.6	0.500	381.6
Pozzolan, BP-2	0.00	--	0.100	76.3
Sand, C109	2.000	1526.5	1.872	1428.8
Totals	3.500	2671.4	3.472	2650.1

Table 5.7.2

Observed Concentrations of Ions in Expressed Pore Solution (Not Corrected for Bound Water)

Mix 34, Control for Mix Series 34 - 35

(Concentrations in millimoles/liter)

Age, Days at 20° C	Si ⁴⁺ *	Al ³⁺	Fe ³⁺	Mg ⁺⁺	Ca ⁺⁺	Na ⁺	K ⁺	Σ^{+**}	OH ⁻	SO ₄ ⁼	Σ^{-**}	Σ^{+-**}
0.017	2.4	0.6	0.2	0.6	24.	134.	405.	587.	179.	n.d.		
0.042	0.4	0.2	0.0	0.4	20.	135.	405.	581.	166.	n.d.		
0.125	0.2	0.1	0.0	0.0	19.	137.	412.	589.	179.	n.d.		
0.25	0.7	0.4	0.0	0.0	14.	144.	424.	596.	203.	n.d.		
0.60	0.7	0.4	0.0	0.0	2.	163.	474.	640.	607.	7.	621.	+ 19.
1.125	0.8	0.7	0.0	0.0	2.	198.	496.	697.	650.	2.	654.	+ 43.
3.95	0.0	0.4	0.1	0.0	1.	200.	547.	749.	717.	4.	725.	+ 24.
9.	5.2	0.4	0.0	0.0	1.	204.	532.	738.	732.	2.	736.	+ 2.
15.	0.3	0.0	0.0	0.0	1.	215.	554.	771.	733.	0.	733.	0.
49.	1.0	0.0	0.0	0.0	2.	242.	594.	838.	772.	2.	776.	+ 62.
70.	1.0	0.2	0.0	0.0	0.	218.	575.	793.	751.	8.	767.	+ 26.
149.	0.6	0.6	0.0	0.0	2.	233.	602.	839.	797.	12.	821.	+ 18.
177.	2.1	0.8	0.1	0.0	1.	244.	628.	874.	785.	5.	796.	+ 78.
585.	8.8	0.8	0.1	0.0	0.	236.	575.	811.	781.	n.d.		

* See remarks under Section 4.4.1

** milliequivalents.liter

n.d. = not determined

Table 5.7.2 (Continued)

Observed Concentrations of Ions in Expressed Pore Solution (Not Corrected for Bound Water)

Mix 34, Control for Mix Series 34 - 35

(Concentrations in millimoles/liter)

Age, Days at 40° C	Si ⁴⁺ *	Al ³⁺	Fe ³⁺	Mg ⁺⁺	Ca ⁺⁺	Na ⁺	K ⁺	Σ^{+**}	OH ⁻	SO ₄ ⁼	Σ^{-**}	Σ^{+-**}
3.95	0.0	0.0	0.1	0.0	1.	199.	521.	722.	673.	12.	696.	+ 25.
9.	0.5	0.3	0.0	0.0	1.	208.	510.	720.	680.	18.	716.	+ 4.
15.	0.3	0.0	0.0	0.0	1.	231.	544.	777.	711.	13.	737.	+ 40.
49.	0.8	0.0	0.0	0.0	1.	266.	596.	864.	753.	14.	781.	+ 83.
70.	0.0	0.1	0.0	0.0	1.	226.	537.	765.	677.	31.	739.	+ 26.
149.	0.8	0.2	0.0	0.0	2.	239.	490.	733.	714.	n.d.		
177.	2.4	0.4	0.0	0.0	1.	236.	568.	806.	657.	18.	714.	+ 92.
585.	12.6	0.6	0.0	0.0	0.	242.	548.	790.	634.	n.d.		

* See remarks under Section 4.4.1

** milliequivalents/liter

n.d. = not determined

Table 5.7.3

Observed Concentrations of Ions in Expressed Pore Solution (Not Corrected for Bound Water)Mix 35, 10. Percent Opal Pozzolan, BP-2

(Concentrations in millimoles/liter)

Age, Days at 20° C	Si^{4+} *	Al^{3+}	Fe^{3+}	Mg^{++}	Ca^{++}	Na^+	K^+	$\Sigma +**$	OH^-	$\text{SO}_4^=$	$\Sigma -**$	$\Sigma +-*$
0.017	0.5	0.1	0.0	0.0	19.	126.	394.	558.	144.	n.d.		
0.042	0.3	0.1	0.0	0.0	17.	123.	392.	549.	162.	n.d.		
0.125	0.5	0.1	0.0	0.0	19.	126.	394.	558.	155.	n.d.		
0.25	1.0	0.4	0.0	0.0	9.	135.	407.	560.	227.	n.d.		
0.60	1.1	0.7	0.0	0.0	2.	148.	445.	597.	585.	6.	598.	- 1.
1.125	1.5	0.0	0.0	0.0	2.	190.	454	646.	610.	2.	612.	+ 34.
3.95	0.0	0.4	0.1	0.0	1.	173.	468.	643.	606	3.	612.	+ 31.
9.	0.5	0.3	0.0	0.0	1.	153.	442.	597.	584.	8.	600.	- 3.
15.	0.4	0.0	0.0	0.0	1.	197.	447.	646.	665.	1.	667.	- 21.
49.	0.7	0.0	0.0	0.0	1.	186.	384.	572.	508.	2.	510.	+ 62.
70.	0.9	0.2	0.0	0.0	0.	170.	345.	515.	453.	6.	465.	+ 50.
149.	0.7	0.5	0.0	0.0	1.	153.	300.	455.	447.	10.	467.	- 12.
177.	2.4	0.4	0.0	0.0	0.0	147.	317.	464.	429.	5.	439.	+ 25.
585.	10.2	0.7	0.0	0.0	0.0	145.	304.	449.	435.	n.d.		

* See remarks under Section 4.4.1

** Milliequivalents/liter

n.d. = not determined

Table 5.7.3 (Continued)

Observed Concentrations of Ions in Expressed Pore Solution (Not Corrected for Bound Water)

Mix 35, 10. Percent Opal Pozzolan, BP-2

(Concentrations in millimoles/liter)

Age Days at 40° C	Si ⁴⁺ *	Al ³⁺	Fe ³⁺	Mg ⁺⁺	Ca ⁺⁺	Na ⁺	K ⁺	$\Sigma +**$	OH ⁻	SO ₄ ⁼	$\Sigma -**$	$\Sigma +--**$
3.95	0.0	0.4	0.1	0.0	1.	142.	353.	497.	462.	7.	476.	+ 21.
9.	0.9	0.2	0.0	0.0	1.	80.	288.	370.	384.	14.	412.	- 42.
15.	0.1	0.0	0.0	0.0	1.	165.	284.	451.	378.	6.	390.	+ 61.
49.	1.2	0.0	0.0	0.0	2.	178.	306.	488.	406.	8.	422.	+ 66.
70.	0.8	0.2	0.0	0.0	0.	163.	287.	450.	382.	17.	416.	+ 34.
149.	1.5	0.4	0.0	0.0	1.	152.	278.	432.	392.	21.	434.	- 2.
177.	3.0	0.3	0.0	0.0	1.	144.	287.	433.	386.	10.	407.	+ 26.
585.	10.6	0.5	0.0	0.1	0.	138.	258.	396.	331.	n.d.		

* See remarks under Section 4.4.1

** milliequivalents/liter

n.d. = not determined

Table 5.7.4
Mix 34, Control for Mix Series 34 - 35
(Concentrations in millimoles/liter)

Age, days at 20° C	W_n/c	bulk	Cations Found			Cation Concentration Corrected for W_n/c			Σ^{*M^+}	Δ^{*M^+}	$*K^+ / *Na$
			Na^+	K^+	ΣM^+	$*Na^+$	Δ^{*Na^+}	$*K^+$			
0.017	0.002	0.996	134	405	539	133	-	403	-	537	-
0.042	0.004	0.922	135	405	540	134	-	402	-	536	-
0.125	0.006	0.983	136	412	548	134	-	407	-	541	-
0.25	0.017	0.966	144	424	568	139	-	410	-	549	-
0.6	0.060	0.880	163	474	637	143	-	417	-	561	-
1.125	0.111	0.778	197	496	693	153	-	386	-	539	-
3.95	0.152	0.696	201	547	748	140	-	381	-	521	-
9.	0.160	0.680	204	532	736	139	-	362	-	500	-
15.	0.178	0.614	215	554	769	138	-	357	-	495	-
49.	0.191	0.618	212	549	791	150	-	339	-	489	-
70.	0.194	0.612	218	575	793	133	-	352	-	485	-
149.	0.200	0.600	233	602	835	140	-	361	-	501	-
177.	0.202	0.596	244	628	872	145	-	374	-	520	-
585.	0.206	0.588	236	575	811	139	-	338	-	477	-
											2.436

Table 5.7.4 (Continued)

Concentrations of Alkali Metal Cations in Expressed Pore Solution (Corrected for Bound Water)

Age, Days at 40°C	W_n/c	bwk	Cations Found			Cation Concentration Corrected for W_n/c						$*K^+/\Sigma *Na^+$
			Na^+	K^+	ΣM^+	$*Na^+$	$\Delta *Na^+$	$*K^+$	$\Delta *K^+$	$\Sigma *M^+$	$\Delta *M^+$	
4.	0.156	0.688	199	521	720	137	-	358	-	495	-	2.618
9.	0.166	0.668	208	510	718	139	-	341	-	480	-	2.452
15.	0.179	0.642	231	544	775	148	-	349	-	498	-	2.355
49.	0.196	0.608	266	596	862	162	-	362	-	524	-	2.241
70.	0.198	0.604	226	537	763	137	-	324	-	461	-	2.376
149.	0.204	0.592	239	550	789	141	-	326	-	467	-	2.301
177.	0.206	0.583	236	568	804	139	-	334	-	473	-	2.407
585.	0.210	0.580	242	548	790	140	-	318	-	458	-	2.264

Table 5.7.5
 Concentrations of Alkali Metal Cations in Expressed Pore Solution (Corrected for Bound Water)
 Mix 35, 10. percent Opal Pozzolan, RP-2
 (Concentrations in millimoles/liter)

Age, days at 20° C	i_n/c	bulk	Cations Found			Cation Concentration Corrected for i_n/c			$*K^+/\Sigma Na^+$
			Na^+	K^+	ΣK^+	$*Na^+$	$\Delta *Na^+$	$*K^+$	
0.017	0.002	0.996	126	394	520	125	- 8	392	- 11
0.042	0.004	0.992	123	392	515	122	- 12	389	- 13
0.125	0.006	0.988	126	394	520	124	- 10	389	- 18
0.25	0.017	0.966	135	407	542	130	- 9	393	- 16
0.6	0.060	0.880	148	445	593	130	- 13	392	- 26
1.125	0.111	0.778	190	454	644	148	- 5	353	- 33
3.95	0.151	0.698	173	468	641	121	- 19	327	- 54
9.	0.158	0.684	153	442	595	105	- 34	302	- 59
15.	0.173	0.654	197	447	644	129	- 10	292	- 64
49.	0.179	0.642	186	384	570	119	- 30	247	- 93
70.	0.180	0.640	200	345	545	128	- 5	221	- 131
149.	0.182	0.636	153	300	453	97	- 42	191	- 170
177.	0.183	0.634	147	317	464	93	- 52	201	- 173
585.	0.184	0.632	145	304	449	92	- 47	192	- 146
								284	-193
									2.097

Table 5.7.5 (Continued)

Concentrations of Alkali Metal Cations in Expressed Pore Solution (Corrected for Bound Water)

Mix 35, 10. Percent Opal Pozzolan, BP-2

(Concentrations in millimoles/liter)

Age, Days at 40° C	W _{n/c}	bulk	Cations Found			Cation Concentration Corrected for W _{n/c}			*K / *Na
			+ Na	+ K ⁺	ΣM^+	+ *Na	+ *K ⁺	Δ^{*M} ⁺	
3.95	0.150	0.700	142	353	195	99	- 38	247	-149
9.	0.157	0.686	80	288	368	55	- 84	198	-143
15.	0.167	0.666	165	284	449	110	- 38	189	-160
19.	0.179	0.642	178	306	484	114	- 47	196	-166
70.	0.181	0.638	163	287	450	104	- 33	183	-141
149.	0.184	0.632	152	278	430	96	- 45	176	-150
177.	0.185	0.630	144	287	431	91	- 48	181	-153
585.	0.187	0.626	138	258	396	86	- 54	162	-156

Review of the experimentally determined values of W_n/c for Mix Series 59 - 64, and for Series 78 - 81, revealed that W_n/c for these series could be related to time by a hyperbolic estimating equation (see Eq. 4.11.8 and Eq. 4.11.9). It was also noted that, at a given age, W_n/c decreased linearly with increased loading of the reactive mix component. The reactive component used in the selected mixes is a pozzolan identified as "L". In the following equations "P" represents the percent of pozzolan L (by weight of portland cement) present in the mix. To apply these equations the simplifying assumption is made that the reactive portion of any pozzolan is its content of SiO_2 . In consequence "P" in these equations must be multiplied by the ratio of SiO_2 in the pozzolan of the test mix whose W_n/c is to be estimated to that of pozzolan L. For the ground opal BP-2 the ratio is $87.96/67.98 = 1.294$. Thus, for 10 percent loading of ground opal pozzolan BP-2, P in the following equations is 12.94.

W_n/c at $20^\circ C$ for $t < 10$ days =

$$\frac{t}{4.0223 + 5.3722 t + 0.0470 t^2} + \frac{t P}{-39044. + 722.26 t - 144.392 t^2} \dots \quad (\text{Eq. 5.7.1})$$

W_n/c at $20^\circ C$ for $10 \text{ days} \leq t \leq 422 \text{ days}$ =

$$\frac{t}{7.1626 + 5.1626 t - 0.0015 t^2} + \frac{t P}{-32611. - 490.626 t + 0.0947 t^2} \dots \quad (\text{Eq. 5.7.2})$$

W_n/c at 40°C for $t < 10$ days =

$$\frac{t}{0.8216 + 6.4171 t - 0.0526 t^2} +$$

$$\frac{t P}{-10823. + 944.81 t - 108.16 t^2} \dots \quad (\text{Eq. 5.7.3})$$

W_n/c at 40°C for $10 \leq t \leq 422$ days =

$$\frac{t}{9.8603 + 4.9551 t - 0.00083 t^2} +$$

$$\frac{t P}{-7571. - 647.9 t + 0.2999 t^2} \dots \quad (\text{Eq. 5.7.4})$$

Beyond the range of these equations, 422 days, values of W_n/c were estimated by fitting an equation of the type illustrated by Eq. 4.11.8 to the last three estimated points and then extrapolating to 585 days.

As noted in Section 4.12, the final disposition of alkali metal ions in hydraulic cement pastes and mortars cannot be stated without ambiguity. However, if one considers two mortars that are in all respects identical with the exception of the substitution of an alkali-silica reactive component for a fraction of the aggregate component of one, it is reasonable to assume any differences in alkali metal ion concentrations observed in expressed pore solutions are due to reactions between alkalies and the alkali-silica reactive component. This difference, Δ^*M^+ , can be considered a measure of the extent of the reaction. Values of Δ^*M^+ from Table 5.7.5 have been plotted against time on a logarithmic scale in Figure 5.7.1. The plots indicate that Δ^*M^+ becomes constant at about 10 days for specimens stored at 40°C,

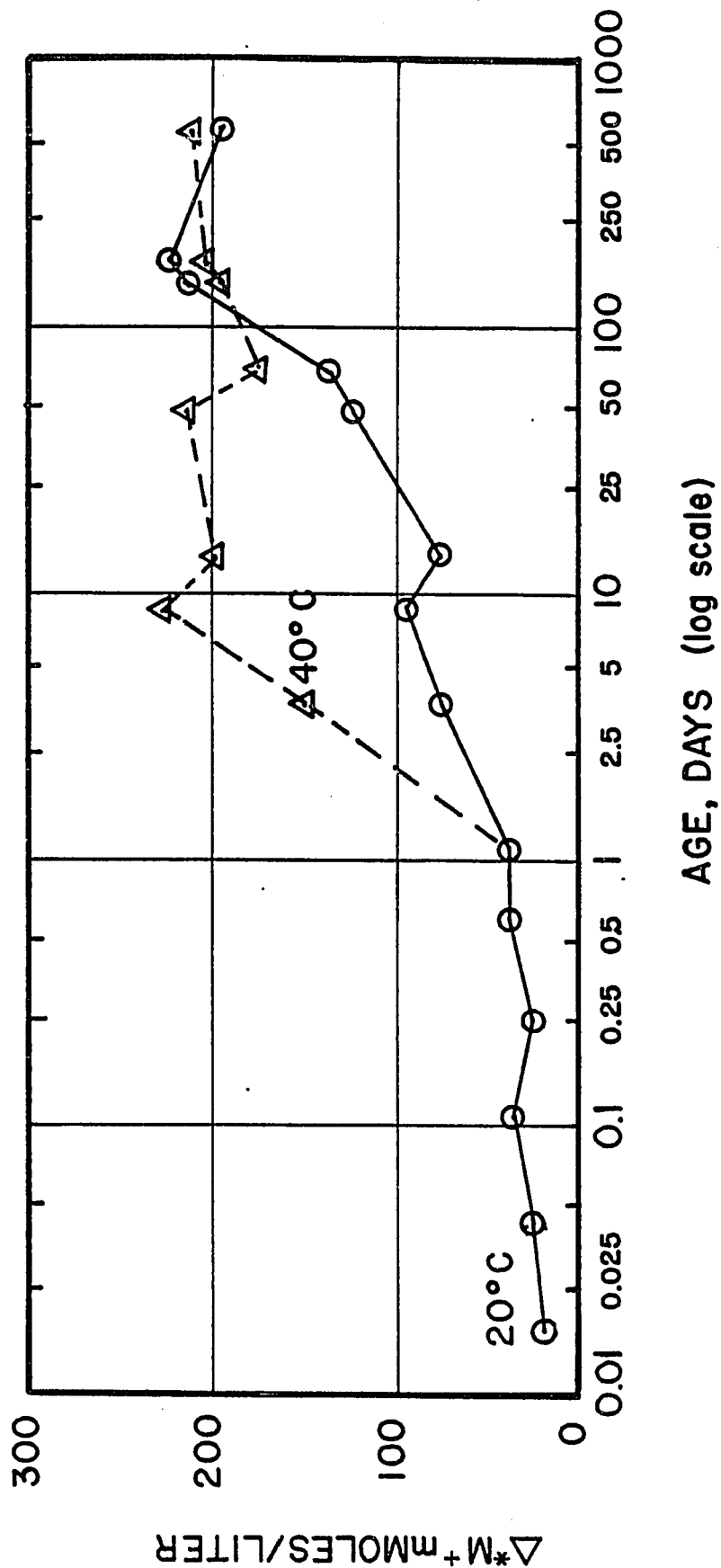


Figure 5.7.1 - Change in Combined Alkali Metal Ion Concentration vs. Time
as a Result of Alkali-Silica Reaction

Table 5.7.6

Observed Expansions of Mortar Prisms ($\mu\text{in/in}$), Mixes 34 - 35

Time, Days	Mix 34 Series a	Mix 34 Series b	Mix 35 Series a	Mix 35 Series b
1.7	-140	+ 60	-235	+187
3.3	- 80	140	-120	173
6.7	+ 20	100	- 80	187
7.4	- 40	140	- 80	133
15.	+ 60	80	+ 13	187
94.	160	200	120	293
185.	300	340	253	347
452.	440	133*	387	213
773.	440	420	440	213

Temperature of:				
Storage	20°C	40°C	20°C	40°C
Measurement	20°C	40°C	20°C	40°C
Cross- Section	0.25 in 6.35 mm	0.25 in 6.35 mm	0.25 in 6.35 mm	0.25 in 6.35 mm

* Anomalous value probably due to reading error.

while more than 100 days are required for this condition to be attained at 20°C. Attainment of a constant value of Δ^*M^+ implies that the chemical attack phase of the alkali-silica reaction has gone to completion.

In Table 5.7.6 the observed expansions of mortar prisms cast from mixes of this series have been listed. Observed expansion of the mix containing opal ground to pozzolan fineness was about the same as that of the control mix for specimens stored at 20°C, but was significantly reduced for specimens stored at 40°C.

5.8 - This section not used

5.9 - This section not used

5.10 - Mix Series 44-45

In this series an attempt was made to verify the observation made in Mix Series 32 - 33 that the magnitude of expansion was an inverse function of specimen storage temperature for Beltane Opal.

Concentrations of ions in expressed pore solutions were determined, and measurements were made of 0.50-in (12.7-mm) cross section prisms of hardened mortar stored at 20° and 40°C to determine expansion potential as a function of storage temperature.

Batch weights for the mixtures studied are listed in Table 5.10.1. Weight ratios of the component materials, oven-dry/batch, and ignited/batch, are listed in Table 5.10.2. These values were required to reduce the data for determination of W_n/c at 3, 8, and 27 hours for this series. Estimating equations (see Section 4.11.3) were fitted to these data, and to data from other sources (see Table 5.10.5) to allow estimation of W_n/c at all test ages.

Observed concentrations of ions found in pore solutions are listed in Tables 5.10.3 and 5.10.4. Concentrations of alkali metal ions, compensated for W_n/c , have been listed in Tables 5.10.6 and 5.10.7, and plotted against the logarithm of time in Figures 5.10.1 and 5.10.2.

In Figures 5.10.1 and 5.10.2 the concentration of alkali metal ions is seen to be nearly constant in the time period 0.017 days (25 minutes) through 0.33 days (8 hours). This plateau is followed by a small increase to a peak near 1.1 days. At this point half of the samples were transferred to storage at 40°C and the remainder left at 20°C. Concentrations of alkali metal ions in the expressed pore solutions fell slowly in the control mix, mix 44, out to 60 days.

Table 5.10.1

Batch Weights, grams, for Mixes 44 - 45

Materials	Mix 44, Control		Mix 45, 8% Opal Sand	
	Parts by Weight	Batch Weights	Parts by Weight	Batch Weights
Cement, AT-1	1.000	763.3	1.000	759.2
Water	0.500	381.6	0.500	379.6
Beltane Sd.*	0.000	--	0.080	30.4
Sand, C109	2.000	1526.5	1.920	1457.6
Totals	3.500	2671.4	3.500	2657.2

Table 5.10.2

Weight Ratios of Component MaterialsOven-Dry/Batch, Ignited/Batch

Material	Wod/Wo	Wig/Wo
Cement, AT-1	0.99809	0.99483
Beltane Sand*	0.99445	0.95298
Sand, C109	0.99993	0.99868

*Beltane opal sand, 50% 600 x 300 μ m, 50% 300 x 150 μ m.

Table 5.10.3

Observed Concentrations of Ions in Expressed Pore Solution (Not Corrected for Bound Water)Mix 44, Control for Mix Series 44 - 45

(Concentrations in millimoles/liter)

Age, Days at 20°C	Si^{4+*}	Al^{3+}	Fe^{3+}	Mg^{++}	Ca^{++}	Na^+	K^+	$+**$	OH^-	$\text{SO}_4^=$	$-**$	$+**$
0.017	0.2	0.0	0.0	0.0	42.	122.	375.	539.	162.	195.	552.	- 13.
0.04	n.d.	0.0	0.0	0.0	27.	125.	379.	531.	169.	206.	581.	- 50.
0.125	0.2	0.0	0.0	0.0	26.	128.	382.	536.	197.	195.	587.	- 51.
0.333	0.2	0.0	0.0	0.0	10.	139.	400.	549.	276.	138.	552.	- 3.
1.125	0.4	0.1	0.0	0.0	2.	182.	480.	666.	650.	3.	656.	+ 10.
20.***	0.0	3.0	1.2	2.5	25.	228.	575.	853.	n.d.	n.d.	--	--
56.	0.8	0.5	0.0	0.0	2.	220.	572.	796.	770.	8.	787.	+ 9.

*** Sample recovered very small and may have been contaminated by cement paste particles.

Age, Days at 40°C	Si^{4+}	Al^{3+}	Fe^{3+}	Mg^{++}	Ca^{++}	Na^+	K^+	$+**$	OH^-	$\text{SO}_4^=$	$-**$	$+**$
20.	0.0	0.5	0.0	0.0	1.	232.	554.	788.	775.	n.d.	--	--
56.	1.3	0.4	0.0	0.0	2.	220.	525.	749.	683.	27.	737.	+ 12.

*See remarks under Section 4.4.1

** milliequivalents/liter

n.d. = not determined

Table 5.10.4

Observed Concentrations of Ions in Expressed Pore Solution (Not Corrected for Bound Water)Mix 45, 8% Opal Sand

(Concentrations in milliequivalents/liter)

Age, Days at 20°C	Si^{4+} *	Al^{3+}	Fe^{3+}	Mg^{++}	Ca^{++}	Na^+	K^+	$+\text{**}$	OH^-	$\text{SO}_4^{=}$	$-\text{**}$	$+\text{-**}$
0.017	0.0	0.0	0.0	0.0	18.	127.	380.	543.	153.	187.	509.	+ 34.
0.04	0.1	0.1	0.0	0.0	14.	128.	379.	535.	167.	182.	531.	+ 4.
0.125	0.1	0.0	0.0	0.0	17.	127.	383.	544.	164.	185.	534.	+ 10.
0.333	0.7	0.0	0.0	0.0	5.	138.	400.	548.	289.	130.	549.	- 1.
1.125	0.6	0.1	0.0	0.0	2.	168.	455.	627.	606.	5.	616.	+ 11.
20.***	0.0	0.6	0.0	0.1	3.	146.	307.	459.	n.d.	n.d.	--	--
56.	11.1	0.3	0.0	0.0	2.	102.	196.	302.	336.	9.	354.	- 52.

*** Sample recovered very small.

Age, Days at 40°C	Si^{4+} *	Al^{3+}	Fe^{3+}	Mg^{++}	Ca^{++}	Na^+	K^+	$+\text{**}$	OH^-	$\text{SO}_4^{=}$	$-\text{**}$	$+\text{-**}$
20.***	0.0	0.3	0.0	0.0	1.	120.	240.	632.	n.d.	n.d.	--	--

56. No sample recovered.

* See remarks under Section 4.4.1

** milliequivalents/liter

n.d. = not determined

Table 5.10.5
Nonevaporable Water, W_n/c , as a Function of
 Beltane Opal Addition and Time

Time, Days	Temp. °C	Mix 44	Mix 45
0.125	20	0.0069	0.0048
0.333	20	0.0329	0.0336
1.125	20	0.0781	0.0740
Beltane Sand, %		0.00	8.00

Equations fit to the above data and used to estimate W_n/c for $0.125 \leq t \leq 1.125$:

$$\text{For Mix 44, est } W_n/c = t/(25.728 - 58.363t + 43.722t^2)$$

$$\text{For Mix 45, est } W_n/c = t/(39.216 - 115.905t + 84.053t^2)$$

Equation used to estimate W_n/c at 0.017 and 0.40 days

(fitted to points picked from curve of Copeland and Kantro (511, p. 352)):

$$\text{est } W_n/c = t/(6.092 + 122.637t - 27.608t^2)$$

Equations used to estimate W_n/c at 20 days and beyond:

(see Section 5.7, Equations 5.7.2 and 5.7.4)

Table 5.10.6

Concentrations of Alkali Metal Cations in Expressed Pore Solution (Corrected for Bound Water)

Mix 44, Control for Mix Series 44 - 45

(Concentrations in millimoles/liter)

Age, Days at 20°C	$\text{W}_{\text{n}}/\text{c}$	bwk	Cations Found			Cation Concentration Corrected for $\text{W}_{\text{n}}/\text{c}$						$*\text{K}^+/\text{*Na}^+$
			Na^+	K^+	M^+	$*\text{Na}^+$	$*\text{Na}^+$	$*\text{K}^+$	$*\text{K}^+$	$*\text{M}^+$	$*\text{M}^+$	
0.017	0.002	0.996	122.	357.	497.	122.	--	374.	--	495.	--	3.074
0.04	0.004	0.992	125.	379.	504.	124.	--	376.	--	500.	--	3.032
0.125	0.007	0.986	128.	382.	510.	126.	--	377.	--	503.	--	2.984
0.333	0.033	0.935	139.	400.	539.	130.	--	374.	--	503.	--	2.878
1.125	0.078	0.844	182.	480.	662.	154.	--	405.	--	559.	--	2.637
20.	0.182	0.636	228.	575.	803.	145.	--	366.	--	511.	--	2.522
56.	0.192	0.616	220.	572.	792.	136.	--	352.	--	488.	--	2.600

Age, Days at 40°C	$\text{W}_{\text{n}}/\text{c}$	bwk	Cations Found			Cation Concentration Corrected for $\text{W}_{\text{n}}/\text{c}$						$*\text{K}^+/\text{*Na}^+$
			Na^+	K^+	M^+	$*\text{Na}^+$	$*\text{Na}^+$	$*\text{K}^+$	$*\text{K}^+$	$*\text{M}^+$	$*\text{M}^+$	
20.	0.184	0.632	232.	554.	786.	147.	--	350.	--	497.	--	2.388
56.	0.197	0.607	220.	525.	745.	133.	--	318.	--	452.	--	2.386

Table 5.10.7

Concentrations of Alkali Metal Cations in Expressed Pore Solution (Corrected for Bound Water)

Mix 45, 8% Opal Sand

(Concentrations in millimoles/liter)

Age, Days at 20°C	$W_{n/c}$	bwk	Cations Found			Cation Concentration Corrected for $W_{n/c}$						$*\text{K}^+/\text{*Na}^+$
			Na^+	K^+	M^+	$*\text{Na}^+$	$*\text{Na}^+$	$*\text{K}^+$	$*\text{K}^+$	$*\text{M}^+$	$*\text{M}^+$	
0.017	0.002	0.996	127.	380.	507.	126.	+ 5.	378.	+ 5.	505.	+10.	2.992
0.04	0.004	0.992	128.	379.	507.	127.	+ 3.	376.	0.	503.	+ 3.	2.961
0.125	0.005	0.990	127.	383.	510.	126.	0.	379.	+ 3.	505.	+ 2.	3.016
0.333	0.034	0.932	138.	400.	538.	129.	- 1.	373.	- 1.	501.	- 2.	2.899
1.125	0.074	0.852	168.	455.	623.	143.	-10.	388.	-17.	531.	-28.	2.708
20.	0.177	0.646	146.	307.	453.	94.	-51.	198.	-167.	293.	-218.	2.103
56.	0.182	0.636	102.	196.	298.	65.	-71.	125.	-228.	189.	-299.	1.922

Age, Days at 40°C	$W_{n/c}$	bwk	Cations Found			Cation Concentration Corrected for $W_{n/c}$						$*\text{K}^+/\text{*Na}^+$
			Na^+	K^+	M^+	$*\text{Na}^+$	$*\text{Na}^+$	$*\text{K}^+$	$*\text{K}^+$	$*\text{M}^+$	$*\text{M}^+$	
20.	0.174	0.652	120.	240.	360.	78.	-68.	156.	-194.	235.	-262.	2.000
56.			No Sample Recovered									

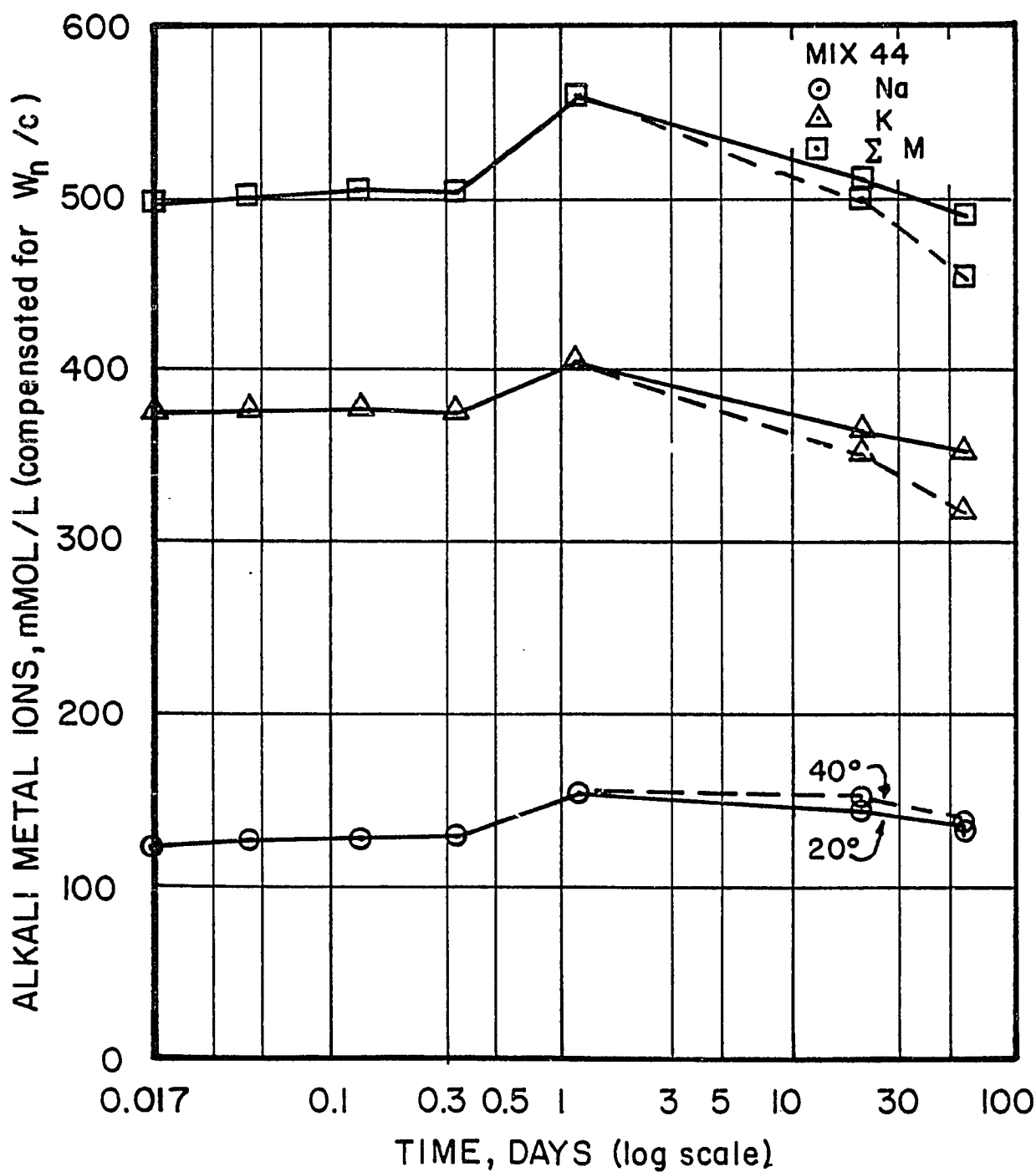


Figure 5.10.1 - Alkali Metal Ion Concentration vs. Time

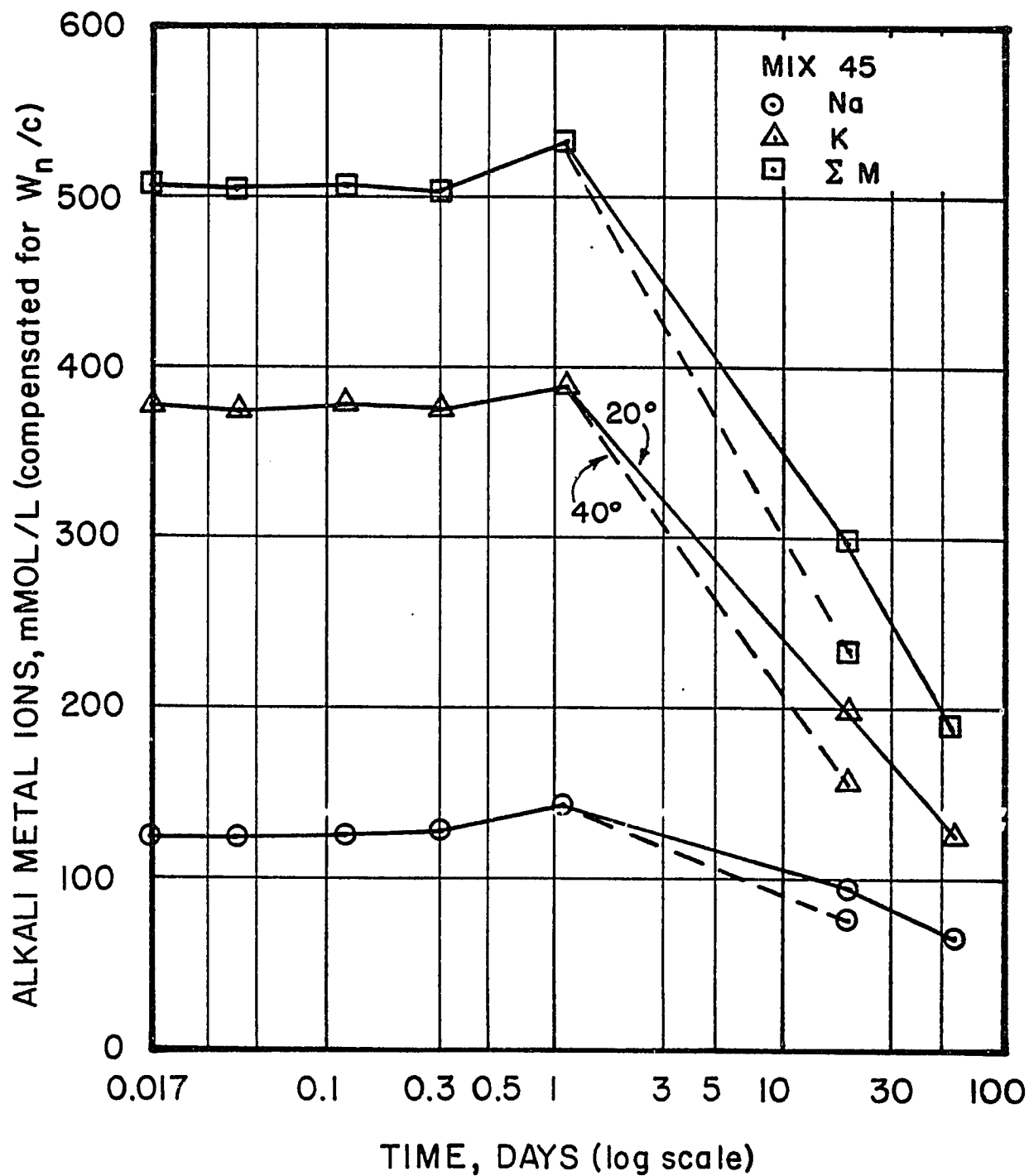


Figure 5.10.2 - Alkali Metal Ion Concentration vs. Time

Table 5.10.8

Observed Expansions of Mortar Prisms ($\mu\text{in/in}$), Mixes 44 - 45

Time, Days	Mix 44 Series a	Mix 44 Series b	Mix 45 Series a	Mix 45 Series b
2.0	67	40	0	507
9.5	27	0	2840	1267
31.	187	213	4840	2960
91.	307	200	5960	3453
359.	467	Lost Seal	6360	3991

Temperature of:				
Storage	20° C	40° C	20° C	40° C
Measurement	20° C	40° C	20° C	40° C
Cross section	0.50-in 12.7-mm	0.50-in 12.7-mm	0.50-in 12.7-mm	0.50-in 12.7-mm

Storage temperature appears to have had little effect on concentrations of alkali metal ions in the control mix. Alkali metal ion concentrations fell rapidly in the mix containing 8 percent Beltane opal sand, Mix 45, and even more rapidly for specimens of this mix stored at 40°C. As will be noted in Mix Series 46 - 48, very rapid depletion of alkali metal ion concentration takes place in mixes containing highly reactive aggregate constituents, e.g. opal sand the final concentration plateau being reached in 10 to 30 days.

Observed expansion of hardened mortar prisms for this series are listed in Table 5.10.8. From observations of mix 45 at 91 days, the effect of storage temperature in the range of 20° - 40°C is to reduce potential expansion by approximately 125 $\mu\text{in/in}$ for each degree Celsius increase in storage temperature. This change is a little more than twice that observed in Mix Series 32 - 33.

5.11 - Mix Series 46 - 48

In this series the effects of the addition of a single level of Beltane opal sand, with and without a single addition level of pozzolan BP-2, were studied. Pozzolan BP-2 was prepared by grinding crushed Beltane opal in a porcelain jar mill with a charge of steel balls (see Section 4.9). BP-2 was ground to a Blaine specific surface of $10,860 \text{ cm}^2/\text{g}$ ($22,480 \text{ cm}^2/\text{cm}^3$).

Concentrations of ions in expressed pore solutions were determined and measurements were made of prisms of the hardened mortars to determine the potential length change of the mixtures.

Batch weights for the mixtures studied are listed in Table 5.11.1. Weight ratios of the component materials, oven-dry/batch, and ignited/batch, are listed in Table 5.11.2. These values were required to reduce the data for determination of W_n/c . Observed concentrations of ions found in expressed pore solutions are listed in Tables 5.11.3 through 5.11.5. In Table 5.11.6 the observed values of W_n/c have been listed. Interpolation, where necessary, was carried out as outlined in Section 4.11.3. The interpolating equations used to estimate values of W_n/c have been appended to Table 5.11.6. These estimated values were used to calculate the compensated alkali metal ion concentrations listed in Tables 5.11.7 through 5.11.9. Data from these tables were used to construct Figures 5.11.1 through 5.11.3.

Figure 5.11.1, for the control mix containing no additions of opaline materials, indicates a gradual although erratic reduction in $*K^+$ concentration with time. The concentration of $*Na^+$ increased slightly with time. At 30.5 days nearly 90 percent of the total potential K^+ present in the portland cement was in solution, while more than 60 percent of the Na^+ was in solution. In Figure 5.11.2 the addition of 8 percent Beltane opal sand is shown to reduce the concentration of both $*Na^+$ and $*K^+$. The alkali metal ion concentration fell more rapidly at 40°C, particularly that of $*K^+$. For specimens stored at 20°C concentrations decreased slowly, requiring about 30 days to fall to the same level reached in only 3 days for specimens stored at 40°C. In Figure 5.11.3 the addition of 19.6 percent BP-2 to a mix that also contained 8 percent opal sand resulted in a pattern similar to that seen in Figure 5.11.2, except that the residual concentrations of alkalies were lower.

Table 5.11.1

Batch Weights, Grams, for Mixes 46 - 48

Materials	Mix 46, Control		Mix 47, 8% Opal Sand		Mix 48, 8% Opal Sd., 20% Pozzolan	
	Parts by Weight	Batch Weights	Parts by Weight	Batch Weights	Parts by Weight	Batch Weights
Cement, RZ-354	1.00	763.3	1.00	759.2	1.00	763.3
Water	0.50	381.6	0.50	379.6	0.50	381.6
Pozzolan, BP-2	0.00	--	0.00	--	0.196	149.8
Beltane Sd.*	0.00	--	0.08	60.8	0.08	60.8
Sand, C109	2.00	1526.5	1.92	1457.6	1.642	1253.3
Totals	3.50	2671.4	3.50	2657.2	3.418	2608.0

* Beltane opal sand, 50% 600 x 300 μm , 50% 300 x 150 μm .

Table 5.11.2

Weight Ratios of Component MaterialsOven-Dry/Batch, Ignited/Batch

Material	W _{od} /W _o	W _{ig} /W _o
Cement, RZ354	0.99809	0.99297
Pozzolan, BP-2	0.96539	0.93334
Beltane Sd.	0.99445	0.95298
Sand, C109	0.99993	0.99868

Table 5.11.3

Observed Concentrations of Ions in Expressed Pore Solution (Not Corrected for Bound Water)

Mix 46, Control for Mix Series 46 - 48

(Concentrations in millimoles/liter)

Age Days at 20° C	Concentrations in millimoles/liter							$\Sigma +**$	$\Sigma -**$	$\Sigma +**$
	Si ⁴⁺ *	Al ³⁺	Fe ³⁺	Mg ⁺⁺	Ca ⁺⁺	Na ⁺	K ⁺			
0.25	0.5	0.1	0.0	0.8	12.	111.	508.	643.	>74.	817.
1.	3.1	0.4	0.0	0.0	2.	158.	587.	759.	801.	8.
3.4	2.1	0.1	0.0	0.0	1.	185.	780.	967.	898.	23.
8.5	27.4	0.0	0.0	0.0	2.	187.	704.	895.	919.	9.
30.5	11.6	0.4	0.0	0.0	1.	212.	788.	1002.	963.	20.
										- 1.
Age Days at 40° C	Concentrations in millimoles/liter							$\Sigma +**$	$\Sigma -**$	$\Sigma +**$
	Si ⁴⁺ *	Al ³⁺	Fe ³⁺	Mg ⁺⁺	Ca ⁺⁺	Na ⁺	K ⁺			
3.4	0.7	0.1	0.0	0.0	1.	189.	764.	955.	792.	51.
8.5	45.5	0.3	0.0	0.0	1.	210.	678.	890.	816.	40.
30.5	14.6	0.3	0.0	0.0	1.	215.	730.	947.	843.	>73.
370.	26.9	0.7	0.0	0.1	0.	208.	702.	910.	774.	n.d.
										--

* See remarks under Section 4.4.1

** Milliequivalents/liter

n.d. = not determined
> greater than

Table 5.11.4

Observed Concentrations of Ions in Expressed Pore Solution (Not Corrected for Bound Water)

Mix 47, 8% Opal Sand

(Concentrations in millimoles/liter)

Age, Days at 20° C	Si ⁴⁺ *	Al ³⁺	Fe ³⁺	Mg ⁺⁺	Ca ⁺⁺	Na ⁺	K ⁺	Σ^{+**}	OH ⁻	SO ₄ ⁼	Σ^{-**}	Σ^{+-**}
0.25	0.6	0.1	0.0	0.9	8.	113.	653.	311.	>73.	--	--	--
1.0	5.5	0.4	0.0	0.0	2.	143.	556.	703.	717.	10.	737.	-34.
3.4	7.0	0.3	0.0	0.1	2.	143.	537.	684.	648.	23.	694.	-10.
8.5	43.2	0.9	0.0	0.0	0.	127.	416.	543.	527.	n.d.	--	--
30.5	11.5	0.4	0.0	0.0	0.	108.	320.	428.	403.	14.	431.	-3.

Age, Days at 40° C	Si ⁴⁺ *	Al ³⁺	Fe ³⁺	Mg ⁺⁺	Ca ⁺⁺	Na ⁺	K ⁺	Σ^{+**}	OH ⁻	SO ₄ ⁼	Σ^{-**}	Σ^{+-**}
3.4	8.9	0.2	0.0	0.1	0.	94.	298.	392.	363.	22.	407.	-15.
8.5	33.8	0.2	0.0	0.0	1.	89.	254.	345.	326.	9.	344.	+1.
30.5	14.4	0.0	0.0	0.0	0.	108.	299.	407.	381.	21.	423.	-16.
370.	11.7	0.7	0.1	0.1	0.	100.	273.	373.	348.	n.d.	--	--

* See remarks under Section 4.4.1

** milliequivalents/liter

n.d. = not determined
> greater than

Table 5.11.5

Observed Concentrations of Ions in Expressed Pore Solution (Not Corrected for Bound Water)

Mix 48, 8% Opal Sand, 19.6% Pozzolan BP-2

(Concentrations in millimoles/liter)

Age, Days at 20°C	Concentrations in millimoles/liter						$\Sigma +**$	$\Sigma -**$	$\Sigma +**$
	Si ⁴⁺ *	Al ³⁺	Fe ³⁺	Mg ⁺⁺	Ca ⁺⁺	Na ⁺			
0.25	2.8	0.4	0.0	0.9	9.	107.	485.	610.	367.
1.0	7.0	0.9	0.0	0.5	8.	128.	519.	653.	9.
3.4	3.9	0.2	0.1	0.0	2.	120.	441.	565.	18.
8.5	32.9	0.4	0.0	0.0	1.	100.	318.	420.	414.
30.5	13.2	0.5	0.0	0.0	0.	66.	172.	238.	240.
									9.
									258.
									- 20.

Age, Days at 40°C	Concentrations in millimoles/liter						$\Sigma +**$	$\Sigma -**$	$\Sigma +**$
	Si ⁴⁺ *	Al ³⁺	Fe ³⁺	Mg ⁺⁺	Ca ⁺⁺	Na ⁺			
3.4	1.2	0.1	0.0	0.0	1.	58.	151.	211.	199.
8.5	24.5	0.0	0.0	0.0	1.	50.	117.	169.	163.
30.5	12.7	0.4	0.0	0.0	1.	49.	105.	156.	146.
370.	6.8	0.5	0.1	0.1	0.	44.	102.	146.	134.
									n.d.
									--

* See remarks under Section 4.4.1

** milliequivalents/liter

n.d. = not determined

> greater than

Table 5.11.6

Nonevaporable Water, W_n/c , as a Function ofBeltane Opal Addition* and Time

Time, Days	Temp. °C	Mix 46	Mix 47	Mix 48
0.46	20	0.0466	0.0477	0.0486
4.0	20	0.1651	0.1580	0.1708
4.0	40	0.1784	0.1692	0.1699
9.25	20	0.1769	0.1721	0.1736
9.25	40	0.1845	0.1790	0.1743
30.5	20	0.1920	0.1846	0.1877
30.5	40	0.1914	0.1914	0.1668

Equations used to estimate W_n/c for $0.25 \leq t \leq 30.5$ days at $20^\circ C$:

$$\text{Mix 46, est } W_n/c = t/(6.7831 + 4.7572t + 0.0076t^2)$$

$$\text{Mix 47, est } W_n/c = t/(7.2743 + 4.8398t + 0.0112t^2)$$

$$\text{Mix 48, est } W_n/c = t/(5.9598 + 4.9249t + 0.0069t^2)$$

Equations used to estimate W_n/c for $3.4 \leq t \leq 30.5$ days at $40^\circ C$.

$$\text{Mix 46, est } W_n/c = t/(1.1117 + 5.3485t - 0.0053t^2)$$

$$\text{Mix 47, est } W_n/c = t/(1.8993 + 5.4765t - 0.0103t^2)$$

$$\text{Mix 48, est } W_n/c = t/(1.7222 + 5.3823t + 0.0182t^2)$$

* Beltane Opal Additions to Mixes 46 - 48

Material	Mix 46	Mix 47	Mix 48
Beltane Sand, %	0.0	8.0	8.0
Pozzolan, BP-2, %	0.0	0.0	19.6
Total Opal Added, %	0.0	8.0	27.6

Table 5.11.7

Concentrations of Alkali Metal Cations in Expressed Pore Solution (Corrected for Bound Water)

Mix 46, Control for Mix Series 46 - 48									
(Concentrations in millimoles/liter)									
Age, Days at 20° C.	W_n/c	b _{wk}	Cations Found			Cation Concentration Corrected for W_n/c			$*K^+ / *Na^+$
			Na^+	K^+	ΣM^+	$*Na^+$	$\Delta *Na^+$	$*K^+$	
0.25	0.031	0.994	111.	508.	619.	110.	--	505.	--
1.	0.087	0.826	158.	598.	755.	131.	--	493.	--
3.4	0.148	0.704	185.	780.	965.	130.	--	549.	--
8.5	0.178	0.644	187.	704.	891.	120.	--	453.	--
30.5	0.192	0.616	212.	788.	1000.	131.	--	485.	--
								616.	--
									3.717

Mix 46, Control for Mix Series 46 - 48									
(Concentrations in millimoles/liter)									
Age, Days at 40° C.	W_n/c	b _{wk}	Cations Found			Cation Concentration Corrected for W_n/c			$*K^+ / *Na^+$
			Na^+	K^+	ΣM^+	$*Na^+$	$\Delta *Na^+$	$*K^+$	
3.4	0.177	0.646	189.	764.	953.	122.	--	494.	--
8.5	0.184	0.632	210.	678.	888.	133.	--	428.	--
30.5	0.191	0.618	215.	730.	945.	133.	--	451.	--
370.	0.193	0.614	208.	702.	910.	128.	--	431.	--
								616.	--
									4.042

Table 5.11.8
 Concentrations of Alkali Metal Cations in Expressed Pore Solution (corrected for Bound Water)
Mix 47, 8% Opal Sand
 (Concentrations in millimoles/liter)

Age, Days at 20° C	W _n /c	bwk	Cations Found	Corrected for W _n /c				*K ⁺ / ⁺ *Na ⁺
				Na ⁺	K ⁺	ΣM^+	*Na ⁺ $\Delta *Na^+$	
0.25	0.029	0.942	113.	524.	637.	113.	+ 3.	4.368
1.	0.082	0.836	143.	556.	699.	120.	- 11.	- 9.
3.4	0.143	0.714	143.	537.	680.	102.	- 28.	3.888
8.5	0.173	0.654	127.	416.	543.	83.	- 283.	3.755
30.5	0.192	0.616	108.	320.	428.	67.	- 64.	3.276
							- 197.	2.963
							- 288.	
							- 264.	
							- 352.	
							- 352.	

Age, Days at 40° C	W _n /c	bwk	Cations Found	Corrected for W _n /c				*K ⁺ / ⁺ *Na ⁺
				Na ⁺	K ⁺	ΣM^+	*Na ⁺ $\Delta *Na^+$	
3.4	0.167	0.666	94.	298.	392.	63.	- 59.	3.170
8.5	0.178	0.644	89.	254.	343.	57.	- 75.	- 355.
30.5	0.191	0.618	108.	299.	407.	67.	- 66.	- 340.
370.	0.195	0.610	100.	273.	373.	61.	- 67.	2.769
							- 167.	2.730
							- 264.	
							- 228.	
							- 331.	

Table 5.11.9
 Concentrations of Alkali Metal Cations in Expressed Pore Solution (Corrected for Bound Water)
Mix 48, 8% Opal Sand, 19.6% Pozzolan BP-2
 (Concentrations in millimoles/liter)

Age, Days at 20°C	W_n/c	bulk	Cations Found			Cation Concentration Corrected for W_n/c	$*K^+ / *Na^+$
			Na^+	K^+	ΣM^+		
0.25	0.035	0.930	107.	485.	592.	100. - 11. $\frac{*Na^+}{\Delta *Na^+}$ $\frac{*K^+}{\Delta *K^+}$ $\frac{\Sigma *M^+}{\Delta *M^+}$	4.533
1.	0.092	0.816	128.	519.	647.	104. - 26. $\frac{451.}{54.}$ $\frac{424.}{70.}$ $\frac{551.}{65.}$	4.055
3.4	0.149	0.702	120.	441.	561.	84. - 46. $\frac{424.}{310.}$ $\frac{240.}{240.}$ $\frac{528.}{96.}$	3.675
8.5	0.176	0.648	100.	318.	418.	65. - 56. $\frac{310.}{206.}$ $\frac{247.}{247.}$ $\frac{394.}{286.}$	3.180
30.5	0.188	0.624	66.	172.	238.	41. - 89. $\frac{206.}{107.}$ $\frac{271.}{303.}$ $\frac{378.}{303.}$	2.606
Age, Days at 40°C	W_n/c	bulk	Cations Found			Cation Concentration Corrected for W_n/c	$*K^+ / *Na^+$
			Na^+	K^+	ΣM^+		
3.4	0.168	0.664	58.	151.	209.	39. - 84. $\frac{*Na^+}{\Delta *Na^+}$ $\frac{*K^+}{\Delta *K^+}$ $\frac{\Sigma *M^+}{\Delta *M^+}$	2.603
8.5	0.174	0.652	50.	117.	167.	33. - 100. $\frac{100.}{76.}$ $\frac{393.}{139.}$ $\frac{352.}{477.}$	2.340
30.5	0.167	0.666	49.	105.	154.	33. - 100. $\frac{76.}{100.}$ $\frac{100.}{109.}$ $\frac{109.}{452.}$	2.143
370.	0.166	0.668	44.	102.	146.	29. - 98. $\frac{100.}{70.}$ $\frac{103.}{103.}$ $\frac{103.}{481.}$	2.318

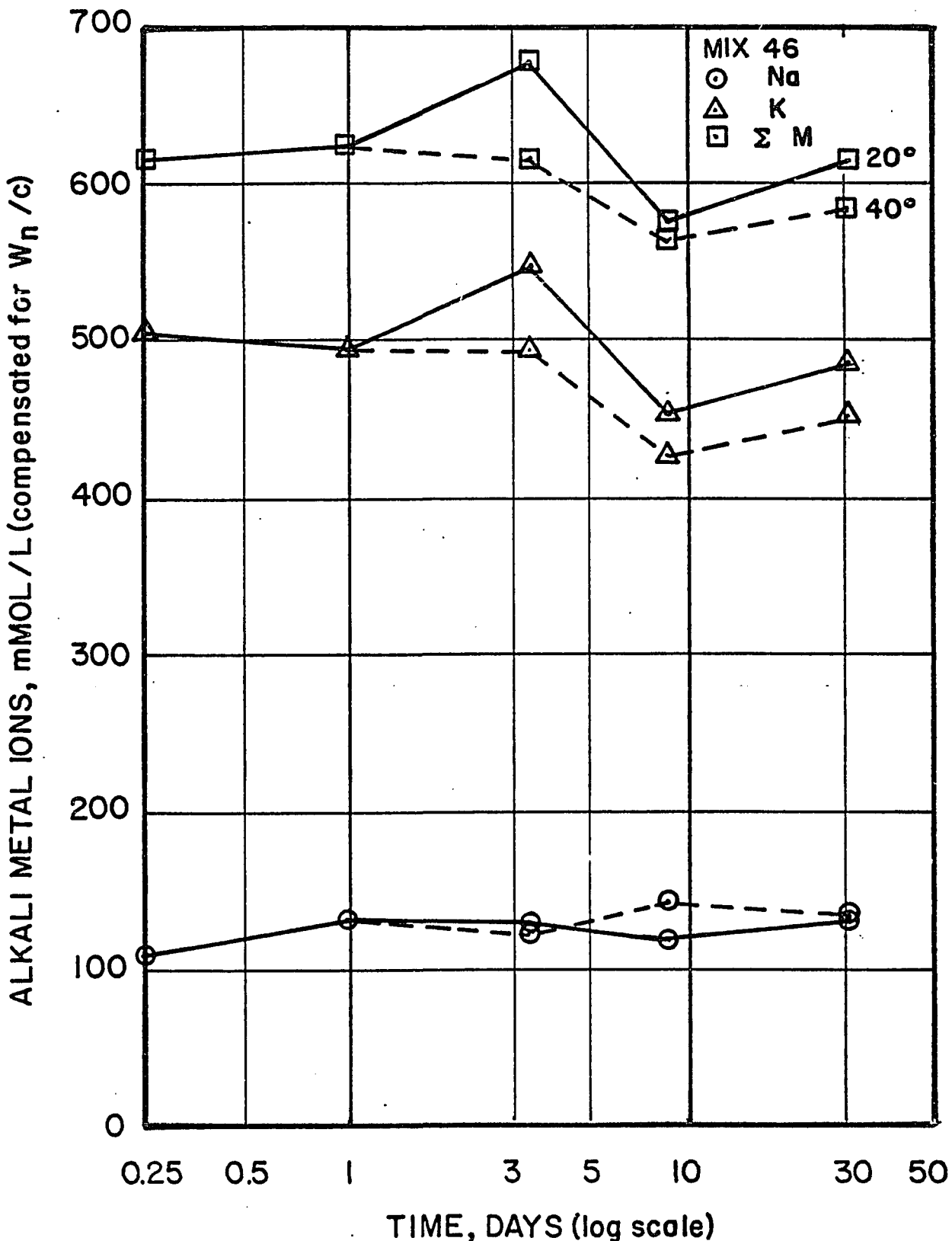


Figure 5.11.1 - Alkali Metal Ion Concentrations (Compensated for W_n/c)
as a Function of Time for Mix 46, Control for Mix Series 46 - 48.

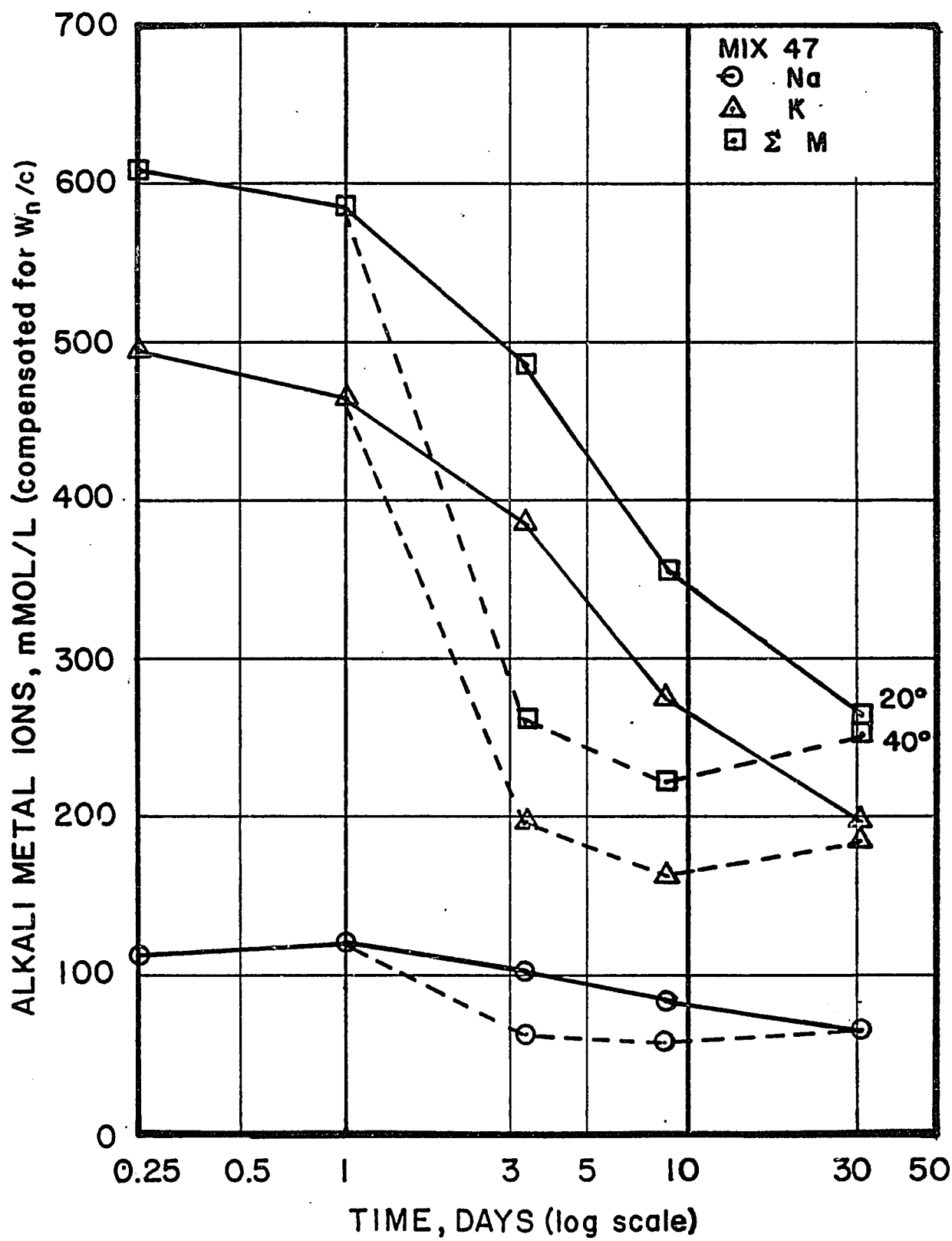


Figure 5.11.2 - Alkali Metal Ion Concentrations (Compensated for W_n/c) as a Function of Time for Mix 47, 8% Beltane Opal Sand.

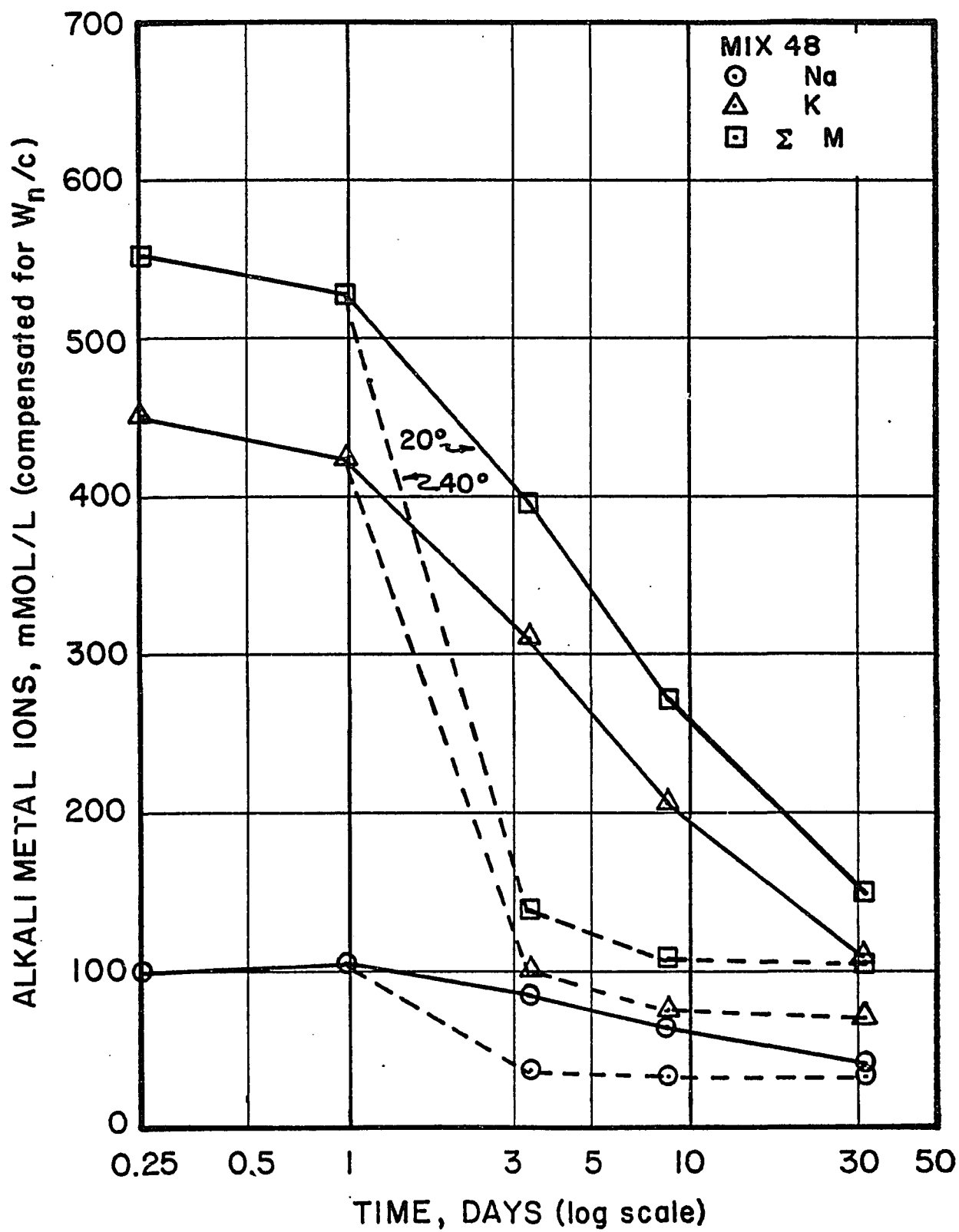


Figure 5.11.3 - Alkali Metal Ion Concentration (Compensated for W_n/c)
as a Function of Time for Mix 48, 8% Beltane Opal Sand and 19.6% EP-2.

For most chemical reactions involving mixtures of solid and liquid reactants the rate of the reaction is an inverse function of the particle size, and is directly related to the specific surface of the solid reactant. Thus it would be expected that Beltane opal added to a mortar mix as a fine powder, e.g. BP-2, should more rapidly and perhaps more efficiently reduce the alkali concentration level than Beltane opal added as sand-sized particles.

In Figures 5.11.4 through 5.11.6 the total alkali metal ion concentration, Σ^*M^+ , has been plotted against the total amount of Beltane opal added, as either sand-sized particles (Mix 47, 8 percent opal sand) or as both sand-sized particles and as BP-2 (Mix 48, 8 percent opal sand, 19.6 percent opal pozzolan).

It is instructive to examine the pattern of alkali removal from solution indicated in Figures 5.11.4 through 5.11.6. To begin with, the amount of alkali removed from solution at either test temperature, beyond one day, is not linearly related to the total percentage of opal added. Secondly, it will be noted that the alkali reduction resulting from the addition of 19.6 percent BP-2 to the mix containing 8 percent Beltane sand is nearly constant from 3.4 to 370 days, the maximum test age for specimens stored at 40°C. Subsequently it will be shown that for a commercial pozzolan (Pozzolan L, Mix Series 59 - 64) a linear relationship exists between alkali removed from pore solution and pozzolan added.

The implication of the pattern seen in Figures 5.11.4 through 5.11.6 is that the two forms of opal, differing only in particle size,

are not equally effective in removing alkalis; paradoxically the sand-sized opal seems more effective than the finely ground opal pozzolan.

Finally, it should be noted that at 40°C, the concentration of alkalis remaining in expressed pore solution approaches a constant value at about 30 days for mixes that contain either opal sand or opal sand and pozzolan. Essentially no change occurs between 30.5 days and 370 days. At 20°C, the responses are similar, but slower; however samples were not available for determinations beyond 30 days. Experience with other mix series suggests that the alkali concentrations in pore solutions at 370 days for either 20°C or 40°C storage usually approach a common value. Thus Figure 5.11.6 apparently represents attainment of an equilibrium condition and no further changes in concentration would be expected. Thus it can be inferred from the data that opal sand has a larger capacity for removing alkalis from the pore solution than an equal amount of finely ground opal, Pozzolan BP-2, prepared from the same material. This inference is of considerable importance in attempting to understand and model the reactions observed, and it will be referred to subsequently in Section 6.

The observed expansion of hardened mortar prisms for this series are listed in Table 5.11.10, and have been plotted against the logarithm of time in Figures 5.11.7 and 5.11.8. The values of Σ^*M^+ to 30.5 days at 20°C and to 370 days at 40°C have been included in these figures. For specimens stored at 20°C, expansion and Σ^*M^+ appear to follow similar paths, both approaching apparent equilibrium

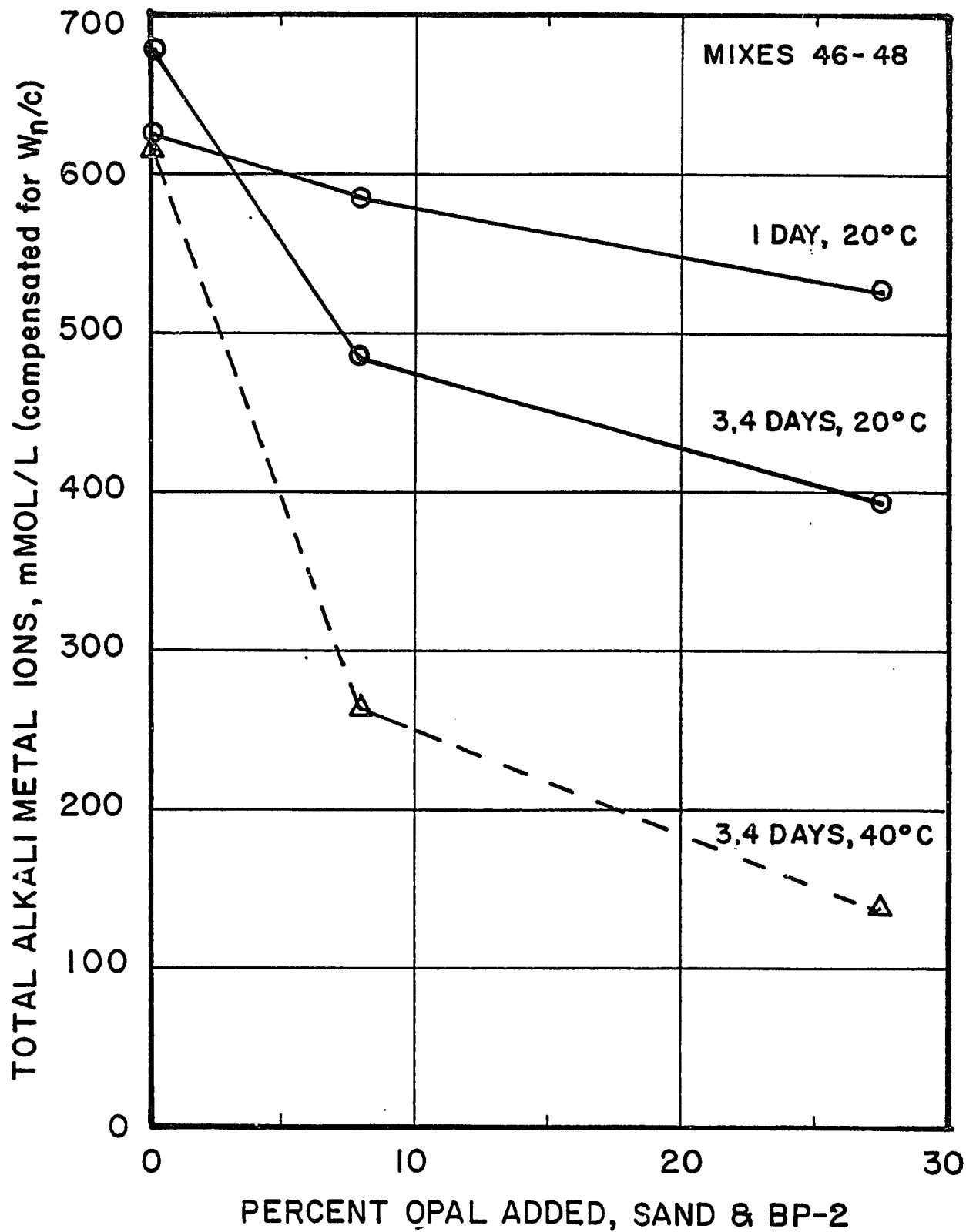


Figure 5.11.4 - Total Alkali Metal Ion Concentration

(Compensated for W_n/c) as a Function of Added Beltane Opal.

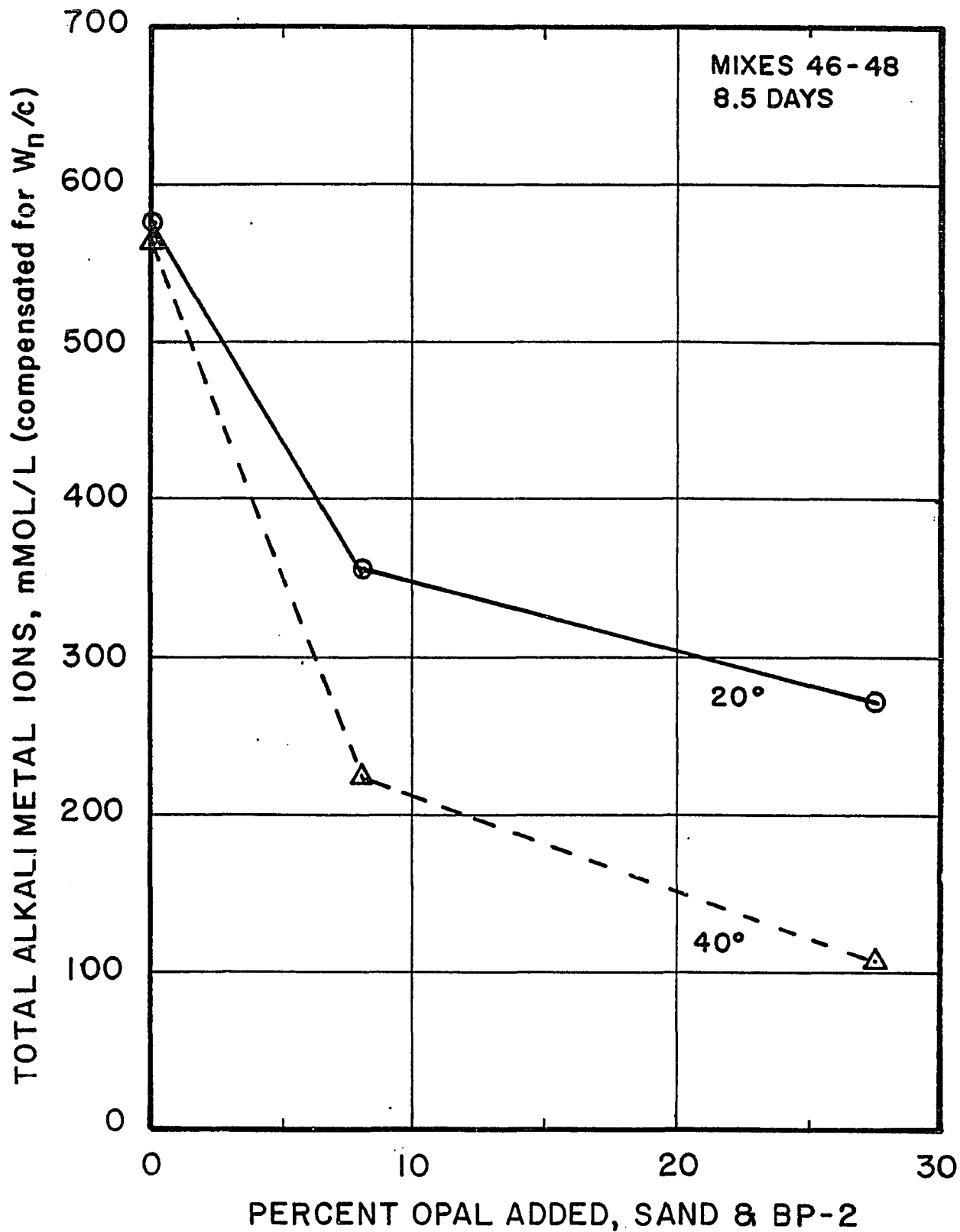


Figure 5.11.5 - Total Alkali Metal Ion Concentration
(Compensated for W_n/c) as a Function of Added Beltane Opal.

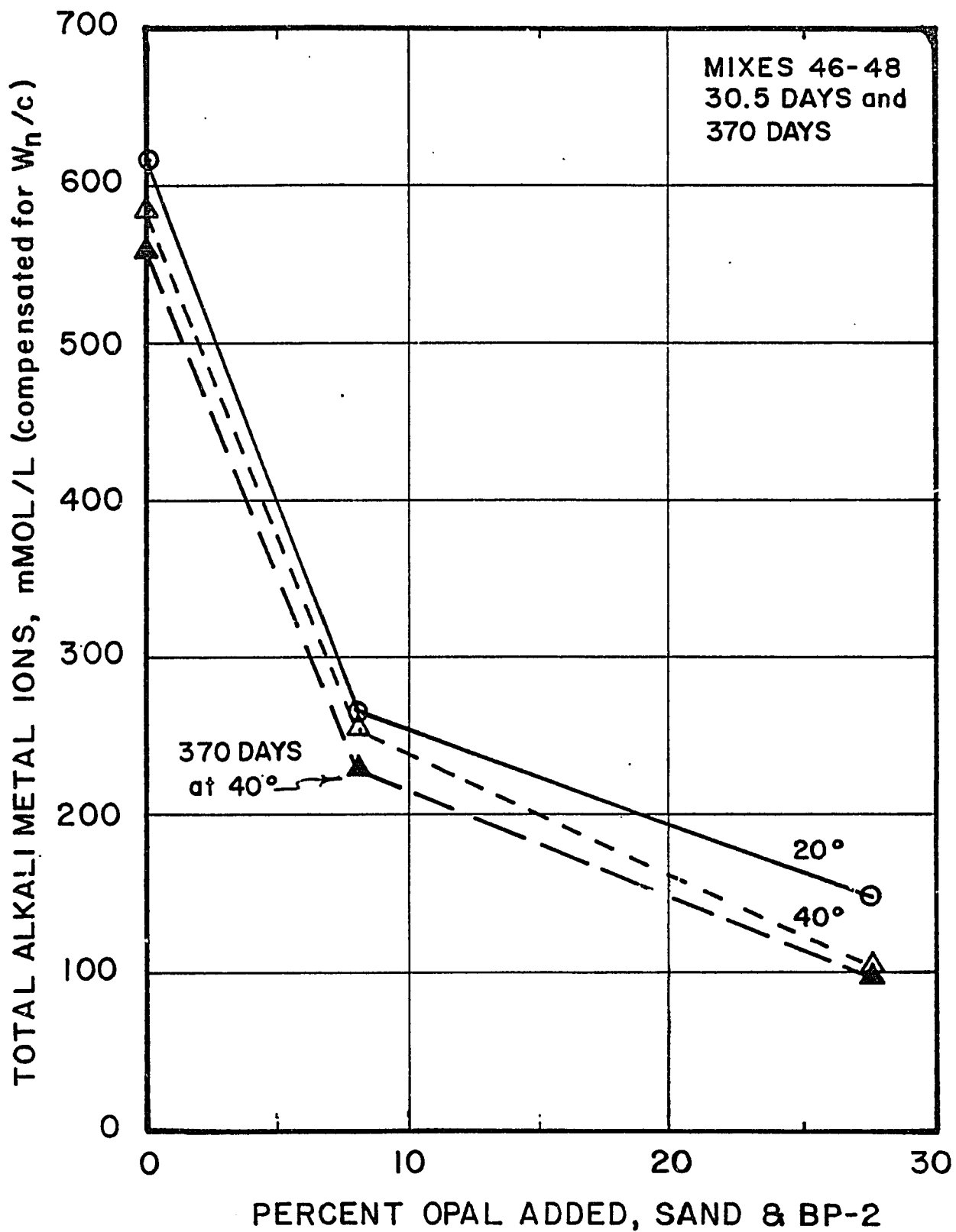


Figure 5.11.6 - Total Alkali Metal Ion Concentration

(Compensated for W_n/c) as a Function of Added Beltane Opal.

Table 5.11.10

Observed Expansions ($\mu\text{in/in}$) of Mortar Prisms, Mixes 46 - 48

Time, Days	Mix 46 20° C	Mix 46 40° C	Mix 47 20° C	Mix 47 40° C	Mix 48 20° C	Mix 48 40° C
0.8	-20	+93	+93	+587	+133	+373
3.7	-20	133	493	1227	787	680
11.8	+40	80	2013	2227	1840	773
23.	-20	173	2587	2720	2200	947
33.	+40	187	2853	2907	2373	1080
60.	40	133	2720	2987	2307	1320
235.	160	213	2747	3413	2427	1960

All specimens 0.5-in (12.7-mm) square cross-section rectangular prisms.
 Measurements made at same temperature as storage temperature.
 Negative values denote shrinkage.

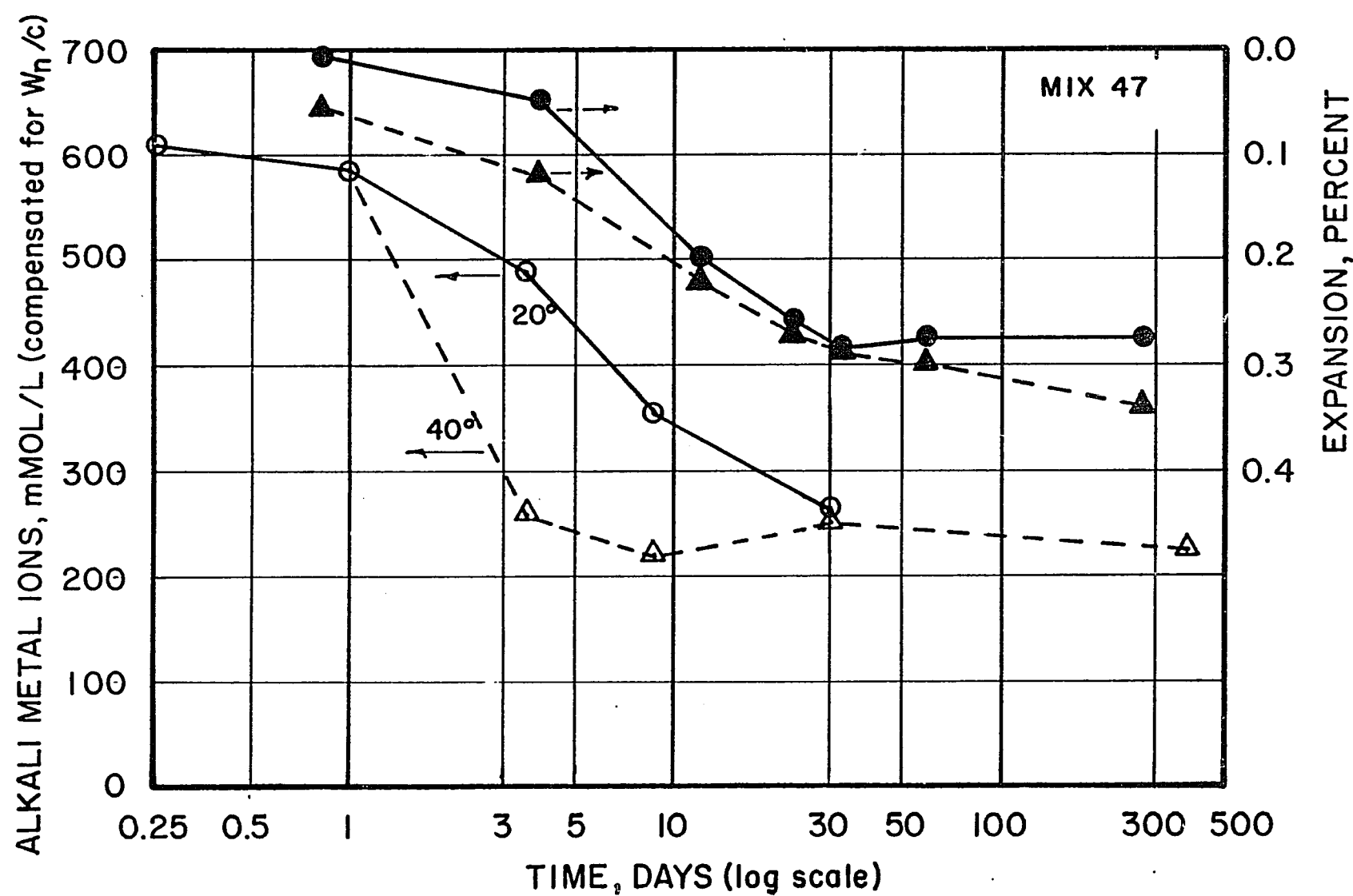


Figure 5.11.7 - Comparison of Total Alkali Metal Ion Concentration

(Compensated for W_n/c) and Expansion of Hardened Mortar Prisms With Time.

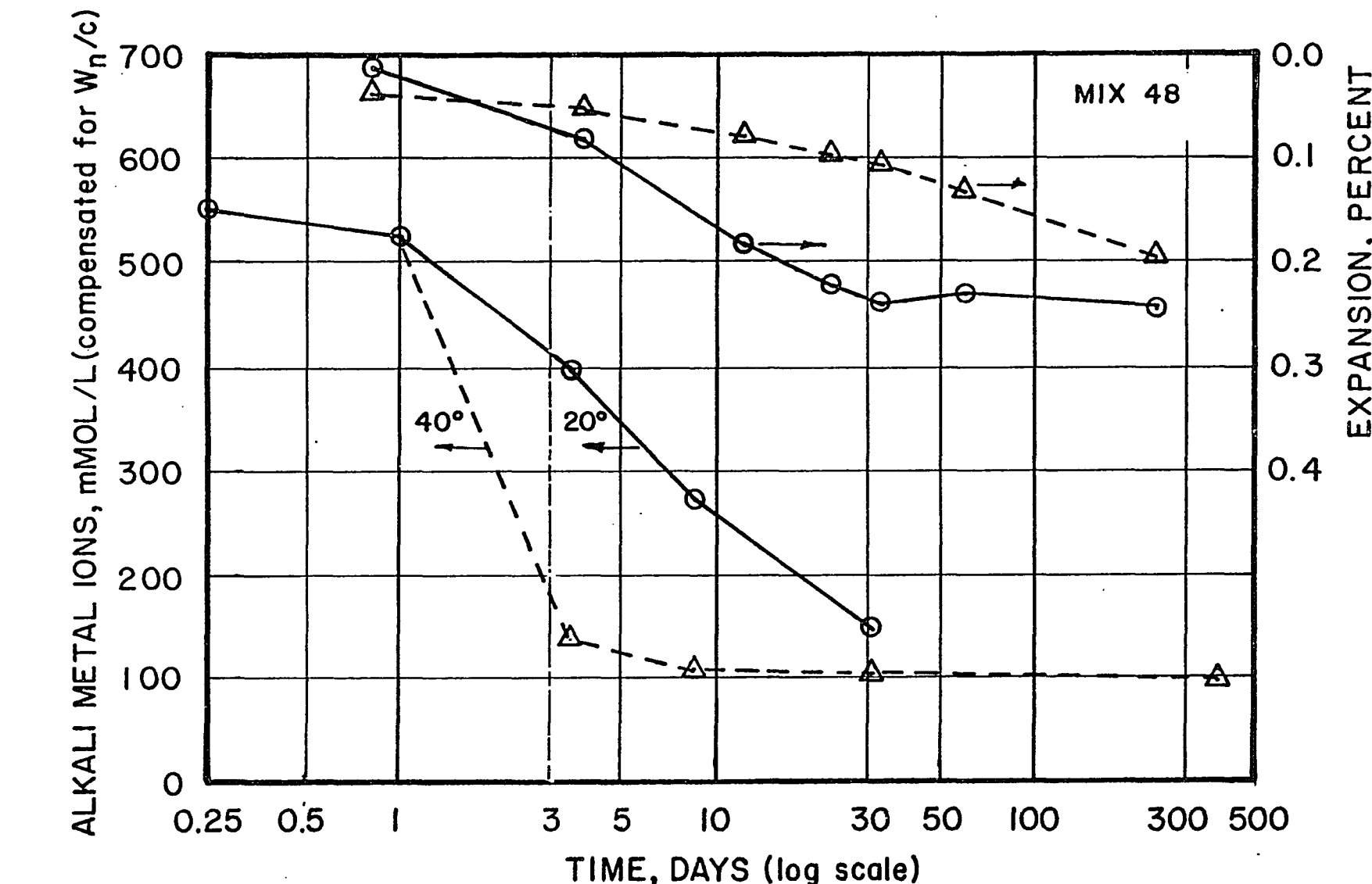


Figure 5.11.8 - Comparison of Total Alkali Metal Ion Concentration

(Compensated for W_n/c) and expansion of Hardened Mortar Prisms With Time.

at about the same time, i.e. 30 days. At 40°C values of Σ^*M^+ fell to a constant level within 3 to 10 days. However at 40°C the expansion of companion prisms was slower and lagged significantly behind both expansion at 20°C and removal of alkalis, the maximum expansion plateau not being reached before 300 days. This result suggests that while expansion requires products resulting from the alkali-silica reaction, its rate may be limited by other factors.

5.12. Mix Series 49 - 51

This series was conducted simultaneously with Mix Series 46 - 48, and supplements Mix Series 28 - 31, by providing chemical data on expressed pore solutions from mortars containing opal sand and Li_2CO_3 in the time period 0.25 through 30.5 days at both 20° and 40°C, and to 370 days at 40° only. The test mixes contained 8 percent Beltane opal sand, with and without the addition of 1.0 percent Li_2CO_3 . No prisms were cast for measurement of expansion potential of the hardened mortars. (See Mix Series 28 - 31 for length change data from equivalent mixes.)

Batch weights for the mixes studied are listed in Table 5.12.1. Weight ratios of the component materials, oven-dry/batch, and ignited/batch, are listed in Table 5.12.2. Observed concentrations of ions found in expressed pore solutions are listed in Tables 5.12.3 through 5.12.5. In Table 5.12.6 the observed values of W_n/c have been listed. Interpolation, where necessary, was carried out as outlined in Section 4.18.3. Nonevaporable water contents of the hardened specimens were estimated using the equations listed at the foot of Table 5.12.6.

Table 5.12.1

Batch Weights, Grams, for Mixes 49 - 51

Materials	Mix 49, Control		Mix 50, 8% Opal Sand		Mix 51, 8% Opal Sd., 1.0% Li ₂ CO ₃	
	Parts by Weight	Batch Weights	Parts by Weight	Batch Weights	Parts by Weight	Batch Weights
Cement, AT-1	1.00	763.3	1.00	759.2	1.00	763.3
Water	0.50	381.6	0.50	379.6	0.50	381.6
Li ₂ CO ₃	0.00	--	0.00	--	0.01	7.6
Beltane Sd.*	0.00	--	0.08	60.8	0.08	61.0
Sand, C 109	2.00	1526.5	1.92	1457.6	1.898	1448.7
Totals	3.5	2671.4	3.50	2657.2	3.488	2662.2

* Beltane opal sand, 50% 600 x 300 μm , 50% 300 x 150 μm .

Table 5.12.2

Weight Ratios of Component MaterialsOven-Dry/Batch, Ignited/Batch

Material	W _{od} /W _o	W _{ig} /W _o
Cement, AT-1	0.99809	0.99483
Beltane Sd.	0.99445	0.95298
Sand, C 109	0.99993	0.99868

Table 5.12.3

Observed Concentrations of Ions in Expressed Pore Solution (Not Corrected for Bound Water)

Mix 49, Control for Mix Series 49 - 51

(Concentrations in millimoles/liter)

Age, Days at 20° C	Mix 49, Control for Mix Series 49 - 51						Mix 49, Control for Mix Series 49 - 51					
	Si ⁴⁺ *	Al ³⁺	Fe ³⁺	Mg ⁺⁺	Ca ⁺⁺	Na ⁺	K ⁺	Li ⁺	Σ+**	OH ⁻	SO ₄ ⁼	Σ-**
0.25	0.5	0.1	0.0	1.0	54.	120.	401.	2.	631.	166.	n.d.	--
1.0	4.8	0.3	0.0	0.0	2.	169.	514.	1.	688.	648.	3.	654.
3.4	2.5	0.3	0.1	0.0	2.	197.	562.	2.	765.	706.	23.	752.
8.5	28.9	0.4	0.0	0.0	1.	202.	529.	1.	734.	732.	3.	738.
30.5	14.8	0.4	0.0	0.0	1.	229.	585.	4.	820.	817.	14.	845.
Age, Days at 40° C	Si ⁴⁺ *	Al ³⁺	Fe ³⁺	Mg ⁺⁺	Ca ⁺⁺	Na ⁺	K ⁺	Li ⁺	Σ+**	OH ⁻	SO ₄ ⁼	Σ-**
3.4	0.7	0.1	0.1	0.0	1.	206.	553.	5.	766.	654.	24.	703.
8.5	40.9	0.1	0.0	0.0	1.	211.	517.	1.	731.	663.	29.	721.
30.5	15.8	0.3	0.0	0.0	1.	231.	530.	2.	738.	611.	46.	703.
370.	9.3	0.7	0.1	0.1	1.	234.	531.	2.	769.	678.	n.d.	--

** See remarks under Section 4.4.1

* milliequivalents/liter

n.d. = not determined

Table 5.12.4

Observed Concentrations of Ions in Expressed Pore Solution (Not Corrected for Bound Water)

Mix 50, 8% Opal Sand

(Concentrations in millimoles/liter)

Age, Days at 20° C										
	Si ⁴⁺ *	Al ³⁺	Fe ³⁺	Mg ⁺⁺	Ca ⁺⁺	Na ⁺	K ⁺	Li ⁺	Σ^{+**}	Σ^{-**}
0.25	0.8	0.2	0.0	0.8	32.	120.	388.	2.	574.	184.
1.0	4.0	0.3	0.2	0.0	2.	164.	461.	1.	630.	n.d.
3.4	4.2	0.3	0.1	0.0	0.	156.	419.	2.	574.	622.
8.5	52.1	0.4	0.0	0.0	2.	151.	334.	0.	489.	524.
30.5	27.4	n.d.	0.0	n.d.	129.	265.	4.	398.	472.	22.
									361.	568.
									10.	22.
									381.	+11.
										+17.

Age, Days at 40° C										
	Si ⁴⁺ *	Al ³⁺	Fe ³⁺	Mg ⁺⁺	Ca ⁺⁺	Na ⁺	K ⁺	Li ⁺	Σ^{+**}	Σ^{-**}
3.4	27.1	0.2	0.0	0.1	3.	105.	214.	2.	327.	302.
8.5	41.7	0.2	0.0	0.1	0.	98.	178.	0.	276.	262.
30.5	13.8	0.4	0.0	0.0	1.	129.	250.	4.	385.	352.
370.	11.5	0.5	0.1	0.1	0.	97.	194.	0.	291.	23.
									270.	n.d.
										--

** See remarks under Section 4.4.1

* milliequivalents/liter

n.d. = not determined

Table 5.12.5
Observed Concentrations of Ions in Expressed Pore Solution (Not Corrected for Bound Water)

Mix 51, 8% Opal Sand, 1% Li ₂ CO ₃									
(Concentrations in millimoles/liter)									
Age, Days at 20° C	Si ⁴⁺ *	Al ³⁺	Fe ³⁺	Mg ⁺⁺	Ca ⁺⁺	Na ⁺	K ⁺	Li ⁺	Σ^{+**}
0.25	1.5	0.7	0.6	0.0	43.	115.	378.	363	942.
1.0	0.7	0.4	0.0	0.0	2.	159.	466.	266.	895.
3.4	1.8	0.2	0.0	0.1	2.	174.	502.	324.	1004.
8.5	46.5	0.3	0.0	0.0	1.	176.	423.	314.	915.
30.5	15.9	0.3	0.0	0.0	1.	188.	411.	237.	838.
Age, Days at 40° C	Si ⁴⁺ *	Al ³⁺	Fe ³⁺	Mg ⁺⁺	Ca ⁺⁺	Na ⁺	K ⁺	Li ⁺	Σ^{+**}
3.4	4.5	0.0	0.0	0.1	1.	144.	352.	227.	725.
8.5	38.0	0.1	0.0	0.0	1.	154.	306.	183.	645.
30.5	13.7	0.4	0.0	0.0	1.	159.	277.	132.	570.
370.	13.1	0.5	0.1	0.1	1.	137.	218.	55.	412.
									Σ^{+**}

** See remarks under Section 4.4.1

* milliequivalents/liter

n.d. = not determined

Table 5.12.6

Nonevaporable Water, W_n/c , as a Function ofBeltane Opal Sand Addition* and Time

Time, Days	Temp. °C	Mix 49	Mix 50	Mix 51
0.46	20	0.0360	0.0336	0.0251
4.0	20	0.1563	0.1521	0.1436
4.0	40	--	0.1508	0.1437
9.25	20	0.1692	0.1618	0.1436
9.25	40	0.1687	0.1660	0.1530
30.5	20	0.1835	0.1784	0.1986
30.5	40	--	0.1665	0.1712

Equations used to estimate W_n/c for $0.25 \leq t \leq 30.5$ days at $20^\circ C$

$$\text{Mix 49, est } W_n/c = t/(9.3650 + 4.5988t + 0.0179t^2)$$

$$\text{Mix 50, est } W_n/c = t/(9.8782 + 4.8010t + 0.0158t^2)$$

$$\text{Mix 51, est } W_n/c = t/(13.4833 + 4.8651t - 0.0088t^2)$$

Equations used to estimate W_n/c for $0.25 \leq t \leq 30.5$ days at $40^\circ C$

$$\text{Mix 49, est } W_n/c = t/(3.4174 + 5.8366t - 0.0141t^2)$$

$$\text{Mix 50, est } W_n/c = t/(4.8890 + 5.3431t - 0.2165t^2)$$

$$\text{Mix 51, est } W_n/c = t/(2.0387 + 6.5512t - 0.0255t^2)$$

Components Added to Mixes	Mix 49	Mix 50	Mix 51
% Beltane Opal Sand	0.0	8.0	8.0
% Li ₂ CO ₃	0.0	0.0	1.0

'1

Alkali metal ion concentrations, compensated for $\frac{W}{n}/c$, have been listed in Tables 5.12.7 through 5.12.9, and plotted against the logarithm of time in Figures 5.12.1 through 5.12.4.

In Figure 5.12.1 the alkali metal ion concentrations (including Li^+) in pore solutions from the control mix, Mix 49, appear to have increased slightly during the period from 0.25 to one day, after which the K^+ concentration fell back to its 0.25 day concentration at 10 days. Through 30.5 days the alkali metal ion concentration appeared independent of temperature in the range 20° to 40°C, and there was no significant change after 370 days of storage at 40°C.

In Figure 5.12.2 the alkali metal ion concentrations in pore solutions expressed from Mix 50, containing 8 percent Beltane opal sand, increased to a maximum at one day and then fell rapidly, reflecting the changes observed in a similar mix, Mix 47, in Mix Series 46 - 48. Specimens stored at 20°C reached a minimum value at, or just beyond, 30 days, while those stored at 40°C attained a minimum alkali ion content between 3 and 10 days. The large increase in K^+ concentration between 10 and 30.5 days for specimens stored at 40°C appears to be unique to this Mix Series and to Mix Series 46 - 48. Concentrations observed at 370 days lie approximately midway between values observed at 8.5 and 30.5 days for Mix 50.

In Figures 5.12.3 and 5.12.4 data for Mix 51, containing 8 percent Beltane opal sand and 1.0 percent Li_2CO_3 , have been plotted. Because of the number of lines and the large scale reduction required to show all of the concentration values, it was desirable to separate 20° and 40°C values. The one day values for specimens stored at 20°C

Table 5.12.7
 Concentrations of Alkali Metal Cations in Expressed Pore Solution (Corrected for Bound Water)
 Mix 49, Control for Mix Series 49 - 51
 (Concentrations in millimoles/liter)

Age, Days at 20° C	W_n/c	bwk	Cations Found			Cation Concentration Corrected for W_n/c			$*K^+/_*$ $*Na^+$
			Na^+	K^+	M^+	$*Na^+$	$\Delta *Na^+$	$*K^+$	
0.25	0.024	0.952	120	401	521	114	--	382	--
1.0	0.072	0.856	169	514	683	145	--	440	--
3.4	0.135	0.730	197	562	759	144	--	410	--
8.5	0.171	0.658	202	530	732	133	--	349	--
30.5	0.183	0.634	229	585	814	145	--	371	--
									516
									--
Age, Days at 40° C	W_n/c	bwk	Cations Found			Cation Concentration Corrected for W_n/c			$*K^+/_*$ $*Na^+$
			Na^+	K^+	M^+	$*Na^+$	$\Delta *Na^+$	$*K^+$	
3.4	0.147	0.706	206	553	759	145	--	390	--
8.5	0.163	0.674	211	517	728	142	--	348	--
30.5	0.181	0.638	231	530	761	147	--	338	--
370.	0.187	0.626	234	531	765	146	--	332	--
									479
									--

Table 5.12.8

Concentrations of Alkali Metal Cations in Expressed Pore Solution (Corrected for Bound Water)

Mix 50, 8% Opal Sand												
		(Concentrations in millimoles/liter)										
Age, Days at 20° C	W_n/c	bwk	Cations Found			Cation Concentration Corrected for W_n/c			$*K^+ / *Na^+$			
			Na^+	K^+	M^+	$*Na^+$	$\Delta *Na^+$	$*K^+$		$\Delta *K^+$		
0.25	0.023	0.954	120	388	508	114	0	370	-12	485	-11	3.233
1.0	0.068	0.864	164	461	625	142	-3	398	-42	540	-45	2.811
3.4	0.129	0.742	156	419	575	116	-28	311	-99	427	-127	2.686
8.4	0.164	0.672	151	334	485	101	-31	224	-124	326	-156	2.212
30.5	0.178	0.644	129	265	394	83	-62	171	-200	254	-262	2.054

Age, Days at 40° C	W_n/c	bwk	Cations Found			Cation Concentration Corrected for W_n/c			$*K^+ / *Na^+$			
			Na^+	K^+	M^+	$*Na^+$	$\Delta *Na^+$	$*K^+$				
3.4	0.146	0.708	105	214	319	74	-71	152	-239	226	-310	2.038
8.5	0.165	0.670	98	178	276	66	-77	119	-229	185	-306	1.816
30.5	0.166	0.668	129	250	379	86	-61	167	-171	253	-232	1.938
370.	0.168	0.664	97	194	291	64	-82	129	-204	193	-286	2.000

Table 5.12.9

Concentrations of Alkali Metal Cations in Expressed Pore Solution (Corrected for Bound Water)					
Mix 51, 8% Opal Sand, 1% Li ₂ CO ₃					
(Concentrations in millimoles/liter)					
Age, Days at 20° C	V _n /c	bwk	Cations Found	Cation Concentration Corrected for W _n /c	
			Na ⁺	*Na ⁺	*Li ⁺
0.25	0.017	0.966	K ⁺	Δ*K ⁺	Δ*Li ⁺
1.0	0.55	0.890	Li ⁺	Δ*Li ⁺	
3.4	0.114	0.772	M [†]		
8.5	0.157	0.686			
30.5	0.198	0.604			

Age, Days at 20° C	V _n /c	bwk	Cations Found	Cation Concentration Corrected for W _n /c	
			Na ⁺	*Na ⁺	*Li ⁺
0.25	0.017	0.966	K ⁺	Δ*K ⁺	Δ*Li ⁺
1.0	0.55	0.890	Li ⁺	Δ*Li ⁺	
3.4	0.114	0.772	M [†]		
8.5	0.157	0.686			
30.5	0.198	0.604			

Age, Days at 20° C	V _n /c	bwk	Cations Found	Cation Concentration Corrected for W _n /c	
			Na ⁺	*Na ⁺	*Li ⁺
0.25	0.017	0.966	K ⁺	Δ*K ⁺	Δ*Li ⁺
1.0	0.55	0.890	Li ⁺	Δ*Li ⁺	
3.4	0.114	0.772	M [†]		
8.5	0.157	0.686			
30.5	0.198	0.604			

Table 5.12.9 (Continued)

Concentrations of Alkali Metal Cations in Expresssed Pore Solution (Corrected for Bound Water)

Mix 51, 8% Opal Sand, 1% Li₂CO₃

(Concentrations in millimoles/liter)

Age, Days at 40° C	w _{n/c}	bwk	Cations Found			Cation Concentration Corrected for w _{n/c}		
			Na ⁺	K ⁺	Li ⁺	*Na ⁺	*K ⁺	*Li ⁺
3.4	0.142	0.716	144	352	227	723	103	-42
8.5	0.152	0.696	154	306	183	643	107	-35
30.5	0.171	0.658	159	277	132	568	105	-43
370.	0.177	0.646	137	218	55	410	89	-58
							141	-192
								36
								+36
Age, Days at 40° C						*K ⁺ / *Na ⁺		
3.4						2.444		
8.5						1.987		
30.5						1.742		
370.						1.591		

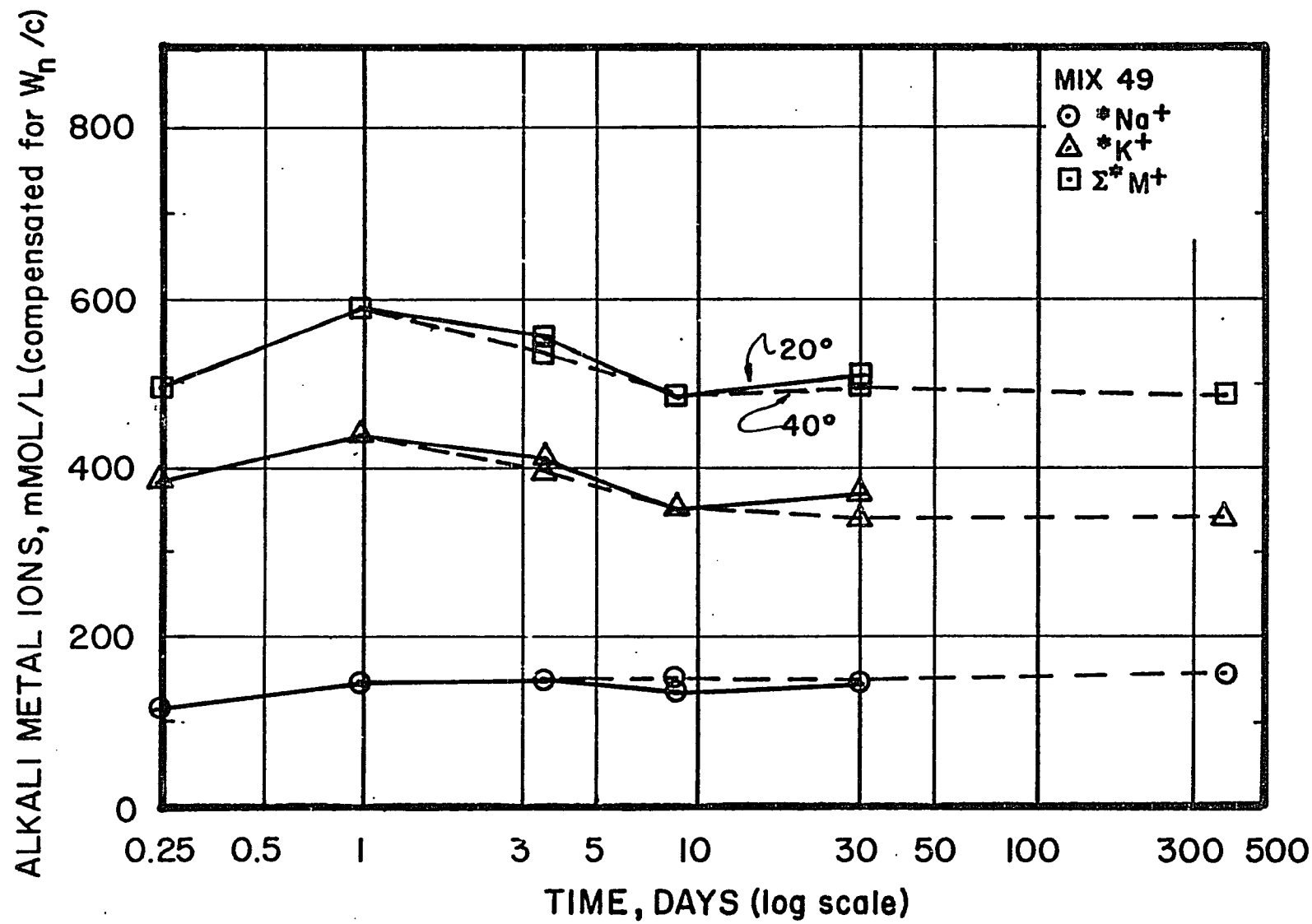


Figure 5.12.1 - Alkali Metal Ion Concentrations (Compensated for W_n/c)

as a Function of Time for Mix 49, Control for Mix Series 49 - 51.

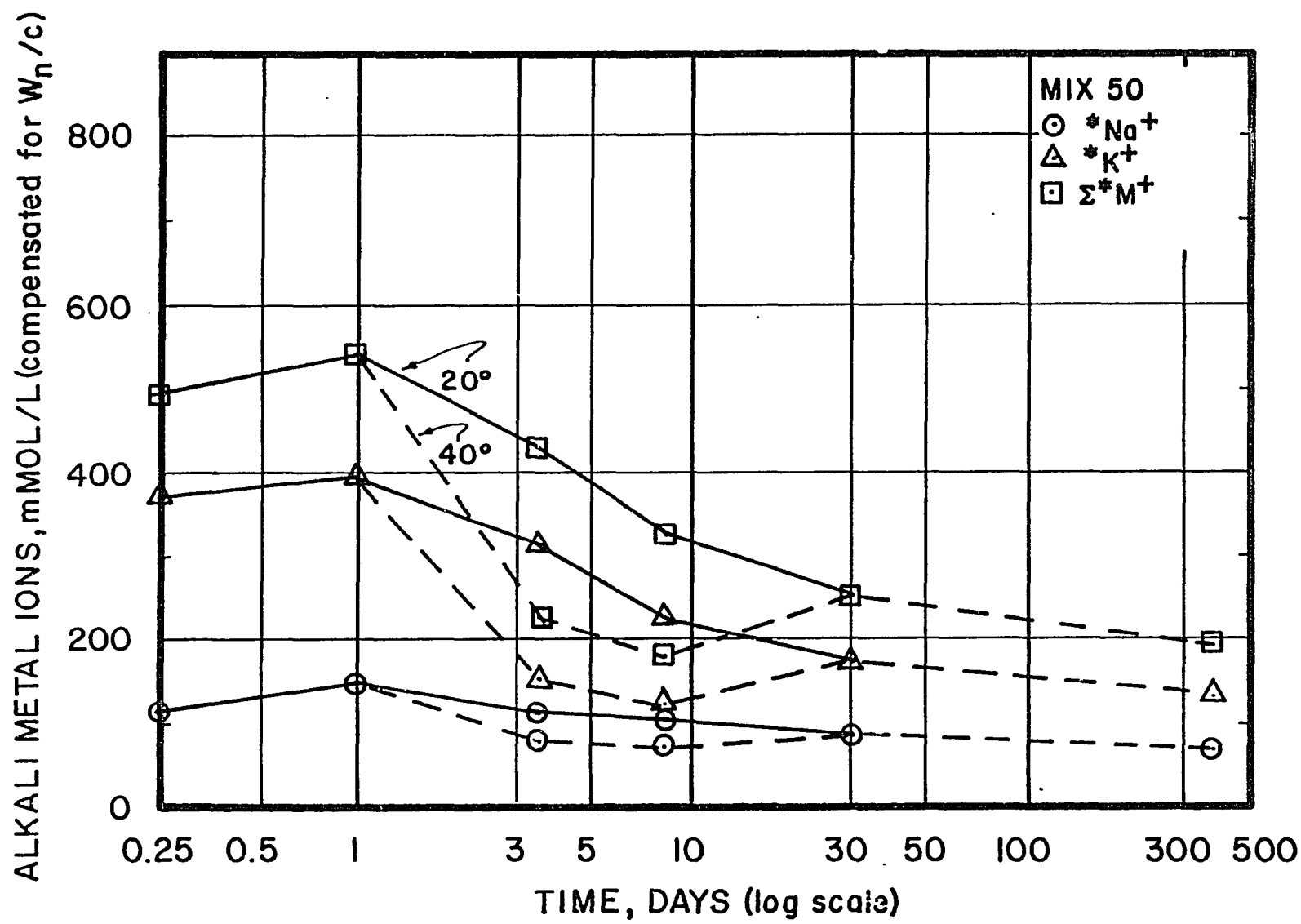


Figure 5.12.2 - Alkali Metal Ion Concentrations (Compensated for W_n/c)
as a Function of Time for Mix 50, *% Beltane Opal Sand.

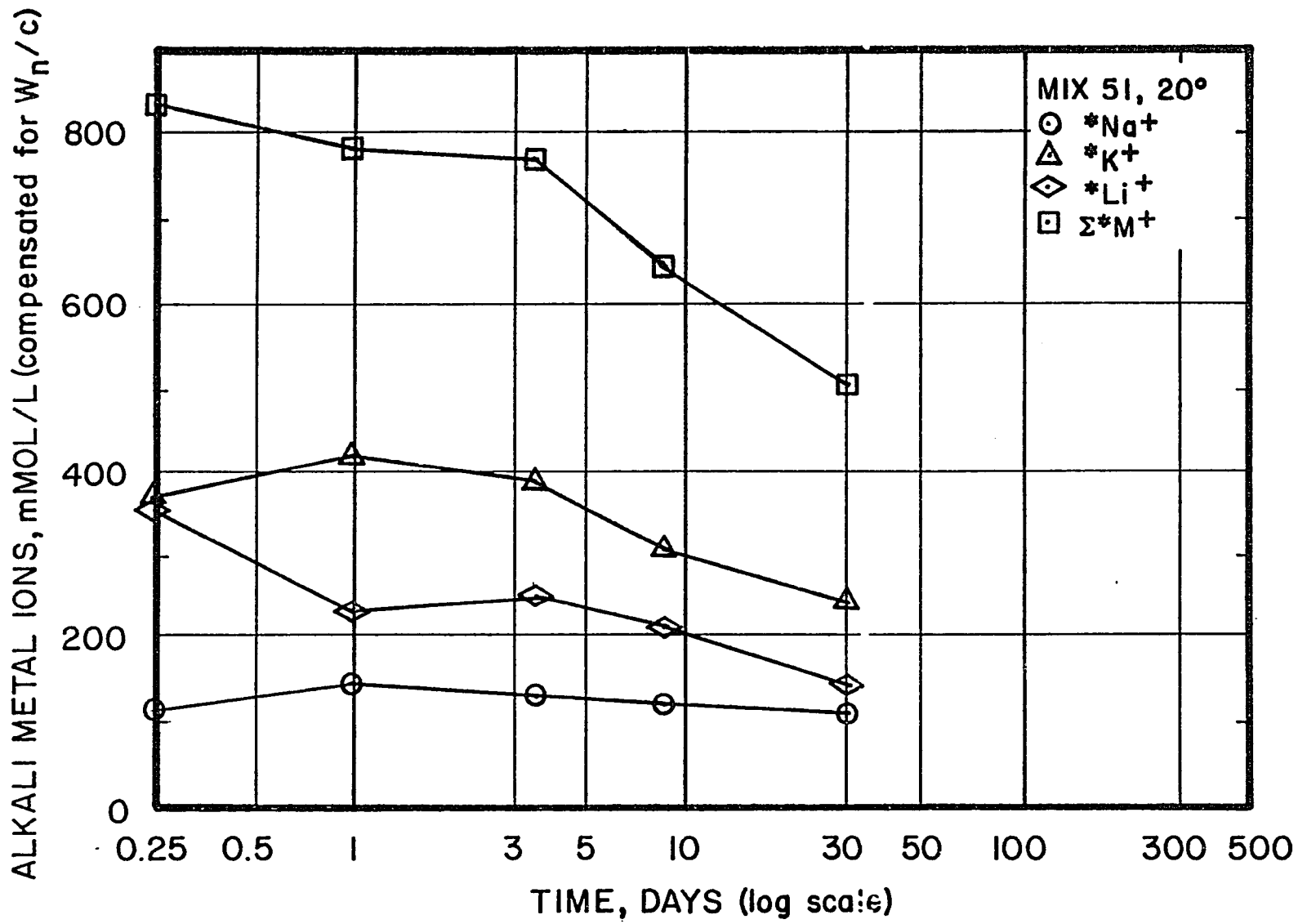


Figure 5.12.3 - Alkali Metal Ion Concentrations (Compensated for W_n/c)

as a Function of Time for Mix 51, 8% Beltane Opal Sand, 1.0% Li_2CO_3

for Specimens Stored at 20° C.

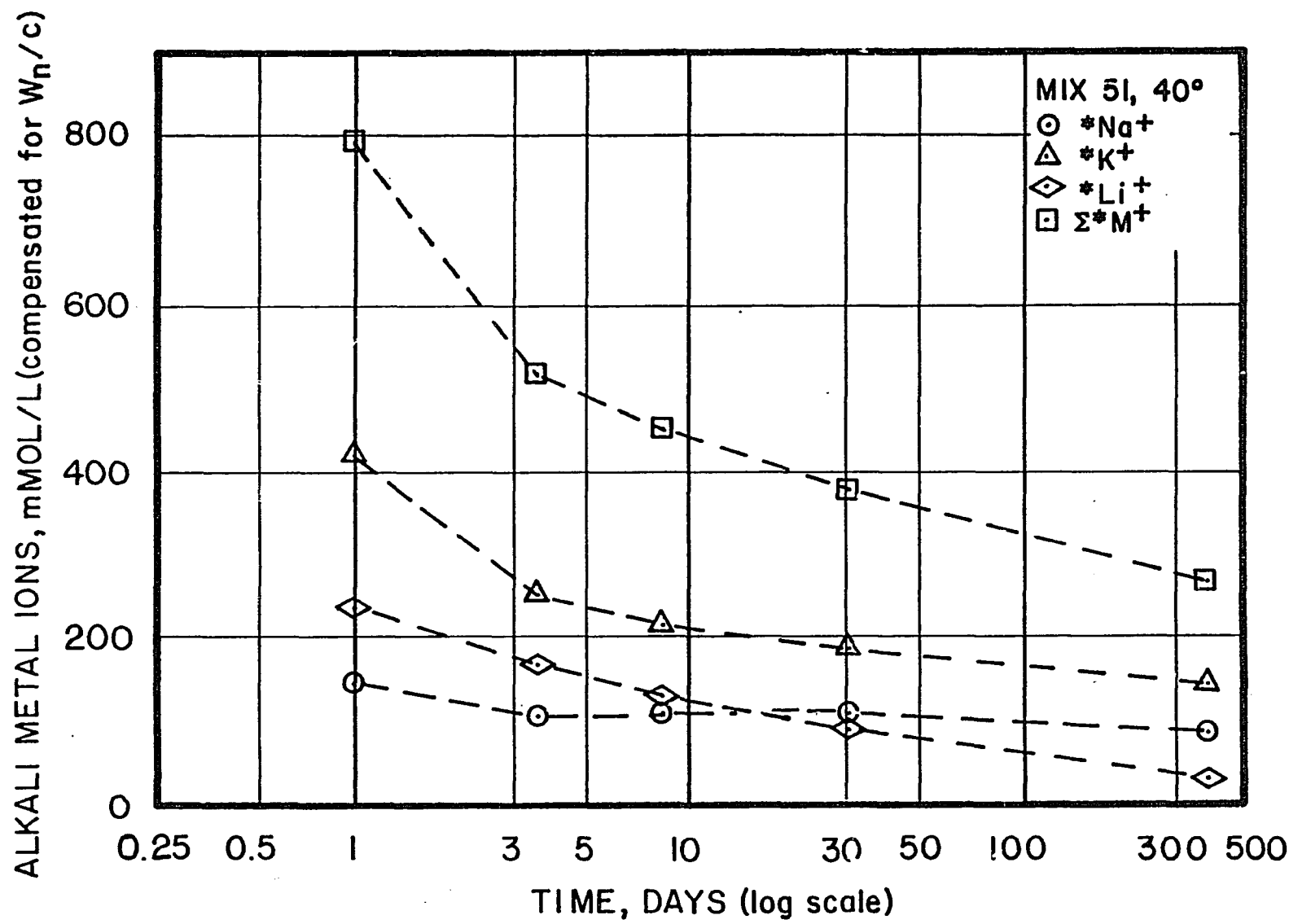


Figure 5.12.4 - Alkali Metal Ion Concentrations (Compensated for W_n/c)

as a Function of Time for Mix 51, 8% Beltane Opal Sand, 1.0% Li_2CO_3

for Specimens Stored at 40° C.

have been plotted in Figure 5.12.4 with the 40°C data to provide a reference point. At 20°C the K⁺ and Na⁺ concentrations followed the same patterns observed in Mix 50 except that in the presence of Li⁺ the rate of removal of these cations from solution as a result of the alkali-silica reaction was reduced. At 40°C the rate of removal of Na⁺ and K⁺ were virtually identical to those observed for Mix 50. The Li⁺ concentration fell throughout the period 1 through 370 days and appears to have been asymptotically approaching zero concentration.

At 1.0 percent addition of Li₂CO₃, by weight of portland cement the potential concentration of the solutions was 0.271 molar with respect to Li₂CO₃, or 0.541 normal with respect to Li⁺. It should be noted that the solubility of Li₂CO₃ (508, Vol. II, pp. 384, f.). pure water is 0.180 moles per liter at 20°C, equivalent to 0.360 normal Li⁺, and 0.158 moles per liter at 40°C, equivalent to 0.317 normal Li⁺. The maximum concentration observed in solutions uncorrected for bound water was 0.363 normal at 0.25 days and 20°C (see Table 5.12.5).

This matter will be addressed more fully in Section 6, but it seems desirable to point out the curious behavior of the Li⁺ at this point. Until this series of experiments, it appeared that the rate at which alkali metal ions were removed from pore solutions was inversely related to their hydrated radii. In this series it appears the Li⁺ ion is preferentially removed from solution, in spite of its large radius relative to the radii of Na⁺ and K⁺, followed by K⁺ that has the least radius of the three, which is in turn followed by Na⁺ that has an intermediate radius.

5.13 - This section not used

5.14 - Mix Series 58

In this series a single mix (see Table 5.14.1) containing Beltane opal sand was used. Two types of specimens were used to measure potential expansion; a Butyl rubber jacketed 50-mm diameter cylinder (see Section 4.14.5) and 0.50-in (12.7-mm) cross-section rectangular prisms (see Section 4.14.3). No chemical tests were made in this series. Chemical data are available for identical mixes, e.g. mixes 30, 50, and 60.

The purpose of this experiment was to verify that specimens identical in size, shape, composition and treatment to those actually used in measuring chemical responses of pore solutions do in fact undergo expansion, and can be used to provide accurate expansion-time data that can be related specifically to the pore solution compositional changes.

Although the shape of the expansion-time curves for the 50-mm jacketed cylinder is similar to that of the 0.50-in (12.7-mm) prism, the magnitude of the expansion of the cylindrical specimen was several times that of the small prisms. Specific reasons for this difference were not investigated, but the following are probable:

- differences in cross-sectional area of the two types of specimen,
- dilution of the pore solutions in the unjacketed prisms resulting from unlimited access to free water,
- leaching of alkalies from unjacketed prisms.

The last cause was documented qualitatively. To prevent growth of mold and bacteria in the wet storage containers a 5 percent solution of copper sulfate ($5\text{ g CuSO}_4 \cdot 5\text{H}_2\text{O}$ in $95\text{ g H}_2\text{O}$) was used in

Table 5.14.1

Batch Weights, grams, for Mix 58

Materials	Mix 58, 8% Opal Sand	
	Parts by Weight	Batch Weights
Cement, AT-1	1.00	143.1
Water	0.50	71.6
Beltane Sd.*	0.08	11.4
Sand, C109	1.57	271.6
Totals	3.15	479.7

* Beltane opal sand, 50% 600 x 300 μm ,
50% 300 x 150 μm .

Table 5.14.2
Expansion Measurements ($\mu\text{in/in}$) of
Specimens Representing Mix Series 58

Age, Days at 40° C	50-mm Butyl Rubber Jacketed Cylinders	0.5-in (12.7-mm) Rectangular Prisms
1.	0	0
2.9	364	282
5.3	1491	582
8.	2764	763
14.2	6036	1245
17.2	6654	1236
19.7	7840	1482
25.4	8509	1763
32	9564	1836
35	9673	--
38	10764	--
54	11382	2345
57	13309	--
70	13345	2700
92	14035	3145
123	--	3281
166	14835	3545
297	15634	4236
549	16289	4345
Estimated		
Ultimate	16942	4783

Estimating equation for 50-mm jacketed cylinders:

$$\epsilon_t = t / (1.3323 \times 10^{-3} + 5.9024 \times 10^{-5} t)$$

Estimating equation for 0.5-in (12.7-mm) prisms:

$$\epsilon_t = t / (1.0729 \times 10^{-2} + 2.0910 \times 10^{-4} t)$$

place of pure water. After several months of storage it was noted that the pool of solution in the storage containers was no longer blue and that a dark green precipitate had collected in the bottoms of the containers. The precipitate was identified by X-ray diffraction as brochantite, $\text{CuSO}_4 \cdot 3\text{Cu}(\text{OH})_2$. The published peaks for brochantite (JCPDS 13-398) accounted for all of the significant peaks in the pattern obtained from the precipitate. Presumably the OH^- came from alkali metal hydroxides leached from the mortar specimen.

The observed expansions of the two types of specimens, expressed in $\mu\text{in/in}$, are listed in Table 5.14.2 and plotted in Figure 5.14.1. Hyperbolic estimating equations were fitted to the data starting at 25.4 days, and they have been appended to Table 5.14.2.

The results of this series indicate that the observed changes in chemical composition of pore solutions expressed from hardened mortars do reflect changes that in fact result from alkali-silica reactions. These changes do not necessarily signal expansion of the mortars. In the series that follow it will be seen that whether or not expansion takes place depends on the amount and on the physical form of the added reactive constituents, but that it may be possible to predict whether or not expansion will ultimately take place from early changes in expressed pore solution properties.

5.15 - Mix Series 59 - 64

In this series the effects of two addition levels of Pozzolan L to plain mortars and to mortars containing Beltane opal sand were studied. In addition to the determination of chemical properties of

expressed pore solutions, two different types of specimens were prepared for measurement of length changes of the hardened mortars. Both pozzolan and opal sand were added as percentages, by weight, of the portland cement in the mixes. Batch weights of C 109 sand were adjusted for those mixes containing opal sand or pozzolan to maintain a constant batch volume of 2230 cm³. The batch weights are listed in Table 5.15.1. Weight ratios of the component materials, oven-dry/batch, and ignited/batch, are listed in Table 5.15.2. These values were required to reduce the data for W_n/c as outlined in Section 4.12.2. Tabulations of W_n/c and Ca(OH)₂ found in the hardened mortars, both as a function of % POZZ_{eq} (the ratio of the weight percent SiO₂ in the reactive component under test to the weight percent SiO₂ in pozzolan L, times the percent loading of the reactive component used in the mix) indicate that reductions in W_n/c and in free Ca(OH)₂ are related to % POZZ_{eq}.

Observed chemical properties of the expressed pore solutions have been listed in Tables 5.15.3 through 5.15.8. The concentrations of the alkali metal ions found, compensated for W_n/c, have been listed in Tables 5.15.10 through 5.15.15. These data indicate that the apparent ability of the reactive components to reduce Σ*M⁺ is not necessarily related to % POZZ_{eq} as defined above, but is more likely related to the microstructure or state of order in the reactive material, or possibly to differences in the reaction products as a function of the sizes of the reacting particles.

Table 5.15.1
Batch Weights, grams, for Mixes 59 - 64

Materials	Mix 59, Control		Mix 60, 8% Opal Sand		Mix 61, 8% Opal Sd., 10% Pozzolan	
	Parts by Weight	Batch Weights	Parts by Weight	Batch Weights	Parts by Weight	Batch Weights
Cement, AT-1	1.00	1418.0g	1.00	1418.0g	1.00	1418.0g
Pozzolan, L	0.00	--	0.00	--	0.10	142.0
Water	0.50	709.0	0.50	709.0	0.50	709.0
Beltane Sd.*	0.00	--	0.08	113.4	0.08	113.4
Sand, C109	2.00	2837.0	1.898	2692.0	1.787	2534.0
Totals	3.50	4964.0g	3.478	4932.4g	3.467	4916.4g

Materials	Mix 62, 8% Opal Sd., 25% Pozzolan		Mix 63, 10% Pozzolan		Mix 64, 25% Pozzolan	
	Parts by Weight	Batch Weights	Parts by Weight	Batch Weights	Parts by Weight	Batch Weights
Cement AT-1	1.00	1418.0g	1.00	1418.0g	1.00	1418.0g
Pozzolan, L	0.25	354.6	0.10	142.0	0.25	354.6
Water	0.50	709.0	0.50	709.0	0.50	709.0
Beltane Sd.*	0.08	113.4	0.00	--	0.00	--
Sand, C109	1.62	2297.0	1.89	2679.0	1.72	2442.0
Totals	3.45	4892.0	3.490	4948.0	3.47	4924.0

* Beltane opal sand, 50% 600 x 300 μm , 50% 300 x 150 μm .

Table 5.15.2
Weight Ratios of Component Materials
Oven-Dry/Batch, Ignited/Batch

Material	Wod/Wo	Wig/Wo
Cement, AT-1	0.99809	0.99483
Pozzolan, L	0.99807	0.98924
Beltane Sand	0.99445	0.95298
Sabd, C109	0.99993	0.99868

Table 5.15.3
Observed Concentrations of Ions in Expressed Pore Solution (Not Corrected for Bound Water)
Mix 59, Control for Mix Series 59 - 64
(Concentrations in millimoles/liter)

Age, Days at 20° C							Σ^{+}	Σ^{-}
	Si ⁴⁺ *	Al ³⁺	Fe ³⁺	Mg ⁺⁺	Ca ⁺⁺	K ⁺		
0.021	2.1	0.3	0.0	0.0	15.	125.	374.	529.
2.	3.5	0.3	0.0	0.0	2.	201.	524.	729.
32.	13.8	0.4	0.0	0.1	1.	209.	521.	732.
128.	2.2	0.7	0.0	0.0	1.	238.	575.	815.
	Si ⁴⁺ *	Al ³⁺	Fe ³⁺	Mg ⁺⁺	Ca ⁺⁺	K ⁺	Σ^{+}	Σ^{-}
2.	8.8	0.5	0.0	0.0	1.	203	532.	737.
32.	7.1	0.5	0.0	0.0	1.	220.	496.	718.
128.	8.0	0.8	0.0	0.0	1.	243.	541.	786.

* See remarks in Section 4.4.1
** milliequivalents/liter
n.d. = not determined

Table 5.15.4
 Observed Concentrations of Ions in Expresssed Pore Solution (Not Corrected for Bound Water)
Mix 60, 8 Percent Opal Sand
 (Concentrations in millimoles/liter)

Age, Days at 20° C							Σ^{+-}	Σ^-
	Si ⁴⁺ *	Al ³⁺	Fe ³⁺	Mg ⁺⁺	Ca ⁺⁺	Na ⁺		
0.021	3.6	0.1	0.0	0.0	19.	125.	377	161.
2.	6.3	0.4	0.0	0.0	1.	165.	439.	582.
32.	13.1	0.8	0.0	0.1	1.	102.	194.	298.
128.	10.9	0.6	0.0	0.0	1.	100.	189.	291.
							288.	0.
							288.	+ 3.

Age, Days at 40° C							Σ^{+-}	Σ^-
	Si ⁴⁺ *	Al ³⁺	Fe ³⁺	Mg ⁺⁺	Ca ⁺⁺	Na ⁺		
2.	10.1	0.4	0.0	0.0	1.	148.	355.	475.
32.	14.5	0.5	0.0	0.0	0.	101.	172.	212.
128.	4.5	0.3	0.0	0.0	1.	104.	193.	299.
							290.	0.
							290.	+ 9.

* See remarks in Section 4.4.1

** milliequivalents/liter

n.d. = not determined

Table 5.15.5
 Observed Concentrations of Ions in Expressed Pore Solution (Not Corrected for Bound Water)
Mix 61, 8 Percent Opal Sand, 10 Percent Pozzolan L.
 (Concentrations in millimoles/liter)

Age, Days at 20° C	Si ⁴⁺ *	Al ³⁺	Fe ³⁺	Mg ⁺⁺	Ca ⁺⁺	Na ⁺	K ⁺	Σ^{+**}	SO ₄ ²⁻	Σ^{-**}
0.021	4.1	0.2	0.0	0.0	17.	125.	378.	573.	159.	176.
2.	9.0	0.4	0.0	0.0	1.	164.	429.	595.	569.	511.
32.	14.0	0.4	0.0	0.0	0.	99.	178.	277.	276.	575.
128.	7.1	0.4	0.0	0.0	0.	75.	132.	207.	206.	n.d.
									0.	206.
										+ 1.

Age, Days at 40° C	Si ⁴⁺ *	Al ³⁺	Fe ³⁺	Mg ⁺⁺	Ca ⁺⁺	Na ⁺	K ⁺	Σ^{+**}	OH ⁻	SO ₄ ²⁻	Σ^{-**}
2.	5.9	0.1	0.0	0.0	0.	136.	326.	462.	438.	6.	450.
32.	22.5	0.8	0.0	0.0	0.	80.	124.	204.	207.	n.d.	+ 12.
128.	3.5	0.4	0.0	0.0	1.	71.	118.	191.	187.	0.	187.

* See remarks in Section 4.4.1
 ** milliequivalents/liter
 n.d. = not determined

Table 5.15.6
Observed Concentrations of Ions in Expressed Pore Solution (Not Corrected for Bound Water)

Age, Days at 20° C	Mix 62, 8 Percent Opal Sand, 25 Percent Pozzolan L							Σ^{+-}
	Si ⁴⁺ *	Al ³⁺	Fe ³⁺	Mg ⁺⁺	Ca ⁺⁺	Na ⁺	K ⁺	
0.021	6.6	0.1	0.0	0.0	15.	124.	371.	525.
2.	14.6	0.1	0.0	0.0	1.	162.	414.	578.
32.	13.1	0.7	0.0	0.1	0.	78.	131.	209.
128.	3.2	0.3	0.0	0.0	0.	64.	110.	174.
Age, Days at 140° C <th>Si⁴⁺*</th> <th>Al³⁺</th> <th>Fe³⁺</th> <th>Mg⁺⁺</th> <th>Ca⁺⁺</th> <th>Na⁺</th> <th>K⁺</th> <th>Σ^{+-}</th>	Si ⁴⁺ *	Al ³⁺	Fe ³⁺	Mg ⁺⁺	Ca ⁺⁺	Na ⁺	K ⁺	Σ^{+-}
2.	7.1	0.3	0.0	0.0	0.	117.	262.	379.
32.	6.5	1.8	0.0	0.1	1.	69.	102.	173.
128.	4.5	0.6	0.0	0.0	0.	61.	100.	161.

* See remarks in Section 4.4.1

** milliequivalents/liter
n.d. = not determined

Table 5.15.7

Observed Concentrations of Ions in Expressed Pore Solutions (Not corrected for Bound Water)

Mix 63, 10 percent Pozzolan L

Age, Days at 20°C	Si^{4+*}	Al^{3+}	Fe^{3+}	Mg^{++}	Ca^{++}	Na^+	K^+	Σ^{+**}	OH^-	$\text{SO}_4^{=}$	Σ^{-**}	Σ^{+-**}
0.021	6.4	0.1	0.0	0.0	22.	126.	377.	547.	161.	207.	575.	- 28.
2.	7.4	0.1	0.0	0.0	1.	180.	486.	668.	642.	0.	642.	+ 26.
32.	7.9	n.d.	0.0	0.0	1.	188.	444.	634.	617.	n.d.		
128.	5.1	0.5	0.0	0.0	1.	204.	459.	665.	661.	1.	663.	+ 2.

Age, Days at 40°C	Si^{4+*}	Al^{3+}	Fe^{3+}	Mg^{++}	Ca^{++}	Na^+	K^+	Σ^{+**}	OH^-	$\text{SO}_4^{=}$	Σ^{-**}	Σ^{+-**}
2.	13.3	0.0	0.0	0.0	1.	182.	475.	659.	619.	6.	631.	+ 28.
32.	12.4	0.7	0.0	0.1	1.	196.	409.	607.	569.	n.d.		
128.	5.1	0.6	0.0	0.0	1.	216.	448.	666.	651.	16.	683.	- 17.

* See remarks in Section 4.4.1

** milliequivalents/liter

n.d. = not determined

Table 5.15.8

Observed Concentrations of Ions in Expressed Pore Solutions (Not Corrected for Bound Water)

Mix 64, 25 Percent Pozzolan L

Age, Days at 20°C	Si^{4+*}	Al^{3+}	Fe^{3+}	Mg^{++}	Ca^{++}	Na^+	K^+	$\Sigma +^{**}$	OH^-	$\text{SO}_4^{=}$	$\Sigma -^{**}$	$\Sigma + -^{**}$
0.021	2.4	0.1	0.0	0.0	22.	126.	378.	584.	151.	200.	551.	- 3.
2.	7.4	0.1	0.0	0.0	1.	174.	478.	654.	620.	0.	620.	+ 34.
32.	6.5	0.9	0.0	0.0	1.	120.	249.	371.	352.	n.d.		
128.	4.5	0.7	0.0	0.0	1.	115.	227.	344.	333.	4.	341.	+ 3.

Age, Days at 40°C	Si^{4+*}	Al^{3+}	Fe^{3+}	Mg^{++}	Ca^{++}	Na^+	K^+	$\Sigma +^{**}$	OH^-	$\text{SO}_4^{=}$	$\Sigma -^{**}$	$\Sigma + -^{**}$
2.	5.7	0.2	0.0	0.0	1.	146.	375.	523.	484.	2.	488.	+ 35.
32.	4.3	0.6	0.0	0.1	1.	111.	210.	323.	284.	n.d.		
128.	3.9	0.3	0.0	0.0	1.	114.	117.	333.	305.	14.	333.	0.

* See remarks in Section 4.4.1

** milliequivalents/liter

n.d. = not determined

The tabulation of length change data indicate that the type of specimen used has a major effect on the magnitude of the observed expansion; indeed some of the mixes that expanded in one type of specimen shrunk in another type.

In Table 5.15.9 the nonevaporable water, W_n/c , found in mortar specimens has been listed. In these tables the percent pozzolan equivalent, % POZZ_{eq}, has been substituted for percent pozzolan or percent opal sand. For pozzolan L, these units are interchangeable. In the case of Beltane opal sand, the ratio of SiO₂ in the opal sand to that in pozzolan L is:

$$87.96/67.98 = 1.294 \dots \dots \dots \dots \dots \dots \dots \dots \quad \text{Eq. 5.15.1}$$

Thus, the pozzolan equivalent of Beltane opal sand is approximately 1.3, i.e. 1 gram of opal is approximately equivalent to 1.3 grams of pozzolan L on the basis of SiO₂ content. The percent pozzolan equivalent (% POZZ_{eq}) of 8 percent Beltane opal sand is approximately 10.35. Table 5.15.9 also contains the estimating equations fit to the observed values of W_n/c at each age of test.

In Figure 5.15.1 data have been drawn from Table 5.15.9 to illustrate the effect of reactive mix component addition on W_n/c found in mortars of this series. In the lower part of the figure the points represent mixes stored at either 20° or 40°C for a period of 32 days. In the upper part of the figure the points represent specimens stored at 40°C for 423 days and for specimens stored at 20°C for 432 days.

Table 5.15.9

Nonevaporable Water, W_n/c , as a Function of

		<u>% POZZ_{eq}</u>					
Time, Days	Temp. °C	Mix 59	Mix 60	Mix 61	Mix 62	Mix 63	Mix 64
2	20	0.1331	0.1327	0.1324	0.1318	0.1327	0.1322
		Estimated from data for Mix Series 78 - 81					
2	40	0.1332	0.1311	0.1291	0.1261	0.1321	0.1282
		Estimated from data for Mix Series 78 - 81					
32	20	0.1847	0.1766	0.1682	0.1563	0.1977	0.1627
		est $W_n/c = 0.1913 - 1.0067 \times 10^{-3} \times \% \text{ POZZ}_{\text{eq}}$					
32	40	0.1861	0.1818	0.1662	0.1668	0.1805	0.1484
		est $W_n/c = 0.1858 - 0.8427 \times 10^{-3} \times \% \text{ POZZ}_{\text{eq}}$					
128	20	0.1958	0.1848	0.1716*	0.1531	0.1956	0.1582
		est $W_n/c = 0.2000 - 1.3968 \times 10^{-3} \times \% \text{ POZZ}_{\text{eq}}$					
128	40	0.1962	0.1870	0.1716*	0.1510	0.2033	0.1540
		est $W_n/c = 0.2040 - 1.5817 \times 10^{-3} \times \% \text{ POZZ}_{\text{eq}}$					
432	20	0.2167	0.1988	0.1804	0.1569	0.2125	0.1645
		est $W_n/c = 0.2204 - 1.9081 \times 10^{-3} \times \% \text{ POZZ}_{\text{eq}}$					
432	40	0.2016	0.2017	0.1831	0.1503	0.2150	0.1569
		est $W_n/c = 0.2160 - 1.8531 \times 10^{-3} \times \% \text{ POZZ}_{\text{eq}}$					
Reactive Component		Mix 59	Mix 60	Mix 61	Mix 62	Mix 63	Mix 64
% Beltane Opal Sand		0.0	8.0	8.0	8.0	0.0	0.0
% Pozzolan L		0.0	0.0	10.0	25.0	10.0	25.0
% POZZ _{eq}		0.0	10.35	20.35	35.35	10.0	25.0

* Original samples lost during ignition. Value estimated by use of cited estimating equations.

Three things should be noted about Table 5.15.9 and Figure 5.15.1:

1. For periods beyond about 30 days, variation of storage temperature in the range of 20° to 40°C appears to have little influence on W_n/c .
2. W_n/c appears to depend mainly on the amount of siliceous material added to the mix rather than on its mineralogical character, i.e. it appears that sand-size opal and finely ground pozzolan are equally effective in reducing the apparent value of W_n/c . A similar although nonlinear trend will be noted for these components in reducing the amount of $\text{Ca}(\text{OH})_2$ found, as will be discussed later.
3. In the period 32 to about 425 days, the change in the slope constant relating W_n/c to % POZZ_{eq} is relatively small.

In Tables 5.15.10 through 5.15.15 the concentrations of alkali metal ions, both as observed and compensated for W_n/c , have been listed. In Figures 5.15.2 through 5.15.7 the alkali metal ion concentrations, compensated for W_n/c , have been plotted against the logarithm of time. As anticipated from previous results, the alkali-silica reaction at 40°C apparently resulted in a rapid initial reduction in the alkali concentrations found in pore solutions. While the reduction in concentration was slower for specimens stored at 20°C, the differences in concentration levels at 128 days were small. If the attainment of a relatively constant concentration level of alkali metal ions in solution is assumed to indicate attainment of equilibrium, the chemical phase of alkali-silica attack in these mixes stored at 40°C appears to have stopped at or before 30 days. Mixes stored at 20°C required about four times as long to attain equilibrium.

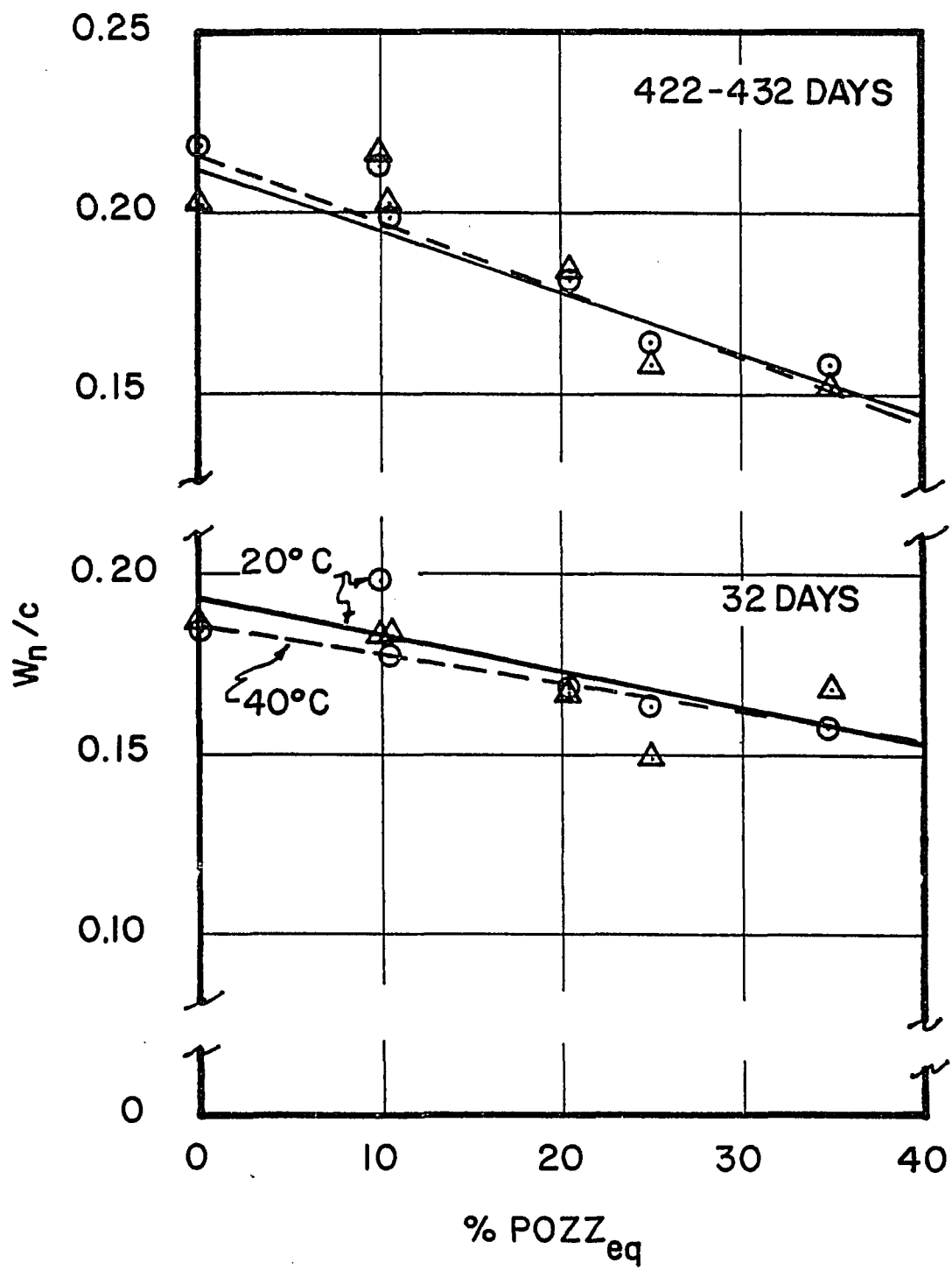


Figure 5.15.1 - Effect of Reactive Mix Component,
% POZZ_{eq}, on W_n/c

Table 5.15.10

Concentrations of Alkali Metal Cations in Expressed Pore Solution (Corrected for Bound Water)

Mix 59, Control for Mix Series 59 - 64

(Concentrations in millimoles/liter)

Age, Days at 20° C	W_n/c	bwk	Cations Found			Cation Concentration Corrected for W_n/c			$*K^+ / *Na^+$
			Na^+	K^+	ΣM^+	$*Na^+$	$\Delta *Na^+$	$*K^+$	
0.021	0.002	0.995	125	374	499	124	-	372	-
2.	0.133	0.734	201	524	725	147	-	385	-
32.	0.185	0.631	209	521	730	132	-	329	-
128.	0.196	0.606	238	575	813	145	-	350	-

Age, Days at 40° C	W_n/c	bwk	Cations Found			Cation Concentration Corrected for W_n/c			$*K^+ / *Na^+$
			Na^+	K^+	ΣM^+	$*Na^+$	$\Delta *Na^+$	$*K^+$	
2.	0.133	0.734	203	532	735	149	-	390	-
32.	0.186	0.628	220	496	716	138	-	311	-
128.	0.196	0.608	243	541	784	148	-	329	-

Table 5.15.11
 Concentrations of Alkali Metal Cations in Expressed Pore Solution (Corrected for Bound Water)
 Mix 60, 8 Percent Opal Sand
 (Concentrations in millimoles/liter)

Age, Days at 20°C	$\frac{W_n}{c}$	b/w _K	Cations Found			Cation Concentration Corrected for W_n/c $\frac{*Na^+}{\Sigma M^+}$	$\frac{*K^+}{\Sigma M^+}$	$\frac{\Delta *K^+}{\Delta *Na^+}$	$\frac{*K^+/}{*Na^+}$
			Na^+	K^+	ΣM^+				
0.021	0.002	0.995	125	377	502	124	0	375	+ 3
2.	0.133	0.735	165	439	604	121	- 26	322	- 62
32.	0.177	0.647	102	194	296	66	- 66	125	- 203
128.	0.185	0.630	100	189	289	63	- 82	119	- 231
								182	- 312
									1.890

Age, Days at 40°C	$\frac{W_n}{c}$	b/w _K	Cations Found			Cation Concentration Corrected for W_n/c $\frac{*Na^+}{\Sigma M^+}$	$\frac{*K^+}{\Sigma M^+}$	$\frac{\Delta *K^+}{\Delta *Na^+}$	$\frac{*K^+/}{*Na^+}$
			Na^+	K^+	ΣM^+				
2.	0.131	0.738	143	355	503	109	- 40	262	- 128
32.	0.182	0.636	101	172	273	64	- 74	109	- 202
128.	0.187	0.626	104	193	297	65	- 83	121	- 208
								186	- 290
									1.856

Table 5.15.12

Concentrations of Alkali Metal Cations in Expressed Pore Solution (Corrected for Bound Water)

Mix 61, 8 Percent Opal Sand, 10 Percent Pozzolan L

(Concentrations in millimoles/liter)

Age, Days at 20°C	W_n/c	bwk	Cations Found			Cation Concentration Corrected for W_n/c						$*K^+ / *Na^+$
			Na^+	K^+	ΣM^+	$*\text{Na}^+$	$\Delta *\text{Na}^+$	$*\text{K}^+$	$\Delta *\text{K}^+$	$\Sigma *\text{M}^+$	$\Delta *\text{M}^+$	
0.021	0.002	0.995	125	378	503	124	0	376	+ 4	501	+ 4	3.204
2.	0.132	0.735	164	429	593	121	- 27	315	- 69	436	- 96	2.616
32.	0.168	0.664	99	178	277	66	- 66	118	- 210	184	- 277	1.798
128.	0.172	0.657	75	132	207	49	- 96	87	- 263	136	- 359	1.760

Age, Days at 40°C	W_n/c	bwk	Cations Found			Cation Concentration Corrected for W_n/c						$*K^+ / *Na^+$
			Na^+	K^+	ΣM^+	$*\text{Na}^+$	$\Delta *\text{Na}^+$	$*\text{K}^+$	$\Delta *\text{K}^+$	$\Sigma *\text{M}^+$	$\Delta *\text{M}^+$	
2.	0.129	0.742	136	326	462	101	- 48	242	- 148	343	- 196	2.397
32.	0.166	0.668	80	124	204	53	- 85	83	- 229	136	- 313	1.550
128.	0.172	0.657	71	118	189	47	- 101	78	- 251	124	- 352	1.662

Table 5.15.13
Concentrations of Alkali Metal Cations in Impressed pore Solution (Corrected for Bound Water)
Mix: 62, 8 Percent Oyal Sand, 25 Percent Pozzolan L
(Concentrations in millimoles/liter)

Age, Days at 20° C	$\frac{w_n}{c}$	bulk	Cations Found			Cation Concentration Corrected for $\frac{w_n}{c}$			$\frac{*K^+}{*Na^+}$
			$\frac{Na^+}{K^+}$	$\frac{K^+}{\Sigma M^+}$	$\frac{*Na^+}{\Delta *Na^+}$	$\frac{*K^+}{\Delta *K^+}$	$\frac{\Sigma *M^+}{\Delta *M^+}$		
0.021	0.002	0.995	124	371	495	123	- 1	369	- 3
2.	0.132	0.736	162	414	576	119	- 28	305	- 80
32.	0.156	0.687	78	131	209	54	- 78	90	- 238
128.	0.153	0.694	64	110	174	44	- 100	76	- 274
								121	- 374
									1.719

Age, Days at 40° C	$\frac{w_n}{c}$	bulk	Cations Found			Cation Concentration Corrected for $\frac{w_n}{c}$			$\frac{*K^+}{*Na^+}$
			$\frac{Na^+}{K^+}$	$\frac{K^+}{\Sigma M^+}$	$\frac{*Na^+}{\Delta *Na^+}$	$\frac{*K^+}{\Delta *K^+}$	$\frac{\Sigma *M^+}{\Delta *M^+}$		
2.	0.126	0.748	117	262	379	87	- 61	196	- 194
32.	0.167	0.666	69	102	171	46	- 92	63	- 243
128.	0.151	0.698	61	100	161	43	- 105	70	- 259
								112	- 364
									1.639

Table 5.15.1₄
Concentrations of Alkali Metal Cations in Expressed Pore Solution (Corrected for Bound Water)
Mix 63, 10 Percent Pozzolan L

Age, Days at 20° C	M_n/c	bulk	Cations Found			Cation Concentration Corrected for M_n/c	$\frac{\text{*K}^+}{\text{*Na}^+}$
			Na^+	K^+	ΣM^+		
0.021	0.002	0.995	126	377	503	125	+ 1
2.	0.133	0.735	180	486	666	132	- 15
32.	0.198	0.605	188	444	632	114	- 18
128.	0.196	0.609	204	459	663	124	- 21
						279	- 70
						404	- 91
							2.250

Age, Days at 40° C	M_n/c	bulk	Cations Found			Cation Concentration Corrected for M_n/c	$\frac{\text{*K}^+}{\text{*Na}^+}$
			Na^+	K^+	ΣM^+		
2.	0.131	0.738	182	475	657	134	- 15
32.	0.180	0.639	196	409	605	125	- 13
128.	0.203	0.593	216	448	664	128	- 19
						350	- 40
						261	- 50
						266	- 63
						394	- 82
							2.074

Table 5.15.15
Concentrations of Alkali Metal Cations in Expressed Pore Solution (Corrected for Bound Water)
Mix 64, 25 Percent Pozzolan L

Age, Days at 20°C	W_n/c	b/wk	Cations Found			Cation Concentration Corrected for W_n/c			$*K^+/\frac{*Na^+}{*Na}$
			Na^+	K^+	ΣM^+	$*Na^+$	$\Delta *Na^+$	$*K^+$	
0.021	0.002	0.995	126	378	504	125	+ 1	376	+ 5
2.	0.132	0.736	174	478	652	128	- 19	352	- 52
32.	0.163	0.675	120	249	369	81	- 51	168	2.747
128.	0.158	0.684	115	227	342	79	- 66	155	2.075
								195	1.974
Age, Days at 40°C	W_n/c	b/wk	Cations Found			Cation Concentration Corrected for W_n/c			$*K^+/\frac{*Na^+}{*Na}$
			Na^+	K^+	ΣM^+	$*Na^+$	$\Delta *Na^+$	$*K^+$	
2.	0.128	0.744	146	375	521	109	- 40	279	- 152
32.	0.143	0.703	111	210	321	78	- 60	148	2.568
128.	0.154	0.692	114	217	331	79	- 69	150	1.892
								179	1.904

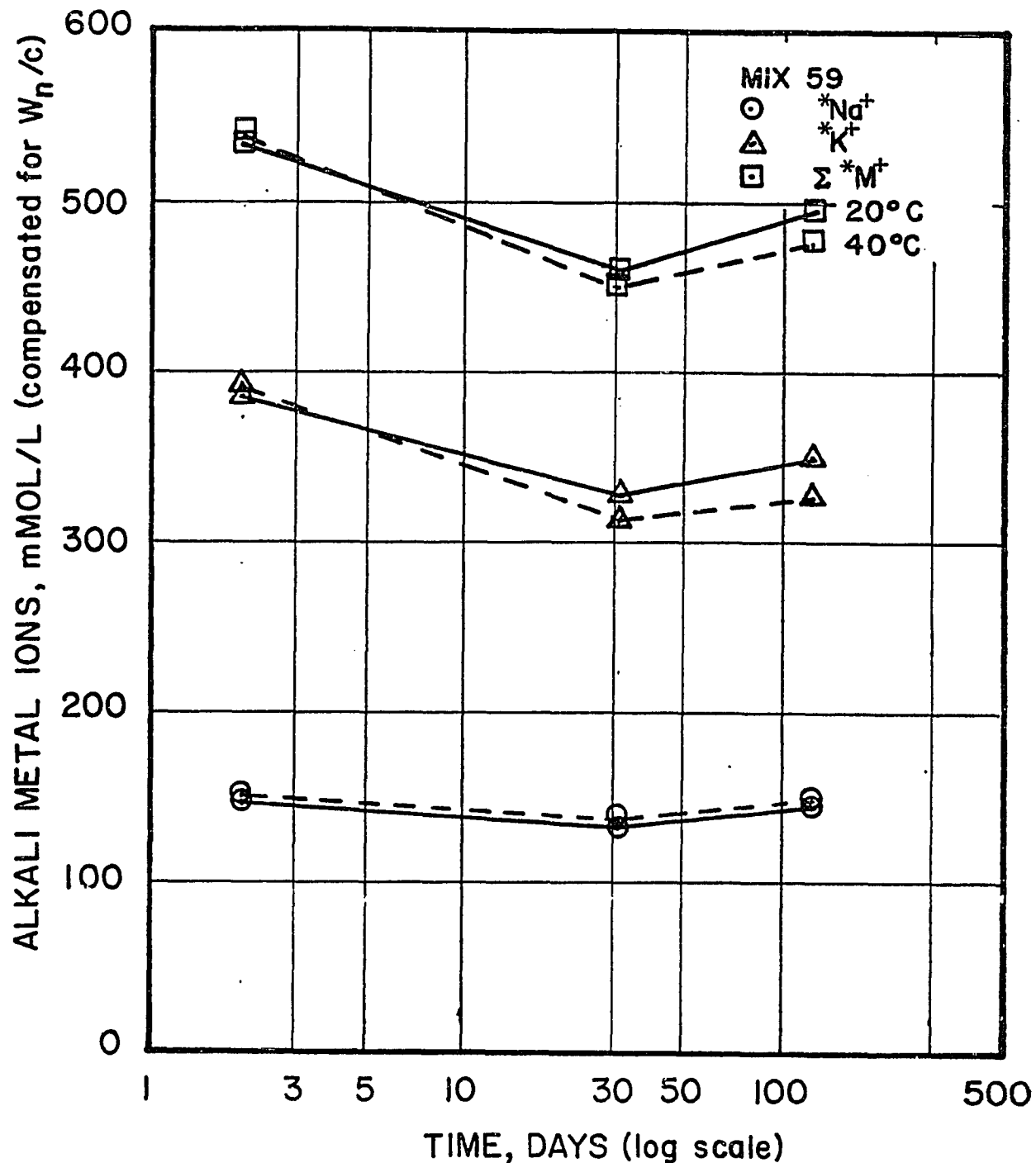


Figure 5.15.2 - Alkali Metal Ion Concentration (Compensated for W_n/c) as a Function of Time for Mix 59, Control for Mix Series 59 - 64.

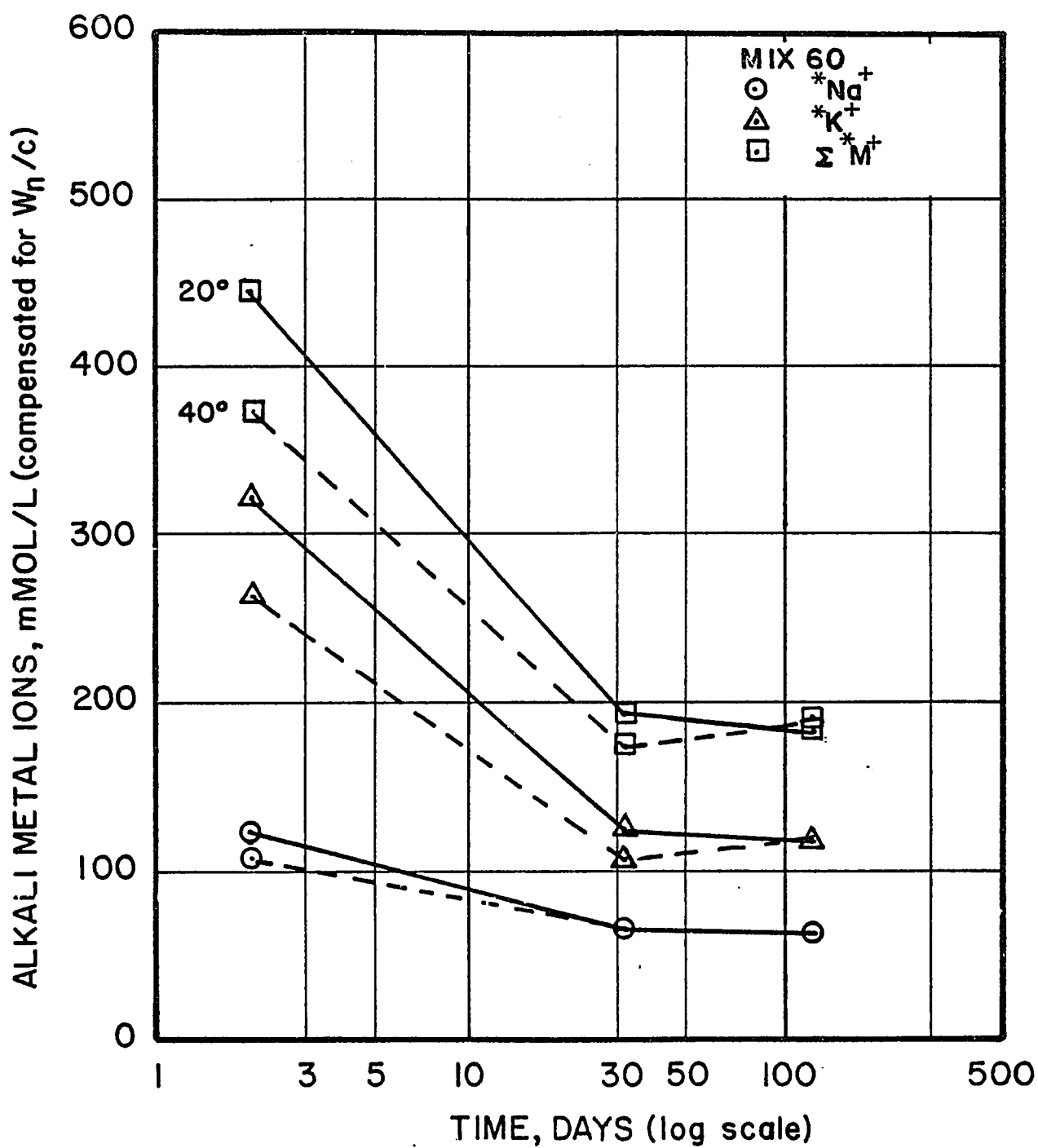


Figure 5.15.3 - Alkali Metal Ion Concentration (Compensated for W_n/c) as a Function of Time for Mix 60, 8% Beltane Opal Sand.

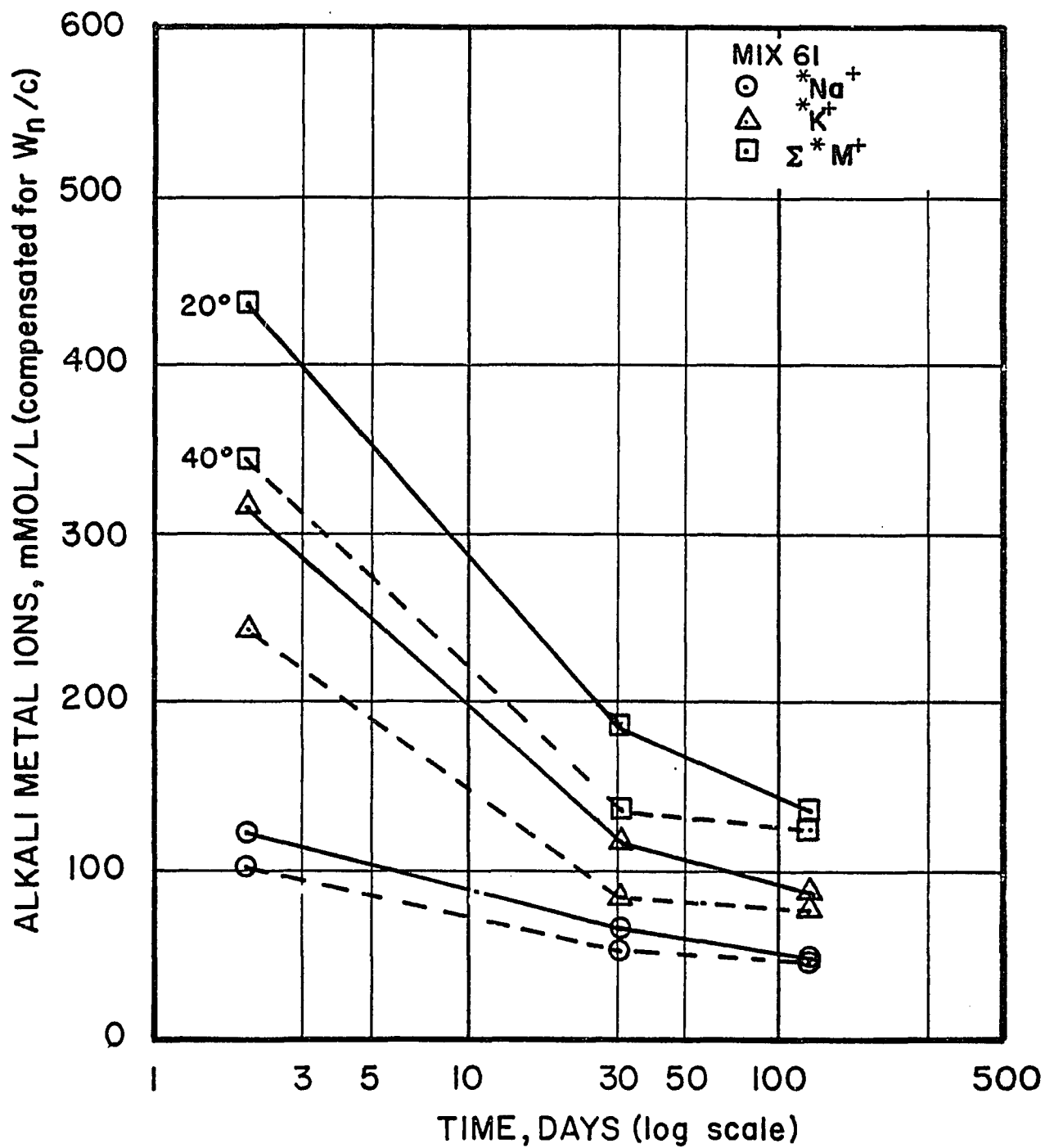


Figure 5.15.4 - Alkali Metal Ion Concentration (Compensated for W_n/c)
as a Function of Time for Mix 61, 8% Beltane Opal Sand, 10% Pozzolan L.

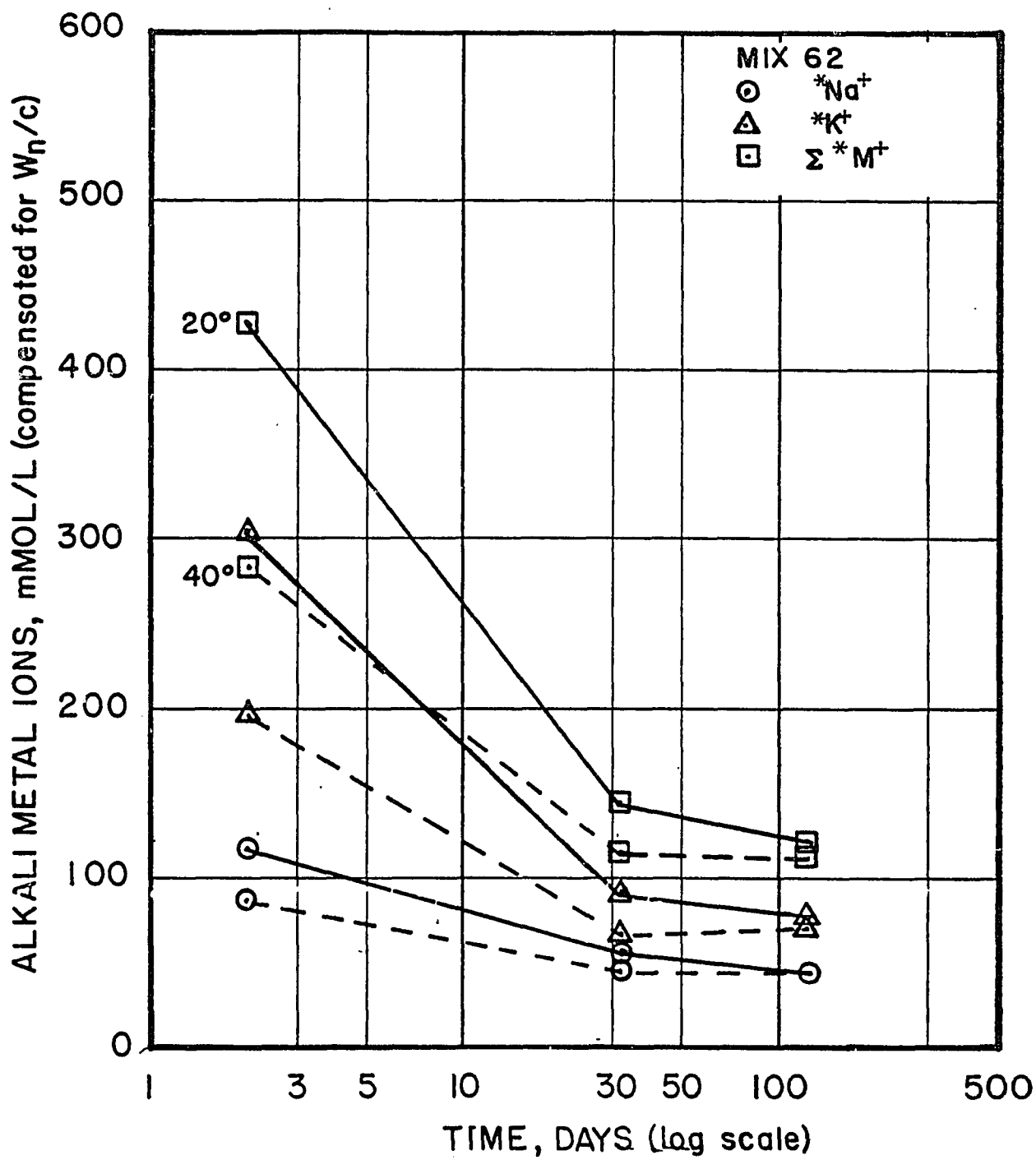


Figure 5.15.5 - Alkali Metal Ion Concentration (Compensated for W_n/c)
as a Function of Time for Mix 62, 8% Beltane Opal Sand, 25% Pozzolan L.

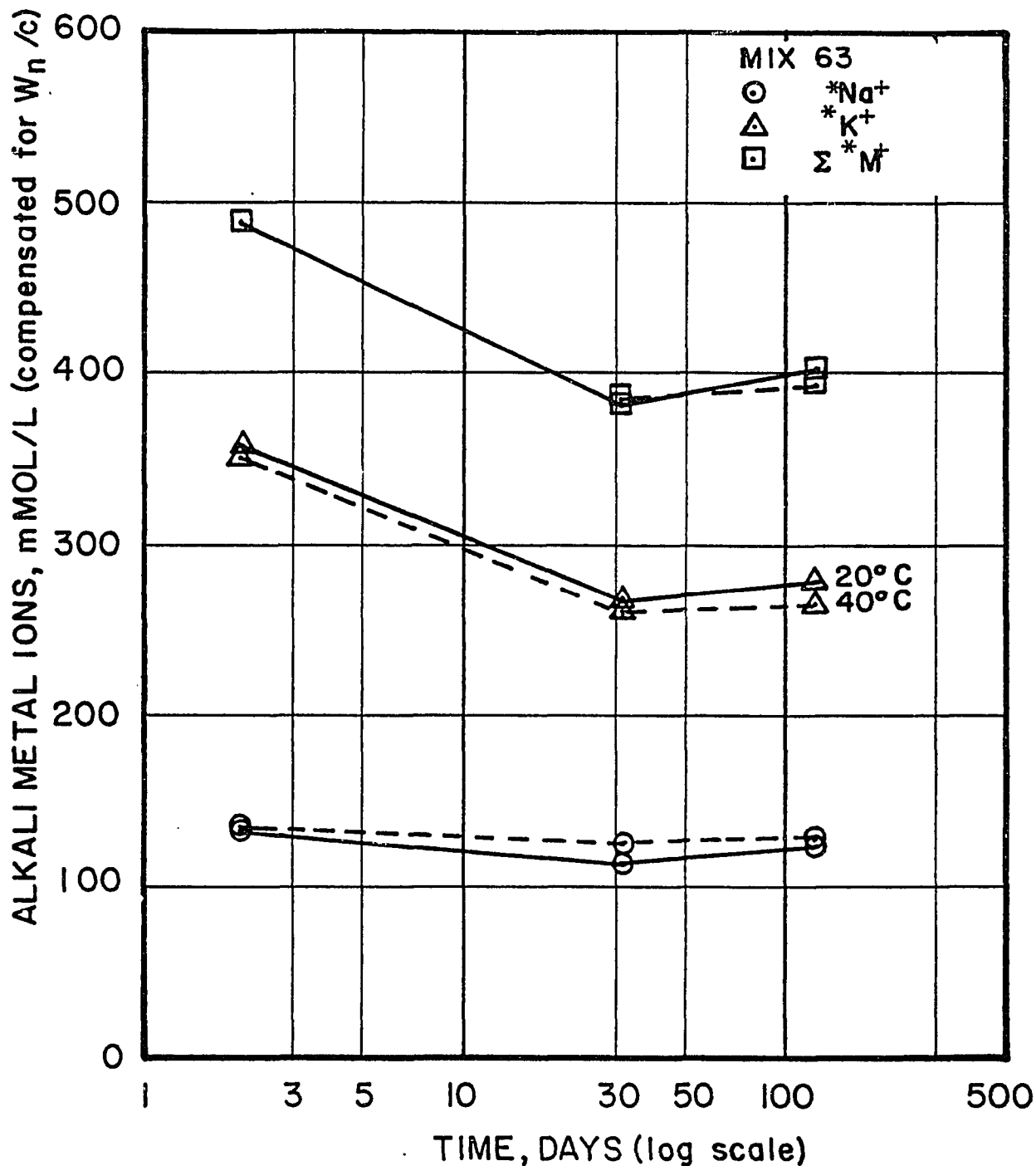


Figure 5.15.6 - Alkali Metal Ion Concentration (Compensated for W_n/c)
as a Function of Time for Mix 63, 10% Pozzolan L.

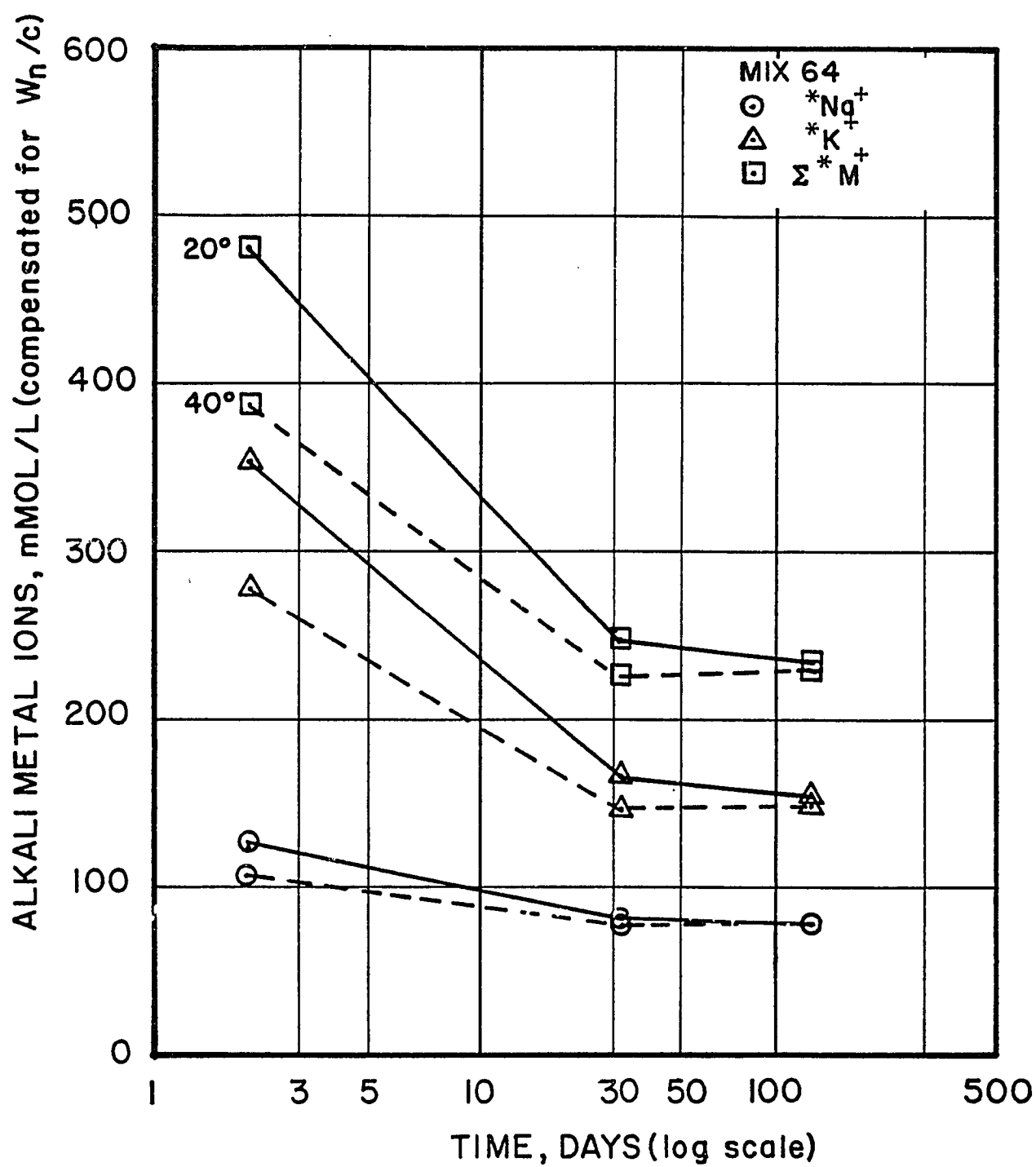


Figure 5.15.7 - Alkali Metal Ion Concentration (Compensated for W_n/c)
as a Function of Time for Mix 64, 25% Pozzolan L.

In Figures 5.15.8 through 5.15.10 the total concentration of alkali metal ions in expressed pore solution, compensated for W_n/c , has been plotted against the percent addition of pozzolan L for specimens aged 2, 32, and 128 days.

At 2 days (Figure 5.15.8) it is apparent that the alkali concentration in pore solutions was a linear function of the pozzolan addition and was significantly affected by storage temperature. The reduction in alkali concentration owing to the addition of 8 percent Beltane opal sand (Mix 60) was greater than that resulting from the addition of 25 percent pozzolan L. It is of interest to note that the effectiveness of pozzolan additions in removal of alkali metal ions from pore solutions, when combined with Beltane opal sand (Mixes 61 and 62), was reduced. This effect remained nearly constant with time while the effect of different storage temperatures on alkali metal ion concentrations decreased with time to become negligibly small by 128 days.

Linear estimating equations were fitted to the points in Figures 5.15.8 through 5.15.10 and have been listed in Table 5.15.16. By using the intercept constants for mixes containing only 8 percent Beltane opal sand and the equations for mixes containing three levels of pozzolan L, but no opal sand, it is possible to compute the percent addition level of pozzolan L equivalent to 8 percent addition of Beltane opal sand, with respect to reduction of Σ^+M .

$$P = (a_p - a_o) / -b_p \dots \dots \dots \dots \dots \dots \quad \text{Eq. 5.15.2}$$

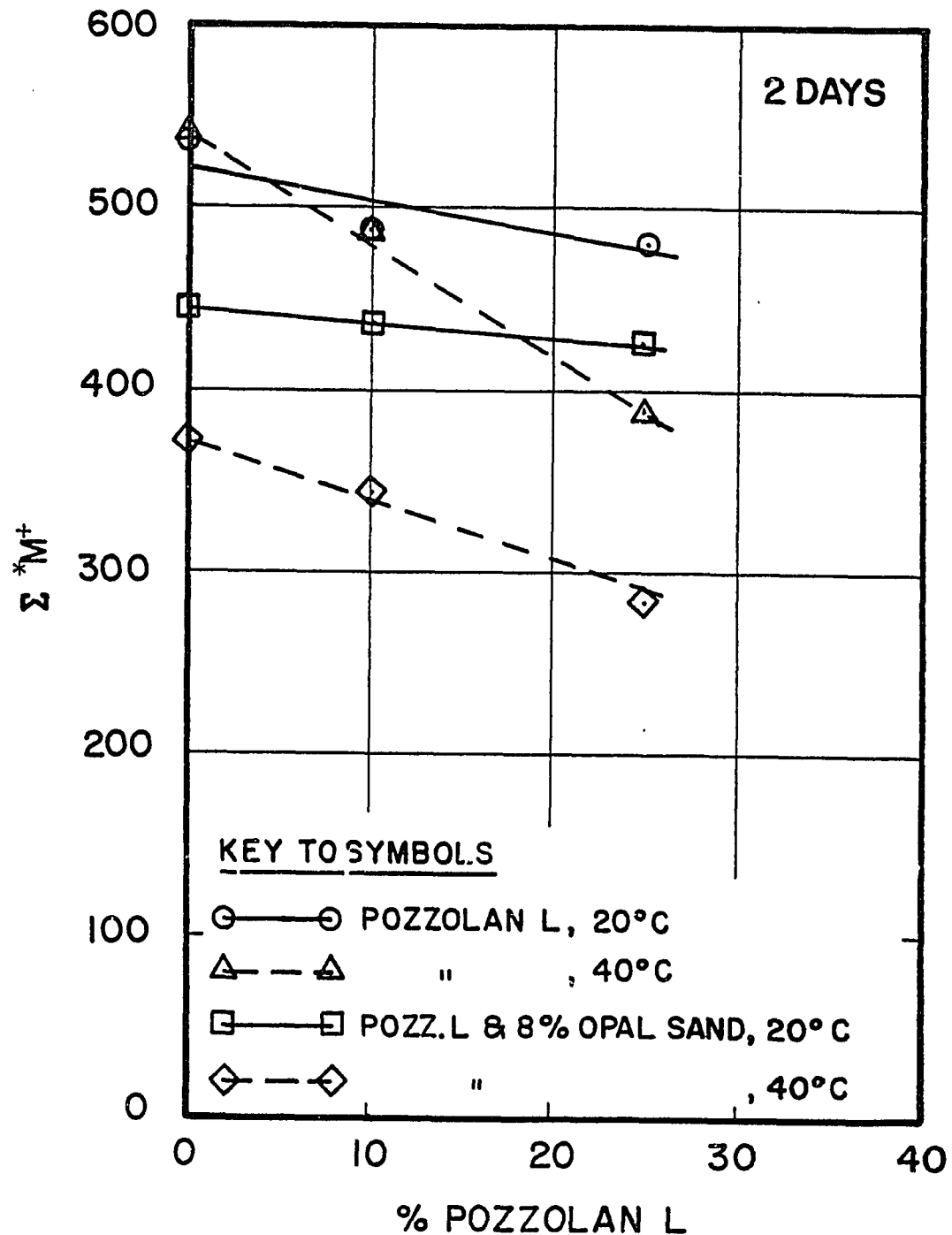


Figure 5.15.8 - Total Alkali Metal Ion Concentration (Compensated for $\frac{W}{n} / c$) as a Function of % Pozzolan L Addition.

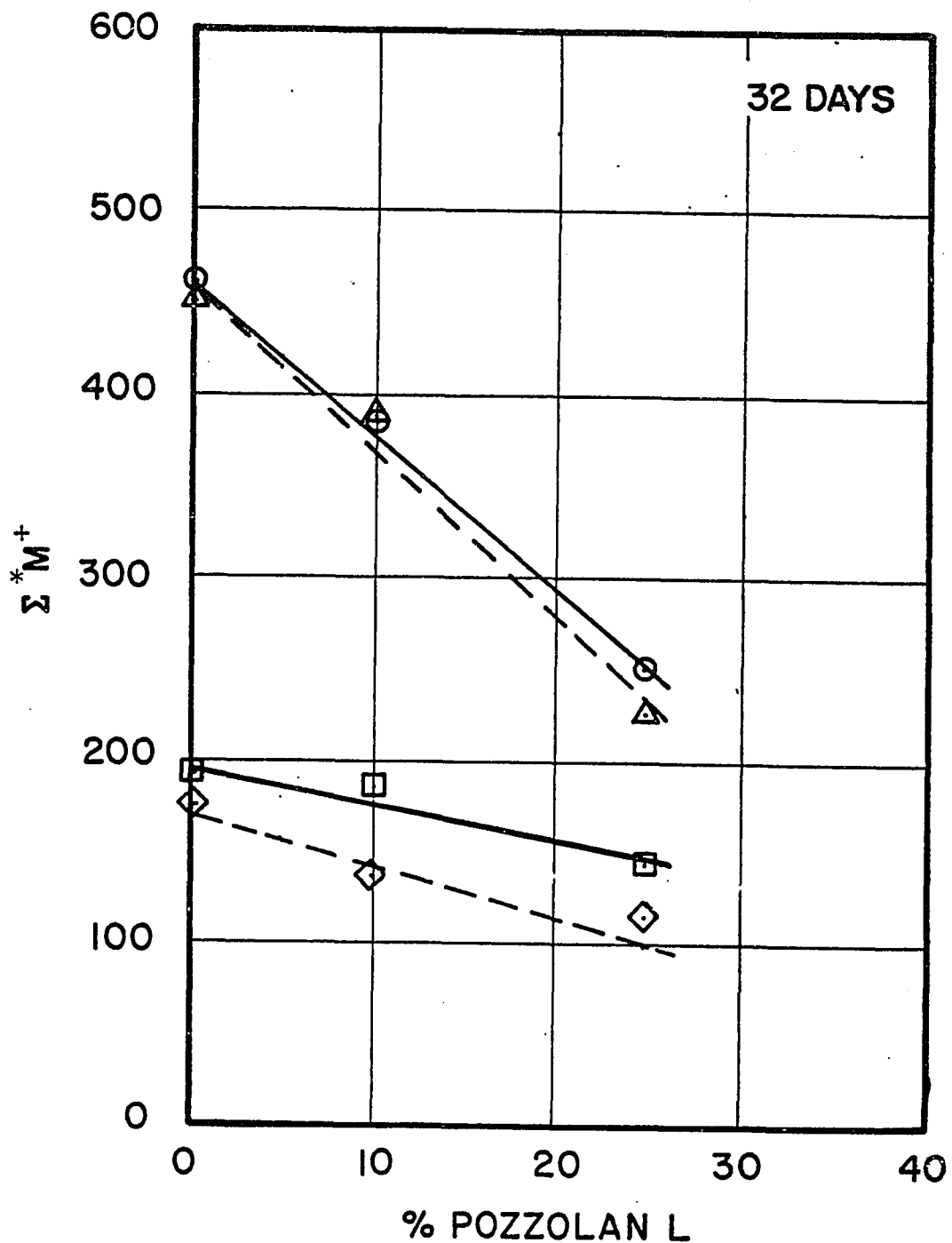


Figure 5.15.9 - Total Alkali Metal Ion Concentration (Compensated for $\frac{W}{C}$) as a Function of % Pozzolan L Addition.

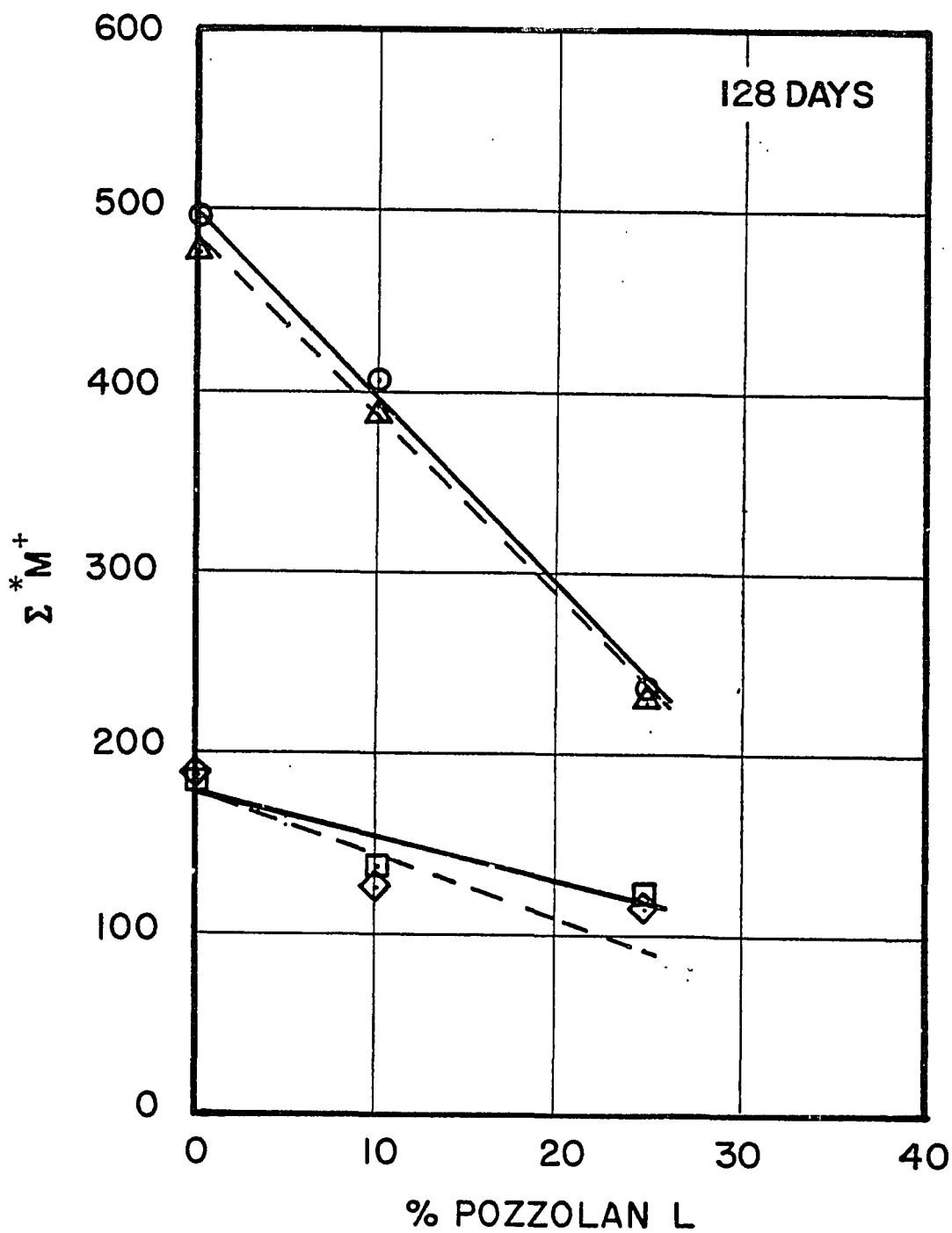


Figure 5.15.10 - Total Alkali Metal Ion Concentration (Compensated for w_n/c) as a function of % Pozzolan L Addition.

Table 5.15.16

Equations of Trend Lines Relating
 $*M^+$ to Percent Added Pozzolan L

Mixes without Beltane opal sand, at 20° C.

$$\begin{aligned} 2 \text{ Days } \Sigma *M^+ &= 532.2 - 1.963 P \\ 32 \text{ Days } \Sigma *M^+ &= 462.5 - 8.474 P \\ 128 \text{ Days } \Sigma *M^+ &= 500.3 - 10.510 P \end{aligned}$$

Mixes with 8 percent Beltane opal sand, at 20° C.

$$\begin{aligned} 2 \text{ Days } \Sigma *M^+ &= 444.0 - 0.800 P \\ 32 \text{ Days } \Sigma *M^+ &= 195.6 - 1.942 P \\ 128 \text{ Days } \Sigma *M^+ &= 173.5 - 2.326 P \end{aligned}$$

Mixes with Beltane opal sand, at 40° C.

$$\begin{aligned} 2 \text{ Days } \Sigma *M^+ &= 541.7 - 6.116 P \\ 32 \text{ Days } \Sigma *M^+ &= 460.5 - 9.100 P \\ 128 \text{ Days } \Sigma *M^+ &= 482.6 - 9.968 P \end{aligned}$$

Mixes with 8 percent Beltane opal sand, at 40° C.

$$\begin{aligned} 2 \text{ Days } \Sigma *M^+ &= 373.8 - 3.558 P \\ 32 \text{ Days } \Sigma *M^+ &= 168.5 - 2.326 P \\ 128 \text{ Days } \Sigma *M^+ &= 173.2 - 2.790 P \end{aligned}$$

Where: P = Percent pozzolan L

where:

a_p = Constant term from linear estimating equation relating

Σ^*M^+ to percent pozzolan added, i.e. $\Sigma^*M^+ = a_p + b_p P$.

b_p = First derivative term from above equation.

a_0 = Constant term from linear estimating equation relating

Σ^*M^+ to percent pozzolan added to mixes containing 8 percent
Beltane opal sand.

P = Percent pozzolan required to bind the same amount of Σ^*M^+
as is bound by the opal sand.

Substituting appropriate constants from Table 5.15.16 for
specimens 2 days old into Eq. 5.15.2:

$$P = (541.7 - 373.8)/6.116 = 27.54 \text{ percent pozzolan L.}$$

Constants from the equations listed in Table 5.15.16 have been used in Eq. 5.15.2 to generate Table 5.15.17.

In construction of Figure 5.15.1 the simplifying assumption was made that amorphous or disordered SiO_2 was the reactive component in both Beltane opal and pozzolan L. From Eq. 5.15.1 Beltane opal was found to contain about 1.3 times as much SiO_2 as pozzolan L. Using this factor, Figure 5.15.1 was constructed, relating W_n/c to % POZZ_{eq}. The fact that the plotted points in Figure 5.15.1 lie relatively close to the trend lines suggests that this was a reasonable assumption for the relationship.

Consideration of Table 5.15.17 suggests that the addition of one percent Beltane opal sand is equivalent to the addition of 3.9 percent of pozzolan L in reducing Σ^*M^+ . This is three times the factor of 1.3 noted above with respect to the effect on W_n/c .

Table 5.15.17

Percent Addition of Pozzolan L Required to Effect the Same
Alkali Metal Ion Concentration Reduction as Effected by Addition
of One Percent Beltane Opal Sand

<u>Age, Days</u>	<u>Storage Temperature</u>	
	<u>20° C</u>	<u>40° C</u>
2	5.62	3.43
32	3.94	4.01
128	3.89	3.88

The amount of free $\text{Ca}(\text{OH})_2$ present in hardened mortars, in grams of $\text{Ca}(\text{OH})_2$ per gram of batched portland cement, was determined by thermogravimetry on specimens stored 432 days at 20°C and 423 days at 40°C (see Section 4.13). The amounts of $\text{Ca}(\text{OH})_2$ found have been listed in Table 5.15.18 and are plotted against % POZZ_{eq} in Figure 5.15.11. While there is a general trend toward reduced residual $\text{Ca}(\text{OH})_2$ with increasing % POZZ_{eq}, being nearly linear for Mixes 59, 63, and 64, stored at 20°C , the trend appears to become parabolic for mixes containing Beltane opal sand, e.g. mixes 60, 61, and 62. This parabolic trend pattern is more pronounced for mixes stored at 40°C . The pattern suggests that the amount of $\text{Ca}(\text{OH})_2$ reacting with the pozzolan tends to decrease with increasing pozzolan additions and is further reduced in the presence of Beltane opal sand. Note that the amount of residual $\text{Ca}(\text{OH})_2$ in Mix 62, containing 25 percent pozzolan L and 8 percent Beltane opal sand, is slightly greater than that in Mix 64, containing only 25 percent pozzolan L (see Figure 5.15.12).

The derivative thermogravimetric curves (DTG) have been reproduced in Figures 5.15.13 through 5.15.16. The traces have been reduced photographically to approximately half the original scale, and the curves have been nested for ease of comparison. Addition of siliceous material, particularly pozzolan L, reduces the number of "peaks" or troughs in the range 0 - 375°C and results in smoothing of the curves. Before attempting any interpretation of these curves reference should be made to notes in Section 4.13.3.

Two different types of specimens were used to evaluate potential expansion of hardened mortars; 0.50-in (12.7 mm) cross section rectangular prisms (see Section 4.13.3) and 50-mm diameter Butyl rubber

Table 5.15.18

Free Ca(OH)_2 Found by Thermogravimetry in Mix Series 59 - 64

<u>Mortars Stored 432 Days at 20°C</u>							
Mix Number	Percent Pozzolan L Added	Percent Beltane Opal Sd. Added	Percent Pozzolan Equivalent	W_F , mg	ΔW , mg	c, mg	$\frac{\text{g CH}}{\text{g c}}$
59	0	0	0	45.30	0.88	15.245	0.2374
60	0	8	10.35	46.15	0.69	15.666	0.1812
61	10	8	20.35	50.10	0.65	17.075	0.1566
62	25	8	35.35	46.70	0.44	16.016	0.1130
63	10	0	10.0	49.55	0.78	16.737	0.1917
64	25	0	25.0	51.25	0.54	17.436	0.1274

<u>Mortars Stored 423 Days at 40°C</u>							
Mix Number	Percent Pozzolan L Added	Percent Beltane Opal Sd. Added	Percent Pozzolan Equivalent	W_F , mg	ΔW , mg	c, mg	$\frac{\text{g CH}}{\text{g c}}$
59	0	0	0	47.90	0.96	16.120	0.2449
60	0	8	10.35	45.85	0.68	15.563	0.1797
61	10	8	20.35	47.85	0.58	16.308	0.1463
62	25	8	35.35	45.30	0.36	15.536	0.0953
63	10	0	10.0	47.65	0.66	16.095	0.1687
64	25	0	25.0	57.30	0.44	19.494	0.0928

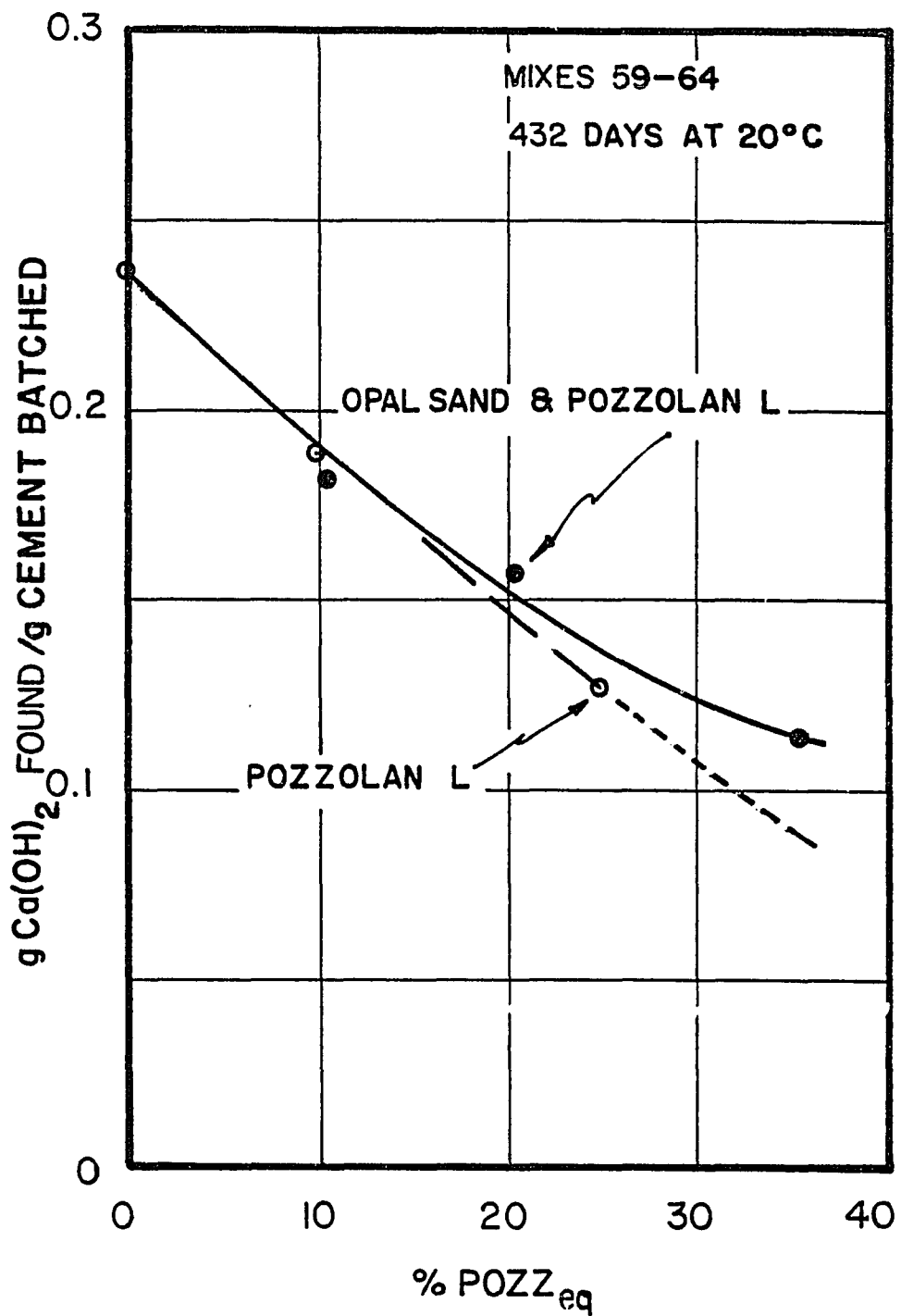


Figure 5.15.11 Grams of Calcium Hydroxide, $\text{Ca}(\text{OH})_2$, Found per Gram of Cement Batched vs. Percent Pozzolan Equivalent

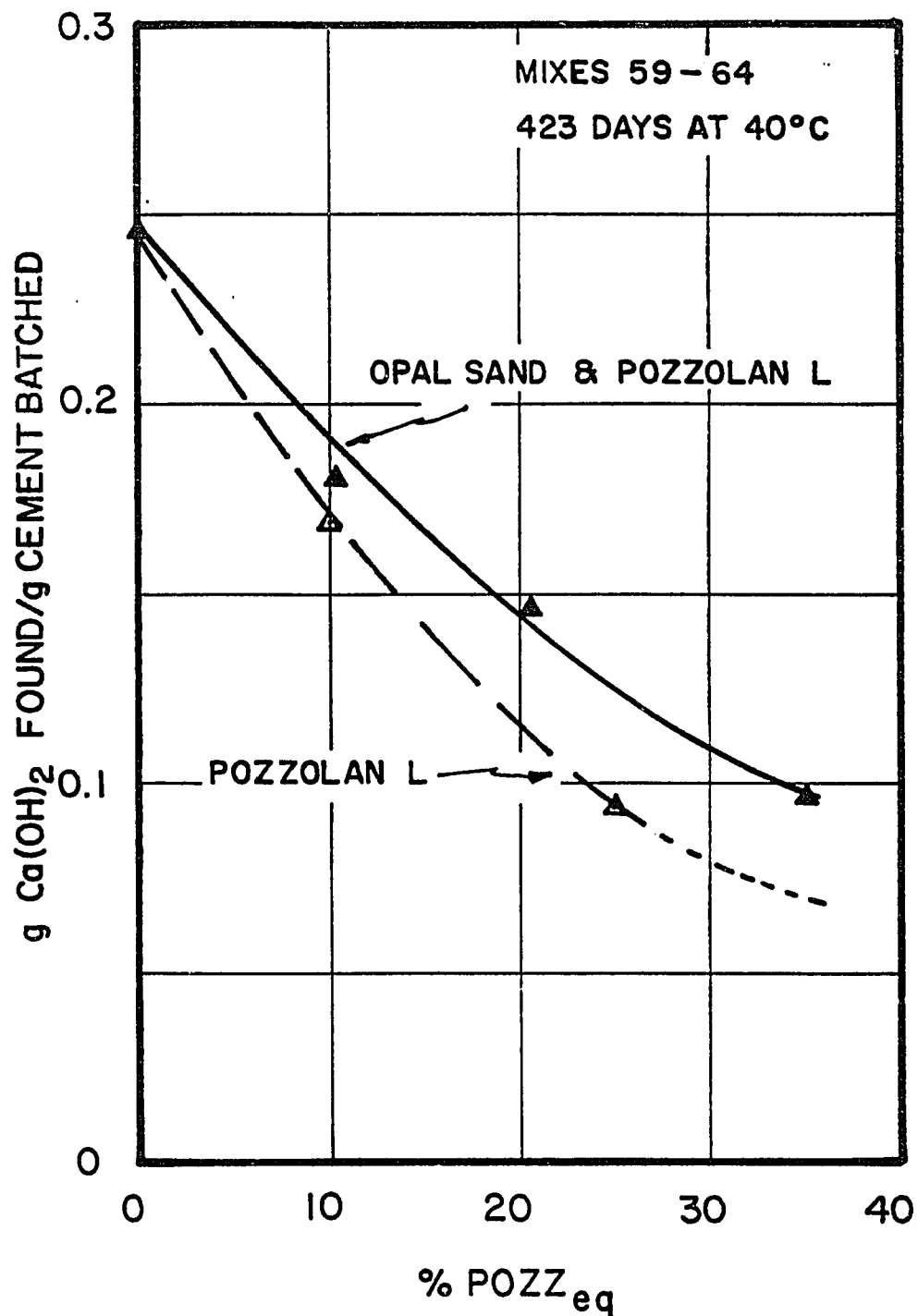


Figure 5.15.12 - Grams of Calcium Hydroxide, $\text{Ca}(\text{OH})_2$, Found per Gram of Cement Batched vs. Percent Pozzolan Equivalent

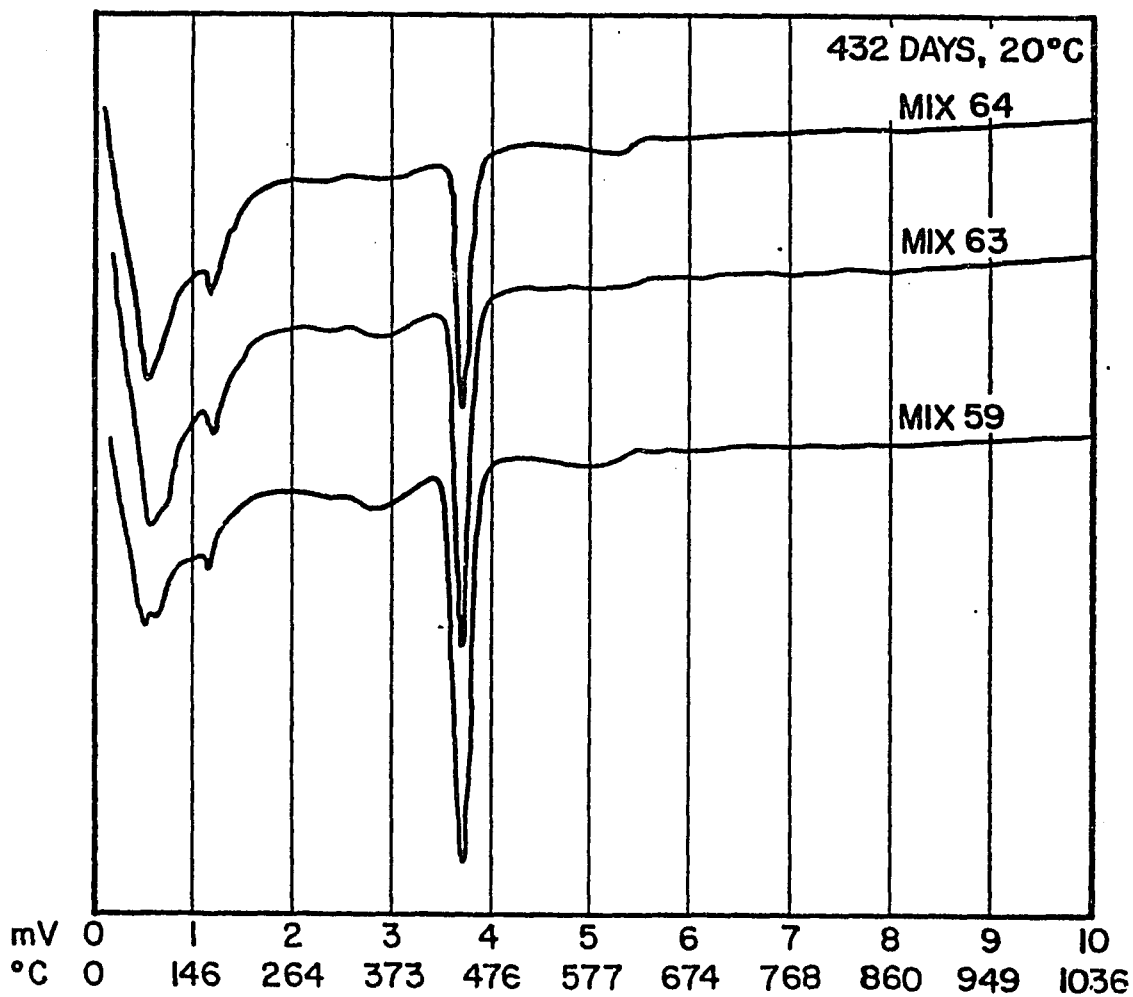


Figure 5.15.13 - Derivative Thermogravimetric Curves

for Mixes 59 (Control), 63 (10% Pozzolan L),
and 64 (25% Pozzolan L), 432 Days at 20°C

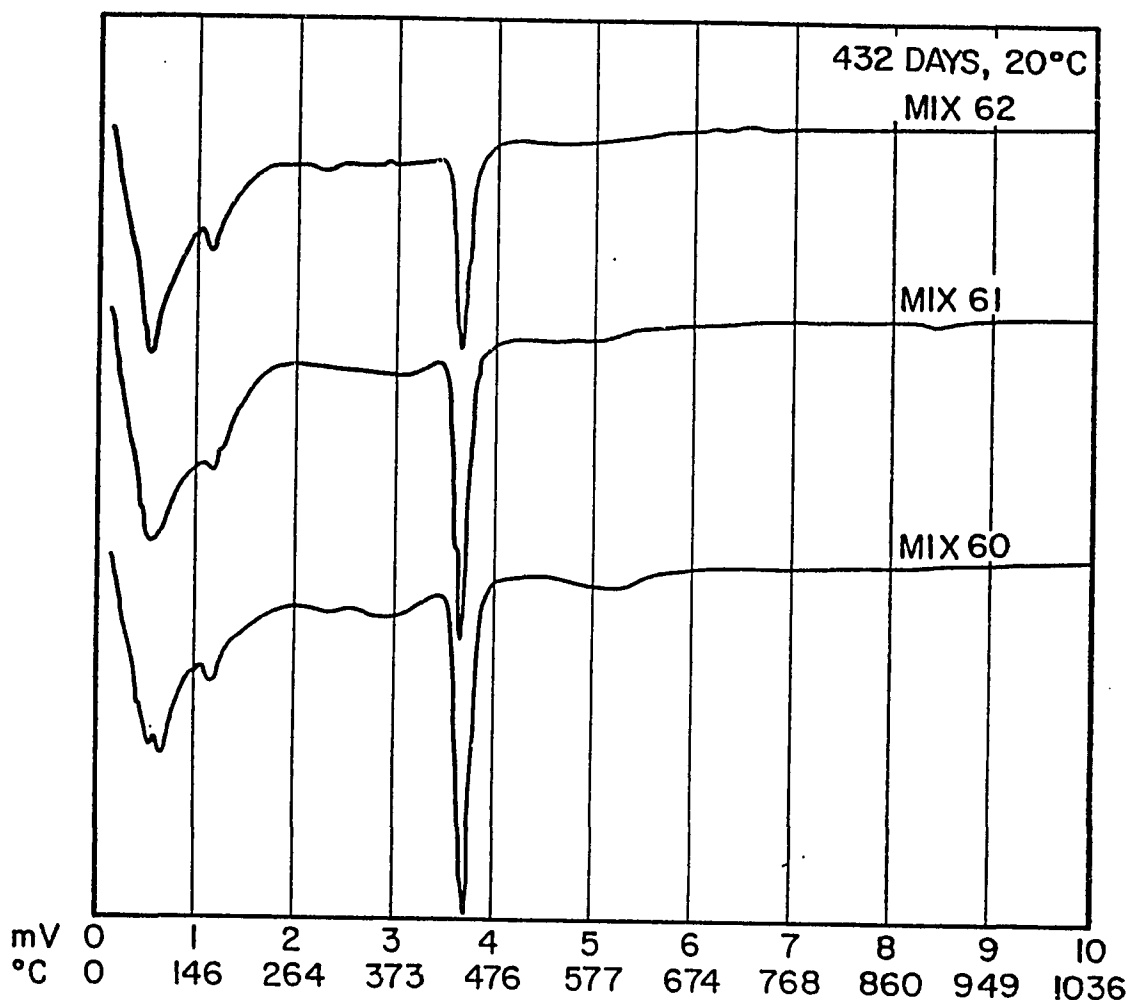


Figure 5.15.14 - Derivative Thermogravimetric Curves for
Mixes 60 (8% Beltane Opal Sand), 61 (8% Beltane Opal Sand + 10%
Pozzolan L), and 62 (8% Beltane Opal Sand + 25% Pozzolan L),
432 Days at 20°C

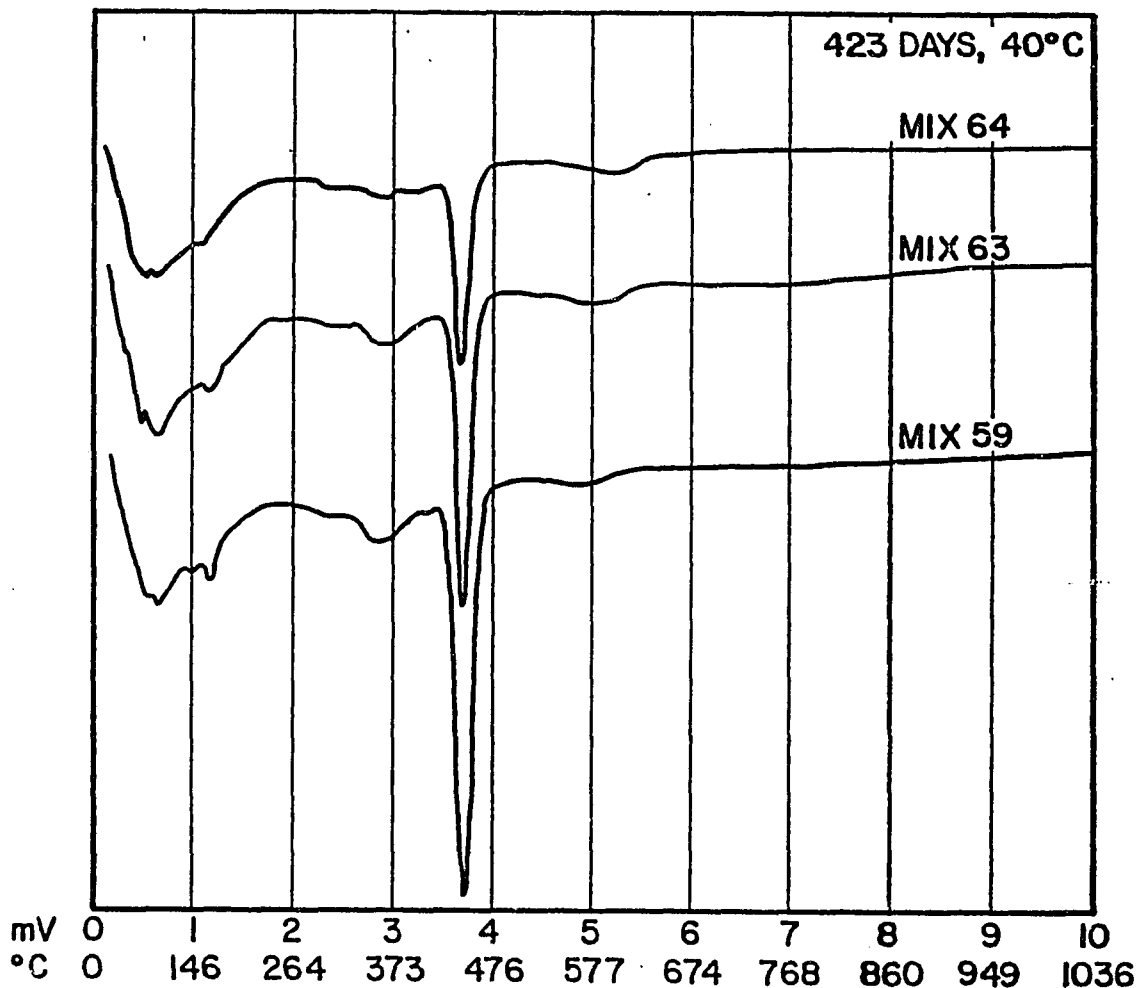


Figure 5.15.15 - Derivative Thermogravimetric Curves

for Mixes 59 (Control), 63 (10% Pozzolan L),
and 64 (25% Pozzolan L), 423 Days at 40°C

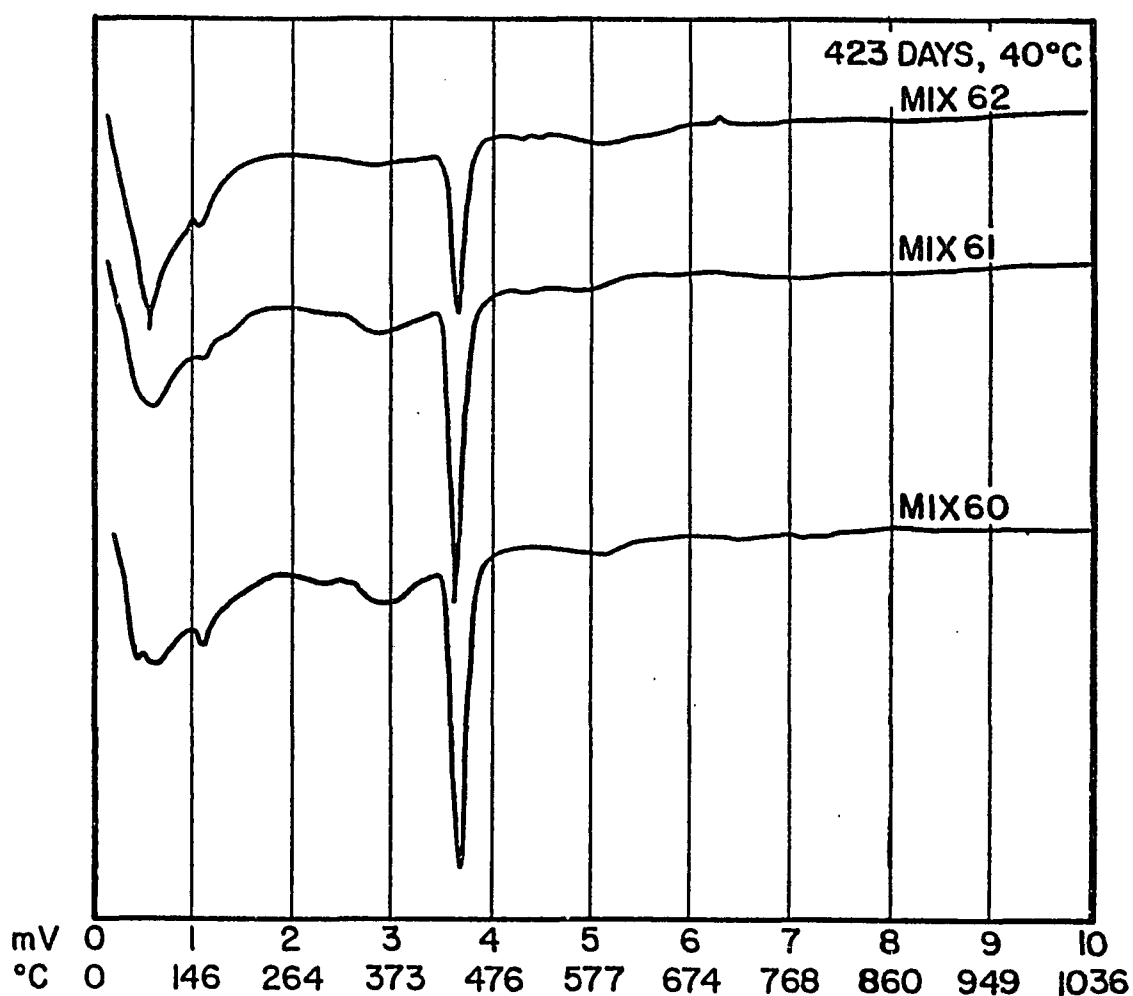


Figure 5.15.16 - Derivative Thermogravimetric Curves for
Mixes 60 (8% Beltane Opal Sand), 61 (8% Beltane Opal Sand + 10%
Pozzolan L), and 62 (8% Beltane Opal Sand + 25% Pozzolan L),
423 Days at 40°C

jacketed cylinders (see Section 4.13.5). Observed expansion measurements of these specimens are listed in Table 5.15.19. In general, specimens stored at 40°C exhibited less expansion than those stored at 20°C, and jacketed specimens containing 8 percent Beltane opal sand with 25 percent pozzolan L shrank while unjacketed companion prismatic specimens of the same mix expanded significantly. When the specimens were 476 days old the Butyl rubber jackets were removed, and the cylinders were placed over water in storage containers similar to those used for the small prisms. All the specimens expanded when exposed in this manner. Specimens from Mixes 60 and 61 were observed to be cracked when the jackets were removed. Subsequent to exposure, their appearance suggested that most of the expansion taking place after storage over water was localized in the cracked areas. Measured expansions of the cylindrical specimens after removal of the rubber jackets are listed in Table 5.15.20. The values tabulated are expansions after 476 days of age, and must be added to the 476 day expansion values listed in Table 5.15.19 to obtain total expansion.

Hyperbolic estimating equations were fitted to the expansion data for sealed specimens (see Section 4.11 and Eq. 4.11.8) and the ultimate expansions of the sealed cylinders, from Table 5.15.19, were estimated. In Figure 5.15.17 the estimated ultimate expansions for specimens stored at 40°C have been plotted against percent pozzolan L added to the mixes. The plot indicates a linear reduction in expansion with increasing Pozzolan addition. Data from Table 5.15.19 for specimens stored at 20°C would yield a similar plot.

Table 5.15.19 - Expansion (Microstrain) of Mortar Specimens, Mix Series 59 - 64

Age, Days at 20°C	Control Mix	Mix 59			8% Beltane Opal Sand			Mix 64		
		0% Pozz	10% Pozz	L	Mix 60	Mix 61	Mix 62	10% Pozzolan L	Mix 63	25% Pozz L
2		-73	-12	-36	-73	-127	+24	-145	+36	-127
4		-36	+12	-55	-109	-164	338	-200	145	-182
18.6		-36	73	+5581	+3036	-109	2230	-236	679	-182
32		-182	36	8745	7454	-127	2691	-327	679	-327
50		-145	12	10926	9908	--	2763	-273	691	-254
93		-36	133	13508	12508	-18	3333	-236	788	-200
224		-145	170	16689	14580	-36	4060	-345	921	-327
476		-218	230	19216	16435	-55	4072	-400	957	-382
<hr/>										
Age, Days at 40°C										
2		0	+12	+636	-36	-127	--	--	+36	-145
4		-18	12	3418	+182	-145	+533	-254	61	-145
18.6		0	36	9563	6345	-200	1382	-254	85	-218
32		-36	85	10109	7654	-218	2218	-273	133	-218
50		-18	97	11690	8145	-291	2666	-218	194	-273
93		-91	121	13308	8654	-327	3018	-236	254	-291
224		-200	230	13835	8490	-509	4194	-473	315	-455
476		-309	267	14999	8254	-673	5224	-709	412	-636

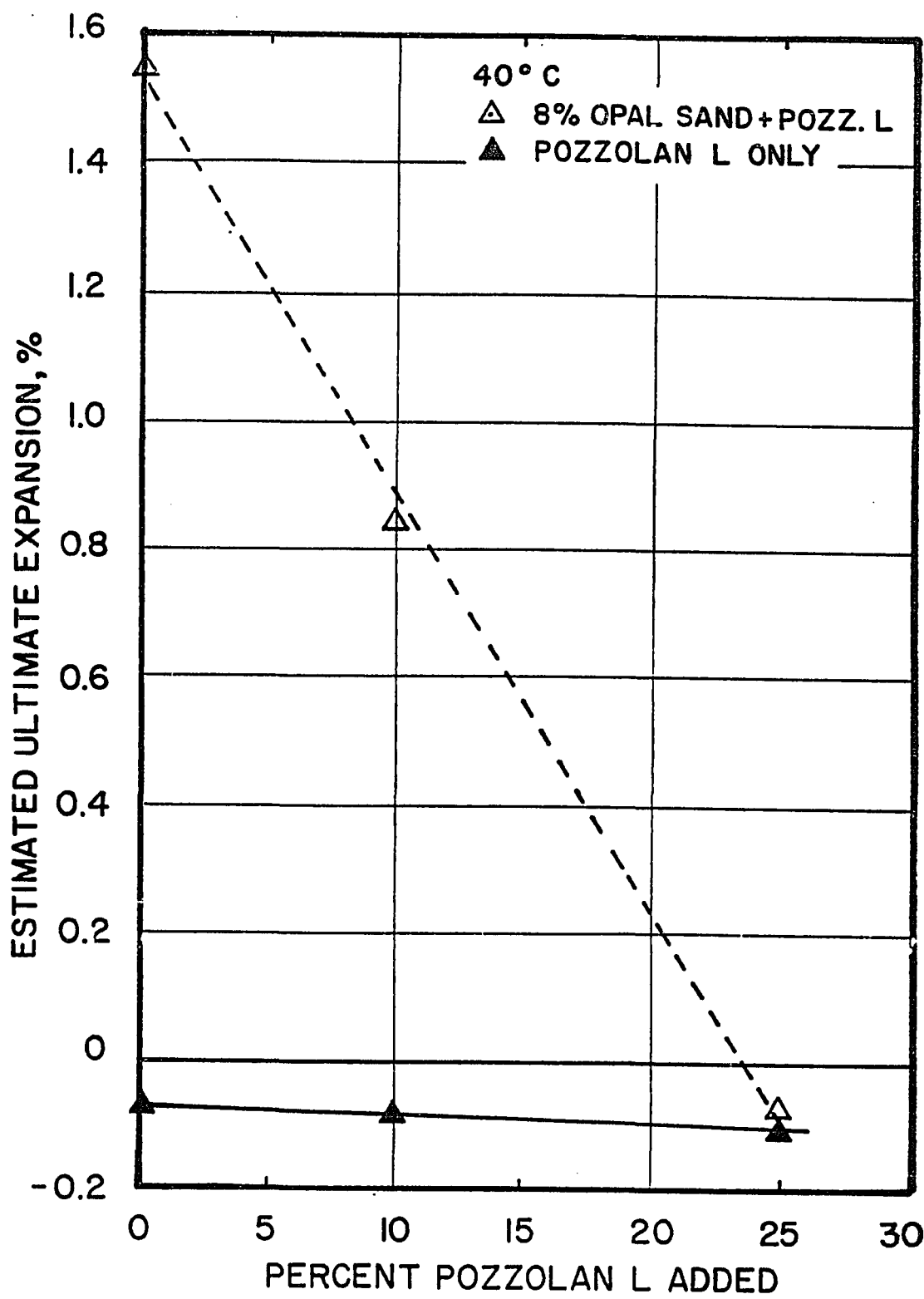


Figure 5.15.16 - Effect of Addition of Pozzolan L on
Estimated Ultimate Expansion of Sealed 50-mm Cylinders

Table 5.15.20 - Expansion (Microstrain) of Mortar Cylinders, Mix Series 59 - 64After Removal of Butyl Rubber Jackets and Storage over Water

Age, Days* at 20° C	Mix 59 Control Mix	8% Beltane Opal Sand					
		Mix 60 0% Pozzolan	Mix 61 10% Pozzolan	Mix 62 25% Pozzolan	Mix 63 10% Pozzolan	Mix 64 25% Pozzolan	
		L	L	L	L	L	
2.5	--	+3009	+3074	+37	+91	+164	
5	--	3218	3436	1746	18	219	
25	--	3745	3763	2073	-18	309	
108	--	7000	4454	2746	+145	255	

Age, Days* at 40° C	8% Beltane Opal Sand					
	Mix 60 0% Pozzolan	Mix 61 10% Pozzolan	Mix 62 25% Pozzolan	Mix 63 10% Pozzolan	Mix 64 25% Pozzolan	
L	L	L	L	L	L	
2.5	-36	+2145	+2854	+328	-36	--
5	-55	2054	2999	346	0	+254
25	-91	4290	3818	658	+91	345
108	+254	6253	5545	1764	291	527

Days after removal of Butyl rubber jackets.

5.15 - This section not used

5.17 - This section not used

5.18 - This section not used

5.19 - Mix Series 78 ~ 81

In this series the effects of three addition levels of pozzolan L on the concentrations of ions in the expressed pore solutions were studied.

Batch weights for the mixes are listed in Table 5.19.1. The pozzolan was added as a percent, by weight, of the portland cement and an equivalent absolute volume of C 109 sand was deleted from the batch to maintain a constant batch volume of 2500 cm³. Weight ratios of the component materials, oven-dry/batch, and ignited/batch, are listed in Table 5.19.2.

Observed properties of the expressed pore solutions are listed in Tables 5.19.3 through 5.19.6. The concentrations of alkali metal ions, compensated for W_n/c , have been listed in Tables 5.19.8 through 5.19.11. These tables have been used to construct figures relating changes in chemical properties of the pore solutions to time and to the addition of pozzolan L.

Values of nonevaporable water, W_n/c , were determined, for these mixes, and are listed in Table 5.19.7 along with the linear estimating equations fitted to them.

Nonevaporable water data from Table 5.19.7, for mixes stored at 20°C and 40°C for periods of 10 and 124 days, have been plotted against the percent addition of pozzolan L in Figure 5.19.1.

Table 5.19.1

Batch Weights, grams, for Mixes 78 - 81

Materials	Mix 78, Control		Mix 79, 10% Pozzolan L		Mix 80, 15% Pozzolan L	
	Parts by Weight	Batch Weights	Parts by Weight	Batch Weights	Parts by Weight	Batch Weights
Cement, AT-1	1.00	1590.2	1.00	1590.2	1.00	1590.2
Water	0.50	795.5	0.50	795.5	0.50	795.5
Pozzolan, L	0.00	--	0.10	159.0	0.15	238.5
Sand, C 109	2.00	3180.3	1.89	3003.2	1.83	2914.7
Totals	3.50	5565.6	3.49	5547.5	3.48	5538.5

Mix 91, 30%
Pozzolan L

Materials	Parts by Weight	Batch Weights
Cement, AT-1	1.00	1590.2
Water	0.50	795.5
Pozzolan, L	0.30	477.0
Sand, C 109	1.666	2649.1
Totals	3.466	5511.4

Table 5.19.2

Weight Ratios of Component MaterialsOven-Dry/Batch, Ignited/Batch

Material	W _{od} /W _o	W _{ig} /W _o
Cement, AT-1	0.99809	0.99483
Pozzolan, L	0.99807	0.98924
Sand, C 109	0.99993	0.99868

Table 5.19.3
 OBSERVED CONCENTRATIONS OF IONS IN EXPRESSED PORE SOLUTION (NOT CORRECTED FOR BOUND WATER)
 MTX 78, CONTROL FOR MIX SERIES 78 - 81
 (Concentrations in millimoles/liter)

AGE DAYS AT 20°C	Si ⁴⁺ *	Al ³⁺	Fe ³⁺	Mg ⁺⁺	Ca ⁺⁺	Na ⁺	K ⁺	$\Sigma^{+}**$	$\Sigma^{-}**$
0.021	3.5	0.3	0.0	0.0	20.	125.	389.	554.	179.
1.0	2.8	0.7	0.0	0.0	2.	168.	478.	650.	649.
2.75	1.4	0.3	0.0	0.0	2.	209.	522.	734.	736.
5.75	2.4	0.4	0.0	0.0	1.	194.	504.	700.	717.
9.75	2.3	0.4	0.0	0.0	1.	206.	536.	745.	744.
27.	5.9	0.5	0.0	0.0	1.	219.	567.	789.	773.
124.	5.8	0.5	0.0	0.0	1.	223.	540.	764.	760.
						n.d.	(0.)	(0.)	(+ 4.)
40°C	Si ⁴⁺ *	Al ³⁺	Fe ³⁺	Mg ⁺⁺	Ca ⁺⁺	Na ⁺	K ⁺	$\Sigma^{+}**$	$\Sigma^{-}**$
2.75	2.4	0.2	0.0	0.0	2.	205.	487.	695.	685.
5.75	3.7	0.3	0.0	0.0	1.	213.	523.	737.	709.
9.75	2.6	0.4	0.0	0.0	1.	214.	511.	728.	709.
27.	6.8	0.4	0.1	0.0	2.	221.	521.	745.	697.
124.	3.8	0.6	0.0	0.0	0.	226.	505.	732.	613.
						n.d.	(613.)	(613.)	(+119.)

* See Remarks under Section 4.4.1

** milliequivalents/liter

n.d. = not determined

Values in parentheses are estimates.

Table 5.19.4

OBSERVED CONCENTRATIONS OF IONS IN EXPRESSED PORE SOLUTION (NOT CORRECTED FOR BOUND WATER)

MIX 79, 10 PERCENT POZZOLAN ADDITION, MIX SERIES 78 - 81

(Concentrations in millimoles/liter)

AGE	DAYS AT 20° C	Si ⁴⁺ *	Al ³⁺	Fe ³⁺	Mg ⁺⁺	Ca ⁺⁺	Na ⁺	K ⁺	Σ^{+**}	OH ⁻	SO ₄ ²⁻	Σ^{-**}	Σ^{+-**}
0.021	2.7	0.3	0.0	0.0	21.	124.	386.	552.	175.	196.	568.	- 16.	
1.0	3.8	0.5	0.0	0.0	2.	170.	477.	650.	654.	0.	654.	- 4.	
2.75	1.1	0.4	0.0	0.0	1.	199.	508.	710.	699.	0.	699.	+ 11.	
5.75	2.4	0.4	0.0	0.0	1.	201.	516.	720.	726.	3.	732.	- 12.	
9.75	2.3	0.4	0.0	0.0	2.	213.	551.	768.	760.	2.	763.	+ 5.	
27.	7.5	0.5	0.1	0.0	1.	195.	479.	677.	689.	4.	697.	- 20.	
124.	3.4	0.7	0.0	0.0	1.	190.	432.	623.	678.	n.d.	(0.)	(- 55.)	
AGE	DAYS AT 40° C	Si ⁴⁺ *	Al ³⁺	Fe ³⁺	Mg ⁺⁺	Ca ⁺⁺	Na ⁺	K ⁺	Σ^{+**}	OH ⁻	SO ₄ ²⁻	Σ^{-**}	Σ^{+-**}
2.75	2.3	0.3	0.0	0.0	1.	187.	620.	620.	608.	8.	625.	- 5.	
5.75	3.3	0.4	0.0	0.0	1.	175.	400.	578.	580.	12.	603.	- 25.	
9.75	2.0	0.3	0.0	0.0	1.	190.	432.	625.	603.	15.	633.	- 8.	
27.	9.2	0.5	0.0	0.0	1.	198.	422.	623.	593.	15.	624.	- 1.	
124.	3.7	0.8	0.0	0.0	0.	212.	442.	654.	608.	n.d.	(608)	(+ 46.)	

*See remarks under Section 4.1.1

** milliequivalents/liter

n.d. = not determined

Values in parentheses are estimates.

Table 5.19.5
 OBSERVED CONCENTRATIONS OF IONS IN EXPRESSED PORE SOLUTION (NOT CORRECTED FOR BOUND WATER)
 MIX 80, 15 PERCENT POZZOLAN ADDITION, MIX SERIES 78 - 81
 (Concentrations in millimoles/liter)

AGE	DAYS	AT 20° C	Si ⁴⁺ *	Al ³⁺	Fe ³⁺	Mg ⁺⁺	Ca ⁺⁺	Na ⁺	K ⁺	Σ^{+**}	Σ^{-**}	Σ^{+-**}
			Si ⁴⁺ *	Al ³⁺	Fe ³⁺	Mg ⁺⁺	Ca ⁺⁺	Na ⁺	K ⁺	Σ^{+**}		
0.021	2.7	0.4	0.0	0.0	21.	122.	383.	546.	167.	175.	516.	+ 30.
1.0	3.1	0.6	0.0	0.0	2.	169.	474.	647.	644.	0.	644.	+ 3.
2.75	2.8	0.4	0.0	0.0	1.	201.	486.	689.	692.	0.	692.	- 3.
5.75	2.3	0.4	0.0	0.0	1.	189.	480.	672.	695.	3.	701.	- 29.
9.75	2.3	0.5	0.0	0.0	2.	197.	500.	700.	699.	5.	709.	- 9.
27.	7.7	0.6	0.0	0.0	1.	173.	404.	579.	518.	3.	524.	+ 55.
124.	3.8	0.8	0.0	0.0	0.	163.	346.	509.	502.	n.d.	(502.)	(+ 7.)
40° C	Si ⁴⁺ *	Al ³⁺	Fe ³⁺	Mg ⁺⁺	Ca ⁺⁺	Na ⁺	K ⁺	Σ^{+**}	Σ^{-**}	Σ^{+-**}	Σ^{+-**}	
		Si ⁴⁺ *	Al ³⁺	Fe ³⁺	Mg ⁺⁺	Ca ⁺⁺	Na ⁺	K ⁺	Σ^{-**}			
2.75	2.6	0.3	0.0	0.0	1.	164.	376.	542.	537.	9.	555.	- 13.
5.75	4.1	0.4	0.0	0.0	1.	153.	337.	491.	477.	16.	509.	- 18.
9.75	1.8	0.4	0.0	0.0	1.	154.	326.	482.	458.	16.	490.	- 8.
27.	8.2	0.5	0.1	0.0	1.	157.	325.	484.	451.	14.	479.	+ 5.
124.	2.4	0.6	0.0	0.0	0.	180.	358.	538.	501.	n.d.	(501.)	(+ 37.)

* See remarks under Section 4.1.1

** milliequivalents/liter

n.d. = not determined

Values in parentheses are estimates.

Table 5.19.6
OBSERVED CONCENTRATIONS OF IONS IN EXPRESSED PORE SOLUTION (NOT CORRECTED FOR BOUND WATER)
MIX 81, 30 PERCENT POZZOLAN ADDITION, MIX SERIES 78 - 81
(Concentrations in milliequivalents/liter)

AGE DAYS	AT 20° C	4+							3+							2+							K ⁺							Σ^{+-**}						
		Si ⁴⁺ *	Al ³⁺	Fe ³⁺	Mg ⁺⁺	Ca ⁺⁺	Na ⁺	K ⁺	OH ⁻	SO ₄ ⁼	Cl ⁻	OH ⁻	SO ₄ ⁼	Cl ⁻	K ⁺	OH ⁻	SO ₄ ⁼	Cl ⁻	K ⁺	OH ⁻	SO ₄ ⁼	Cl ⁻	K ⁺	OH ⁻	SO ₄ ⁼	Cl ⁻	K ⁺	OH ⁻	SO ₄ ⁼	Cl ⁻						
0.021		2.7	0.5	0.0	0.0	17.	122.	384.	541.	157.	175.	507.	649.	0.	649.	0.	649.	0.	649.	0.	649.	0.	649.	0.	649.	0.	649.	0.	+ 34.							
1.0		4.9	0.6	0.0	0.0	2.	170.	476.	650.	649.	649.	649.	649.	0.	649.	0.	649.	0.	649.	0.	649.	0.	649.	0.	649.	0.	649.	0.	+ 1.							
2.75		2.1	0.4	0.0	0.0	2.	202.	485.	690.	692.	692.	692.	692.	0.	692.	0.	692.	0.	692.	0.	692.	0.	692.	0.	692.	0.	692.	0.	- 2.							
5.75		2.6	0.5	0.0	0.0	1.	174.	426.	602.	617.	617.	617.	617.	6.	617.	6.	617.	6.	617.	6.	617.	6.	617.	6.	617.	6.	617.	6.	- 27.							
9.75		1.4	0.9	0.0	0.0	1.	150.	348.	500.	500.	500.	500.	500.	5.	500.	5.	500.	5.	500.	5.	500.	5.	500.	5.	500.	5.	500.	5.	- 10.							
27.		8.4	1.0	0.0	0.0	1.	118.	247.	366.	357.	357.	357.	357.	6.	357.	6.	357.	6.	357.	6.	357.	6.	357.	6.	357.	6.	357.	6.	- 3.							
124.		3.5	1.0	0.0	0.0	0.	107.	211.	318.	300.	300.	300.	300.	n.d.	(300.)	n.d.	(300.)	n.d.	(300.)	n.d.	(300.)	n.d.	(300.)	n.d.	(300.)	n.d.	(300.)	n.d.	(+ 18.)							
40° C		4+							3+							2+							K ⁺							Σ^{+-**}						
		2.75	2.4	0.5	0.0	0.0	1.	127.	261.	390.	390.	390.	390.	390.	13.	390.	13.	390.	13.	390.	13.	390.	13.	390.	13.	390.	13.	390.	13.	- 12.						
5.75		2.7	0.4	0.0	0.0	1.	112.	223.	336.	336.	336.	336.	336.	19.	336.	19.	336.	19.	336.	19.	336.	19.	336.	19.	336.	19.	336.	19.	- 11.							
9.75		2.0	0.7	0.0	0.0	0.	103.	202.	306.	306.	306.	306.	306.	16.	306.	16.	306.	16.	306.	16.	306.	16.	306.	16.	306.	16.	306.	16.	- 3.							
27.		8.2	0.8	0.0	0.0	1.	100.	189.	291.	291.	291.	291.	291.	0.	291.	0.	291.	0.	291.	0.	291.	0.	291.	0.	291.	0.	291.	0.	0.							
124.		3.4	0.9	0.0	0.0	0.	101.	183.	284.	284.	284.	284.	284.	n.d.	(254.)	n.d.	(254.)	n.d.	(254.)	n.d.	(254.)	n.d.	(254.)	n.d.	(254.)	n.d.	(254.)	n.d.	(+ 30.)							

* See remarks under Section 4.1.1

**milliequivalents/liter

n.d. = not determined

Values in parentheses are estimates.

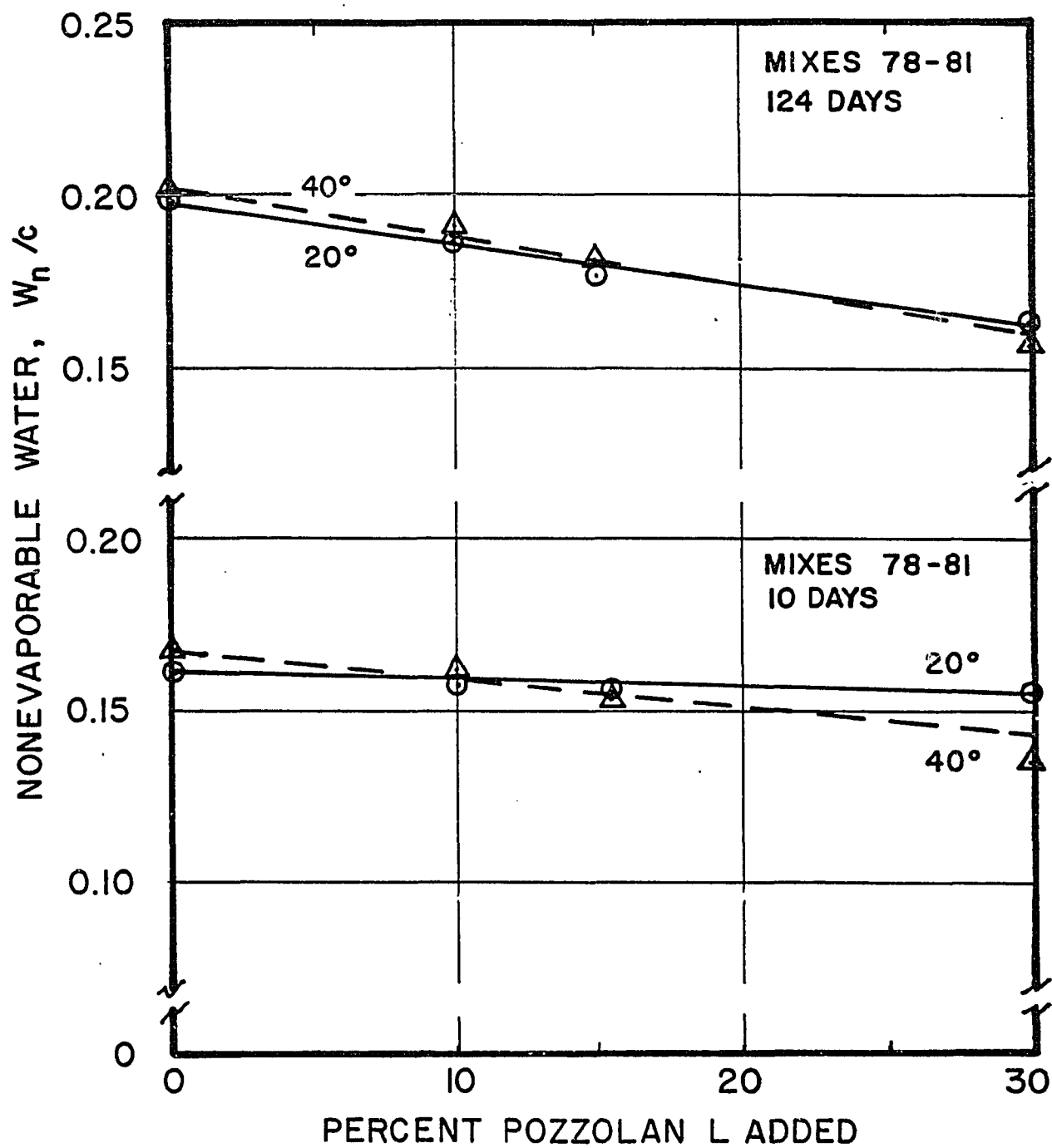


Figure 5.19.1 - Effect of Pozzolan L Addition on
Nonevaporable Water, W_n/c , at 10 and 128 Days

Table 5.19.7

Nonevaporable Water, W_n/c , as a Function ofPercent Pozzolan L Added

Time, Days	Temp. °C	Mix 78	Mix 79	Mix 80	Mix 81
1	20	0.1046 est $W_n/c = 0.1054 + 2.853 \times 10^{-5} x \% P$	0.1055	0.1076	0.1054 $x \% P$
2.75	20	0.1518 est $W_n/c = 0.1520 - 7.547 \times 10^{-5} x \% P$	0.1508	0.1517	0.1494
2.75	40	0.1533 est $W_n/c = 0.1553 - 4.261 \times 10^{-4} x \% P$	0.1528	0.1506	0.1411
5.75	20	0.1572 est $W_n/c = 0.1571 - 1.944 \times 10^{-4} x \% P$	0.1550	0.1544	0.1513
5.75	40	0.1591 est $W_n/c = 0.1598 - 6.413 \times 10^{-4} x \% P$	0.1556	0.1486	0.1406
10.	20	0.1610 est $W_n/c = 0.1602 - 2.109 \times 10^{-4} x \% P$	0.1576	0.1562	0.1545
10.	40	0.1670 est $W_n/c = 0.1674 - 8.203 \times 10^{-4} x \% P$	0.1613	0.1530	0.1341
27.	20	0.1792 est $W_n/c = 0.1789 - 7.968 \times 10^{-4} x \% P$	0.1712	0.1658	0.1554
27	40	0.1842 est $W_n/c = 0.1840 - 1.221 \times 10^{-3} x \% P$	0.1737	0.1629	0.1482
124	20	0.1981 est $W_n/c = 0.1973 - 1.218 \times 10^{-3} x \% P$	0.1859	0.1765	0.1618
124	40	0.2011 est $W_n/c = 0.2027 - 1.444 \times 10^{-3} x \% P$	0.1904	0.1813	0.1585

$\% \text{ Pozzolan L}$ Added		0.	10.	15.	30.

 $\% P$ = percent pozzolan L added

Considering the fact that each of the plotted points represents a single determination, they appear to define reasonably linear relationships between W_n/c and percent pozzolan addition. At early ages the reduction in W_n/c was greater for specimens stored at 40°C than for specimens stored at 20°C . With increasing time the two linear relationships tend to merge, as shown in the upper half of Figure 5.19.1. This effect is understandable if, as suggested in Section 5.15, it is assumed that the loss in W_n/c with increasing pozzolan loading is due to reactions between amorphous or disordered silica in the pozzolan, and free calcium hydroxide and alkali metal compounds released by the hydrating cement, in such a way that a reaction product is produced in which the molar ratio $\text{H}_2\text{O}/\text{CaO}$ is less than unity.

Data from Table 5.19.7 have been used to construct Tables 5.19.8 through 5.19.11. These tables contain observed concentrations of the alkali metal ions found in pore solutions expressed from hardened mortars and concentrations of these ions compensated for W_n/c . In Table 5.19.12 the total alkali metal ion concentrations found in the pore solutions, compensated for W_n/c , are summarized, and the linear estimating equations fitted to these data are listed. Data from this table have been plotted against the logarithm of time for the control mix, Mix 78, stored at 20°C (Figure 5.19.2), and at 40°C (Figure 5.19.3), and for a mix containing 30 percent pozzolan L addition, Mix 81, at 20°C (Figure 5.19.4), and at 40°C (Figure 5.19.5).

The control mix exhibited a nearly constant alkali concentration except for a modest decline in K^+ concentration with time. At 40°C (Figure 5.19.3) the pattern is similar, but the reduction of K^+ was greater. In Figures 5.19.4 and 5.19.5 for mixes with 30% pozzolan L,

Table 5.19.8

Concentrations of Alkali Metal Cations in Expresssed Pore Solution (Corrected for Bound Water)						
Mix 78, Control for Mix Esries 78 - 81						
(Concentrations in millimoles/liter)						
Age, Days at 20° C	W _{n/c}	bwk	Cations Found	Cation Concentration Corrected for W _{n/c}	*K ⁺ / *Na ⁺	
			Na ⁺ K ⁺ M ⁺	*Na ⁺ Δ*K ⁺ *K ⁺ Δ*M ⁺		
0.021	0.004	0.992	125 389 514	124 - 386 -	510	-
1.	0.105	0.791	168 478 646	133 - 378 -	511	-
2.75	0.144	0.711	209 522 731	149 - 371 -	520	-
5.75	0.157	0.686	194 504 698	133 - 346 -	479	-
10.	0.161	0.678	206 536 742	140 - 363 -	503	-
27.	0.179	0.642	219 566 785	141 - 363 -	504	-
124.	0.198	0.604	223 540 763	135 - 326 -	461	-
					2.422	

Age, Days at 20° C	W _{n/c}	bwk	Cations Found	Cation Concentration Corrected for W _{n/c}	*K ⁺ / *Na ⁺	
			Na ⁺ K ⁺ M ⁺	*Na ⁺ Δ*K ⁺ *K ⁺ Δ*M ⁺		
0.021	0.004	0.992	125 389 514	124 - 386 -	510	-
1.	0.105	0.791	168 478 646	133 - 378 -	511	-
2.75	0.144	0.711	209 522 731	149 - 371 -	520	-
5.75	0.157	0.686	194 504 698	133 - 346 -	479	-
10.	0.161	0.678	206 536 742	140 - 363 -	503	-
27.	0.179	0.642	219 566 785	141 - 363 -	504	-
124.	0.198	0.604	223 540 763	135 - 326 -	461	-
					2.422	

Age, Days at 40° C	W _{n/c}	bwk	Cations Found	Cation Concentration Corrected for W _{n/c}	*K ⁺ / *Na ⁺	
			Na ⁺ K ⁺ M ⁺	*Na ⁺ Δ*K ⁺ *K ⁺ Δ*M ⁺		
2.75	0.146	0.709	205 487 692	145 - 345 -	490	-
5.75	0.159	0.682	213 523 736	145 - 357 -	502	-
10.	0.167	0.666	214 511 725	143 - 340 -	483	-
27.	0.184	0.632	221 521 742	140 - 329 -	469	-
124.	0.201	0.598	226 505 731	135 - 302 -	437	-
					2.235	

Table 5.19.9

Concentrations of Alkali Metal Cations in Expressed Pore Solution (Corrected for Bound Water)

Mix 79, 10 Percent Pozzolan L

(Concentrations in millimoles/liter)

Age, Days at 20° C	W _n /c	bwk	Cations Found			Cation Concentration	Corrected for W _n /c	*K ⁺ / *Na ⁺	
			Na ⁺	K ⁺	M ⁺				
0.021	0.004	0.992	124	386	510	123	-1	383	-3
1.	0.106	0.789	170	477	647	134	+1	376	-2
2.75	0.144	0.712	199	508	707	142	-7	362	-10
5.75	0.155	0.690	201	516	717	139	+6	356	+10
10.	0.158	0.685	213	551	764	146	+6	377	+14
27.	0.171	0.658	195	479	674	128	-12	315	-48
124.	0.186	0.628	190	432	622	119	-15	271	-55
								391	-70

Age, Days at 40° C	W _n /c	bwk	Cations Found			Cation Concentration	Corrected for W _n /c	*K ⁺ / *Na ⁺	
			Na ⁺	K ⁺	M ⁺				
2.75	0.146	0.707	187	430	617	132	-13	304	-41
5.75	0.156	0.689	175	400	575	121	-25	276	-81
10.	0.161	0.677	190	432	622	129	-14	293	-54
27.	0.174	0.653	198	422	620	129	-10	275	-54
124.	0.190	0.619	212	442	654	131	-4	274	-28
								405	-32

Table 5.19.10

Concentrations of Alkali Metal Cations in Expressed Pore Solution (Corrected for Bound Water)
Mix 80, 15 Percent Pozzolan L
 (Concentrations in millimoles/liter)

Age, Days at 20° C	W _{n/c}	bwk	Cations Found			Cation Concentration Corrected for W _{n/c}			*K ⁺ / *Na ⁺
			Na ⁺	K ⁺	M ^t	*Na ⁺	*K ⁺	Δ*K ⁺	
0.021	0.004	0.992	122	383	505	112	-3	380	-6
1.	0.108	0.785	168	474	642	132	-1	372	-6
2.75	0.146	0.709	201	486	687	142	-6	344	-27
5.75	0.154	0.691	189	480	669	131	-2	332	-14
10.	0.156	0.688	197	500	697	135	-4	344	-20
27.	0.166	0.668	173	404	577	116	-25	270	-93
124.	0.176	0.647	163	346	509	105	-29	224	-102
									-131
Age, Days at 40° C	W _{n/c}	bwk	Cations Found			Cation Concentration Corrected for W _{n/c}			*K ⁺ / *Na ⁺
			Na ⁺	K ⁺	M ^t	*Na ⁺	*K ⁺	Δ*K ⁺	
2.75	0.144	0.712	164	376	540	117	-29	268	-78
5.75	0.149	0.703	153	337	490	108	-38	237	-120
10.	0.153	0.694	154	326	480	107	-36	226	-114
27.	0.163	0.674	157	325	482	106	-34	219	-110
124.	0.181	0.637	180	360	540	115	-20	229	-72
									-93

Table 5.19.11
 Concentrations of Alkali Metal Cations in Expressed Pore Solution (Corrected for Bound Water)
Mix 81, 30 Percent Pozzolan L
 (Concentrations in millimoles/liter)

Age, Days at 20° C	W _n /c	bwk	Cations Found			Cation Concentration Corrected for W _n /c			*K ⁺ / ^{*Na⁺}
			Na ⁺	K ⁺	M ⁺	*Na ⁺	*K ⁺	*M ⁺	
0.021	0.004	0.992	122	384	506	121	-3	381	-8
1.	0.105	0.789	170	476	646	134	+1	376	3.148
2.75	0.144	0.713	202	485	687	144	-5	346	2.800
5.75	0.151	0.697	174	426	600	121	-12	297	-1
10.	0.154	0.691	150	348	498	104	-36	240	2.401
27.	0.155	0.689	118	247	365	81	-59	170	-30
124.	0.162	0.676	107	211	318	72	-62	143	2.448
								215	-60
									2.320
									2.093
									-246
									1.972

Age, Days at 40° C	W _n /c	bwk	Cations Found			Cation Concentration Corrected for W _n /c			*K ⁺ / ^{*Na⁺}
			Na ⁺	K ⁺	M ⁺	*Na ⁺	*K ⁺	*M ⁺	
2.75	0.137	0.725	127	260	387	92	-53	189	-210
5.75	0.141	0.719	112	223	335	81	-65	160	2.047
10.	0.143	0.714	103	202	305	74	-69	144	-261
27.	0.148	0.704	100	189	289	70	-69	133	1.991
124.	0.158	0.683	101	183	284	69	-66	125	-265
								218	1.961
								203	-265
								194	1.890
								-243	1.812

Table 5.19.12

Total Alkali Metal Ion Concentration, $*M^+$, as a Function
of Percent Pozzolan L Added

Time, Days	Temp. °C	Mix 78	Mix 79	Mix 80	Mix 81
0.02	20	510	506	501	502
		est $\Sigma *M^+$ = 508.5 - 0.269 x % P			
1.	20	511	510	504	510
		est $\Sigma *M^+$ = 509.4 - 0.045 x % P			
2.75	20	520	503	487	490
		est $\Sigma *M^+$ = 513.6 - 0.992 x % P			
	40	490	436	384	281
		est $\Sigma *M^+$ = 495.3 - 7.096 x % P			
5.75	20	479	495	462	418
		est $\Sigma *M^+$ = 495.0 - 2.288 x % P			
	40	502	396	344	241
		est $\Sigma *M^+$ = 489.3 - 8.621 x % P			
10.	20	503	523	479	344
		est $\Sigma *M^+$ = 541.1 - 5.736 x % P			
	40	483	421	333	218
		est $\Sigma *M^+$ = 488.7 - 9.091 x % P			
27	20	504	443	386	252
		est $\Sigma *M^+$ = 514.0 - 8.563 x % P			
	40	469	405	325	203
		est $\Sigma *M^+$ = 475.5 - 9.093 x % P			
124	20	461	391	329	215
		est $\Sigma *M^+$ = 463.4 - 8.320 x % P			
	40	437	405	344	194
		est $\Sigma *M^+$ = 460.7 - 8.416 x % P			
<hr/>					
% Pozzolan L Added		0	10.	15.	30.

% P = percent pozzolan L added

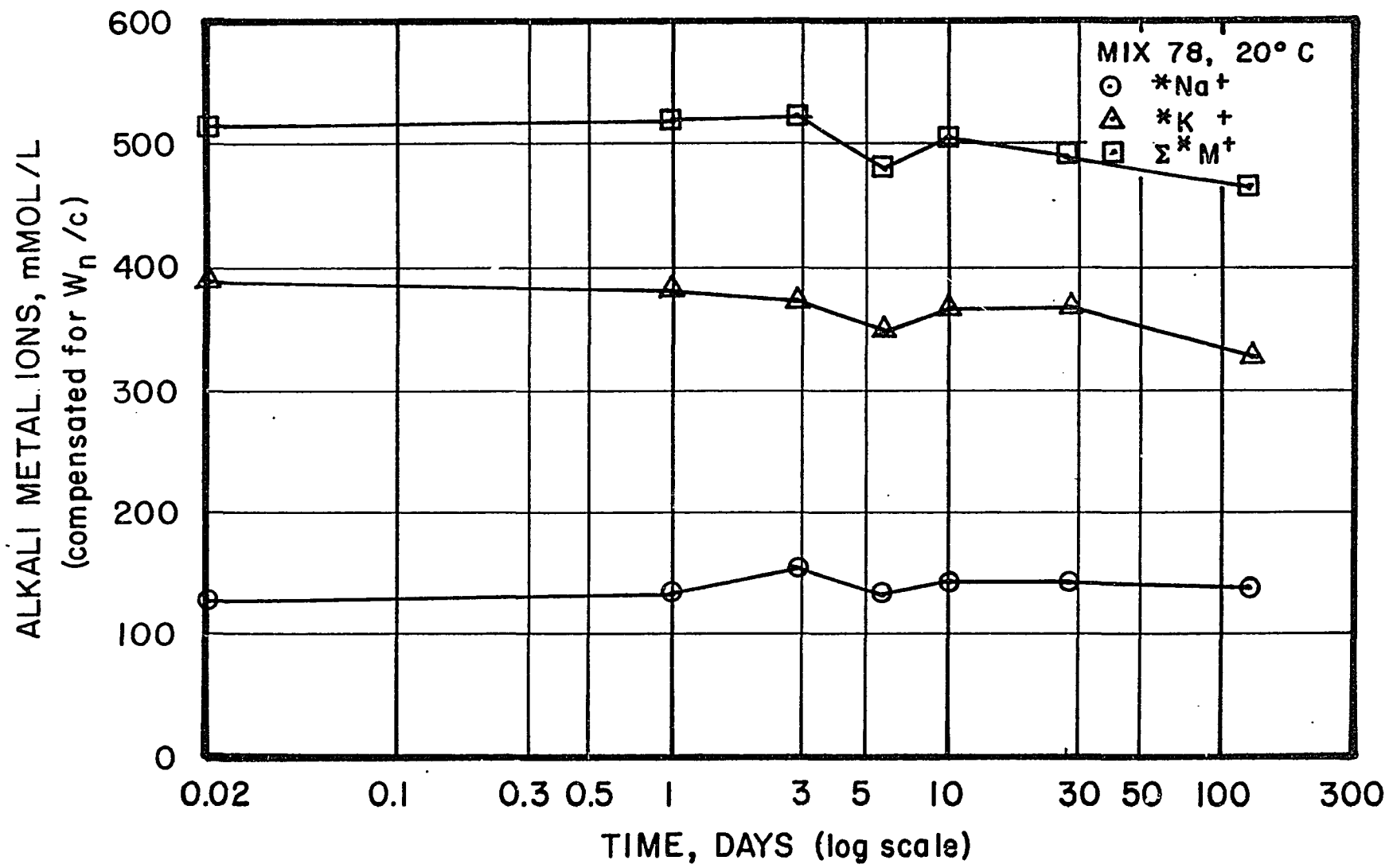


Figure 5.19.2 - Alkali Metal Ion Concentration (mMol/L) in
Expressed Pore Solution, Compensated for W_n/c , Mix 78 Stored at 20° C

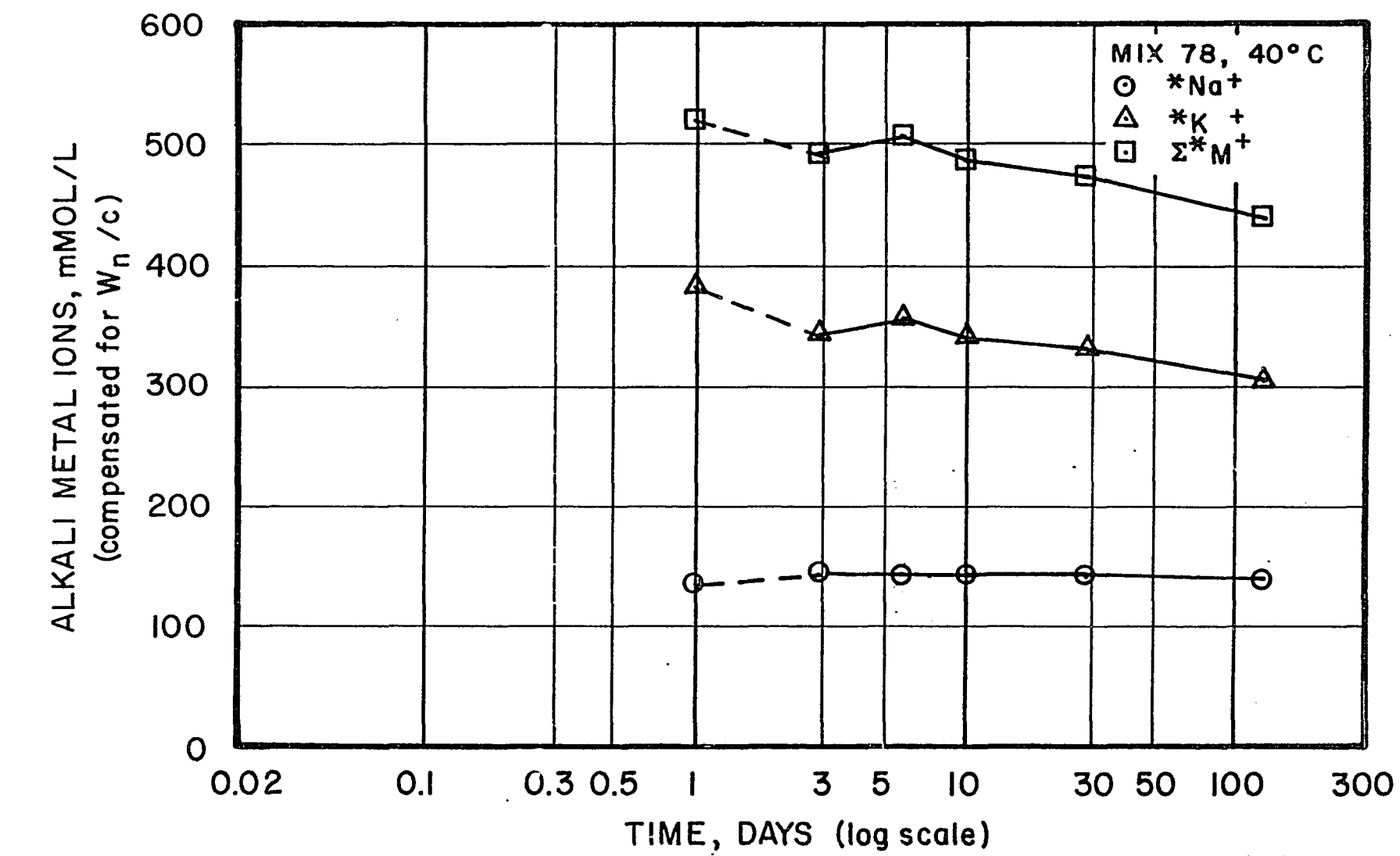


Figure 5.19.3 - Alkali Metal Ion Concentration (mMol/L) in
Expressed Pore Solution, Compensated for $\text{W}_{\text{n}}/\text{c}$, Mix 78 Stored at 40°C

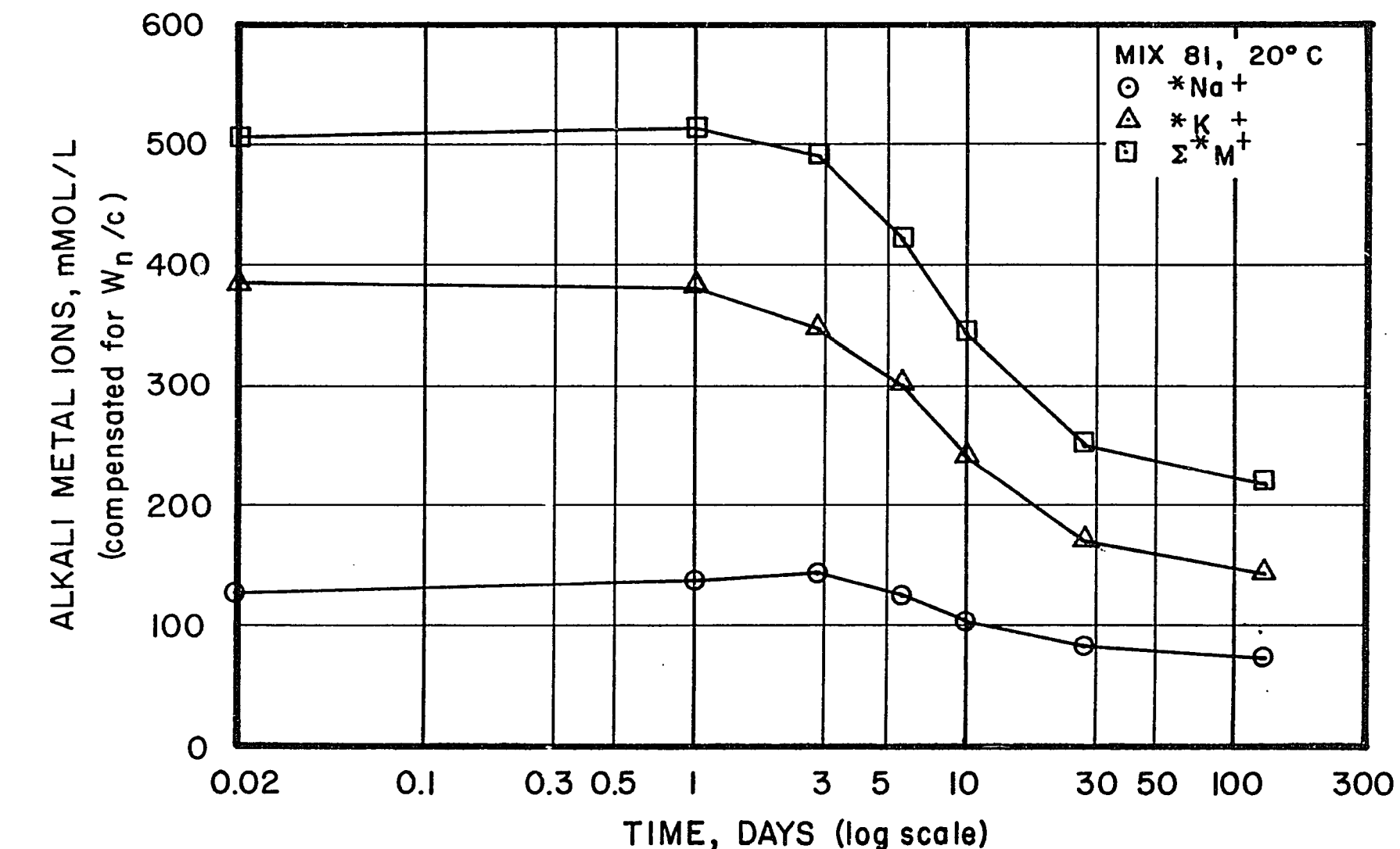


Figure 5.19.4 - Alkali Metal Ion Concentration (mmol/L) in

Expressed Pore Solution, Compensated for W_n/c , Mix 81 Stored at 20°C

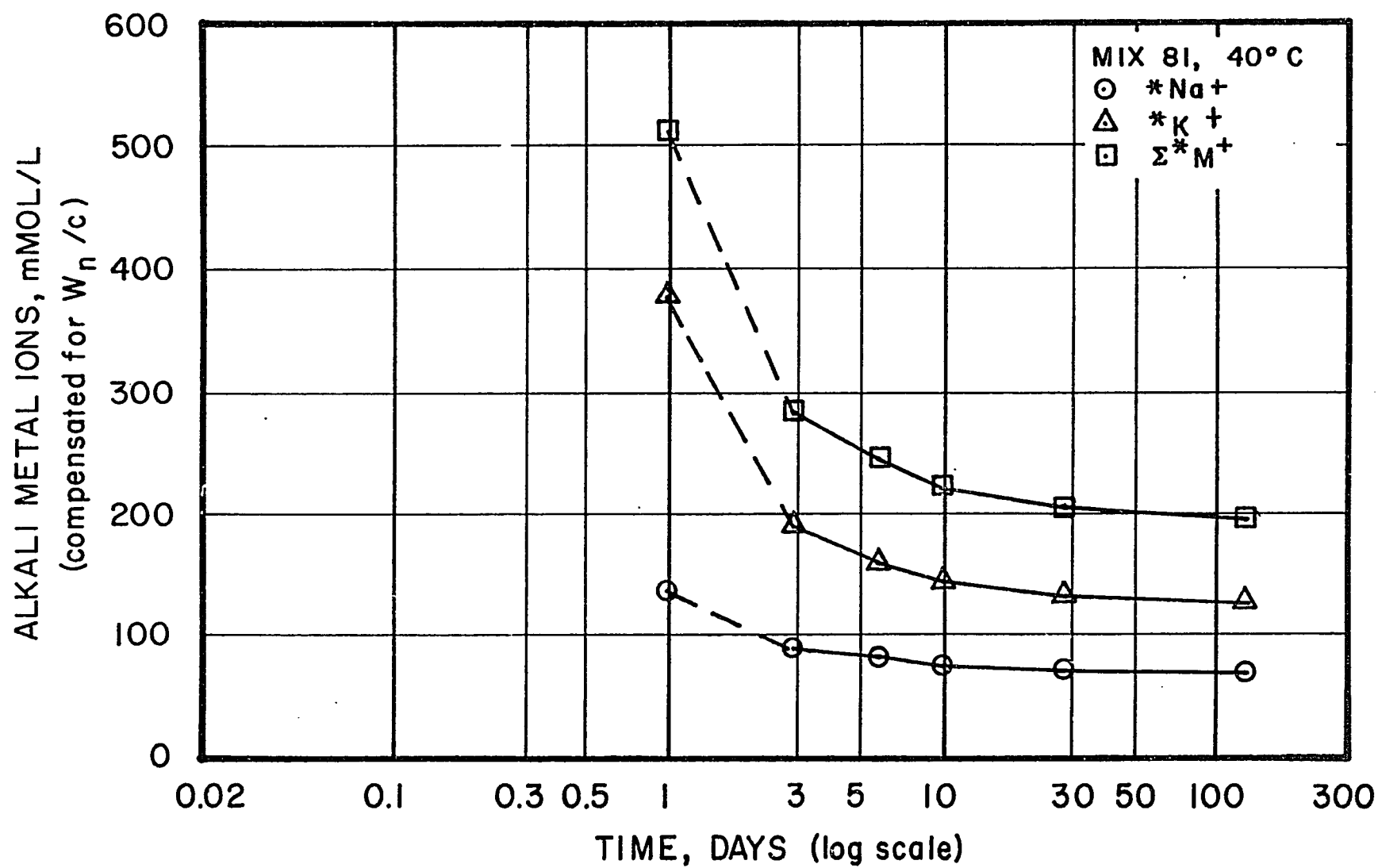


Figure 5.19.5 - Alkali Metal Ion Concentration (mMol/L) in
Expressed Pore Solution, Compensated for W_n/c , Mix 81 Stored at 40° C

the decline in alkali metal ion concentration is seen to have been much more rapid, reaching a nearly constant level at or before 100 days at 20°C, and attaining the same level within about 10 to 15 days for specimens stored at 40°C. The values for the intermediate mixes have not been plotted since, for a given age, the alkali metal ion concentration, in general, tends to be a linear function of pozzolan addition.

The reason for the qualification in the last statement appears in Figures 5.19.7 and 5.19.8. Data from Table 5.19.12 have been plotted in Figures 5.19.6 through 5.19.10 showing the effect of pozzolan addition on Σ^*M^+ at ages 2.75, 5.75, 10, 27, and 124 days. While the normal linear relation between Σ^*M^+ and pozzolan addition is exhibited at 2.75, 27 and 124 days, the data for 5.75 and 10 days exhibit anomalous behavior for specimens stored at 20°C. In Figure 5.19.8 it is apparent that the points for Mixes 79 through 81 define a line whose intercept on the ordinate axis is more than 100 mMol/L above the point plotted for the control mix. A similar, although less severe, anomaly occurs in Figure 5.19.7 for specimens stored at 20°C for 5.75 days. After reaching an apparent peak at 5.75 days the anomaly appears to have disappeared by 27 days. It is of interest that this anomaly is not exhibited by specimens stored at 40°C.

Although there appears to be a significant early temperature effect on alkali removal from the pore solution, data for both 20°C and 40°C specimens appear to approach a single linear relationship at or before 124 days, as is seen in Figure 5.19.10.

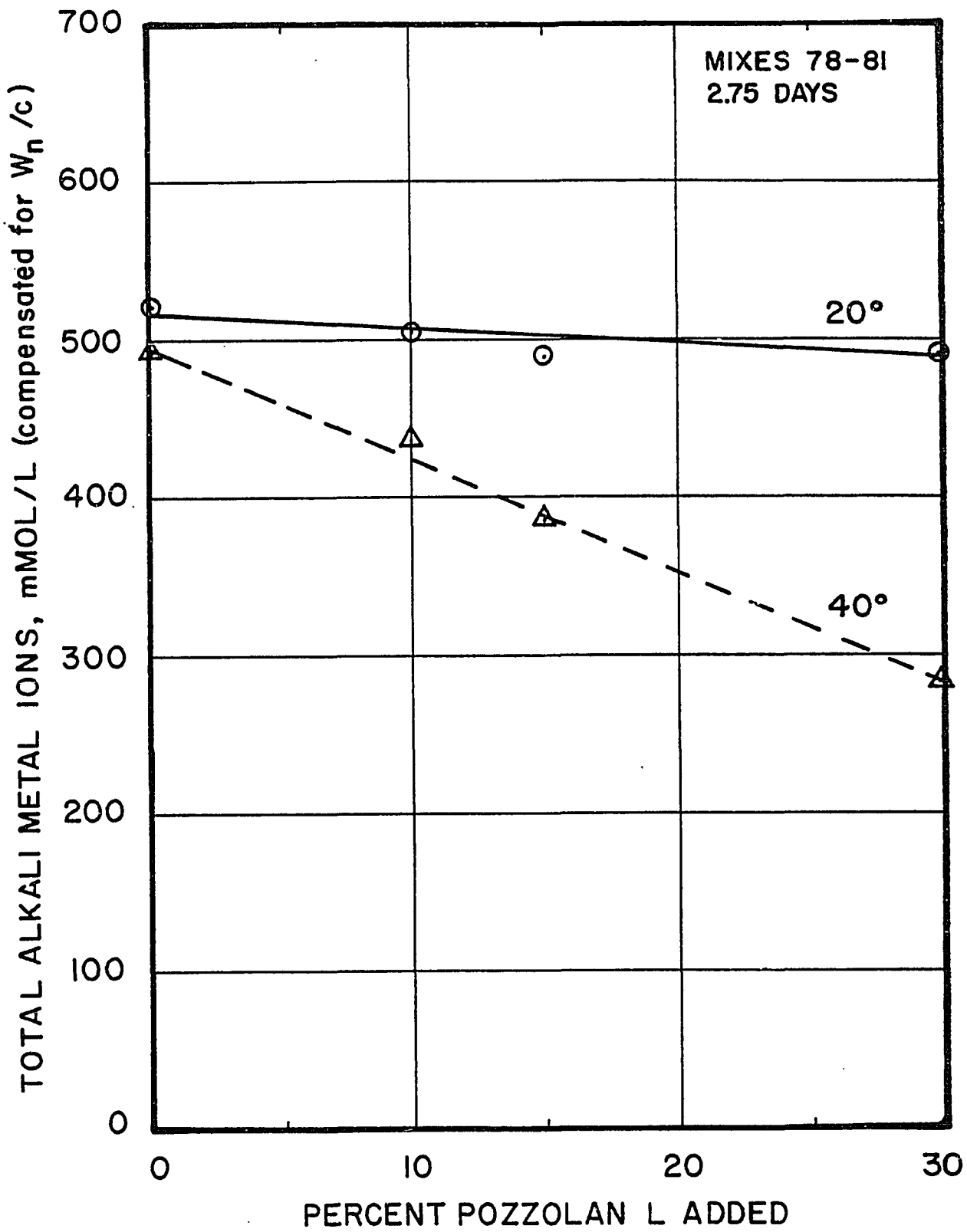


Figure 5.19.6 - Effect of Pozzolan L Addition on Alkali Metal Ion Concentration, Compensated for W_n/c , at 2.75 Days

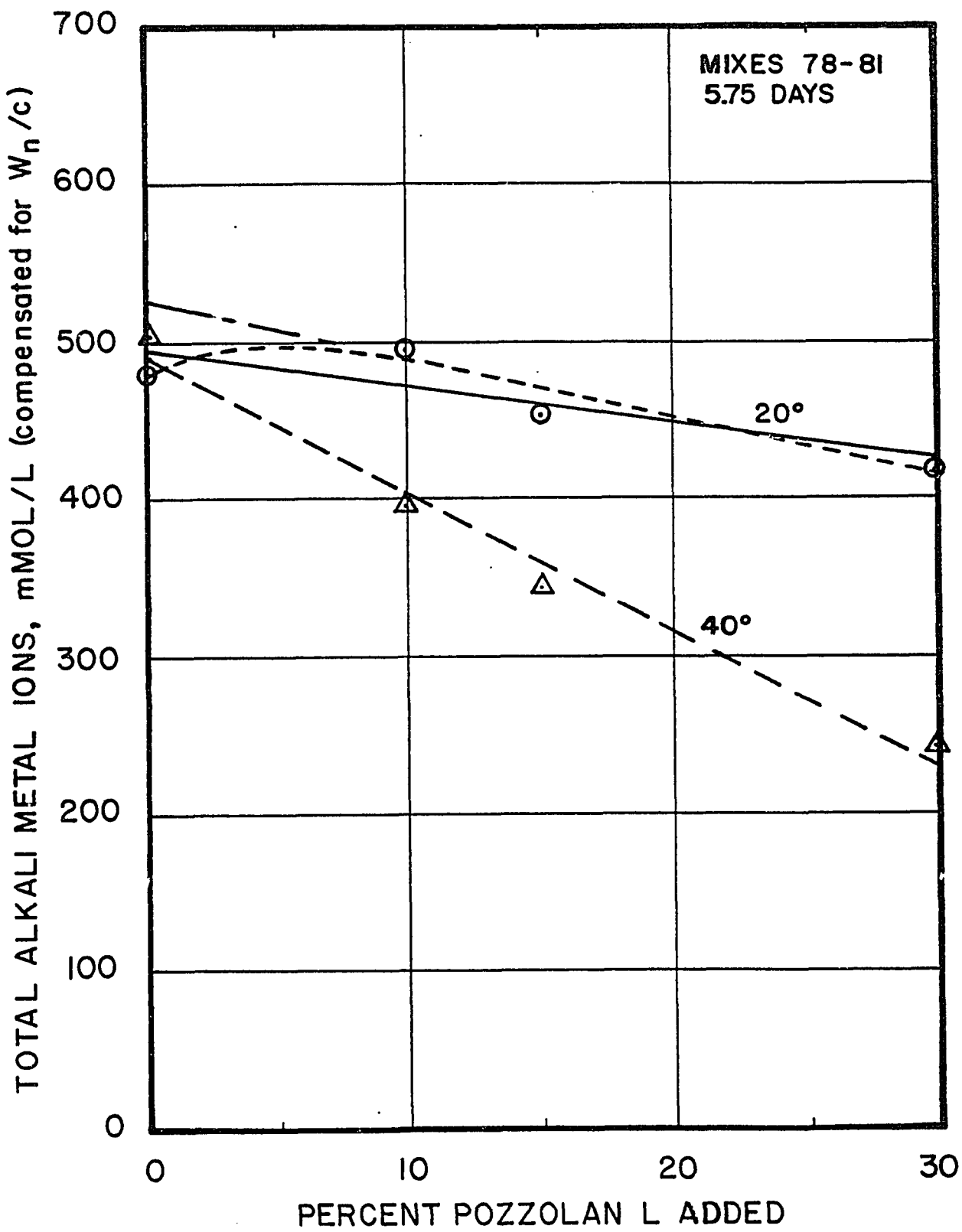


Figure 5.19.7 - Effect of Pozzolan L Addition on Alkali Metal Ion Concentration, Compensated for W_n/c , at 5.75 Days

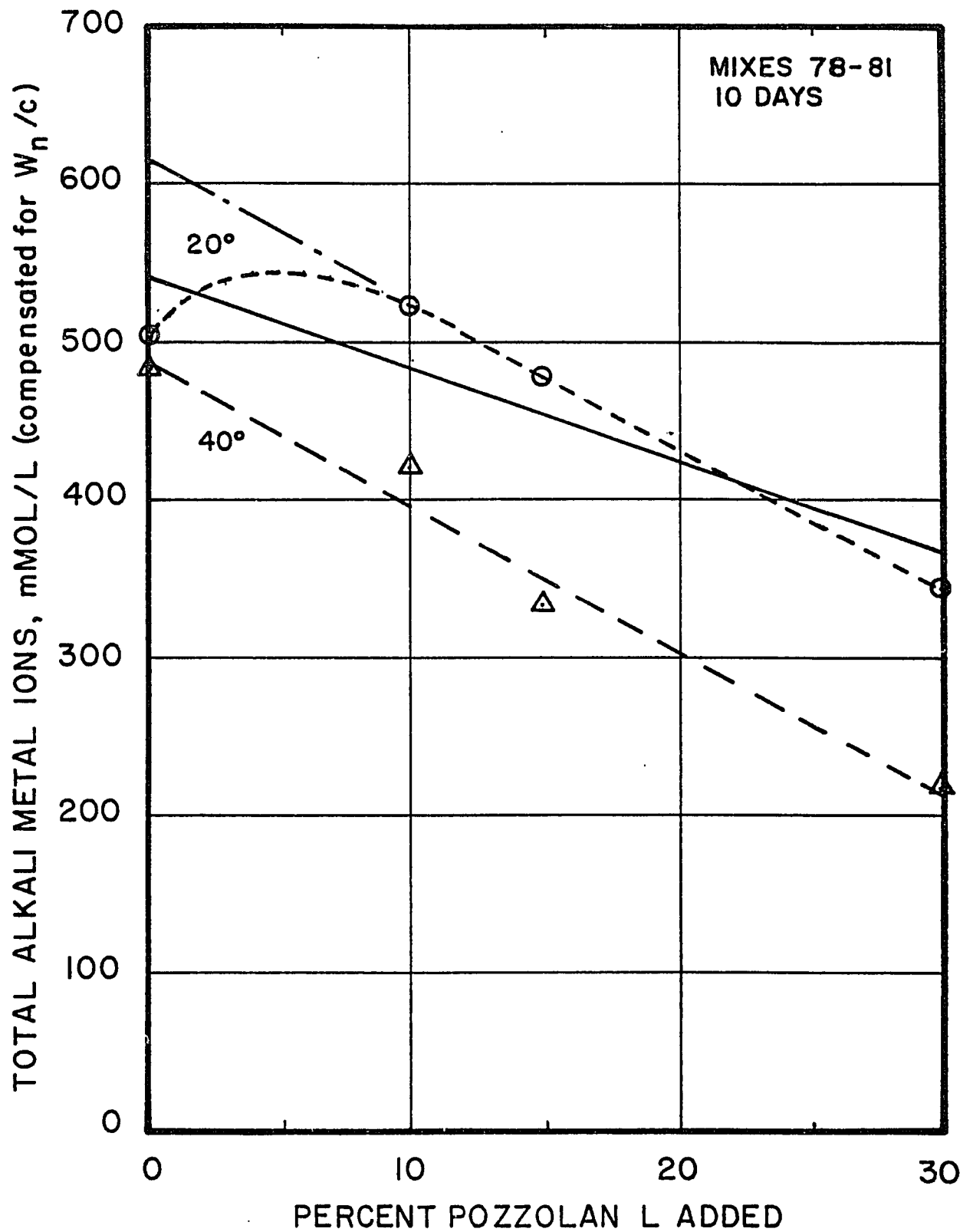


Figure 5.19.8 - Effect of Pozzolan L Addition on Alkali Metal Ion Concentration, Compensated for W_n/c , at 10. Days

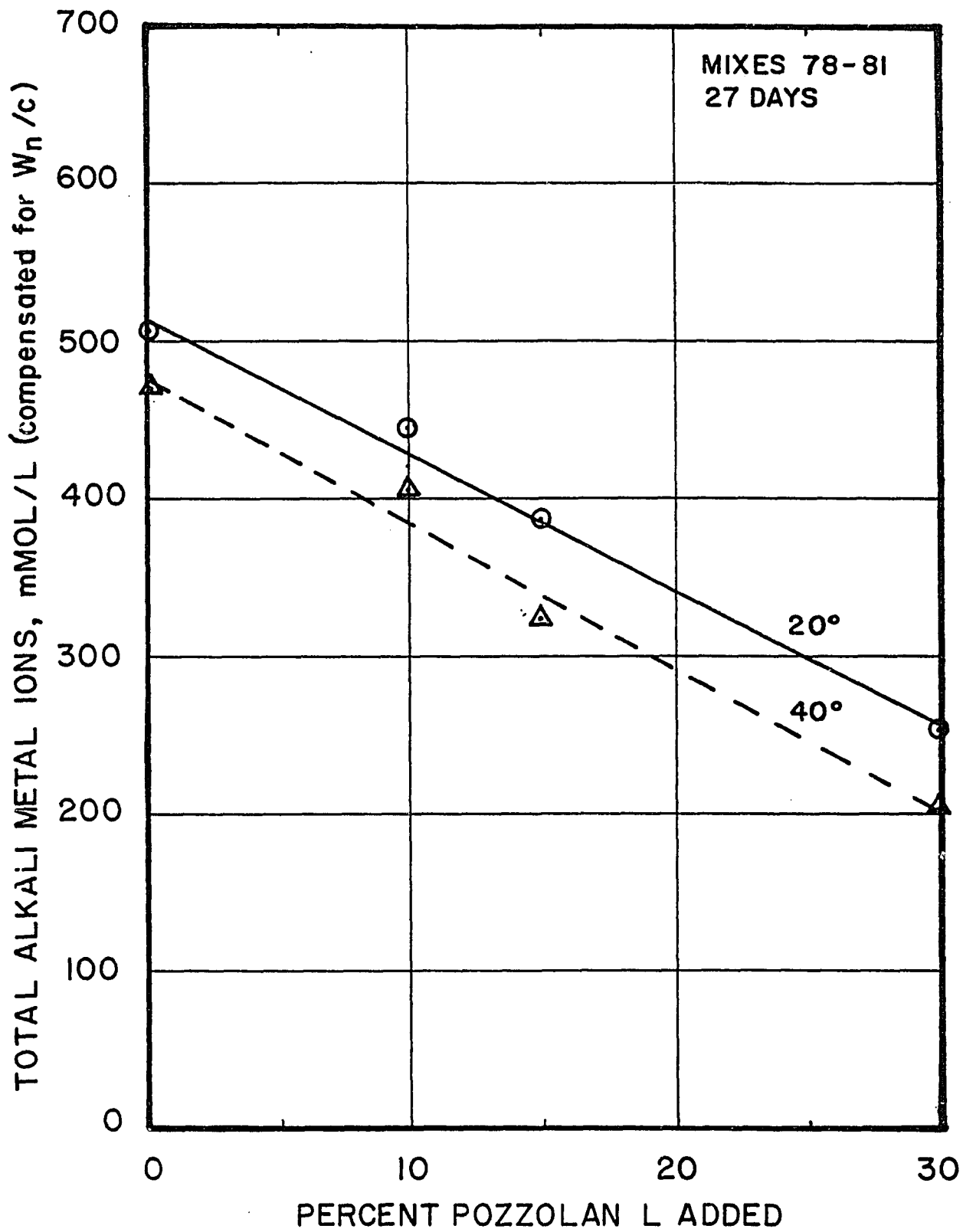


Figure 5.19.9 - Effect of Pozzolan L Addition on Alkali Metal Ion Concentration, Compensated for W_n/c , at 27. Days

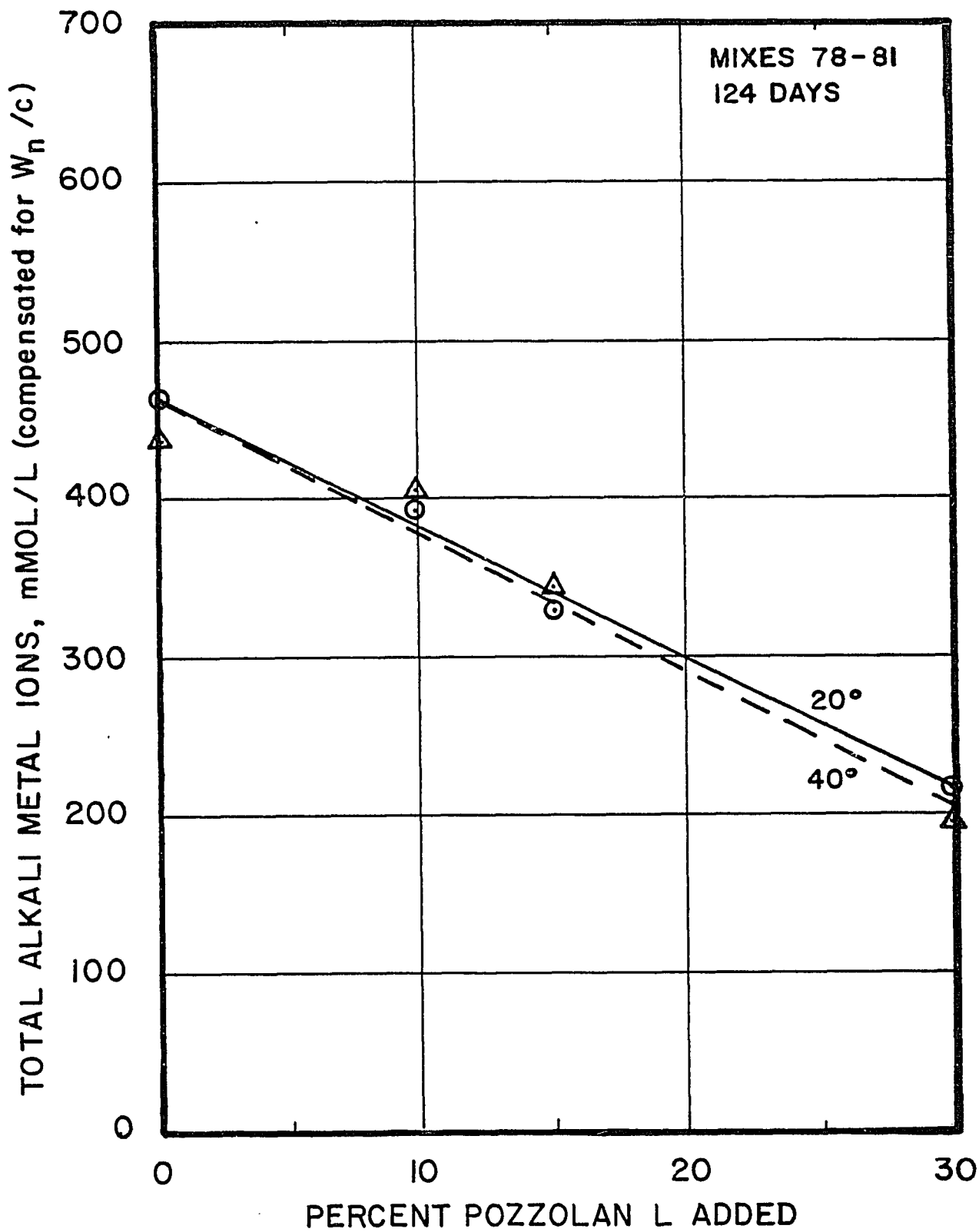


Figure 5.19.10 - Effect of Pozzolan L Addition on Alkali Metal Ion Concentration, Compensated for W_n/c , at 124 Days

5.20 - Mix Series 82 - 91

In the previous series pozzolans were used as additions, with an equivalent absolute volume of C 109 sand being deleted from the batch to maintain constant batch volume. In essence the mix proportions were held constant while the sand gradation was altered by substitution of pozzolanic material. In this series the "pozzolan" was used as a replacement for the portland cement on a percent by weight basis. Even-numbered mixes contain 15 percent replacement and odd-numbered mixes contain 30 percent replacement. This is in closer accord with normal field practice. The properties of the pozzolans used have been described in detail in Section 3 and are briefly identified here as follows:

Pozzolan A - A commercial pozzolan produced from calcined diatomaceous shale.

Pozzolan L - A commercial pozzolan produced from calcined water lain volcanic glass and clays.

Pozzolan Q - A "pozzolan" prepared in the laboratory by ball milling ASTM C 109 Ottawa silica sand (quartz). The ignition loss of this sand is low, and sufficient metal was abraded from the steel grinding media to cause a net increase in weight on ignition due to oxidation of the iron. While abraded metal particles could have been removed by magnetic separation, similar particles are present in all production ground pozzolans.

Pozzolan R - An experimental pozzolan prepared by laboratory grinding crushed rhyolitic pumice. While the other pozzolans, with the exception of pozzolan Q, contain minor amounts of alkali metal compounds, it should be noted that this pozzolan contains 3.05 percent Na_2O and 4.47 percent K_2O , or 5.99 percent Na_2O equivalent.

Pozzolan S - An industrial byproduct consisting mainly of a silica fume with high surface area.

The batch weights for the mixes are listed in Table 5.20.1. Weight ratios, oven-dry/batch, and ignited/batch, are listed in Table 5.20.2. Table 5.20.3 contains a listing of all values of nonevaporable water determined for this series. Nonevaporable water at 0.021 days (30 minutes) was estimated from the data of Copeland and Kantro (511). Extrapolation of the W_n/c values back to one day was done by means of Equation 4.11.7.

The observed concentrations of ions in expressed pore solutions, not corrected for W_n/c , have been listed in Tables 5.20.4 through 5.20.13. Concentrations of alkali metal ions, corrected for W_n/c , have been listed in Tables 5.20.14 through 5.20.23, and are plotted against the logarithm of time in Figures 5.20.1 through 5.20.5.

As a result of the use of pozzolans as cement replacements, the water-cement ratio of the even-numbered mixes, with 15 percent pozzolan replacement, was 0.588, and that of the odd-numbered mixes, with 30 percent pozzolan replacement was 0.724. It is of interest to note

Table 5.20.1

Batch Weights, grams, for Mixes 82 - 91

Materials	Mix 82, Control 15% Pozzolan Q		Mix 84 15% Pozzolan L		Mix 86 15% Pozzolan S	
	Parts by Weight	Batch Weights	Parts by Weight	Batch Weights	Parts by Weight	Batch Weights
Cement, AT-1	0.85	907.2	0.85	907.2	0.85	907.2
Water	0.50	533.7	0.50	533.7	0.50	533.7
Pozzolan	0.15	160.1	0.15	160.1	0.15	160.1
Sand, C 109	2.00	2134.7	2.00	2134.7	2.00	2134.7
Totals	3.50	3735.7	3.5	3735.7	3.50	3735.7

Materials	Mix 88 15% Pozzolan A		Mix 90 15% Pozzolan R	
	Parts by Weight	Batch Weights	Parts by Weight	Batch Weights
Cement, AT-1	0.85	907.2	0.85	907.2
Water	0.50	533.7	0.50	533.7
Pozzolan	0.15	160.1	0.15	160.1
Sand, C 109	2.00	2134.7	2.00	2134.7
Totals	3.50	3735.7	3.50	3735.7

Materials	Mix 83, Control 30% Pozzolan Q		Mix 85 30% Pozzolan L		Mix 87 30% Pozzolan S	
	Parts by Weight	Batch Weights	Parts by Weight	Batch Weights	Parts by Weight	Batch Weights
Cement, AT-1	0.70	737.6	0.70	737.6	0.70	737.6
Water	0.5065	533.7	0.5065	533.7	0.5065	533.7
Pozzolan	0.30	316.1	0.30	316.1	0.30	316.1
Sand, C 109	2.00	2107.5	2.00	2107.5	2.00	2107.5
Totals	3.5065	3694.9	3.5065	3694.9	3.5065	3694.9

	Mix 89 30% Pozzolan A		Mix 91 30% Pozzolan R	
	Parts by Weight	Batch Weights	Parts by Weight	Batch Weights
Cement, AT-1	0.70	737.6	0.70	737.6
Water	0.5065	533.7	0.5065	533.7
Pozzolan	0.30	316.1	0.30	316.1
Sand, C 109	2.00	2107.5	2.00	2107.5
Totals	3.5065	3694.9	3.5065	3694.9

Table 5.20.2

Weight Ratios of Component MaterialsOven-Dry/Batch, Ignited/Batch

Material	W_{od}/W_0	W_{ig}/W_0
Cement, AT-1	0.99809	0.99483
Pozzolan A	0.99591	0.98599
Pozzolan L	0.99807	0.98924
Pozzolan Q	0.99700	1.00019*
Pozzolan R	0.99635	0.97416
Pozzolan S	0.99700	0.98634
Sand, C 109	0.99993	0.99868

* Gain on ignition due to oxidation
of iron from grinding media.

Table 5.20.3

Nonevaporable water, W_n/c , as a Function ofTime at 15 Percent Pozzolan Replacement

Time, Days	Temp. ° C	Mix 82	Mix 84	Mix 86	Mix 88	Mix 90
		20	0.1090	0.1153	0.1247	0.1078
2	40	--	--	--	--	--
	20	0.1338	0.1448	0.1417	0.1371	0.1398
4	40	0.1434	0.1388	0.1381	0.1421	0.1449
	20	0.1541	0.1542	0.1484	0.1517	0.1545
19	40	0.1603	0.1529	0.1392	0.1481	0.1546
	20	--	--	--	--	--
527	40	0.1823	0.1719	0.1538	0.1700	0.1715

Nonevaporable Water, W_n/c as a function ofTime at 30 Percent Pozzolan Replacement

Time, Days	Temp. ° C	Mix 83	Mix 85	Mix 87	Mix 89	Mix 91
		20	0.0937	0.0963	0.1040	0.0941
2	40	--	--	--	--	--
	20	0.1186	0.1228	0.1175	0.1245	0.1208
4	40	0.1270	0.1274	0.1102	0.1268	0.1293
	20	0.1381	0.1311	0.1124	0.1315	0.1398
19	40	0.1430	0.1269	0.1128	0.1231	0.1335
	20	--	--	--	--	--
527	40	0.1577	0.1424	0.1299	0.1359	0.1413

Table 5.20.4

Observed Concentrations of Ions in Expressed Pore Solution (Not Corrected for Bound Water)

Mix 82, Control for Mixes 82, 84, 86, 88, and 90

(Concentrations in millimoles/liter)

Age, Days at 20°C	Si^{4+*}	Al^{3+}	Fe^{3+}	Mg^{++}	Ca^{++}	Na^+	K^+	Σ^{+**}	OH^-	$\text{SO}_4^{=}$	Σ^{-**}	Σ^{+-**}
0.021	3.3	0.3	0.0	0.0	21.	108.	328.	479.	160.	131.	422.	+ 56.
1.	10.0	0.5	0.0	0.0	2.	143.	398.	545.	550.	0.	550.	- 5.
4.	12.0	0.5	0.0	0.0	1.	165.	418.	585.	603.	0.	603.	- 18.
19.	4.9	0.0	0.1	0.0	1.	187.	440.	629.	640.	1.	642.	- 13.

Age, Days at 40°C	Si^{4+*}	Al^{3+}	Fe^{3+}	Mg^{++}	Ca^{++}	Na^+	K^+	Σ^{+**}	OH^-	$\text{SO}_4^{=}$	Σ^{-**}	Σ^{+-**}
4.	8.5	0.6	0.0	0.0	0.	167.	404.	571.	574.	6.	586.	- 15.
19.	3.8	0.0	0.1	0.0	1.	186.	408.	596.	590.	14.	618.	- 22.
527.	4.3	0.8	0.0	0.0	1.	164.	318.	484.	417.	54.	525.	- 41.

* See remarks under Section 4.4.1

** Milliequivalents/liter

n.d. = not determined

Table 5.20.5
Observed Concentrations of Ions in Expressed Pore Solution (Not Corrected for Bound Water)

Mix 84, 15 Percent Pozzolan L

(Concentrations in millimoles/liter)

Age, Days at 20°C							Σ^{+**}	Σ^{-**}	Σ^{+**}
	Si^{4+*}	Al^{3+}	Fe^{3+}	Mg^{++}	Ca^{++}	Na^+			
0.021	3.5	0.3	0.0	0.0	20.	108.	318.	466.	139.
1.	12.3	0.5	0.0	0.0	4.	139.	383.	530.	529.
4.	11.1	0.6	0.0	0.0	0.	166.	409.	575.	587.
19.	3.3	0.0	0.1	0.0	1.	141.	315.	458.	466.

Age, Days at 40°C							Σ^{+**}	Σ^{-**}	Σ^{+**}
	Si^{4+*}	Al^{3+}	Fe^{3+}	Mg^{++}	Ca^{++}	Na^+			
4.	13.0	0.5	0.0	0.0	1.	131.	302.	435.	431.
19.	3.5	0.0	0.2	0.0	1.	121.	235.	358.	339.
527.	6.3	0.8	0.0	0.0	0.	149.	264.	413.	359.

* See remarks under Section 4.4.1

** Milliequivalents/liter

n.d. = not determined

Table 5.20.6

Observed Concentrations of Ions in Expressed Pore Solution (Not Corrected for Bound Water)

Mix 86, 15 Percent Pozzolan S

(Concentrations in millimoles/liter)

Age, Days at 20° C	Concentrations in millimoles/liter						Σ^{+**}	Σ^{-**}	Σ^{+**}
	Si ⁴⁺ *	Al ³⁺	Fe ³⁺	Mg ⁺⁺	Ca ⁺⁺	Na ⁺			
0.021	3.3	0.2	0.0	28.	111.	333.	500.	143.	154.
1.	12.6	0.5	0.0	0.0	2.	412.	572.	580.	582.
4.	14.7	0.2	0.0	0.0	1.	163.	405.	577.	577.
19.	2.5	0.0	0.1	0.0	0.	94.	195.	289.	297.
	Si ⁴⁺ *	Al ³⁺	Fe ³⁺	Mg ⁺⁺	Ca ⁺⁺	Na ⁺	K ⁺	Σ^{+**}	Σ^{-**}
40° C	10.2	0.0	0.0	0.0	1.	95.	205.	302.	255.
4.	1.6	0.0	0.0	0.0	0.	72.	133.	205.	143.
19.	3.6	0.3	0.0	0.0	0.0	94.	168.	262.	192.
527.									

* See remarks under Section 4.4.1

** Milliequivalents/liter

n.d. = not determined

Table 5.20.7
 Observer Concentrations of Ions in Expressed Fore Solution (Not Corrected for Bound Water)

Mix 88, 15 Percent Pozzolan A								
(Concentrations in millimoles/liter)								
Age,	Days at 20° C	Si ⁴⁺ *	Al ³⁺	Fe ³⁺	Mg ⁺⁺	Ca ⁺⁺	Na ⁺	K ⁺
0.021	1.8	0.4	0.0	0.0	22.	108.	322.	474.
1.	12.3	0.3	0.0	0.0	1.	143.	394.	539.
4.	13.5	0.2	0.0	0.0	1.	171.	422.	595.
19.	0.8	0.0	0.1	0.0	1.	150.	344.	496.
Age,	Days at 40° C	Si ⁴⁺ *	Al ³⁺	Fe ³⁺	Mg ⁺⁺	Ca ⁺⁺	Na ⁺	K ⁺
4.	12.7	0.2	0.0	0.0	0.	143.	327.	470.
19.	1.8	0.0	0.0	0.0	0.	119.	231.	350.
527.	4.9	0.5	0.0	0.0	0.	138.	244.	382.

* See remarks under Section 4.4.1

** Milliequivalents/liter
 n.d. = not determined

Table 5.20.8

Observed Concentrations of Ions in Expressed Pore Solution (Not Corrected for Bound Water)Mix 90, 15 Percent Pozzolan R

(Concentrations in millimoles/liter)

Age, Days at 20°C	Si^{4+*}	Al^{3+}	Fe^{3+}	Mg^{++}	Ca^{++}	Na^+	K^+	$\Sigma +**$	OH^-	$\text{SO}_4^=$	$\Sigma -**$	$\Sigma +-*$
0.021	2.2	0.4	0.0	0.0	18.	110.	325.	471.	153.	168.	489.	- 18.
1.	4.1	0.2	0.0	0.0	2.	142.	387.	533.	536.	1.	538.	- 5.
4.	13.8	0.2	0.1	0.0	1.	178.	427.	607.	622.	0.	622.	- 15.
19.	3.1	0.0	0.1	0.0	1.	190.	433.	625.	632.	0.	632.	- 7.

Age, Days at 40°C	Si^{4+*}	Al^{3+}	Fe^{3+}	Mg^{++}	Ca^{++}	Na^+	K^+	$\Sigma +**$	OH^-	$\text{SO}_4^=$	$\Sigma -**$	$\Sigma +-*$
4.	14.9	0.1	0.1	0.0	1.	182.	413.	597.	595.	7.	609.	- 12.
19.	2.5	0.0	0.1	0.0	0.	184.	341.	525.	489.	20.	529.	- 4.
527.	3.0	0.3	0.0	0.0	1.	229.	343.	574.	444.	72.	588.	- 14.

* See remarks under Section 4.4.1

** Milliequivalents/liter

n.d. = not determined

Table 5.20.9
 Observed Concentrations of Ions in Expressed Pore Solution (Not Corrected for Bound Water)
Mix 83, Control for Mixes 83, 85, 87, 89, and 91
 (Concentrations in millimoles/liter)

Age, Days at 20° C	Si ⁴⁺ * C	Al ³⁺ C	Fe ³⁺ C	Mg ⁺⁺ C	Ca ⁺⁺ C	Na ⁺ C	K ⁺ C	Σ^{+**}	OH ⁻ C	SO ₄ ⁼ C	Σ^{-**}	Σ^{+-**}
0.021	4.0	0.3	0.0	0.0	21.	87.	264.	393.	133.	96.	325.	+ 68.
1.	11.1	0.5	0.0	0.0	2.	116.	314.	434.	437.	0.	437.	- 3.
4.	12.1	0.4	0.0	0.0	2.	138.	329.	471.	484.	0.	484.	- 13.
19.	4.2	0.0	0.1	0.0	0.	149.	324.	473.	485.	0.	485.	- 12.
Age, Days at 40° C	Si ⁴⁺ * C	Al ³⁺ C	Fe ³⁺ C	Mg ⁺⁺ C	Ca ⁺⁺ C	Na ⁺ C	K ⁺ C	Σ^{+**}	OH ⁻ C	SO ₄ ⁼ C	Σ^{-**}	Σ^{+-**}
4.	9.9	0.5	0.0	0.0	0.	145.	335.	480.	481.	3.	487.	- 7.
19.	4.1	0.0	0.1	0.0	1.	152.	308.	462.	463.	8.	479.	- 17.
527.	4.3	0.8	0.0	0.0	1.	121.	226.	349.	300.	41.	382.	- 33.

* See remark: under Section 4.4.1

** Milliequivalents/liter

n.d. = not determined

Table 5.20.10
 Observed Concentrations of Ions in Expressed Pore Solution (Not Corrected for Bound Water)
Mix 85, 30 Percent Pozzolan L
 (Concentrations in millimoles/liter)

Age, Days at 20° C	Si ⁴⁺ *	Al ³⁺	Fe ³⁺	Mg ⁺⁺	Ca ⁺⁺	Na ⁺	K ⁺	Σ^{+**}	OH ⁻	$\overline{SO_4^=}$	Σ^{-**}	Σ^{+-**}	
0.021	2.6	0.3	0.0	0.0	0.0	21.	84.	256.	382.	114	120.	354.	+ 28.
1.	12.2	0.4	0.0	0.0	0.0	1.	110.	291.	403.	407.	0.	407.	- 4.
4.	11.6	0.5	0.0	0.0	0.0	0.	133.	302.	435.	444.	0.	444.	- 9.
19.	2.8	0.0	0.1	0.0	0.0	0.	93.	179.	272.	272.	1.	274.	- 2.
Age, Days at 40° C	Si ⁴⁺ *	Al ³⁺	Fe ³⁺	Mg ⁺⁺	Ca ⁺⁺	Na ⁺	K ⁺	Σ^{+**}	OH ⁻	$\overline{SO_4^=}$	Σ^{-**}	Σ^{+-**}	
4.	6.9	0.8	0.0	0.0	0.0	0.	86.	171.	257.	254.	4.	262.	- 5.
19.	4.6	0.0	0.1	0.0	0.0	0.	74.	125.	199.	187.	9.	205.	- 6.
527.	3.4	0.8	0.0	0.0	0.0	0.	80.	120.	200.	182.	17.	216.	- 16.

* See remarks under Section 4.4.1

** Milliequivalents/liter

n.d. = not determined

Table 5.20.11

Observed Concentrations of Ions in Expressed Pore Solution (Not Corrected for Bound Water)Mix 87, 30 Percent Pozzolan S

(Concentrations in millimoles/liter)

Age, Days at 20°C	Si^{4+*}	Al^{3+}	Fe^{3+}	Mg^{++}	Ca^{++}	Na^+	K^+	$\Sigma +**$	OH^-	$\text{SO}_4^{=}$	$\Sigma -**$	$\Sigma +--**$
0.021	2.6	0.3	0.0	0.0	22.	93.	271.	408.	118.	130.	378.	+ 30.
1.	7.9	0.4	0.0	0.0	2.	134.	333.	471.	475.	0.	475.	- 4.
4.	11.6	0.1	0.0	0.0	1.	123.	294.	419.	422.	0.	422.	- 3.
19.	2.8	0.0	0.1	0.0	0.	48.	87.	135.	110.	11.	132.	+ 3.

Age, Days at 40°C	Si^{4+*}	Al^{3+}	Fe^{3+}	Mg^{++}	Ca^{++}	Na^+	K^+	$\Sigma +**$	OH^-	$\text{SO}_4^{=}$	$\Sigma -**$	$\Sigma +--**$
4.	8.2	0.0	0.0	0.0	0.	54.	96.	150.	99.	25.	149.	+ 1.
19.	0.6	0.0	0.0	0.0	4.	26.	33.	67.	2.	29.	60.	+ 7.
527.	2.0	0.0	0.4	0.8	0.	46.	56.	102.	19.	49.	117.	- 15.

* See remarks under Section 4.4.1

** Milliequivalents/liter

n.d. = not determined

Table 5.20.12
 Observed Concentrations of Ions in Expressed Pore Solution (Not Corrected for Bound Water)

Mix 89, 30 Percent Pozzolan A

(Concentration in millimoles/liter)

Age, Days at 20° C	Si ⁴⁺ *	Al ³⁺	Fe ³⁺	Mg ⁺⁺	Ca ⁺⁺	Na ⁺	K ⁺	Σ^{+**}	OH ⁻	SO ₄ ⁼	Σ^{-**}	Σ^{+-**}
0.021	2.6	0.4	0.0	0.0	21.	89.	261.	392.	124.	124.	372.	+ 20.
1.	10.2	0.2	0.0	0.0	2.	120.	307.	431.	434.	2.	438.	- 7.
4.	13.5	0.0	0.0	0.0	1.	148.	327.	477.	481.	0.	481.	- 4.
19.	1.3	0.0	0.1	0.0	1.	101.	200.	303.	296.	0.	296.	+ 7.
Age, Days at 40° C	Si ⁴⁺ *	Al ³⁺	Fe ³⁺	Mg ⁺⁺	Ca ⁺⁺	Na ⁺	K ⁺	Σ^{+**}	OH ⁻	SO ₄ ⁼	Σ^{-**}	Σ^{+-**}
4.	7.1	0.2	0.0	0.0	0.	98.	198.	296.	289.	9.	301.	- 5.
19.	0.8	0.0	0.0	0.0	0.	81.	136.	217.	188.	14.	216.	+ 1.
527.	4.3	0.8	0.0	0.0	0.	88.	129.	217.	164.	38.	240.	- 23.

* See remarks under Section 4.4.1

** Milliequivalents/liter

n.d. = not determined

Table 5.20.13
 Observed Concentrations of Ions in Expressed Pore Solution (Not Corrected for Bound Water)
Mix 91, 30 Percent Pozzolan R
 (Concentrations in millimoles/liter)

Age, Days at 20° C	Si ⁴⁺ *	Al ³⁺	Fe ³⁺	Mg ⁺⁺	Ca ⁺⁺	Na ⁺	K ⁺	Σ^{+**}	SO ₄ ⁼	Σ^{-**}	Σ^{+-**}
0.021	2.8	0.4	0.0	0.0	21.	93.	260.	395.	143.	128.	399.
1.	7.8	0.2	0.0	0.0	2.	118.	3001.	423.	426.	2.	430.
4.	14.1	0.0	0.1	0.0	1.	150.	328.	480.	491.	0.	491.
19.	0.0	0.0	0.1	0.0	1.	166.	332.	500.	507.	0.	507.
Age, Days at 40° C	Si ⁴⁺ *	Al ³⁺	Fe ³⁺	Mg ⁺⁺	Ca ⁺⁺	Na ⁺	K ⁺	Σ^{+**}	OH ⁻	SO ₄ ⁼	Σ^{-**}
4.	12.8	0.0	0.0	0.0	2.	162.	326.	492.	492.	3.	498.
19.	0.8	0.0	0.0	0.0	0.	153.	245.	398.	351.	25.	401.
527.	2.2	0.8	0.0	0.0	0.	208.	287.	495.	250.	79.	408.
											+ 87.

* See Remarks under Section 4.4.1

** Milliequivalents/liter

n.d. = not determined

Table 5.20.14
Concentrations of Alkali Metal Cations in Expressed Pore Solution (Corrected for Bound Water)

Age, Days at 20° C	w_n/c	bwk	Cations Found	Cation Concentration Corrected for w_n/c			$*K^+ / *Na^+$
				ΣM^+	$*K^+$	$\Delta *K^+$	
0.021	0.002	0.996	Na ⁺ K ⁺ ΣM^+	108	108	-	3.037
1.	0.109	0.815	143	398	541	-	2.783
4.	0.134	0.773	165	418	583	-	2.533
19.	0.154	0.738	187	440	627	-	2.353
Mix 82, Control for Mixes 82, 84, 86, 88, and 90							
Age, Days at 40° C	w_n/c	bwk	Cations Found	Cation Concentration Corrected for w_n/c			$*K^+ / *Na^+$
				ΣM^+	$*K^+$	$\Delta *K^+$	
4.	0.143	0.756	Na ⁺ K ⁺ ΣM^+	167	404	571	434
19.	0.160	0.728	186	408	594	-	441
527.	0.182	0.690	164	318	482	11.3	450
						-	463
						-	435

Table 5.20.15

Concentrations of Alkali Metal Cations in Expressed Pore Solution (Corrected for Bound Water)

Mix 84, 15 Percent Pozzolan L

(Concentrations in millimoles/liter)

Age, Days at 20° C	W _{n/c}	bwk	Cations Found			Cation Concentration Corrected for W _{n/c}						*K ⁺ / *Na ⁺
			Na ⁺	K ⁺	Σ M ⁺	*Na ⁺	Δ*Na ⁺	*K ⁺	Δ*K ⁺	Σ*M ⁺	Δ*M ⁺	
0.021	0.002	0.996	108	318	426	108	0	317	-10	424	-10	2.944
1.	0.115	0.804	139	383	522	112	-5	308	-16	420	-21	2.755
4.	0.134	0.773	166	409	575	128	+1	316	-7	444	-6	2.464
19.	0.154	0.738	141	315	456	104	-34	232	-92	337	-126	2.234

Age, Days at 40° C	W _{n/c}	bwk	Cations Found			Cation Concentration Corrected for W _{n/c}						*K ⁺ / *Na ⁺
			Na ⁺	K ⁺	Σ M ⁺	*Na ⁺	Δ*Na ⁺	*K ⁺	Δ*K ⁺	Σ*M ⁺	Δ*M ⁺	
4.	0.139	0.764	131	302	433	100	-26	231	-75	331	-101	2.305
19.	0.153	0.740	121	235	356	90	-46	174	-123	263	-169	1.942
527	0.172	0.708	149	264	313	105	-8	187	-33	292	-40	1.772

Table 5.20.16
Concentrations of Alkali Metal Cations in Expresssed Pore Solution (Corrected for Bound Water)

Mix 86, 15 Percent Pozzolan S

(Concentrations in millimoles/liter)

Age, Days at 20° C	$\frac{W_n}{c}$	bwk	Cations Found			Cation Concentration Corrected for W_n/c			$\frac{*K^+}{*Na^+}$
			Na^+	K^+	ΣM^+	$*Na^+$	$\Delta *Na^+$	$*K^+$	
0.021	0.002	0.996	111	333	444	111	+3	332	+5
1.	0.125	0.788	156	412	568	123	+6	325	0
4.	0.142	0.759	163	405	568	124	-4	307	-15
19.	0.148	0.748	94	195	289	70	-68	146	-179

Age, Days at 140° C	$\frac{W_n}{c}$	bwk	Cations Found			Cation Concentration Corrected for W_n/c			$\frac{*K^+}{*Na^+}$
			Na^+	K^+	ΣM^+	$*Na^+$	$\Delta *Na^+$	$*K^+$	
4.	0.138	0.765	95	205	300	73	-54	157	-149
19.	0.139	0.763	72	133	205	55	-80	102	-195
527.	0.154	0.739	94	168	262	69	-44	124	-95

Table 5.20.17
 Concentrations of Alkali Metal Cations in Expressed Pore Solution (Corrected for Bound Water)
 Mix 88, 15 Percent Pozzolan A
 (Concentrations in millimoles/liter)

Age, Days at 20° C	W_n/c	bwk	Cations Found			Cation Concentration Corrected for W_n/c			$*K^+/\Delta *Na^+$
			Na^+	K^+	ΣM^+	$*Na^+$	$\Delta *Na^+$	$*K^+$	
0.021	0.002	0.996	108	322	430	108	0	321	-6
1.	0.108	0.817	143	394	537	117	0	322	-2
4.	0.137	0.767	171	422	593	131	+4	324	+1
19.	0.152	0.742	150	344	494	111	-27	255	-69
								367	-96
									2.293

Age, Days at 40° C	W_n/c	bwk	Cations Found			Cation Concentration Corrected for W_n/c			$*K^+/\Delta *Na^+$
			Na^+	K^+	ΣM^+	$*Na^+$	$\Delta *Na^+$	$*K^+$	
4.	0.142	0.758	143	327	470	108	-18	248	-58
19.	0.148	0.748	119	231	350	89	-46	173	-124
527.	0.170	0.711	138	244	382	98	-15	173	-46
								272	-61
									1.768

Table 5.20.18
 Concentrations of Alkali Metal Cations in Expressed Pore Solution (Corrected for Bound Water)
Mix 90, 15 Percent Pozzolan R
 (Concentrations in millimoles/liter)

Age, Days at 20° C	w_n/c	bwk	Cations Found			Cation Concentration Corrected for w_n/c			$*K^+ / *Na$
			$*Na^+$	K^+	ΣM^+	$*Na^+$	$\Delta *Na^+$	$*K^+$	
0.021	0.002	0.996	110	325	435	110	+2	324	-3
1.	0.104	0.823	142	387	529	117	0	318	-6
4.	0.140	0.762	178	427	605	136	+8	326	+3
19.	0.154	0.737	190	433	623	140	+2	319	-5
									-3
									2.279

Age, Days at 40° C	w_n/c	bwk	Cations Found			Cation Concentration Corrected for w_n/c			$*K^+ / *Na$
			$*Na^+$	K^+	ΣM^+	$*Na^+$	$\Delta *Na^+$	$*K^+$	
4.	0.145	0.754	182	414	596	137	+11	312	+7
19.	0.155	0.737	184	341	525	136	0	251	-45
527.	0.172	0.708	229	343	572	162	+49	243	+24
									+73
									1.498

Table 5.20.19
 Concentrations of Alkali Metal Cations in Expressed Pore Solution (Corrected for Bound Water)

		Mix 83, Control for Mixes 83, 85, 87, 89, and 91							
		(Concentrations in millimoles/liter)							
Age, Days at 20° C	w_n/c	bwk	Cations Found		Cation Concentration Corrected for w_n/c		$*K^+ / *Na^+$		
			Na^+	K^+	ΣM^+	$*Na^+$	$\Delta *Na^+$	$*K^+$	
0.021	0.002	0.997	87	264	351	87	-	263	
1.	0.094	0.871	116	314	430	101	-	273	
4.	0.119	0.836	138	329	467	115	-	275	
19.	0.138	0.809	149	324	473	121	-	262	
								383	
								-	
Age, Days at 40° C	w_n/c	bwk	Cations Found		Cation Concentration Corrected for w_n/c		$*K^+ / *Na^+$		
			Na^+	K^+	ΣM^+	$*Na^+$	$\Delta *Na^+$	$*K^+$	
4.	0.127	0.824	145	335	480	120	-	276	
19.	0.143	0.802	152	308	460	122	-	247	
527.	0.158	0.782	121	226	347	95	-	177	
								396	
								369	
								271	
								-	

Table 5.20.20
 Concentrations of Alkali Metal Cations in Expresssed Pore Solution (Corrected for Bound Water)
 Mix 85, 30 Percent Pozzolan L
 (Concentrations in millimoles/liter)

Age, Days at 20° C	W _{n/c}	b _{wk}	Cations Found			Cation Concentration Corrected for W _{n/c}			*K ⁺ / *Na ⁺
			Na ⁺	K ⁺	ΣM^+	*Na ⁺	*K ⁺	$\Delta *K^+$	
0.021	0.002	0.997	84	256	340	84	-3	255	-8
1.	0.096	0.867	110	291	401	95	-6	252	-21
4.	0.123	0.830	133	302	435	110	-5	251	-24
19.	0.131	0.819	93	179	272	76	-44	147	-116
								223	-160
									1.925

Age, Days at 40° C	W _{n/c}	b _{wk}	Cations Found			Cation Concentration Corrected for W _{n/c}			*K ⁺ / *Na ⁺
			Na ⁺	K ⁺	ΣM^+	*Na ⁺	*K ⁺	$\Delta *K^+$	
4.	0.127	0.824	86	171	257	71	-49	141	-135
19.	0.127	0.825	74	125	199	61	-61	103	-144
527.	0.142	0.803	80	120	200	64	-30	96	-80
								161	-111
									1.500

Table 5.20.21
 Concentration of Alkali Metal Cations in Expressed Pore Solution (Corrected for Bound Water)
Mix 87, 30 Percent Pozzolan S
 (concentrations in millimoles/liter)

Age, Days at 20° C	W_n/c	bvk	Cations Found			Cation Concentration Corrected for W_n/c			$*K^+ / *Na^+$
			Na ⁺	K ⁺	ΣM^+	*Na ⁺	Δ^*Na^+	*K ⁺	
0.021	0.002	0.997	93	271	364	93	+6	270	+7
1.	0.104	0.856	134	333	467	115	+14	285	+12
4.	0.118	0.838	123	294	417	103	-12	246	-29
19.	0.112	0.845	48	87	138	41	-80	73	-189
			Na ⁺	K ⁺	ΣM^+	*Na ⁺	Δ^*Na^+	*K ⁺	Δ^*M^+

Age, Days at 40° C	W_n/c	bvk	Cations Found			Cation Concentration Corrected for W_n/c			$*K^+ / *Na^+$
			Na ⁺	K ⁺	ΣM^+	*Na ⁺	Δ^*Na^+	*K ⁺	
4.	0.110	0.848	54	96	150	46	-74	81	-195
19.	0.113	0.844	26	33	59	22	-100	28	-219
527.	0.130	0.820	46	56	102	38	-57	46	-131
			Na ⁺	K ⁺	ΣM^+	*Na ⁺	Δ^*Na^+	*K ⁺	Δ^*M^+

Table 5.20.22

Concentrations of Alkali Metal Cations in Expressed Pore Solution (Corrected for Bound Water)

Mix 89, 30 Percent Pozzolan A

(Concentrations in millimoles/liter)

Age, Days at 20° C	W _n /c	bwk	Cations Found			Cation Concentration Corrected for W _n /c	*K ⁺ / *Na ⁺
			Na ⁺	K ⁺	Σ M ⁺		
0.021	0.002	0.997	89	261	350	89	+2
1.	0.094	0.870	120	307	427	104	+3
4.	0.124	0.828	148	327	475	123	+7
19.	0.132	0.818	101	200	301	83	-38
						164	-99
						246	-136
						176	-95
Age, Days at 40° C	W _n /c	bwk	Cations Found			Cation Concentration Corrected for W _n /c	*K ⁺ / *Na ⁺
			Na ⁺	K ⁺	Σ M ⁺		
4.	0.127	0.825	98	198	296	81	-39
19.	0.123	0.830	81	136	217	67	-55
527.	0.136	0.812	88	129	217	71	-23
						105	-72
						244	-152
						180	-189
						176	-95

Table 5.20.23
 Concentrations of Alkali Metal Cations in Expresssed Pore Solution (Corrected for Bound Water)
Mix 91, 30 Percent Pozzolan R
 (Concentrations in millimoles/liter)

Age, Days at 20° C	W_n/c	bwk	Cations Found			Cation Concentration Corrected for W_n/c			$*K^+ / *Na^+$		
			Na ⁺	K ⁺	ΣM^+	*Na ⁺	$\Delta *Na^+$	*K ⁺	$\Delta *K^+$	$\Sigma *M^+$	$\Delta *M^+$
0.021	0.002	0.997	93	260	353	93	+6	259	-4	352	+2
1.	0.090	0.875	118	301	419	103	+2	264	-10	367	-7
4.	0.121	0.833	150	328	478	125	+10	273	-2	398	+8
19.	0.140	0.807	166	332	498	124	+13	268	+6	402	+19
Age, Days at 40° C	W_n/c	bwk	Cations Found			Cation Concentration Corrected for W_n/c			$*K^+ / *Na^+$		
			Na ⁺	K ⁺	ΣM^+	*Na ⁺	$\Delta *Na^+$	*K ⁺	$\Delta *K^+$	$\Sigma *M^+$	$\Delta *M^+$
4.	0.129	0.821	162	326	488	133	+14	268	-8	401	+5
19.	0.134	0.816	153	245	398	125	+3	200	-47	325	-45
527.	0.142	0.805	208	287	495	167	+73	231	+54	398	+127

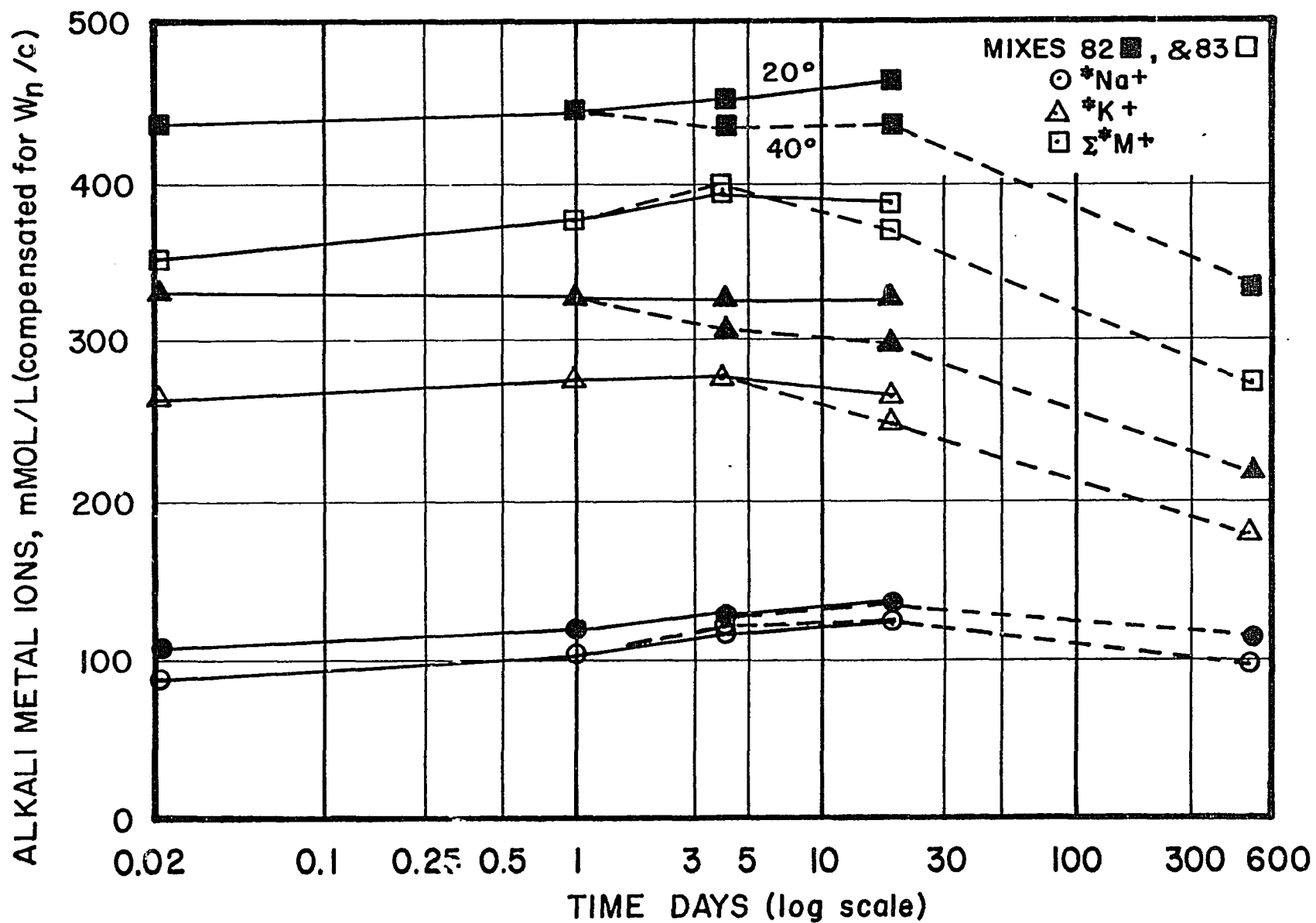


Figure 5.20.1 - Alkali Metal Ion Concentration (Compensated for W/c) vs. Time.

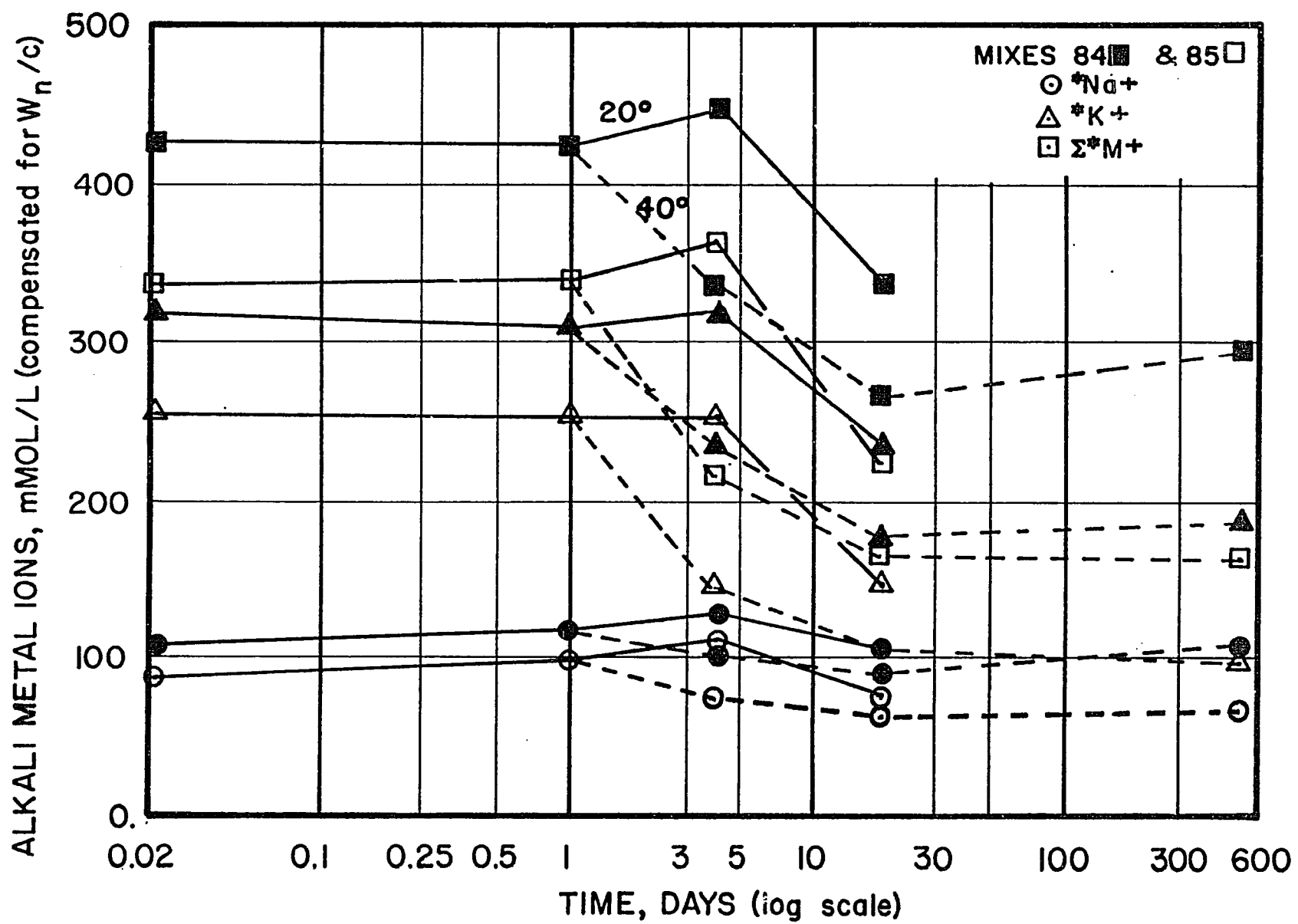


Figure 5.20.2 - Alkali Metal Ion Concentration (Compensated for W_n/c) vs. Time.

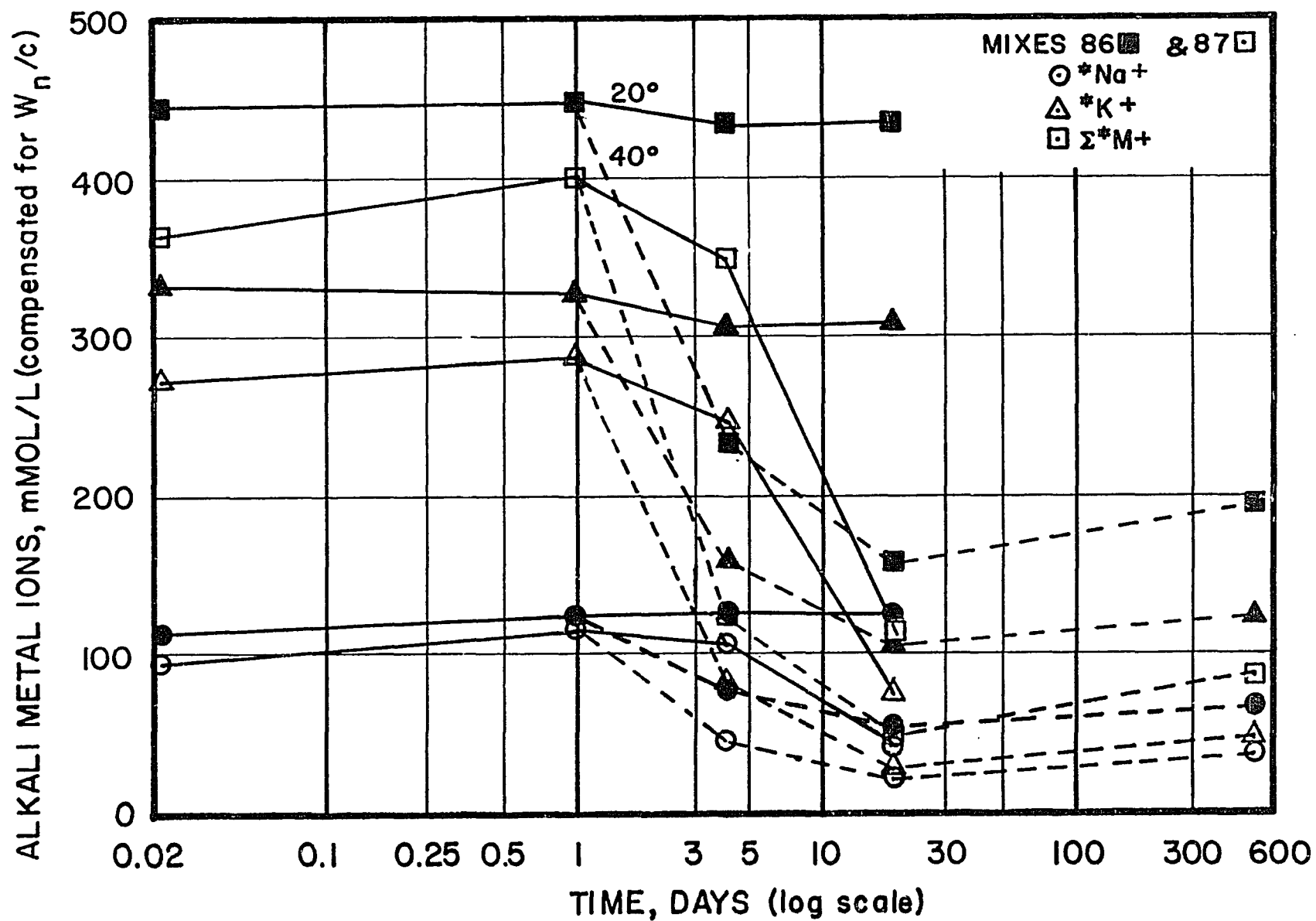


Figure 5.20.3 - Alkali Metal Ion Concentration (Compensated for W_n/c) vs. Time.

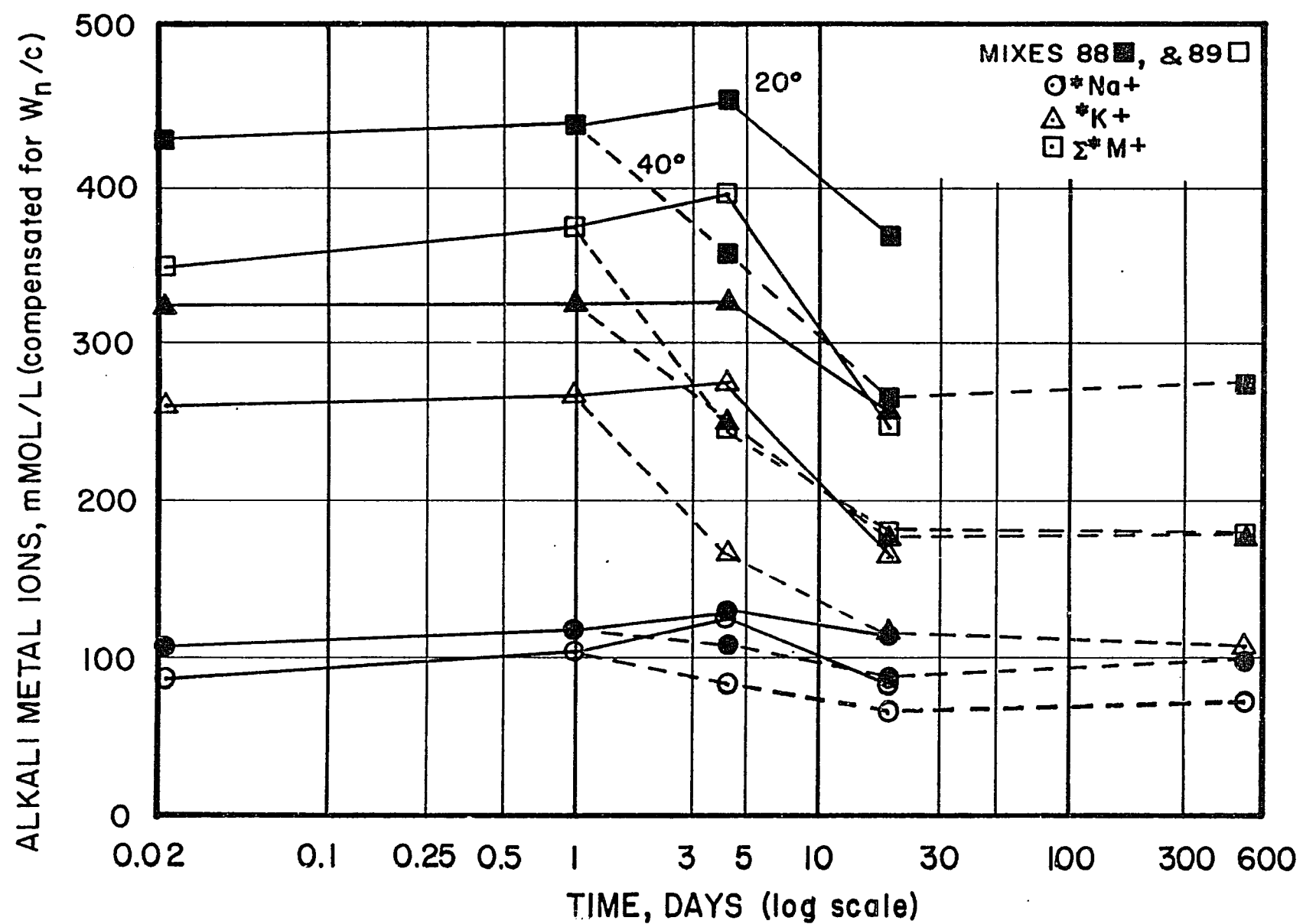


Figure 5.20.4 - Alkali Metal Ion Concentration (Compensated for $\frac{W}{n} / c$) vs. Time.

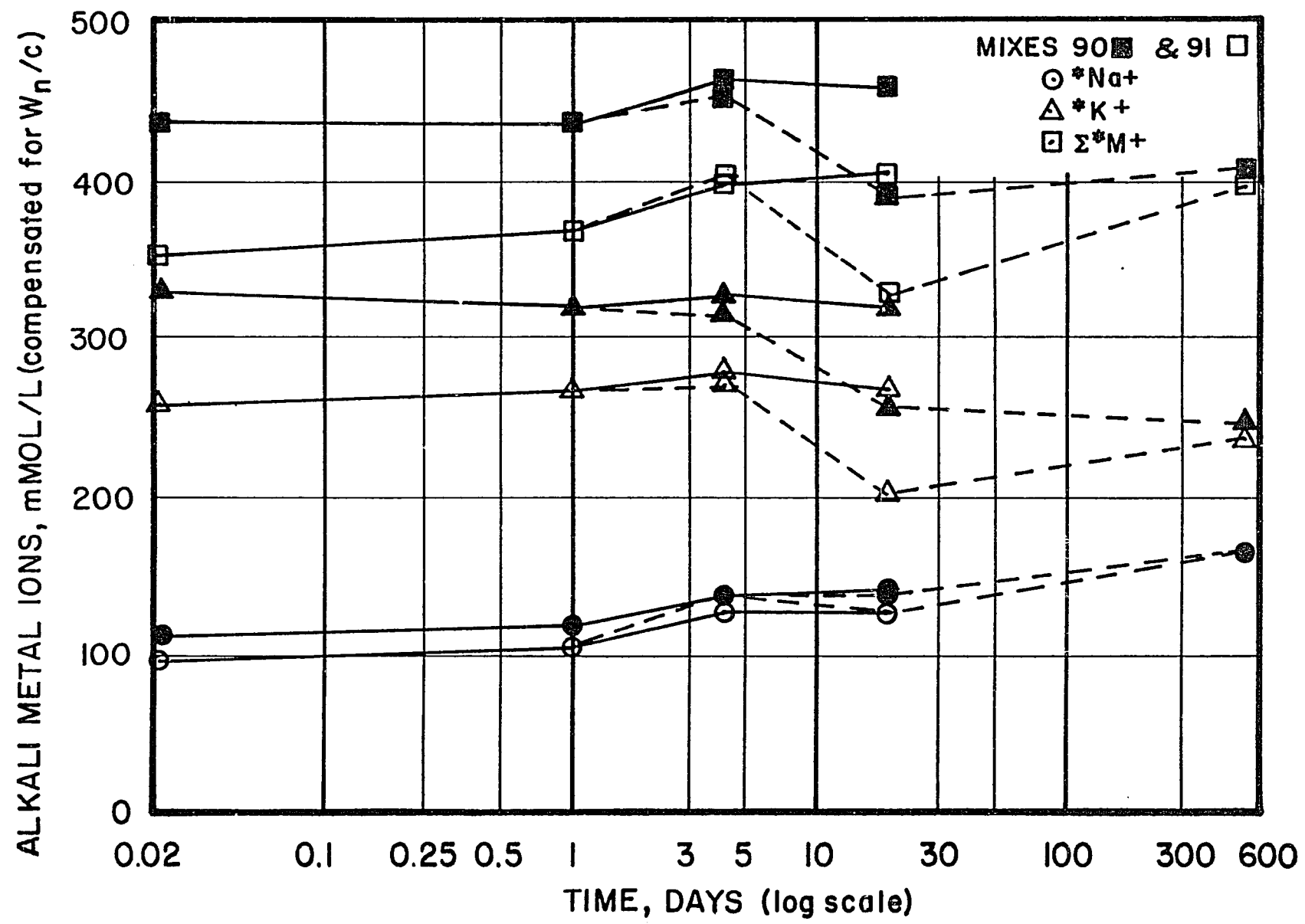


Figure 5.20.5 - Alkali Metal Ion Concentration (Compensated for $\frac{W}{c}$) vs. Time.

that the total concentrations of alkali metal ions found in the expressed pore solutions at 30 minutes, when compensated for differences in water-cement ratio, are nearly identical to the concentrations found in the control mixes for series 5.15 and 5.19*.

Previous experience has suggested that the chemical properties of pore solutions expressed from mixes stored at either 20° or 40° C tend to approach common values as time increases. For this reason, only specimens representing mixes that had been stored at 40°C were expressed and tested at 527 days.

The results of the determinations for chemically bound water were not surprising, in that pozzolan S, nearly pure SiO₂ with high surface area, exhibited the smallest value of W_n/c, while pozzolan Q, consisting of finely ground crystalline quartz, exhibited the largest value of W_n/c. As will be demonstrated, this difference results from the reduced contents of Ca(OH)₂ in the mixes containing the most active pozzolans. As discussed in Section 5.19, this result seems to imply that the reaction products formed from active siliceous pozzolans and Ca(OH)₂ contains a C-S-H product that does not incorporate all of the water available that would otherwise have formed part of the Ca(OH)₂.

Reference to Figures 5.20.1 through 5.20.5 suggests that, as in all previous series, the concentrations of alkali metal ions in the expressed pore solutions, compensated for W_n/c, tend to remain nearly

*Using data for the total alkali metal ion concentration at 30 minutes for mixes 59 and 78 compensated for W_n/c, the mean value is: (497+510)/2=504 mMol/L. For Mix 82: ⁿ(0.588/0.50)x434=510, for Mix 83: (0.724/0.50)x350=507. The mean of these two values is 508 which, for practical purposes is identical to 504 mMol/L.

constant during the first 24 hours after the initiation of mixing. Depending on the activity of the pozzolan, the concentrations of alkali metal ions in solution, compensated for W_n/c , tend to fall to a level approximating that observed at 527 days within the first 4 to 19 days for mixes stored at 40°C. Two significant anomalies should be noted. The alkali concentrations of mixes containing pozzolan Q fell more than one would have anticipated from previous experience for control mixes. This is probably owing to the alkali reactivity of the finely ground quartz that constitutes pozzolan Q. The other anomaly appears in Figure 5.20.5. As previously noted pozzolan R has a high alkali metal oxide content, nearly 6 percent Na_2O equivalent. In contrast to the behavior of the other pozzolans, this material did not reduce the concentration of alkali metal ions in pore solution significantly. Three explanations are possible: the alkalies are being released to solution from the rhyolite glass as a result of chemical attack; the alkalies in the glass are being removed by local reaction directly to reaction products leaving the alkalies in the pore solution unaffected; or some of the alkalies are being recycled to pore solution from previously formed reaction products.

As an aside, it is of interest to note that lightweight aggregates produced from raw materials similar to those used for this pozzolan fall well within the reactive, or deleterious, range when tested by the chemical test for alkali-silica reactivity (ASTM Designation C 289), and that they are only marginally effective in reducing expansion resulting from alkali-silica reaction when finely ground and added as pozzolans. Pozzolans prepared from these materials are,

however, effective cement replacements, allowing approximately 30 percent reductions in cement content without affecting 28 day compressive strength.

CHAPTER 6

THE ROLE OF DIFFUSION IN ALKALI-SILICA REACTIONS

6.1 - Alkali Diffusion in Mortars and Cement Paste

Portland cement paste is a relatively porous solid and a number of ions can diffuse through it. "The factors which affect diffusion of ions through a solid include the following: chemical composition, electrical potential, chemical reaction, porosity (including texture), solution concentration, pressure and temperature. A cementitious composite typically behaves as an electronegative semi-permeable membrane, the permeability depending upon the initial preparation parameters; but the electronegative character suggests that anions should diffuse faster than cations" (601, p. 363). Roy (601, p. 363) reports diffusion coefficients for sodium chloride in a 0.45 w/c paste, cured 7 days, to be $D_{Na} = 1.35 \times 10^{-8} \text{ cm}^2/\text{sec}$ and $D_{Cl} = 8.26 \times 10^{-6} \text{ cm}^2/\text{sec}$.

Vivian (602) demonstrated the effect of diffusion of alkalis in mortar prisms. He prepared four kinds of mortar using a nonreactive quartz sand, a reactive sand consisting of 90 percent nonreactive quartz and 10 percent reactive siliceous magnesian limestone, low alkali (0.12 percent Na_2O equivalent), and high alkali (0.86 percent Na_2O equivalent) portland cement. Mortar prisms, similar to those described in Section 4.14.2, were cast using various combinations of these mortars in segments. Vivian found that the rate and magnitude of the expansion of these composite specimens depended on

the proximity of the reactive aggregate to the high alkali cement.

Expansion was more rapid and greater when the diffusion path between the reactive aggregate and the high alkali cement was shortest. Although the experiment was not designed to yield data for determination of diffusion coefficients, it clearly demonstrated the ability of alkali hydroxides to diffuse through the paste phase of the mortars to reactive aggregate particles.

6.2 - Alkali Diffusion in Reactive Aggregate

Review of the published work on the distribution of ions in reacting siliceous aggregate reveals a number of studies (603, 604, 605, 606), but the results tend to be qualitative rather than quantitative.

Diamond (607), using Energy Dispersive X-Ray Analysis (EDXA), has conducted a series of experiments that do provide quantitative data.

A series of opal cylinders were prepared from an apparently homogeneous mass of opal. These cylinders were machined to a diameter of 10.0 mm and were approximately 20 mm in length. The cylinders were subjected to alkali attack at ambient laboratory temperature (20-25° C) for various time periods before being fractured for EDXA. Figure 6.1 illustrates the experimental arrangements for alkali treatment of a typical specimen.

Cylinders for the Series K experiments were packed in a matrix consisting of 6 grams of quartz mortar sand, to which was added 3.0 ml of 1.0 normal KOH solution. Cylinders for the series KL experiments were prepared for storage similarly, but 1.5 grams of powdered

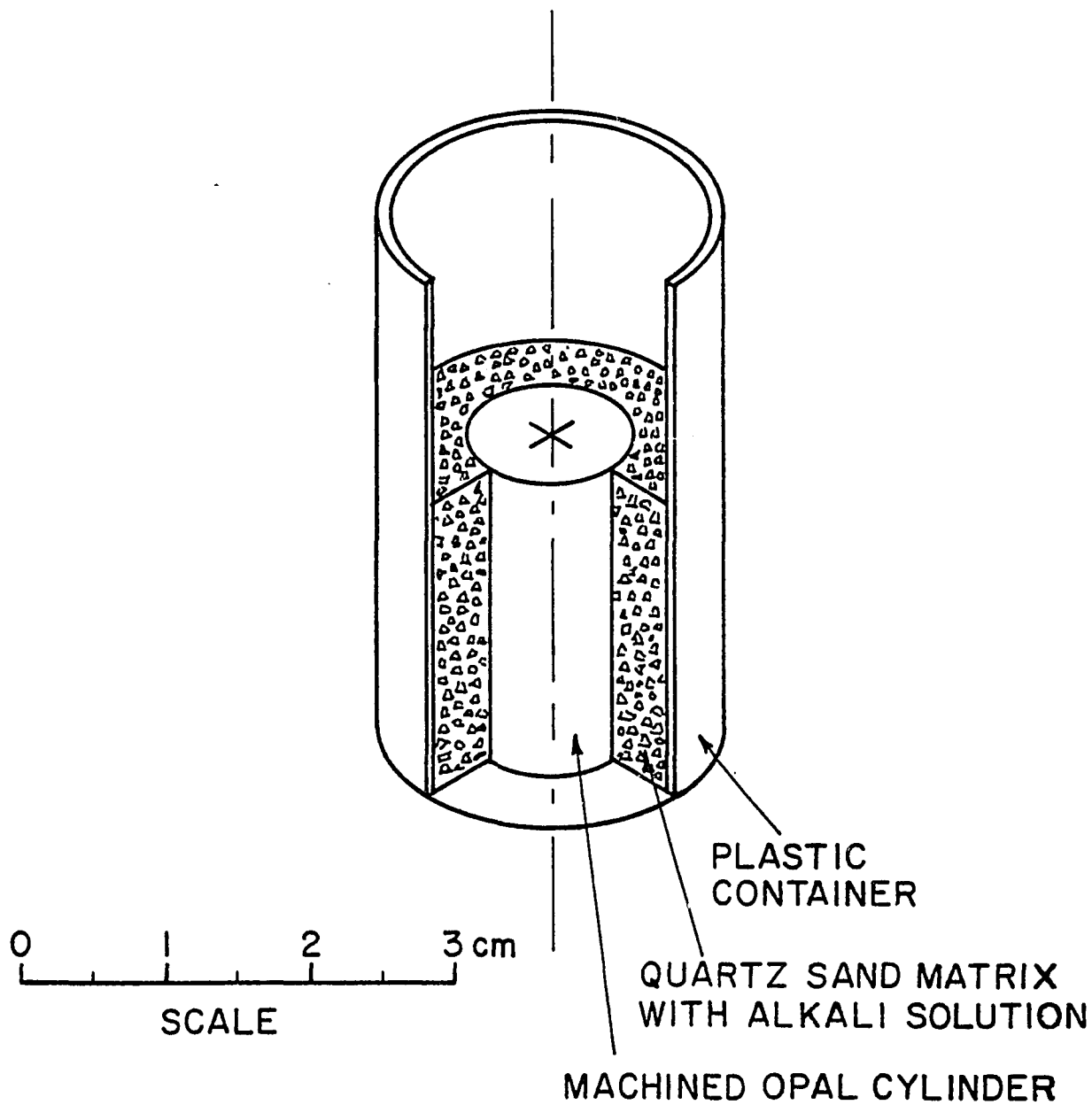


Figure 6.1 - Isometric Half Section of Reaction Cell

Containing an Opal Cylinder

crystalline $\text{Ca}(\text{OH})_2$ was mixed with the sand prior to packing it around the opal specimen. This matrix was then flooded with 3.0 ml of 1.0 normal KOH solution. The specimen containers were sealed during storage to minimize carbonation. One specimen was prepared for each series on three successive dates so that all of the specimens could be fractured and subjected to EDXA at one time.

The data for K series of experiments are presented in Tables 6.1 through 6.3 and shown graphically in Figure 6.2. In the first column the radial distance inward from the machined surface of the opal core, X in microns (μm) is listed, followed by the ratio of the accumulated counts for $\text{K}_{\text{Ka}1}$ to the accumulated counts for $\text{Si}_{\text{Ka}1}$ (K/Si). Since the atomic structure of these elements, with respect to their inner electron shells, is relatively similar, this ratio may be taken as a first approximation of the concentration on the basis of atoms of potassium or, in Series KL, calcium per atom of silicon. In the third and fourth columns are listed the ratio of the K/Si counts at some variable location to the counts at some base location, and the inverse error function complement equivalent to the ratio in column three. This last value has been tabulated under the symbol β . The use of the inverse error function complement will be discussed in Section 6.3. Table 6.7 contains values of this function and the error function for selected arguments. Ordinarily the ratio of concentration at some arbitrary point to that at the surface, C/C_0 , would be used in studies of this nature. Examination of Figure 6.2 reveals a situation in which the maximum concentration of the potassium is 50 to 400 μm inside of the specimens. The reason for this is not clear. The pattern of decreasing potassium concentration from some

Table 6.1

Diffusion Data for Series K-3, 7 Days
from Diamond (607)

X, μm	K/Si	C/C ₅₀	β
25	0.0123	--	--
50	0.0140	1.0000	0.0000
100	0.0073	0.5214	0.4534
150	0.0049	0.3500	0.6609
200	0.0039	0.2786	0.7662
300	0.0065	0.0464	1.4084
5000	0.0000	--	--

$$\text{INVVerfc } (C/C_{50}) = - 65.49 \times 10^{-3} + 47.34 \times \text{cm}^*$$

$$r^2 = 0.964$$

$$D_K \approx 184.4 \times 10^{-12} \text{ cm}^2/\text{sec}^*$$

*For points 100 - 300 μm

Table 6.2

Diffusion Data for Series K-2, 16 Days
from Diamond (607)

X, μm	K/Si	C/C ₂₀₀	β
0	n.d.		
25	0.0196	--	--
50	0.0218	--	--
100	0.0234	1.0000	0.0000
200	0.0217	0.9274	0.0644
300	0.00403	0.1722	0.9653
350	0.00213	0.0910	1.1951
450	0.0000	--	--
500	0.0000	--	--
600	0.0000	--	--

$$\text{INVerfc } (C/C_{200}) = -2.651 + 113.1 \times \text{cm}^*$$

$$r^2 = 0.895$$

$$D_K \approx 14.2 \times 10^{-12} \text{ cm}^2/\text{sec}^*$$

* For points 250 - 350 μm

Table 6.3

Diffusion Data for Series K-1, 21 Days
from Diamond (607)

X, μm	K/Si	C/C ₄₀₀	β
0			
25	0.0251	--	--
50	0.0268	--	--
100	0.0261	--	--
150	0.0317	--	--
200	0.0323	--	--
250	0.0324	--	--
300	0.0305	--	--
350	0.0346	--	--
400	0.0346	1.0000	0.0000
450	0.00779	0.2251	0.8578
500	0.00732	0.2116	0.8833
550	0.00419	0.1211	0.0961
600	0.00342	0.0988	1.1672
650	0.0042	0.1214	1.0953
700	0.0040	0.1156	1.1127
800	0.0000	--	--
1000	0.0000	--	--

$$\text{INVerfc (C/C}_{400}\text{)} = 0.3843 + 11.32 \times \text{cm}^*$$

$$r^2 = 0.658$$

$$D_K \approx 1.08 \times 10^{-9} \text{ cm}^2/\text{sec}^*$$

* For points 400 - 700 μm

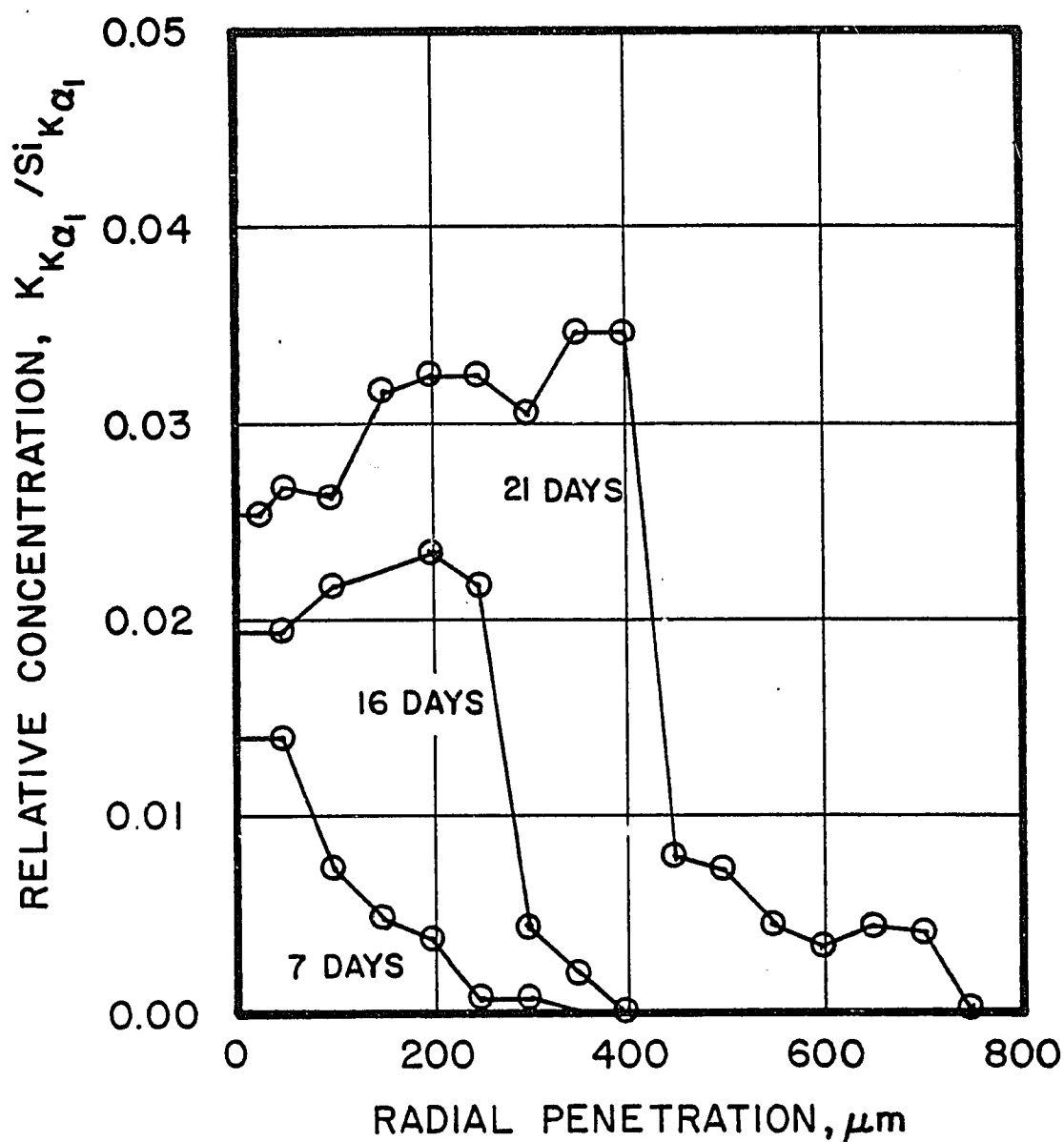


Figure 6.2 - Relative Concentration of K/Si (from EDXA)
Versus Radial Penetration in Opal Cylinder

high inside the specimen to a lower value at the exterior of the specimen suggests a possible loss of potassium through leaching during the process of preparing the specimen for examination. Because of this unusual pattern, the base value has been taken at the maximum concentration and the diffusion coefficient estimated from the remaining portion of the concentration vs. distance curve.

In Tables 6.4 and 6.5 this same column heading arrangement is used, with the addition of data for calcium. These data are plotted in Figures 6.3 and 6.4. The data for KL-3 and KL-2 are confusing and no attempt has been made to interpret them, although approximate diffusion constants have been computed from the data. The method of computation will be discussed in Section 6.3.

The data for Series Kl-1 have been listed in Table 6.6 and are plotted in Figure 6.5. These data produce a pattern for which a possible interpretation is offered in Section 6.4.

6.3 - Computation of Diffusion Coefficients

The mathematics of diffusion has been addressed by a number of authors, e.g. Crank (608), Jost (609), and Shewmon (610).

The solution for Fick's general law of diffusion for the case where the surface concentration of the initially solute-free specimen is maintained at some constant composition, C_0 , for all the time greater than $t = 0$, is:

$$C_{(x,t)} = C_0 \left[(1 - \operatorname{erf} \left(\frac{x}{(4Dt)^{1/2}} \right)) \right] \quad . \quad \text{Eq. 6.3.1}$$

Where: C = Concentration of the diffusing element (solute)

C_0 = Reference concentration, generally at $x = 0$

X = Depth of diffusion, cm

t = Time, seconds

D = Diffusion coefficient, $\text{cm}^2/\text{second}$

erf = Gauss error function (610, pp. 11-15)

Table 6.4

Diffusion Data for Series KL-3, 7 Days
from Diamond (607)

X, μm	K/Si	C/C ₂₅	β_K	Ca/Si	C/C ₀	β_{Ca}
0				(0.0675)	1.0000	0.0000
12.5	0.0425	--	--	0.0592	0.8770	0.1094
25	0.0507	1.0000	0.0000	0.0554	0.8207	0.1603
50	0.0441	0.8698	0.1159	0.0713	1.0563	--
75	0.0346	0.6824	0.2893	0.0180	0.2667	0.7854
100	0.0417	0.8225	0.1586	0.0038	0.0563	1.3497
125	0.00927	0.1828	0.9420	--	--	--
150	0.0040	0.0789	1.2425	0.0027	0.0400	1.4522
200	0.00174	0.0343	1.4966	0.0000	--	--
250	0.00191	0.0377	1.4694			
300	0.0000	--	--			

Equation for Potassium

$$\text{INVerfc } (C/C_{25}) = -0.270 + 80.02 \times \text{cm}^*$$

$$r^2 = 0.835 \quad D_K \approx 64.6 \times 10^{-12} \text{ cm}^2/\text{sec}^*$$

* For points 25 - 200 μm , omit point 100 μm

Equation for Calcium

$$\text{INVerfc } (C/C_0) = -0.018 + 108.9 \times \text{cm}^*$$

$$r^2 = 0.929 \quad D_{Ca} \approx 34.9 \times 10^{-12} \text{ cm}^2/\text{sec}^*$$

* For points 0 - 150 μm

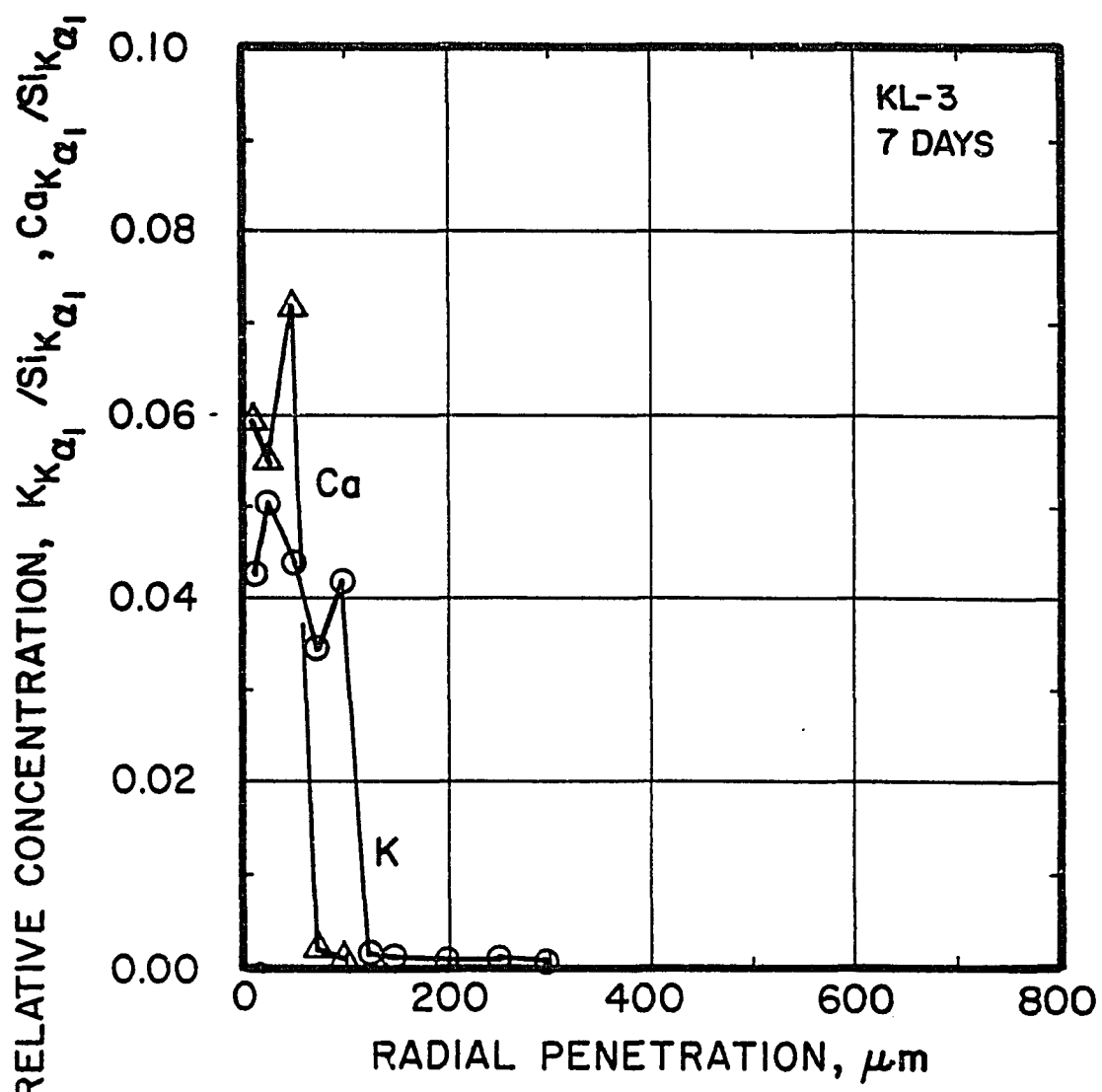


Figure 6.3 - Relative Concentration of K/Si, and Ca/Si (from EDXA)
Versus Radial Penetration in Opal Cylinder.

Table 6.5

Diffusion Data for Series KL-2, 16 Daysfrom Diamond (607)

X, μm	K/Si	C/C ₇₅	β K	Ca/Si	C/C ₀	β Ca
0				(0.1691)	1.0000	0.0000
12.5	0.0459	--	--	0.0867	0.5127	0.4629
25	0.0480	--	--	0.0043	0.0254	1.5806
50	0.0458	--	--	0.0006	0.0035	2.0601
75	0.0644	1.0000	0.0000	0.1267	0.7493	0.2260
100	0.0516	0.8012	0.1780	0.0029	0.0171	1.6861
150	0.0346	0.5372	0.4362	0.00179	0.0106	1.8071
200	0.0203	0.3152	0.7102	0.0000	--	--
300	0.00215	0.0334	1.5042			
350	0.00144	0.0224	1.6147			
400	0.00226	0.0351	1.4900			
500	0.0000	--	--			

Equation for Potassium

$$\text{INVerfc (C/C}_{75}\text{)} = -0.463 + 61.43 \times \text{cm}^*$$

$$r^2 = 0.985 \quad D_K \approx 47.9 \times 10^{-12} \text{ cm}^2/\text{sec}^*$$

* For points 75 - 350 μm

Equations for Calcium

$$\text{INVerfc (C/C}_0\text{)} = 0.223 + 392.5 \times \text{cm}^*$$

$$r^2 = 0.836 \quad D_{Ca_1} \approx 1.17 \times 10^{-12} \text{ cm}^2/\text{sec}^*$$

* For points 0 - 50 μm

$$\text{INVerfc (C/C}_0\text{)} = -0.755 + 184.2 \times \text{cm}^*$$

$$r^2 = 0.639 \quad D_{Ca_2} \approx 10.67 \times 10^{-12} \text{ cm}^2/\text{sec}^*$$

* For points 75 - 150 μm

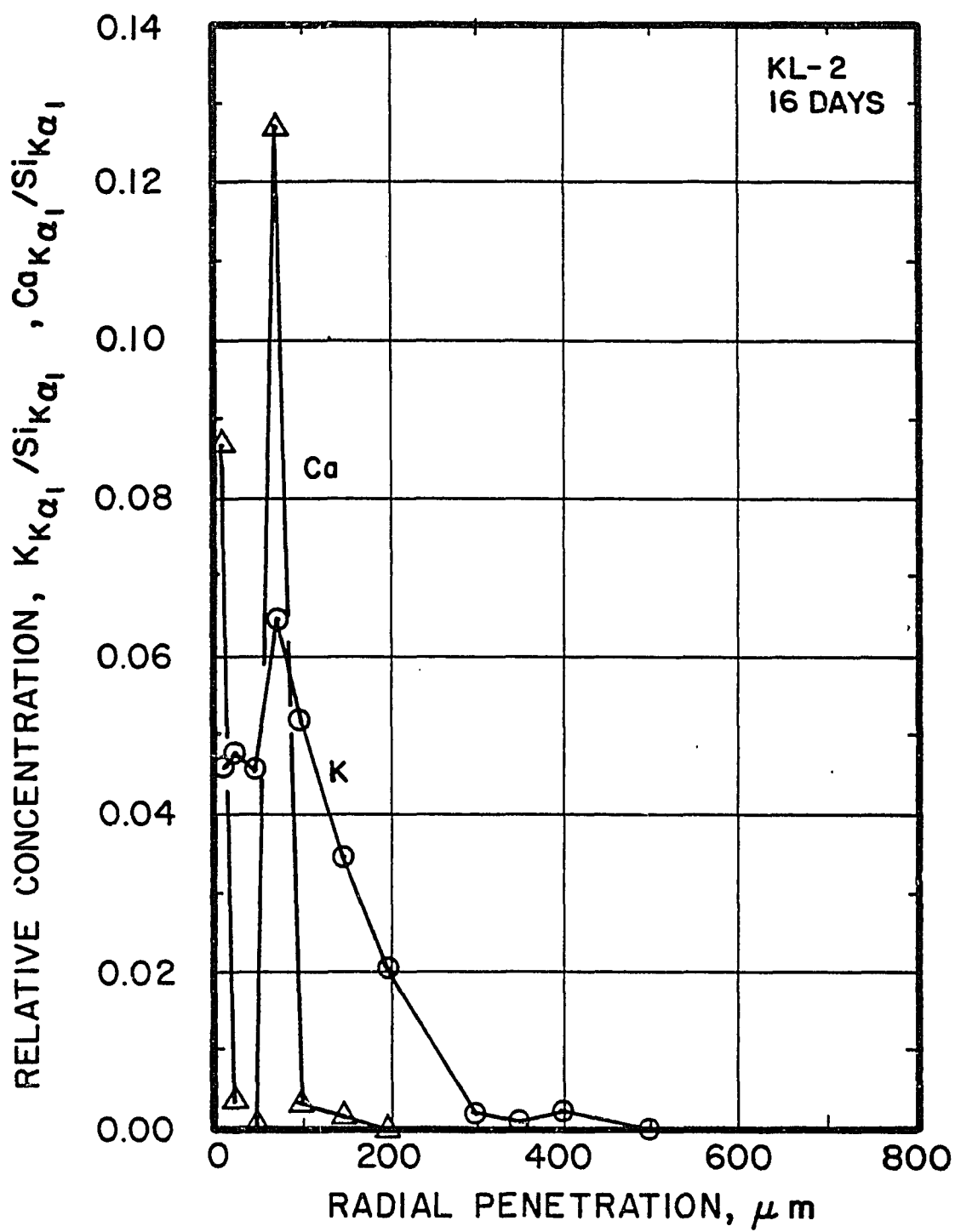


Figure 6.4 - Relative Concentrations of K/Si, and Ca/Si (from EDXA)
Versus Radial Penetration in Opal Cylinder.

Table 6.6

Diffusion Data for Series KL-1, 21 Days

from Diamond (607)

X, μm	K/Si	C/C ₀	β K	Ca/Si	C/C ₀	β Ca
0	(0.2837)	1.0000	0.0000	(0.0298)	1.0000	0.0000
12.5	0.2390	0.8424	0.1406	0.0243	0.8154	0.1651
25	0.2227	0.7850	0.1929	0.0167	0.5604	0.4117
50	0.1223	0.4311	0.5567	0.00568	0.1906	0.9255
75	0.1267	0.4466	0.5382	0.00558	0.1872	0.0326
100	0.0627	0.2210	0.8654	0.00122	0.0409	1.4457
125	0.0489	0.1724	0.9649	0.000	--	--
150	0.0441	0.1554	1.0046			
200	0.0224	0.0790	1.2420			
250	0.0127	0.0448	1.4188			
300	0.0088	0.0310	1.5256			
400	0.0036	0.0127	1.7622			
500	0.0029	0.0102	1.8165			
600	0.00416	0.0147	1.7251			
700	0.00222	0.0078	1.8814			
800	0.0000	--	--			

For equations and diffusion coefficients see continuation of table on next page.

Note: Values of X = 0 have been calculated from linear extrapolation of the first two values of K/Si or Ca/Si.

Table 6.6
(Continued)

Equations for Potassium

$$\text{INVerfc } (C/C_0) = 0.0398 + 79.8 \times \text{cm}^*$$

$$r^2 = 0.924 \quad D_{K_1} \approx 21.6 \times 10^{-12} \text{ cm}^2/\text{sec}^*$$

* For points 0 - 100 μm .

$$\text{INVerfc } (C/C_0) = 0.586 = 30.7 \times \text{cm}^*$$

$$r^2 = 0.982 \quad D_{K_2} \approx 146.2 \times 10^{-12} \text{ cm}^2/\text{sec}^*$$

* For points 100 - 400 μm

$$\text{INVerfc } (C/C_0) = 1.650 + 2.662 \times \text{cm}^*$$

$$r^2 = 0.255 \quad D_{K_3} \approx 19.4 \times 10^{-9} \text{ cm}^2/\text{sec}^*$$

* For points 400 - 700 μm

Equation for Calcium

$$\text{INVerfc } (C/C_0) = 0.065 + 135.4 \times \text{cm}^*$$

$$r^2 = 0.939 \quad D_{Ca} \approx 7.5 \times 10^{-12} \text{ cm}^2/\text{sec}^*$$

* For points 0 - 100 μm

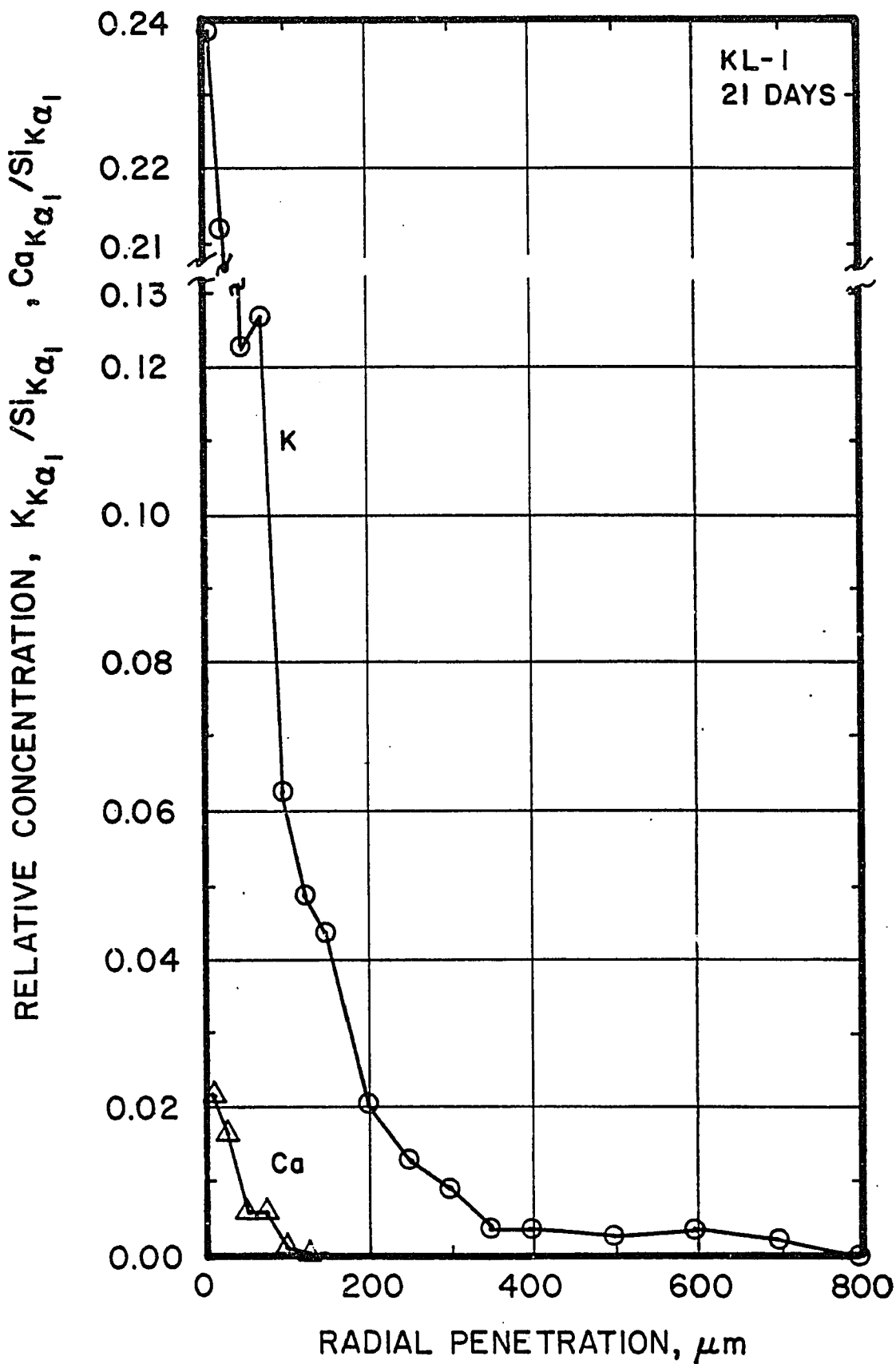


Figure 6.5 - Relative Concentrations of K/Si, and Ca/Si (from EDXA)
Versus Radial Penetration in Opal Cylinder.

Substituting β for $x/(4Dt)$ ⁵, for convenience, the Gauss error function is:

$$\text{erf } (\beta) = \int_0^\beta \exp (-\eta^2) d\eta \quad \text{Eq. 6.3.2}$$

Where: η = an integration variable

The complement of the Gauss error function is:

$$\text{erfc } (\beta) = 1 - \text{erf } (\beta) \quad \text{Eq. 6.3.3}$$

Thus, the concentration of the diffusing ions in the solid as a function of distance and time is:

$$C_{(x,t)} = C_0 [\text{erfc } (\beta)] \quad \text{Eq. 6.3.4}$$

which is equivalent to Eq. 6.3.1.

The value of β for which $C_{(x,t)}/C_0 = \text{erfc } (\beta)$ can be read from tables (611), or abbreviated tables found in most texts on diffusion or heat flow, (612).

For a given value of t , assuming D constant:

$$\beta/X = (4Dt)^{1/2} \quad \text{Eq. 6.3.5}$$

A plot of β vs X yields a straight line with slope β/X , therefore:

$$D = \left(\frac{\Delta \beta}{\Delta X}\right)^2 \times \frac{1}{4t} \quad \text{Eq. 6.3.6}$$

Table 6.7 contains an abbreviated tabulation of values of $\text{erf } (\beta)$ and $\text{erfc } (\beta)$, computed from Eq. 6.3.2, using Gaussian Quadrature (613, pp. 101-105).

These equations assume diffusion into a flat slab rather than a cylinder. Because of the shallow penetration of the potassium and calcium into the opal cylinders this assumption should have little effect on the diffusion coefficient computed from these experiments.

Plots of β versus X for the Series KL-1 specimen, stored 21 days in a solution of KOH and Ca(OH)_2 , are shown in Figure 6.6. The data for calcium diffusion generate a straight line, but the data for potassium

Table 6.7

The Error Function, erf, and the Error Function Complement, erfc, for Selected Values of the Argument β .

β	$erf(\beta)$	$erfc(\beta)$
0.0	0.00000	1.00000
0.1	0.11246	0.88754
0.2	0.22270	0.77730
0.3	0.32863	0.67137
0.4	0.42839	0.57161
0.5	0.52050	0.47950
0.6	0.60386	0.39614
0.7	0.67780	0.32220
0.8	0.74210	0.25790
0.9	0.79691	0.20309
1.0	0.84270	0.15730
1.2	0.91031	0.08969
1.4	0.95229	0.04771
1.6	0.97635	0.02365
1.8	0.98909	0.01091
2.0	0.99532	0.00468
2.2	0.99814	0.00186
2.4	0.99931	0.00069
2.6	0.99976	0.00024
2.8	0.99992	0.00008
3.0	0.99998	0.00002
3.2	0.99999	0.00001
3.4	1.00000	0.00000
∞	1.0	0.0

appear to generate a "curve" composed of three line segments each defined by four or more points. This implies a single diffusion coefficient for calcium, independent of depth of penetration. The data for potassium are anomalous in that there appear to be three diffusion coefficients, increasing step-wise with penetration.

6.4 - Interpretation of Anomalous Diffusion of Potassium in Opal

In polycrystalline materials two diffusion paths are possible; surface diffusion along grain boundaries, dislocations, and free surfaces, and lattice diffusion through the bulk of the crystals. Surface diffusion requires lower activation energy than lattice diffusion and surface diffusion rates are considerably higher than those for lattice diffusion. Bailey (614), in a study of low-temperature diffusion of sodium in albite estimated the activation energy for surface diffusion to be approximately 3kcal/mole sodium and the apparent diffusion coefficient at 25° C to be 0.934×10^{-18} cm²/sec. Using an Arrhenius temperature dependence of volume diffusion coefficient relationship, he extrapolated high-temperature (595 - 940° C) data to 25° C and found the diffusion of sodium in albite at high-temperature to be approximately 8×10^{-13} cm²/sec. His data suggest that at low-temperature the primary mode of diffusion is that of surface diffusion along grain boundaries, free surfaces, lattice defects, and mechanically induced fractures.

Reiman and Stark (615) investigated the phenomenon of the near surface effect (NSE) in metal diffusion. They note that three diffusion coefficients, increasing step-wise with penetration may be found.

If oxidation or some other reaction takes place at or near the surface of the solvent specimen a low diffusion coefficient for the

solute species will be observed. Beyond this, a larger diffusion coefficient indicates lattice or bulk diffusion, and finally a third higher coefficient may be observed at depth. This last, and highest diffusion coefficient is due to surface diffusion. In figure 6.6 the data for diffusion of potassium into the opal core indicate a pattern much like that described by Reiman and Stark.

The equations in Section 6.3 imply that diffusion responds to a concentration gradient of the diffusing species. Actually diffusion responds to a chemical potential gradient and this gradient can be altered by electrical fields (616) and stress (610, pp. 23 - 28). Thus, chemical potential of the diffusing species (609, pp. 68 f.) is the important driving force in these experiments. If diffusing species become involved in chemical reactions with the solute material it may appear that diffusion is proceeding "up hill" against a concentration gradient.

It is of interest to compare the concentrations of potassium and calcium per unit volume of solution surrounding the cores, and per unit volume of core, in the data for the Series KL-1 core experiment. Equation 6.4.2 provides the constant necessary for conversion of the molar ratios of potassium or calcium to silicon into ratios of moles of either potassium or calcium per dm^3 of opal ($1 \text{ dm}^3 = 1000 \text{ cm}^3$). Since no chemical, petrographic, or X-ray diffraction data are available for the opal used by Diamond, it is assumed to be similar to Beltane Opal and is assumed to contain 88 percent SiO_2 and have a specific gravity of 2.07, these values having been taken from Table 3.5.

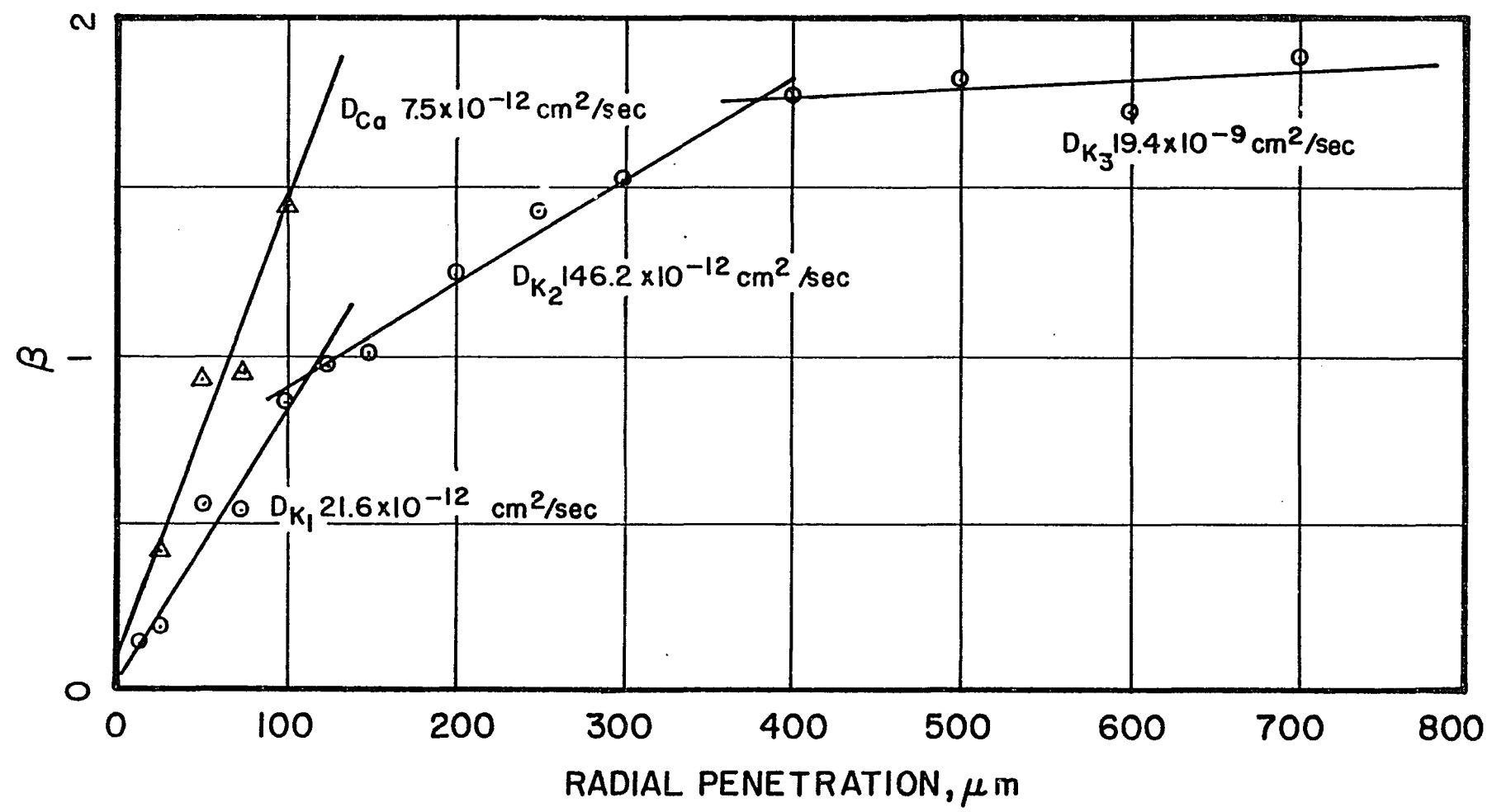


Figure 6.6 - Relationship of β (Inverse Error Function Complement)
to Radial Penetration Distance, μm .

$$\frac{\text{Moles M}}{\text{Moles Si}} \times \frac{\text{Moles SiO}_2}{60.084 \text{ g SiO}_2} \times \frac{0.88 \text{ g SiO}_2}{\text{g Opal}} \times \frac{2.07 \text{ g opal}}{\text{cm}^3 \text{ opal}} = \frac{\text{Moles M}}{\text{cm}^3 \text{ opal}}$$

$$\frac{\text{Moles M}}{\text{Moles Si}} \times 30.32 = \frac{\text{Moles M}}{\text{dm}^3 \text{ opal}} \quad \quad \text{Eq. 6.4.1}$$

Where: M = Either K or Ca

Taking values of M/Si from Table 6.6, the concentrations of K and Ca at the surface of the opal core are:

$$\frac{0.2837 \text{ Mol K}}{\text{Mol Si}} \times 30.32 = \frac{8.60 \text{ Mol K}}{\text{dm}^3 \text{ opal}} \quad \text{and,}$$

$$\frac{0.0298 \text{ Mol Ca}}{\text{Mol Si}} \times 30.32 = \frac{0.90 \text{ Mol Ca}}{\text{dm}^3 \text{ opal}}$$

The volumetric concentration of K in the reaction cell solution during the experiment was probably less than one mole per liter, considering the common ion effect and that some of the K diffused into the opal cylinder. Thus, the K concentration in the surface of the opal core, on a volumetric basis, was on the order of nine times that in the solution surrounding the opal core. Although there was a considerable reservoir of crystalline calcium hydroxide (Ca(OH)_2) the low solubility of Ca(OH)_2 , about 0.023 Moles Ca^{++}/L in pure water in the temperature range $20 - 25^\circ \text{C}$, and the common ion effect due to the presence of the molar solution of K^+ , the concentration of Ca^{++} in solution at any given time was probably close to 1. mMol/L. The volumetric concentration of Ca in the surface of the opal core was on the order of 900 times that in the surrounding solution. If these concentrations are even approximately correct, the chemical potential of the diffusing species must have been reduced due to chemical reactions within the opal in order for diffusion to take place.

Using values from Table 6.6 and the factor in Eq. 6.4.1, a figure similar to Figure 6.5 could be constructed and, using values computed to locate points on this figure, the weighted mean concentrations of K and Ca in the outer 125 μm (0.012 cm) shell of the opal cylinder may be calculated. From this computation, the weighted mean concentration of K is found to be approximately 4.21 Moles/dm³ and that of Ca is 0.37 Moles/dm³.

In Mix Series 59 - 64 (Section 5.15), Mix 60 containing 8 percent Beltane Opal sand, consumes approximately 250 mMol/L of M⁺ (combined Na⁺ and K⁺) from the pore solution at 21 days. The amount of M⁺ consumed per dm³ of opal is:

$$\frac{0.25 \text{ Mol M}^+ \text{ L}}{\text{L} \times 160 \text{ g opal}} \times \frac{2.07 \text{ g opal}}{\text{cm}^3 \text{ opal}} \times \frac{1000 \text{ cm}^3}{\text{dm}^3} = \frac{3.23 \text{ Mol M}^+}{\text{dm}^3 \text{ opal}}$$

The opal sand particles in this mixture have radii ranging from 75 to 300 μm , the approximate mean being close to 185 μm . If the chemical and diffusion properties are similar to those of the opal used by Diamond in his experiments, the K bound, i.e. 4.21 versus 3.23 Mol M⁺/dm³ are in reasonable agreement, considering the range of particle radii. Sealed 50 mm diameter specimens of Mix 60 expanded 8745 microstrain (0.87 percent) in 32 days at 20° C. Mix 63 of this series, containing 10 percent pozzolan L (containing approximately the same amount of SiO₂ as 8 percent Beltane Opal) consumed less than 100 mMol/L of M⁺, an amount approximately equivalent to 1.6 Mol M⁺/dm³. Sealed 50 mm diameter specimens of this mixture shrunk 327 microstrain (0.033 percent) in 32 days at 20° C.

In Mix Series 34 - 35 (Section 5.7) Mix 35, containing 10 percent Beltane Opal pozzolan, consumed about 100 mMol/L of M⁺ at 21

days, equivalent to about $1.0 \text{ Mol } M^+/\text{dm}^3$ opal. Mortar prisms with 6.35 mm square cross sections stored at 20° C for 94 days expanded 120 microstrain (0.012 percent), slightly less than similar prisms made from plain mortar.

These observations suggest that the moles of alkali metal ion consumed per unit volume of reactive opal or pozzolan must be relatively small if expansion is to be prevented and that, within the range of particle size investigated, sand sized ($150 \mu\text{m}$) and larger particles, i.e. opal cylinders, reacted to produce expansive alkali-silicate gels because the relatively large calcium ions were not able to diffuse to the reaction sites while finely ground materials, requiring relatively shorter diffusion paths for calcium ions, produced calcium-alkali-silicate gels that were nonexpansive.

Returning to Figures 6.5 and 6.6, it is of interest to note that the high concentration of K in the opal core is associated with the outer 100 to $125 \mu\text{m}$, the portion containing Ca. At $125 \mu\text{m}$ inside the opal core the Ca concentration falls below the detection limit and it is at this point that the K "curve" first breaks, indicating a greater diffusion coefficient. Beyond this point Ca is not available to form a stable calcium-alkali-silicate gel and a potentially expansive alkali-silicate gel is formed.

There seems to be ample evidence that the introduction of polyvalent cations, e.g. Ca^{++} , Ba^{++} , Al^{3+} etc., into silica gels results in formation of a stable nonexpansive gels (Kalousek, 617, Iler, 618, 619, Powers & Seinour, 620, 621, Struble, 622, and others). Barnes (623), Hadley (624), and others have found that within a few minutes after introduction of mixing water to portland cement mortars,

a coating of crystalline calcium hydroxide (Ca(OH)_2) begins to form on aggregate particles in the mixture. Within a few hours this coating attains a thickness of about $0.5 \mu\text{m}$, independent of the size of the substrate particle. The rate at which Ca(OH)_2 is deposited and the degree to which the coating reaches this thickness is probably independent of the chemical composition of the portland cement unless large quantities of aggregate or mineral admixture particles with high specific surface are added and the cement is predominantly belite. This situation might arise in the case of concrete designed for placement in a massive structure, e.g. a small amount of low-heat portland cement with a high percentage addition (or replacement) of a high specific surface pozzolan.

To aid in visualization of the discussion it is desirable to introduce a reaction model. Two general classes of models suggest themselves, the progressive-conversion model; and the shrinking unreacted-core model. In the former the reactant permeates the entire solid particle and the solid is converted continuously and progressively throughout. In the case of the unreacted-core model the reaction occurs at the outer skin of the particle and progresses inward leaving behind a blanket of reaction product. (616 p. 360). Neither of these models seems entirely satisfactory, but a modification of the second seems best to describe the initial attack of alkalies on unstable aggregate components.

The model selected, that appears appropriate for reactions with opal aggregate, involves a shrinking unreacted-core surrounded by a reaction zone that is in turn surrounded by a reaction product blanket. In this case an additional feature, the Ca(OH)_2 coating, is added to

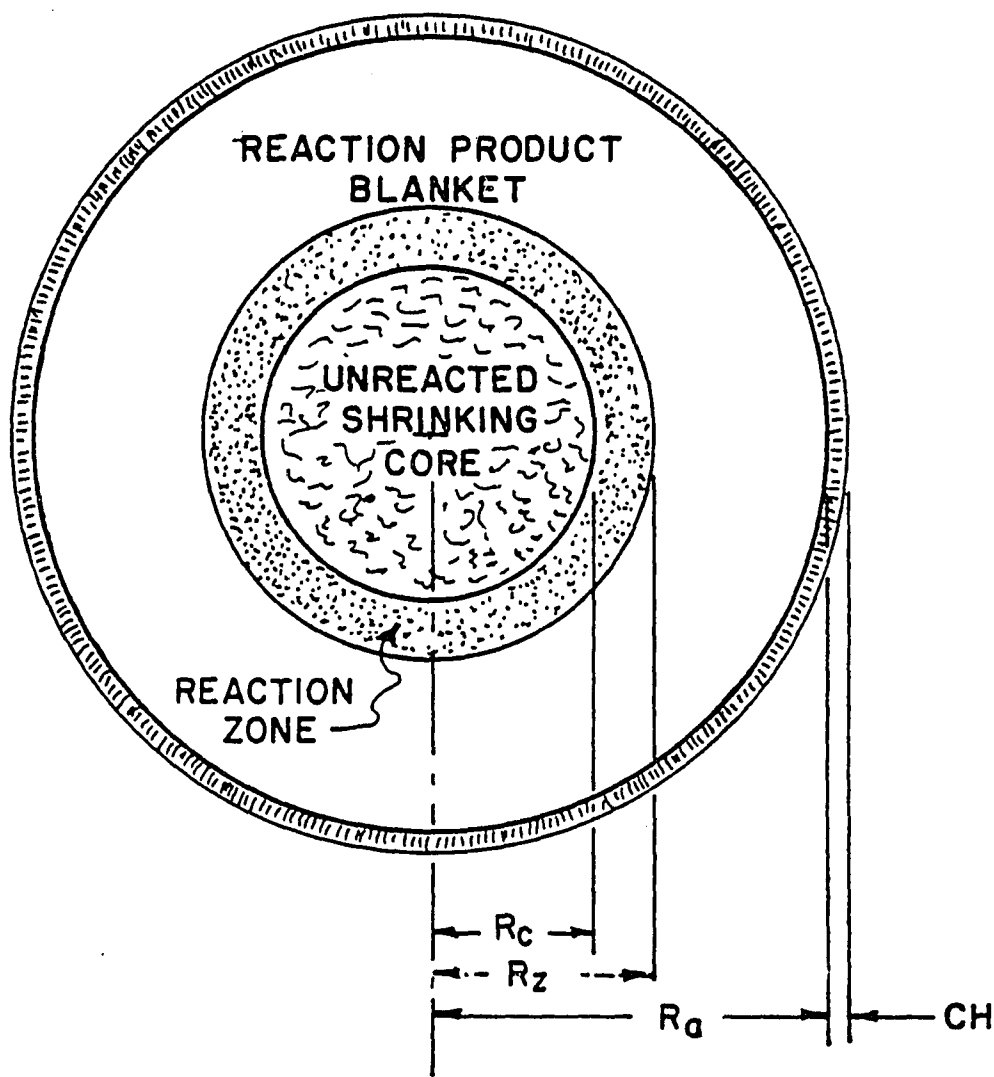


Figure 6.1 - Schematic Diagram of Proposed Reaction Model

R_c = Radius of unreacted core

R_z = Outer radius of reaction zone

R_a = Outer radius of original particle

CH = Ca(OH)_2 (not to scale)

the outside of the whole model. Aside from the addition of the $\text{Ca}(\text{OH})_2$ coating, this is a fairly common model and it is discussed at some length by Levenspiel (625, Ch. 12), and Wen (626, pp. 34 - 54). A schematic drawing of the proposed model, is illustrated in Figure 6.1. In the figure the chemical phase of alkali-silica attack has converted approximately 88 percent of the original particle to reaction product. The original boundary of the $\text{Ca}(\text{OH})_2$ deposit is shown. At this stage some portion of the $\text{Ca}(\text{OH})_2$ would have been mobilized and incorporated in the reaction product.

As previously mentioned, it has been thought that the inclusion of polyvalent cations in the reaction product may result in the production of a stable, i.e. nonswelling, gel. From the chemical data presented in Chapter 5 it is clear that the Ca^{++} content of pore solutions is vanishingly small except during the first 24 hours of hydration, although small amounts of Ca^{++} may also be found in pore solutions expressed from mortars at advanced ages. Thus, except in the case of mortars with high concentrations of active pozzolans, the Ca^{++} available to the reacting particle is primarily limited to that contained in the approximately $0.5 \mu\text{m}$ coating deposited on the particle during the early phases of hydration. The alkali metal ions are in abundant supply in the pore solution and are quite mobile by comparison. If this is the case, the particle size would have a pronounced effect on the character of the reaction product, larger particles having less $\text{Ca}(\text{OH})_2$, or Ca^{++} , available per unit volume than smaller reactive particles of high specific surface.

This does not explain apparently anomalous expansion of mixtures containing small amounts of pozzolan e.g. Mix 17 (Section 5.7),

and Mix 63, Section 5.15, or mixtures containing large quantities of reactive aggregate. Perhaps expansion of mixtures containing small quantities of pozzolan results from displacement of the calcium from reactive silica by an overwhelming concentration of alkali metal ions, analogous to the displacement of calcium ions from zeolites in commercial water softeners by brine solutions. In the second case, if the available surface of the aggregate is sufficiently large, alkali metal ion penetration is probably sufficiently small that a nonexpansive calcium-alkali-silicate gel can be formed.

CHAPTER 7

CONCLUSIONS

The essential conclusions drawn from the experiments conducted using a small suite of cements and pozzolans in mortars containing quartz sand and varying amounts of sand-sized opaline material have been summarized in the following paragraphs. While quartz sand is referred here to as inert, it should be noted that no siliceous material is completely inert in the highly alkaline environment found in most portland cement pastes.

7.1 By the use of equipment and techniques described in this report it is feasible to express and analyze pore solutions from reacting mortars of moderate water contents ($w/c = 0.50$) sealed and allowed to hydrate and react for periods of at least two years.

7.2 Pore solutions expressed from mortars made with inert quartz sand and cements of moderately high alkali contents are found to rapidly become concentrated solutions of potassium and sodium hydroxide. Calcium concentrations fall to levels of 0.001 molar, or less, after the first 24 to 48 hours. Concentrations of sulfate follow a similar pattern, and the concentrations of other cations and anions are negligible.

7.3 The alkali hydroxide solutions thus developed in the pores of mortars or concretes are the primary cause of alkali-aggregate

reactions if reactive aggregates are present.

7.4 The concentrations of the alkali hydroxide pore solutions in sealed mortar specimens containing only inert aggregates increase progressively as solvent water is consumed by cement hydration.

7.5 If the observed concentrations of alkali hydroxides in mortars containing only inert aggregates are quantitatively adjusted for the water consumed by cement hydration, as determined by the amount of nonevaporable water at each age, the adjusted concentrations rapidly approximate constant values. This is interpreted as indicating that no substantial quantities of alkali ions either enter or are removed from solution by cement hydration products after the first few days.

7.6 If reactive aggregate, i.e. sand-size opal grains, are incorporated in the mortar, the alkali hydroxide concentration (adjusted for bound water) diminishes progressively. This decrease represents progressive transfer of alkali cations to the alkali-silica reaction products being produced.

7.7 For any given cement and proportion of reactive aggregate the reduction in alkali content (adjusted for bound water) of the pore solution ceases after some period of time and a constant concentration is approached.

7.8 The same constant concentration level is reached by mortars reacting at either 20° C or 40° C, but it is attained much more rapidly at the higher temperature. The time required to approach equilibrium concentration with opal aggregate present is on the order of 3 to 10 days at 40° C, but may require several months at 20° C.

7.9 Expansion measurements on small mortar specimens incorporating various proportions of a standard opal confirm the existence of a pessimum proportion effect, although a few anomalous results were obtained.

7.10 The pessimum proportion, expressed in terms of the ratio of "reactive" SiO_2 to cement alkalines (as Na_2O equivalent) is on the order of 6 to 10. The actual proportion observed in a given series may be modified by slow release of some of the cement alkalies or by leaching of alkalies from small mortar specimens exposed to 100 percent relative humidity in the expansion test.

7.11 For the Beltane Standard Opal used in these studies, expansions observed in reactive opal-containing mortars of a given composition stored at temperatures ranging from 20° C to 60° C , were inversely related to the exposure temperature.

7.12 Under identical conditions mortar specimens of large cross section exposed to 100 percent relative humidity for prolonged periods tend to expand more than specimens of smaller cross section (although there are some exceptions). This phenomenon is probably due to the higher specific surface of the smaller cross section specimens and the attendant greater potential for leaching of alkalies from the pore solutions of the smaller specimens.

7.13 The observed reduction in alkali hydroxide concentration of the pore solutions of sealed reacting mortars (reflecting the "chemical attack" phase) occurs significantly earlier in time than the expansion

response of the corresponding mortars exposed to 100 percent relative humidity (the "water absorption and expansion" phase).

7.14 Conducting both sets of experiments at 40° C widens the time interval between the two responses, the higher temperature serving to accelerate the "chemical attack" phase markedly while not affecting, or in some cases actually delaying the "water absorption and expansion" phase.

7.15 Large additions of finely-ground reactive opal made to reacting mortars already having approximately the pessimum proportion of sand-size opal result in comparatively modest incremental decreases in alkali hydroxide contents of the pore solutions; substantial amounts of alkalies remain in solution indefinitely.

7.16 Reacting mortars cast as short cylinders and sealed in Butyl rubber jackets to prevent entry or loss of water (or leaching of alkalies) expand significantly more than do small mortar prisms of the same composition exposed to 100 percent relative humidity conditions.

7.17 When reacting mortars sealed in Butyl rubber jackets have ceased to expand, large additional increments of expansion can be obtained by removal of the jackets and exposure of the specimens to 100 percent relative humidity. These additional increments may be much greater than the total expansions of mortar prism specimens of the same mixture exposed in a conventional manner to 100 percent relative humidity. Thus, expansion measurements on conventional mortar prisms exposed to 100 percent relative humidity are of only relative significance and may not adequately represent the expansion potential of the mixture.

7.18 The expansion of opal-containing mortars is substantially reduced, but not eliminated, by addition of one percent of lithium carbonate by weight of cement.

7.19 One percent lithium carbonate added to mortar made with inert quartz sand does not significantly influence the concentration levels of potassium or sodium that would otherwise be observed. A portion, but not all, of the added lithium is found in expressed pore solutions and is accompanied increased levels of OH^- to about one molar. However, the increase in OH^- concentration is significantly less than that required to balance the lithium cations observed. It is suspected that the missing anions are $\text{CO}_3^{=}$.

7.20 One percent of lithium carbonate added to mortars containing approximately the pessimum proportion of sand-sized opal substantially lessens the rate of removal of K^+ and Na^+ from the pore solution that would otherwise occur, and Li^+ is removed at an accelerated rate. Thus, Li^+ shows evidence of being preferentially incorporated in the alkali-silica reaction product, probably changing its character and reducing its expansive potential.

7.21 A commercial pozzolan, consisting primarily of volcanic glass, was added to mortar mixtures already containing approximately the pessimum content of sand-sized opal. It was found to reduce the expansion otherwise occurring in specimens sealed in Butyl rubber jackets. The reduction in expansion was linearly proportional to the percentage of pozzolan added. An addition of 25 percent by weight of cement was sufficient to totally suppress expansion. Secondary

expansions observed after removal of the Butyl rubber jackets and exposure to 100 percent relative humidity are also reduced proportionately with the percentage of pozzolan added.

7.22 The nonevaporable water content per gram of cement as measured at any given time or at equilibrium in the mortars containing volcanic glass pozzolan is also reduced in linear proportion to the amount of pozzolan added. Finely ground opal added as a pozzolan exhibits the same effect, as does sand-size reactive opal. In each case the effect is of similar magnitude per unit of silica added. The effect is independent of temperature in the 20° C to 40° C range investigated.

7.23 The amount of calcium hydroxide per gram of cement found in mortars cured approximately 14 months was reduced significantly by incorporation of silica, either as sand-sized opal grains or as volcanic glass pozzolan. For small additions of silica, up to about 20 percent pozzolan or opal by weight of cement, the reductions in calcium hydroxide appear to be linearly related to the amount of silica added. Beyond this limit, the reduction per unit of silica added diminishes so that, over all, the relation appears to become parabolic, additions of opal and/or pozzolan of more than 25 percent silica being decreasingly effective in reducing the amount of calcium hydroxide found in the mortars.

7.24 Additions of volcanic glass pozzolan to otherwise non-reacting mortar removes alkali hydroxides from the pore solution, but not as effectively as sand-sized opal. The amount of alkali hydroxide removed from the pore solution at equilibrium by a 25 percent addition

of this pozzolan is substantially less than that removed by 8 percent of sand-sized opal.

7.25 Comparison of the effects of incorporating a variety of siliceous pozzolans into otherwise inert mortars as a cement replacement, rather than as an addition:

7.25.1 In all cases there is a reduction in the non-evaporable water content per gram of cement at maturity that is linear with proportion of the pozzolan used. The magnitudes of these reductions were surprisingly similar regardless of the source of the pozzolan. For example, 30 percent replacement reduces the nonevaporable water content per gram of cement from about 20 percent in non-pozzolan containing (control) mortar to about 15 percent for ground quartz and 13 to 14 percent for a variety of more reactive forms of silica.

7.25.2 Four of the five pozzolans used showed no indication of any contribution of alkali from the pozzolan to the pore solution, and were seen to take up alkali roughly proportionately to the extent of pozzolan present (when concentration data were adjusted for reduced cement content alkali source as well as for bound water). However, the amount of alkali removed from the pore solutions varies drastically with the type of pozzolan used,

being almost negligible for ground quartz, substantial and virtually identical to each other for the two commercial pozzolans, and exceedingly high for the silica fume.

7.25.3 The fifth pozzolan, produced by grinding a rhyolitic block pumice, contained a substantial amount of alkalis. This material maintained the pore solution at approximately the same high level regardless of the amount of pozzolan present.

Thus, the influence of added pozzolan on the alkali content of pore solutions, and hence the potential for alkali aggregate attack, varies markedly with the specific pozzolan as well as the replacement level. This does not necessarily mean that all alkalis contained in a pozzolan will find their way into the pore solution. Alkalies bound in feldspars are far less likely to be brought into solution than alkalies in glassy metastable materials.

7.26 It is known that sodium and potassium silicate gels have the ability to imbibe water and swell with sufficient force to cause disruption of portland cement concretes, and that the inclusion of certain polyvalent cations, e.g. Ca^{++} , Ba^{++} , Al^{3+} , in these gels in sufficient amounts results in the formation of stable nonswelling gels. It has been postulated that the relatively large calcium ion can not diffuse into reactive siliceous aggregate particles, on the order of $150 \mu\text{m}$ or larger, rapidly enough to form a stable gel, but that it can do so in particles on the order of $75 \mu\text{m}$ and less. In the case

of finely divided siliceous materials, pozzolans, the product formed is a calcium-silicate-hydrate similar to that produced by the hydration of C_3S and C_2S in portland cements. Quantitative data from EDXA studies indicate that there is a significant difference in diffusion coefficients for potassium in opal when calcium ions are available. The relative concentrations of both potassium and calcium are much greater in the outer 100 to 125 μm of opal cores studied than are present in the surrounding solution indicating that, following diffusion into the opal, there must have been a reaction that decreased the chemical potential of both the calcium and potassium. The diffusion pattern of the potassium is consistent with a material undergoing a chemical reaction (a near surface effect) and then exhibiting diffusion behavior similar to lattice diffusion, followed by surface or grain boundary diffusion.

BIBLIOGRAPHY

BIBLIOGRAPHY

101. Newlon, H., Editor, "Symposium on Alkali-Carbonate Rock Reactions," Highway Research Record No. 45, National Research Council, Washington, D.C., 1964, 244 pp.
102. Diamond, S., Young, J.F., Lawrence, F.V., Jr., "Scanning Electron Microscopy - Energy Dispersive X-Ray Analysis of Cement Constituents - Some Cautions," *Cement and Concrete Research*, Vol. 4, No. 6, 1974, pp. 899-914.
201. Gilmore, Q.A., "Practical Treatise on Limes, Hydraulic Cements, and Mortars," Professional Papers of the Corps of Engineers, U.S.A., No. 9, D. Van Nostrand, Publisher, New York, Fifth Edition 1879, 334 pp.
202. Meade, R.K., "Portland Cement," Chemical Publishing Co., Easton, PA, 1906, 385 pp.
203. Bogue, R.H., "A Digest of the Literature on the Nature of the Setting and Hardening Process in Portland Cement," PCAF Paper No. 17, National Bureau of Standards, October 1982, 48 pp.
204. Blount, B., "Cement," Longmans, Green & Co., London and New York, 1920, 284 pp.
205. Stanton, T.E., "Expansion of Concrete Through Reaction Between Cement and Aggregate," *Proceedings, ASCE*, Vol. 66, 1940, pp. 1781-1811.
206. U.S. Bureau of Reclamation, "Investigation of Crack Development in the Concrete in Parker Dam," Report No. ce-31, Cement Laboratory, USBR, 20 January 1941.
207. U.S. Bureau of Reclamation, "Proceedings of Conference for Discussion of Problems Related to Alkalies in Cement and Their Effect on Aggregates and Concretes," USBR, Denver, 1941.
208. American Society for Testing and Materials, "Symposium on Use of Pozzolanic Materials in Mortars and Concretes," *ASTM STP 99*, ASTM, Philadelphia, PA, 1950, 203 pp.
209. Alderman, A.R., Gaskin, A.J., Jones, R.H., Vivian, A.E., "I. Australian Aggregates and Cements," Bulletin 229, Commonwealth of Australia, Council for Scientific and Industrial Research, 1947.

210. Davis, C.E.S., "XXVI. Comparison of the Effect of Soda and Potash on Expansion," Australian Journal of Applied Science, Vol. 9, 1958, pp. 52-62.
211. Idorn, G.M., "Durability of Concrete Structures in Denmark," Ph.D. Thesis, Technical University of Denmark, Copenhagen, 25 January 1967, 208 pp.
212. Lerch, W., "Chemical Reactions," Significance of Tests and Properties of Concrete and Concrete Aggregates, ASTM STP 169, 1956, pp. 334-345.
213. American Society for Testing and Materials, "1979 Annual Book of Standards, Part 14," ASTM, Philadelphia, PA, 1979, 823 pp.
214. ASTM Designation C227-71(1976), "Standard Test Method Potential Alkali Reactivity of Cement-Aggregate Combinations (Mortar Bar Methods)," in Reference (213).
215. ASTM Designation C289-71(1976), "Standard Method of Test for Potential Reactivity of Aggregate (Chemical Method)," in Reference (213).
216. ASTM Designation C295-65(1973), "Standard Recommended Practice for Petrographic Examination of Aggregate for Concrete," in Reference (213).
217. ASTM Designation C294-69(1975), "Standard Descriptive Nomenclature of Constituents of Natural Mineral Aggregates," in Reference (213).
218. Mielenz, R.C., "Petrographic Examination," in Significance of Tests and Properties of Concrete and Concrete-Making Materials, ASTM STP 169-a, American Society for Testing and Materials, Philadelphia, PA, 1966, pp. 381-403.
219. Mather, B., "Petrographic Identification of Reactive Constituents in Concrete Aggregate," Proceedings ASTM, Vol. 48, American Society for Testing and Materials, Philadelphia, PA, 1948, pp. 1120-1125.
220. ASTM Designation C311-77, "Standard Methods of Sampling and Testing Fly Ash or Natural Pozzolans for Use as a Mineral Admixture in Portland Cement Concrete," in Reference (213).
221. Corps of Engineers, U.S.A., "Standard Practice for Concrete," Engineer Manual E.M. 1110-2-2000, 1 November 1971, Department of the Army, Office of the Chief of Engineers, with Change 1, February 1972.
222. Bailey, S.W., Bell, R.A., Peng, C.J., "Plastic Deformation of Quartz in Nature," Bulletin of the Geological Society of America, Vol. 69, 1958, pp. 1443-1466.

223. De Hills, S.M., Corvalan, J., "Undulatory Extinction of Quartz Grains of Some Chilean Granitic Rocks of Different Ages," Geological Society of America Bulletin, Vol. 75, April 1964, pp. 363-366.
224. White, S., "The Role of Dislocation Processes During Techtonic Deformations, with Particular Reference to Quartz," in "The Physics of Minerals and Rocks," Strens, R.G.J., Editor, John Wiley & Sons, New York, 1974.
225. Spry, A., "Metamorphic Textures," Pergamon Press, Oxford, 1969, 350 pp.
226. Gogte, B.S., "An Evaluation of Some Common Indian Rocks With Special Reference to Alkali-Aggggregate Reactions," Engineering Geology, Vol. 7, 1973, pp. 135-153.
227. Solvay Chemical Co., "Calcium Chloride in Manufacture of Low-Alkali Portland Cement," Solvay Technical Service Report No. 10.61, Syracuse, NY, 1961.
228. Woods, H., "Removing Alkalies by Heating With Admixtures," Rock Products, Vol. 45, February 1942, pp. 66-68.
229. Duda, W.H., "Cement Data Book, International Process Engineering in the Cement Industry," Bauverlag, GmbH, Wiesbaden and Berlin, Germany, Second Edition, 1977, 539 pp.
230. Jawed, I., Skalny, J., "Alkalies in Cement: a Review," Part I, Forms of the Alkalies and Their Effect on Clinker Formation, Cement and Concrete Research, Vol. 7, 1977, pp. 719-730.
231. Jawed, I., Skalny, J., "Alkalies in Cement: a Review," Part II, Effects of Alkalies on Hydration and Performance of Portland Cement, Cement and Concrete Research, Vol. 8, 1978, pp. 37-52.
232. Diamond, S., "A Review of Alkali-Silica Reaction and Expansion Mechanisms, Part I, Alkalies in Cements and in Concrete Pore Solutions," Cement and Concrete Research, Vol. 5, 1975, pp. 329-346.
233. Diamond, S., "A Review of Alkali-Silica Reaction and Expansion Mechanisms, Part II, Reactive Aggregates," Cement and Concrete Research, Vol. 6, 1976, pp. 549-560.
234. Figg, J.W., "Alkali-Aggregate (Alkali-Silica & Alkali-Silicate) Reactivity in Concrete," Bibliography, CEMBUREAU, September 1977, 76 pp.
235. Halldorsson, O.P., Editor, "Symposium on Alkali-Aggregate Reaction Preventive Measures," Reykjavik, August 1975, 270 pp.

236. Poole, A.B., Editor, "The Effect of Alkalies on the Properties of Concrete," Proceedings of Symposium Held in London, September 1976, Cement and Concrete Association, 1976, 374 pp.
237. Diamond, S., Conference Chairman, "Proceedings of the Fourth International Conference on the Effects of Alkalies in Cement and Concrete," June, 1978, Purdue University, West Lafayette, IN, 369 pp.
238. Roller P.S., "The Setting of Portland Cement, Chemical Reactions and the Role of Calcium Sulfate," Industrial and Engineering Chemistry, Vol. 26, No. 6, June 1934, pp. 669-677.
239. Roller, P.S., "The Setting of Portland Cement, Chemical Reactions of Seasoning, Reversion and Restoration," Industrial and Engineering Chemistry, Vol. 26, No. 10, October 1934, pp. 1077-1083.
240. Kalousek, G.L., Jumper, C.H., Tregoning, J.J., "Composition and Physical Properties of Aqueous Extracts from Portland Cement Clinker Pastes Containing Added Materials," Research Paper RP1530, Journal of Research of the National Bureau of Standards, Vol. 30, March 1943, pp. 215-255.
241. Strelkov, M.I. "_____, Trudy Soveshchaniya Khim. Tsementa, Nauch.-Tekh. Obshchestvo Prom. Stroitel. Materialov, 1956, pp. 183-200.
242. Eitel, W., "Silicate Science," Vol. V, Ceramics and Hydraulic Binders, Academic Press, New York, 1966, 618 pp.
243. Kurbatova, I.I., "Effect of Alkalies on the Supersaturation Kinetics of the Liquid Phase During the Hardening of Portland Cement," Translated from Doklady Akademii Nauk SSSR, Vol. 183, No. 6, pp. 1385-1387, December 1968.
244. Lawrence, C.D., "Changes in Composition of the Aqueous Phase During Hydration of Cement Pastes and Suspensions," in Special Report 90, "Symposium on Structure of Portland Cement Paste and Concrete," Highway Research Board, Washington, D.C., 1966, 492 pp.
245. Pequin, P., Rubaud, M., Longuet, P., Zelwer, A., "Etude de la corrosion des aciers et metaux dans le beton," Congres de la Ste Fse de Metallurgie Paris, October 1971.
246. Longuet, P., Burglen, L., Zelwer, A., "La Phase Liquide du Ciment Hydrate," Revue des Materiaux, No. 677, February 1973, pp. 35-41.
247. Longuet, P., "La protection des armatures dans le beton arme elabore avec des ciments de laitier," Silicates Industriels, Vol. 41, No. 7-8, 1976, pp. 321-328.
248. Abbassi, G., "Contribution a l'etude de l'influence des metaux alcalins sur la composition et l'hydration des phases du clinker," Revue des Materiaux, November-December 1974, No. 691, pp. 315-322.

301. U.S. Department of the Interior, Bureau of Reclamation, "Specification No. 1904, Calcined Reactive Siliceous Material for Use in Concrete, Davis Dam Project, Arizona-Nevada," 23 July 1947, 14 pp.
302. A.S.T.M., "Symposium on Use of Pozzolanic Materials in Mortars and Concretes," ASTM STP No. 99, 1950, 203 pp., A.S.T.M., Philadelphia, PA, First Pacific Area National Meeting, San Francisco, CA, 10-14 October 1949.
303. Baes, C.F., Mesmer, R.E., "The Hydrolysis of Cations," John Wiley & Sons, New York, 1976, 489 pp.
304. Hawkins, P., Personal communication, 15 September 1975.
305. Nockolds, S.R., "Average Chemical Compositions of Some Igneous Rocks," Bulletin of the Geological Society of America, Vol. 65, pp. 1007-1032, October 1954.
306. Doremus, R.H., "Glass Science," John Wiley & Sons, New York, 1973, 349 pp.
307. Carmichael, I.S.E., Turner, F.J., Verhoogen, J., "Igneous Petrology," McGraw-Hill Book Co., New York, 1974, 739 pp.
308. Levin, I., Ott, E., "X-Ray Study of Opals, Silica Glass and Silica Gels," Zeit. fur Krist., Vol. 85, 1933, pp. 305-318.
309. Taliferro, N.L., "Some Properties of Opal," American Journal of Science, Fifth Series, Vol. 30, No. 179, November 1935, pp. 450-474.
310. Sosman, R.B., "The Phases of Silica," Rutgers University Press, New Brunswick, NJ, 1965, 388 pp.
311. Krejci, L., Ott, E., "The Structure of Silica Gel (X-Ray Study)," Journal of Physical Chemistry, Vol. 35, No. 7, 1931, pp. 2061-2064.
312. Florke, O.W., "The Problem of the Existence of High-Modification Cristobalite in Opals, Bentonite and Glasses," Neues Jahrb. Mineral Monatsh., Vol. 10, 1955, pp. 217-223 (Chem. Abstracts, Vol. 50, Item 12764g).
313. Jones, J.B., Segnit, E.R., "Differential Thermal and X-Ray Analysis of Opal," Nature, Vol. 198, No. 4886, 22 June 1963, p. 1191.
314. Jones J.B., Sanders, J.V., Segnit, E.R., "Structure of Opal," Nature, Vol. 204, No. 4962, 5 December 1964, pp. 990-991.
315. Tufts, S., "An X-Ray Diffraction Study of Opaline Material," Master of Science Thesis, University of Virginia, Department of Environmental Sciences, 1 June 1971, 69 pp.
316. Barth, T.F.W., "The Cristobalite Structures," I. High-Cristobalite, II. Low Cristobalite, American Journal of Science, Fifth Series, Vol. 23, No. 136, April 1932, pp. 350-356, Vol. 24, No. 140, August 1932, pp. 97-110.

317. Donnay, J.D.H., Onidk, H.M., "Crystal Data Determinative Tables," Vol. II, Inorganic Compounds, Third Ed., U.S. Department of Commerce, National Bureau of Standards, and Joint Committee on Powder Diffraction Standards, 1973.
318. Parker, R.L., "Isomorphous Substitution in Natural and Synthetic Alunite," The Amer. Mineralogist, Vol. 47, Jan-Feb., 1962, pp. 127-136.
319. Buck, A.D., "Personal Communication."
320. Kerr, P.F., "Optical Mineralogy," McGraw-Hill Book Co., New York, Third Edition 1959, 442 pp.
321. Weaver, C.E., Geology and Mineral Deposits of an Area North of San Francisco Bay, California," California Division of Mines & Geology, Ferry Bldg., San Francisco, Calif., Sept. 1949, Bulletin 149, 135 pp. + 20 plates.
322. Burnett, J.L., Barney back, R.S., "Sand and Gravel Resources of the San Francisco Bay Area," U.S. Geological Survey Open File Release, ca. 1973.
323. Shurtz, R.F., "A Hydrothermal Kalonite Deposit in West Texas," Journal of Geology, Vol. 59, 1951, pp. 60-65.
401. Longuet, P., Burglen, L., Zelwer, A., "La phase liquide du ciment hydrate," Rev. Mat. Const., Nov.-Dec. 1973, No. 676, pp. 35-41.
402. Horton, H.L., Schubert, P.B., Garratt, G., Eds., "Machinery's Handbook," Nineteenth Edition, 1973, Industrial Press, Inc., New York, N.Y., 2420 pp.
403. Seely, F.B., Smith, J.O., "Advanced Mechanics of Materials," John Wiley & Sons, Inc., New York, Second Ed., 1952, 680 pp.
404. Bridgman, P.W., "The Physics of High Pressure," G. Bell & Sons, Ltd., 1931, Reprinted by Dover Publications, Inc., New York, 1970, 398 pp.
405. Wainerdi, R.E., Uken, E.A., "Modern Methods of Geochemical Analysis," Plenum Press, New York-London, 1971, 397 pp.
406. Perkin-Elmer Corporation, "Analytical Methods for Atomic Absorption Spectrophotometry," March, Perkin-Elmer Corp., Norwalk, Connecticut, March 1973, (updated periodically).
407. Kolthoff, I.M., Sandell, E.B., Meehan, E.J., Bruckenstein, S., "Quantitative Chemical Analysis," The Macmillan Co., New York, Fourth Edition, 1969, 1199 pp.
408. Dean, J.A., Ed., "Lange's Handbook of Chemistry," Eleventh Ed., 1973, McGraw-Hill Book Co., New York, paged within sections.

409. Ahlberg, J.H., Nilson, E.N., Walsh, J.L., "The Theory of Splines and Their Applications," Academic Press, New York, 1967, 284 pp.
410. Forsythe, G.E., Malcom, M.A., "Computer Methods for Mathematical Computations," Prentice-Hall, Inc., Englewood Cliffs, N.J. 07632, 1977, 257 pp.
411. Conte, S.D., de Boor, C., "Elementary Numerical Analysis" an algorithmic approach, McGraw-Hill Book Co., New York, Second Edition 1972, 396 pp.
412. Brunauer, S., Emmett, P.H., Teller, E., "Adsorption of Gases in Multimolecular Layers," Journal of the American Chemical Society, Vol. 60, No. 2, February 1938, pp. 309-319.
413. Lipka, J., "Graphical and Mechanical Computation," John Wiley & Sons, Inc., New York, 1918, 259 pp.
414. Stein, H.N., Stevels, J.M., "Influence of Silica on the Hydration of 3 CaO, SiO₂," Journal of Applied Chemistry, Vol. 14, pp. 338-346, 1964.
415. de Jong, J.G.M., Stein, H.N., Stevels, J.M., "Influence of Amorphous Silica on the Hydration of Tricalcium Aluminate," Journal of Applied Chemistry, Vol. 19, pp. 25028, 1969.
416. Takemoto, K., Uchikawa, H., "Hydration of Pozzolanic Cement," Seventh International Congress on the Chemistry of Cement, Vol. 1, Principal Reports, Paris, 1980, pp. IV-2/1 - 2/29.
417. Duval, C., "Inorganic Thermogravimetric Analysis," (translated by R.E. Oesper), Second Edition, American Elsevier, New York, 1963.
418. Garn, P.D., Thermoanalytical Methods of Investigation," Academic Press, New York & London, 1965, 606 pp.
419. Schwenker, R.F., Garn, P.D., Eds., "Thermal Analysis," Vol. I, Instrumentation, Organic Materials & Polymers, Vol. II, Inorganic Materials and Physical Chemistry, Academic Press, New York & London, 1969, Vol. I 706 pp., Vol. II, pp. 709-1512.
420. Wendlandt, W.W., "Thermal Methods of Analysis," Vol. 19, Chemical Analysis, Second Edition, Edited by Elving, P.J., Kolthoff, I.M., John Wiley & Sons, Interscience, New York, 1974, 505 pp.
421. Spencer, H.M., "Laboratory Methods for Maintaining Constant Humidity," in: International Critical Tables of Numerical Data; Physics, Chemistry and Technology, Vol. 1, pp. 67-68, McGraw-Hill Book Co., New York, 1926.
422. Biffen, F.M., "Determination of Free Lime and Carbonate in Calcium Silicate Hydrates by Thermobalance," Analytical Chemistry, Vol. 28, #7, July 1956, pp. 1133-1136.

423. Halstead, P.E., Moore, A.E., "The Thermal Dissociation of Calcium Hydroxide," Journal of the Chemical Society, September 1957, pp. 3873-3875.
424. Southard, J.C., Royster, P.H., "The Thermal Dissociation of Calcium Carbonate," Journal of Physical Chemistry, Vol. 40, 1936, pp. 435-438.
425. Webb, T.L., Heystek, H., "The Carbonate Minerals," Chapter XIII, pp. 329-363, in the Differential Thermal Investigation of Clays, Edited by Mackenzie, R.C., Mineralogical Society (Clay Minerals Group), London, 1957, 456, pp.
426. Kantro, D.L., Weise, C.H., Brunauer, S., "Paste Hydration of Beta-Dicalcium Silicate, Tricalcium Silicate, and Alite," Highway Research Board Special Report 90, Symposium on Structure of Portland Cement Paste and Concrete, HRB, Washington, D.C., 1966, 492 pp. (pp. 309-327).
427. Diamond, S., "Identification of Hydrated Cement Constituents Using a Scanning Electron Microscope Energy Dispersive X-Ray Spectrometer Combination," Cement and Concrete Research, Vol. 2, pp. 617-632, 1972.
428. Diamond S., "C/S Mole Ratio of C-S-H Gel in a Mature C₃S Paste as Determined by EDXA," Cement and Concrete Research, Vol. 6, pp. 413-416, 1976.
429. Stucke, M.S., Majumdar, A.J., "The Composition of the Gel Phase in Portland Cement Paste," pp. 31-54, in Hydraulic Cement Pastes: Their Structure and Properties, Proceedings of a conference held at the University of Sheffield, 8-9 April 1976, Cement and Concrete Association, Wexham Springs, U.K., 1976, 334 pp.
430. Taylor, H.F.W., Roy, D.M., "Structure and Composition of Hydrates," Seventh International Congress on the Chemistry of Cement, Vol. I, Principal Reports, Paris, 1980, pp. II-2/1 - 2/13.
501. Vivian, H.E., "Studies in Cement-Aggregate Reaction, X. The Effect on Mortar Expansion of the Amount of Reactive Component in the Aggregate," Bulletin 256, Commonwealth Scientific & Industrial Research Organization, Australia, 1950, pp. 13-20.
502. Meissner, H.S., "Cracking in Concrete Due to Expansive Reaction Between Aggregate and High-Alkali Cement as Evidenced in Parker Dam," Journal, Proceedings of Amer. Conc. Inst., Vol. 37, April 1941, pp. 549-568.
503. Alderman, A.R., Gaskin, A.J., Jones, R.H., Vivian, H.E., "Studies in Cement- Aggregate Reaction, I. Australian Aggregates and Cements," Australian Council for Scientific & Industrial Research, Bulletin 229, pp. 1-46, 1947.

504. Stanton, T.E., Porter, O.J., Meder, L.C., Nicol, A., "California Experience with the Expansion of Concrete Through Reaction Between Cement and Aggregate," Journal Proceedings of American Conc. Inst., Vol. 38, No. 3, January 1942, pp. 209-236.
505. Bredsdorff, P., Poulsen, E., Spohr, H., "Experiments on Mortar Bars Prepared with Selected Danish Aggregates," Progress report I2, Committee on Alkali Reactions in Concrete, Danish National Institute of Building research and the Academy of Technical Sciences, Copenhagen 1966, 223 pp.
506. Wolf, D.O., "Reaction of Aggregate with Low-Alkali Cement," Public Roads, Vol. 27, No. 3, August 1952, Bureau of Public Roads, Washington, D.C., pp. 50-56.
507. Sprung, S., "Influences on the Alkali-Aggregate Reaction in Concrete," pp. 231-244, Symposium on Alkali-Aggregate Reaction Preventive Measures, Reykjavik, Iceland, August 1975, 270 pp.
508. Linke, W.F., "Solubilities, Inorganic and Metal-Organic Compounds," Vol. I, 1958, 1487 pp., Vol. II, 1965, 1914 pp., American Chemical Society, Washington, D.C., (Note: Revision of compilation originated by Seidell, A.)
509. McCoy, W.J., Caldwell, A.G., "New Approach to Inhibiting Alkali-Aggregate Expansion," Journal, Proceedings of Amer. Conc. Inst. Vol. 47, May 1951, pp. 693-708.
510. Bentur, Arnon, "Personal Communication" specific surface measurements of selected Pozzolans by N_2 at University of Illinois.
511. Copeland, L.E., Kantro, D.L., "Chemistry of Hydration of Portland cement at Ordinary Temperature," in The Chemistry of Cements, Ed. H.F.W. Taylor, Vol. I, Chapter 8, pp. 313-370, Academic Press, London and New York, 1964.
601. Roy, D.M., "Geochemical Factors in Borehole and Shaft Plugging Materials Stability," pp. 353-381 in Borehole and Shaft Plugging Proceedings, Columbus, Ohio, United States, May 1980, Organization for Economic Co-operation and development, Paris.
602. Vivian, H.E., "Studies in Cement-Aggregate Reaction: II. The Effect of Alkali Movement in Hardened Mortar," Bulletin No. 229, Commonwealth Scientific and Industrial Research Organization, Melbourne, Australia, 1947, pp. 47-54.
603. Thaulow, N., Kundsen, T., "Quantitative Microanalyses of the Reaction Zone between Cement Paste and Opal," pp. 189-202 in Symposium on Alkali-Aggregate Reaction Preventive Measures, Reykjavik, August 1975, 270 pp.
604. Kundsen, T., Thaulow, N., "Quantitative Microanalyses of Alkali-Silica Gel in Concrete," Cement and Concrete Research, Vol. 5, 1975, pp. 443-454.

605. French, W.J., "The Role of Solvent Migration in Alkali-Silicate Reactivity," pp. 177-190, in The Effect of Alkalies on the Properties of Concrete, Proceedings of a Symposium held in London, September, 1976, Ed. Poole, A.B., Cement and Concrete Association, 1976, 374 pp.
606. Poole, A.B., "Electron Probe Microanalyses of Reaction Zones at Cement/Opal Interfaces," pp. 163-175, in The Effects of Alkalies on the Properties of Concrete, London, September 1976, 374 pp.
607. Diamond, S., unpublished studies of the diffusion of alkalies in opal cores conducted during 1972 in the research laboratories of F.L. Smidth & Co. A/S, in Denmark.
608. Crank, J., "The Mathematics of Diffusion," Second Edition, Clarendon Press, Oxford, 1975.
609. Jost, W., "Diffusion in Solids, Liquids, Gases," Third Printing with Addendum, Academic Press, New York, 1960, 557 pp. + 94 pp. Addendum.
610. Shewmon, P.G., "Diffusion in Solids," McGraw-Hill Book Co., New York, 1963, 203 pp.
611. Abramowitz, M., Stegun, I.A., Editors, "Handbook of Mathematical Functions," Dover Publishing Co., New York, 1965.
612. Carslaw, H., Jaeger, J., "Conduction of Heat in Solids," Oxford University Press, Fair Lawn, New Jersey, 1959.
613. Carnahan, B., Luther H.A., Wilkes, J.O., "Applied Numerical Methods," John Wiley & Sons, Inc., New York, 1969, 604 pp.
614. Bailey, A., "Effects of Temperature on the Reaction of Silicates With Aqueous Solutions in the Low Temperature Range," pp. 375-380, Proceedings of International Symposium on Water-Rock Interaction, Kadek, J. Ed., Prague, Czechoslovakia, September 1974.
615. Reimann, D.K., Stark, J.P., "Oxidation Kinetics and its Influence on the Near-Surface Effect of Diffusion," Acta Metallurgica, Vol. 18, January 1970, pp. 63-70.
616. Stark, J.P., "Solid State Diffusion," John Wiley & Sons, New York, 1976, 237 pp.
617. Kalousek, G.L., "Studies of Portions of the Quaternary System Soda-Lime-Silica-Water at 25°C," Journal of Research, National Bureau of Standards, Vol. 32, 1944, pp. 285-302.
618. Iller, R.K., "Colloid Chemistry of Silicates," Cornell University Press, Ithaca, New York, 1955.

619. Iler, R.K., "The Chemistry of Silica," Wiley-Interscience Publication, John Wiley & Sons, New York, 866 pp.
620. Powers, T.C., Steinour, H.H., "An Interpretation of Some Published Researches on the Alkali-Aggregate Reaction, I. The Chemical Reactions and Mechanisms of Expansion," Journal, Proceedings of the American Concrete Institute, Vol. 51, February 1955, pp. 497-516.
621. Powers, T.C., Steinour, H.H., "An Interpretation of Some Published Researches on the Alkali-Aggregate Reaction, II. A Hypothesis concerning Safe and Unsafe Reactions With Reactive Silica in Concrete," Journal, Proceedings of the American Concrete Institute, Vol. 51, April 1955, pp. 785-812.
622. Struble, L.J., "Swell and Other Properties of Synthetic Gels," Master of Science thesis, Purdue University, August 1979, 150 pp.
623. Barnes, B.D., "Morphology of the Paste-Aggregate Interface," Doctoral Thesis, Purdue University, March 1975, 330 pp.
624. Hadley, D.W., "The Nature of the Paste-Aggregate Interface," Joint Highway Research Project, Purdue University, West Lafayette, Indiana, 9 November 1972, 186 pp.
625. Levenspiel, O., "Chemical Reaction Engineering," John Wiley & Sons, Inc., New York, 1972, 578 pp.
626. Wen, C.Y., "Noncatalytic Heterogeneous Solid Fluid Reaction Models," Industrial and Engineering Chemistry, Vol. 60, No. 9, September 1968, pp. 34 - 55.

VITA

VITA

Robert S. Barneyback, Jr. was born 15
October 1930 in Kansas City, Missouri.